



Vom Fachbereich VI Raum- und Umweltwissenschaften  
der Universität Trier  
zur Verleihung des akademischen Grades  
Doktor der Naturwissenschaften (Dr. rer. nat.)  
genehmigte Dissertation

**Towards Behavioural Model Parameterization:  
Integrated Evaluation of Hydrological Modeling and Parameterization  
Schemes for Improved Water Balance Simulations, Considering Pedo-transfer  
Functions and Spatial Patterns of Runoff Generation Processes**

**Hadis Mohajerani**

Betreuer:  
**Univ.-Prof. Dr. Markus Casper**

Berichterstattende:  
**Univ.-Prof. Dr. Tobias Schütz  
Prof. Dr. Thomas Kreiter**

Datum der wissenschaftlichen Aussprache:

Trier, 22.11.2023



## Kurzfassung

Die vorliegende Dissertation beschäftigt sich mit der Anwendung und Weiterentwicklung physikalisch basierter, räumlich verteilter Niederschlag-Abfluss-Modelle. Diese Modelle simulieren die hydrologischen Prozesse detailliert und berücksichtigen dabei die räumlichen und zeitlichen Dynamiken hydrologischer Variablen. Die konventionelle Modellbewertung basiert überwiegend auf Abflussdaten, was zu einer eingeschränkten Darstellung der Einzugsgebietsdynamik führen kann. Die Arbeit unterstreicht daher die Notwendigkeit, eine umfassendere Bewertung der Modelle zu implementieren, die sowohl interne hydrologische Prozesse als auch andere Wasserbilanzkomponenten einbezieht.

Ein wesentliches Element der Dissertation ist die kritische Analyse der Auswahl und Anwendung von Pedo-Transfer-Funktionen (PTFs). Diese Funktionen sind entscheidend für die Parametrisierung von Bodenwasserretentions- und Hydraulikeigenschaften. Es wird gezeigt, dass die Wahl der PTFs erheblichen Einfluss auf die Modellsensitivität in Bezug auf die räumliche Verteilung dieser Eigenschaften und auf die Simulation der hydrologischen Prozesse hat.

Durch den Einsatz verschiedener PTFs in einem kalibrierten und validierten Modell konnte die Variabilität der Simulationsergebnisse bezüglich der Bodenfeuchte, der Evapotranspiration und der Abflusskomponenten deutlich dargestellt werden.

**1. Manuskript:** Evaluation des hydrologischen Modellverhaltens unter Nutzung eines Multi-Kriterien-Bewertungsschemas, das sowohl quantitative als auch qualitative Daten integriert. Hierdurch konnten optimale Parameterkonfigurationen für Boden und Vegetation identifiziert werden, die zu konsistenten Simulationsergebnissen für Transpiration und Bodenwasser im Vergleich zu gemessenen Daten führten.

**2. Manuskript:** Es behandelt die Sensitivität des Wasserhaushaltsmodells bezüglich der Auswahl von PTFs in einem kleinen Einzugsgebiet in Bayern. Durch Variation der PTFs in einem kalibrierten Modell wurden deren Auswirkungen auf die räumliche Verteilung der Bodenhydraulikeigenschaften sowie auf die Wasserbilanz und die räumlich-zeitliche Variation der Abflusskomponenten aufgezeigt

**3. Manuskript:** Fokussiert auf die Verbesserung der räumlichen Darstellung dominanter Abflussprozesse in einem mesoskaligen Einzugsgebiet in Südwestdeutschland. Die Anwendung einer räumlichen Leistungsmetrik (SPAEF) ermöglichte den Vergleich der simulierten Muster mit den Mustern, die aus digitalen Bodenkarten abgeleitet wurden, und zeigte eine hohe Variabilität in Bezug auf Landnutzung, Topographie und angewandte Niederschlagsraten.

Die Ergebnisse der Dissertation tragen zur Lösung der in der hydrologischen Forschung identifizierten Probleme bei, insbesondere in Bezug auf die räumliche Variabilität und die Methoden der Modellierung. Sie bieten neue Perspektiven für die Kalibrierungsverfahren, die darauf abzielen, plausible Dynamiken (sowohl räumlich als auch zeitlich) der hydrologischen Prozesse innerhalb des Wassereinzugsgebiets zu reproduzieren. Die weiterführenden Untersuchungen, die in dieser Arbeit gefördert werden, sind von großer Bedeutung für die Entwicklung umfassender Modellkalibrierungsstrategien, die multiple Datenquellen simultan berücksichtigen und somit zu nachhaltigeren Wasserwirtschaftsentscheidungen beitragen können.



## Summary

Physically-based distributed rainfall-runoff models as the standard analysis tools for hydrological processes have been used to simulate the water system in detail, which includes spatial patterns and temporal dynamics of hydrological variables and processes (Davison et al., 2015; Ek and Holtslag, 2004). In general, catchment models are parameterized with spatial information on soil, vegetation and topography. However, traditional approaches for evaluation of the hydrological model performance are usually motivated with respect to discharge data alone. This may thus cloud model realism and hamper understanding of the catchment behavior. It is necessary to evaluate the model performance with respect to internal hydrological processes within the catchment area as well as other components of water balance rather than runoff discharge at the catchment outlet only. In particular, a considerable amount of dynamics in a catchment occurs in the processes related to interactions of the water, soil and vegetation. Evapotranspiration process, for instance, is one of those key interactive elements, and the parameterization of soil and vegetation in water balance modeling strongly influences the simulation of evapotranspiration. Specifically, to parameterize the water flow in unsaturated soil zone, the functional relationships that describe the soil water retention and hydraulic conductivity characteristics are important. To define these functional relationships, Pedo-Transfer Functions (PTFs) are common to use in hydrological modeling. Opting the appropriate PTFs for the region under investigation is a crucial task in estimating the soil hydraulic parameters, but this choice in a hydrological model is often made arbitrary and without evaluating the spatial and temporal patterns of evapotranspiration, soil moisture, and distribution and intensity of runoff processes. This may ultimately lead to implausible modeling results and possibly to incorrect decisions in regional water management. Therefore, the use of reliable evaluation approaches is continually required to analyze the dynamics of the current interactive hydrological processes and predict the future changes in the water cycle, which eventually contributes to sustainable environmental planning and decisions in water management.

Remarkable endeavors have been made in development of modelling tools that provide insights into the current and future of hydrological patterns in different scales and their impacts on the water resources and climate changes (Doell et al., 2014; Wood et al., 2011). Although, there is a need to consider a proper balance between parameter identifiability and the model's ability to realistically represent the response of the natural system. Nevertheless, tackling this issue entails investigation of additional information, which usually has to be elaborately assembled, for instance, by mapping the dominant runoff generation processes in the intended area, or retrieving the spatial patterns of soil moisture and evapotranspiration by using remote sensing methods, and evaluation at a scale commensurate with hydrological model (Koch et al., 2022; Zink et al., 2018). The present work therefore aims to give insights into the modeling approaches to simulate water balance and to improve the soil and vegetation parameterization scheme in the hydrological model subject to producing more reliable spatial and temporal patterns of evapotranspiration and runoff processes in the catchment.

An important contribution to the overall body of work is a book chapter included among publications. The book chapter provides a comprehensive overview of the topic and valuable insights into the understanding the water balance and its estimation methods.

Moreover, the first paper aimed to evaluate the hydrological model behavior with respect to contribution of various sources of information. To do so, a multi-criteria evaluation metric including soft and hard data was used to define constraints on outputs of the 1-D hydrological model WaSiM-ETH. Applying this evaluation metric, we could identify the optimal soil and vegetation parameter sets that resulted in a “behavioral” forest stand water balance model. It was found out that even if simulations of transpiration and soil water content are consistent with measured data, but still the dominant runoff generation processes or total water balance might be wrongly calculated. Therefore, only using an evaluation scheme which looks over different sources of data and embraces an understanding of the local controls of water loss through soil and plant, allowed us to exclude the unrealistic modeling outputs. The results suggested that we may need to question the generally accepted soil parameterization procedures that apply default parameter sets.

The second paper attempts to tackle the pointed model evaluation hindrance by getting down to the small-scale catchment (in Bavaria). Here, a methodology was introduced to analyze the sensitivity of the catchment water balance model to the choice of the Pedo-Transfer

Functions (PTF). By varying the underlying PTFs in a calibrated and validated model, we could determine the resulting effects on the spatial distribution of soil hydraulic properties, total water balance in catchment outlet, and the spatial and temporal variation of the runoff components. Results revealed that the water distribution in the hydrologic system significantly differs amongst various PTFs. Moreover, the simulations of water balance components showed high sensitivity to the spatial distribution of soil hydraulic properties. Therefore, it was suggested that opting the PTFs in hydrological modeling should be carefully tested by looking over the spatio-temporal distribution of simulated evapotranspiration and runoff generation processes, whether they are reasonably represented.

To fulfill the previous studies' suggestions, the third paper then aims to focus on evaluating the hydrological model through improving the spatial representation of dominant runoff processes. It was implemented in a mesoscale catchment in southwestern Germany using the hydrological model WaSiM-ETH. Dealing with the issues of inadequate spatial observations for rigorous spatial model evaluation, we made use of a reference soil hydrologic map available for the study area to discern the expected dominant runoff processes across a wide range of hydrological conditions. The model was parameterized by applying 11 PTFs and run by multiple synthetic rainfall events. To compare the simulated spatial patterns to the patterns derived by digital soil map, a multiple-component spatial performance metric (SPAEF) was applied. The simulated DRPs showed a large variability with regard to land use, topography, applied rainfall rates, and the different PTFs, which highly influence the rapid runoff generation under wet conditions.

The three published manuscripts proceeded towards the model evaluation viewpoints that ultimately attain the behavioral model outputs. It was performed through obtaining information about internal hydrological processes that lead to certain model behaviors, and also about the function and sensitivity of some of the soil and vegetation parameters that may primarily influence those internal processes in a catchment. Accordingly, using this understanding on model reactions, and by setting multiple evaluation criteria, it was possible to identify which parameterization could lead to behavioral model realization. This work, in fact, will contribute to solving some of the issues (e.g., spatial variability and modeling methods) identified as the 23 unsolved problems in hydrology in the 21st century (Blöschl et al., 2019). The

results obtained in the present work encourage the further investigations toward a comprehensive model calibration procedure considering multiple data sources simultaneously. This will enable developing the new perspectives to the current parameter estimation methods, which in essence, focus on reproducing the plausible dynamics (spatio-temporal) of the other hydrological processes within the watershed.

## **Affidavit**

I hereby affirm that I wrote this doctoral thesis independently and on my own without illegal assistance of third parties. To the best of my knowledge, all sources that I used to prepare this dissertation are labelled as such. This dissertation has not been received by any examination board, neither in this nor in a similar form.

Trier, 18.04.2024

Hadis Mohajerani



## Acknowledgements

I am deeply inspired by the words of Helen Keller, who once said, 'The only worse thing than being blind is having sight but no vision.' These words resonated with my transformative odyssey in the realm of water and hydrology, just as the word 'W-A-T-E-R' unlocked a world of possibilities for Helen, guided by her teacher, Anne Sullivan. This thesis, a tribute to those who illuminated my path with wisdom and kindness, represents a collective effort, and I am sincerely thankful to each individual who played a role in this journey.

Heartfelt appreciation is extended to my supervisor, Prof. Markus Casper, for his intelligent, wise, and constant guidance in shaping and implementing ideas that guided this work. His commitment to excellence and belief in the potential of every student have not only guided my academic pursuits but also enriched my perspective on the role of education as a catalyst for change.

My deepest gratitude goes to my parents, who navigated the complexities of raising a visually impaired child with grace and love, and encouraged me to widen my horizons beyond the imposed social restrictions.

Special thanks go to all of my friends and colleagues (named and unnamed), whose camaraderie and encouragement made the challenges of this PhD more bearable and the successes more joyful. I am particularly grateful to Dr. Jesus Rodridgo-Comino, and Dr. Manuel Seeger for their collaborative perspectives on research that enhanced my knowledge and integrated me into the broader international research community. In addition, heartfelt thanks to Prof. Johannes Ries for his considerate support and empathetic understanding from my very first day in Physical Geography.

I acknowledge with gratitude the financial support of the German Research Foundation (DFG) for this research project (Projektnummer 426111700 (CA 728/8-1 and VO 1509/8-1), without which this PhD endeavor would not have reached its fruition.

Moreover, I would like to acknowledge the German academic community, in general, for fostering an inclusive, diverse, and empowering environment. In particular, I express my gratitude to the Graduate Center Team and the Equal Opportunities Office at the University of Trier for supporting me during my PhD study and aiding in my academic and personal developments. Special thanks to Dr. Agnes Schindler and Dr. Sabine Hartel-Schenk for their mentorship and invaluable insights in shaping my academic path.

With deepest appreciation,

Hadis Mohajerani - Trier, 2023



# CONTENTS

<b>KURZFASSUNG</b>	<b>I</b>
<b>SUMMARY</b>	<b>III</b>
<b>AFFIDAVIT</b>	<b>VII</b>
<b>ACKNOWLEDGEMENTS</b>	<b>IX</b>
<b>1 INTRODUCTION AND OBJECTIVES</b>	<b>1</b>
<b>2 SCIENTIFIC BACKGROUND</b>	<b>7</b>
2.1 Understanding the water balance and its estimation methods	8
2.2 Modeling water fluxes in the unsaturated zone	38
2.3 Model evaluation and its limitation	46
<b>3 CONCLUSION AND OUTLOOK</b>	<b>53</b>
<b>4 REFERENCES</b>	<b>59</b>
<b>5 APPENDIX</b>	<b>71</b>
5.1 Finding behavioral parameterization for a 1-D water balance model by multi-criteria evaluation	72
5.2 A Comparative Investigation of Various Pedotransfer Functions and Their Impact on Hydrological Simulations	85
5.3 Spatial Evaluation of a Hydrological Model on Dominant Runoff Generation Processes Using Soil Hydrologic Maps	108



# 1 Introduction and Objectives

The current global climate change and land use intensification are causing significant alterations in the terrestrial water cycle. These changes in the process of transforming rainfall into runoff may result in heightened risks of drought and flooding events, which can negatively affect freshwater resources, ecosystem functioning, biodiversity, and various water-dependent socio-economic sectors such as agriculture, forestry, energy, and transportation. The terrestrial water cycle involves intricate interactions among subsurface, surface, and atmospheric processes that have significant impacts on the energy and carbon cycles. Due to the worldwide impact of these issues, extensive efforts have been made to develop modeling tools that can provide a forecast of the future large-scale hydrological patterns and their impacts (Wood et al., 2011; Doell et al., 2014). Predicted changes in the water cycle at subnational, regional, and local levels aren't directly applicable to findings from global assessments. As a result, regional and local assessments of water cycles require either downscaling global climatic and hydrological models or developing models that are able to accurately represent spatial and temporal dynamics of the specific region. Rainfall-runoff models can provide a suitable approach for such analyses (Huang et al., 2013; Surfleet et al., 2012). In the realm of hydrology, rainfall-runoff models have established themselves as the conventional tools for analyzing hydrological processes, due to their versatility and suitability for a wide variety of modelling approaches that can be adapted to fit diverse applications.

In contrast to conceptual models, “physically-based” hydrological models (i.e., models including equations based on principles of physics that incorporates information about the physical properties of the land surface, such as topography, soil properties, vegetation, and meteorological data) offer a more detailed representation of the terrestrial water system, including the spatial patterns and temporal dynamics of state and process variables. This more detailed representation allows for a deeper understanding of the coupling fluxes between land and atmosphere, which are highly sensitive to both the temporal dynamics of atmospheric conditions and the spatial heterogeneity of land surface states. As such, the use of physically-based hydrological

models can facilitate a deeper understanding of land-atmosphere interactions, offering valuable insights into the functioning of the terrestrial water system (Davison et al., 2015; Ek and Holtslag, 2004).

As we face anticipated changes in the terrestrial water cycle, there is a pressing need for modelling frameworks and approaches that are capable of capturing the complex variability in hydrologic processes at scales that are most relevant for local and regional water resource management. Moreover, these modeling frameworks should accurately simulate the interactions between various components of the water cycle at appropriate spatial and temporal scales, taking into account the local variability in environmental conditions. By utilizing such frameworks, it will thus be possible to enhance our understanding of the terrestrial water system and to develop effective strategies for managing water resources at various scales in the face of changing climatic conditions.

When applied at the catchment scale, physically-based hydrological models must account for the local topography and landscape characteristics which regulate the type of runoff generation processes (e.g., infiltration- or saturation excess flow) and the hydrological connectivity in both surface and subsurface flow paths. This is because these factors have a direct impact on the hydrological processes occurring within the catchment, and therefore must be accurately represented in the model to ensure reliable predictions. In other words, the physical features of a landscape, such as the shape of the land and the soil properties, can significantly impact how water flows through it, and this must be accounted for in any hydrological model aimed at predicting runoff patterns at catchment scale (Gupta et al., 2006; Ogden et al., 2013). Within mesoscale catchments (10 - 1000 km<sup>2</sup>), a set of specific questions arise due to future changes in climate and land use. For instance, questions related to water retention capacity and drought stress tolerance of the landscape resulting from water storage in soil and ground-water. These questions can be best addressed by using “distributed physically-based” hydrological models that accurately map the local water cycles (Fatichi et al., 2016).

A calibrated model that accurately mimics the behaviour of a hydrologic system, also known as a "behavioural" model, is essential for predicting runoff patterns in ungagged catchments or when there are significant changes in land use or climate over time. According to Gupta et al. (2006), the fundamental characteristics of a behavioural hydrologic model are: (i) it produces input-state-output behaviour that matches with observed measurements; (ii) it generates accurate predictions that are essentially unbiased; and (iii) its structure and behaviour align with our

current understanding of hydrological processes in the real world. Therefore, it is necessary for "Physically-based" models to exhibit coherence with observational evidence of process dynamics that portray the performance of a natural hydrological system (Beven, 2002). In catchment modeling, spatial data on soil, vegetation, and topography are typically used to parameterize the models. These models simulate all aspects of the hydrological cycle but are often only calibrated using streamflow measurements at the catchment outlet. Available spatially distributed information is often not considered adequately in model calibration and validation procedures. Spatial knowledge on runoff generation processes (with relevant feedbacks on the other hydrological variables) is not usually included in the model parameterization process and not used to define constraints in the parameter space. Furthermore, spatially-distributed land surface parameters, such as soil hydraulic properties, vegetation cover, and land use/cover, are often defined as static parameters without sufficient attention to their spatial and temporal fluctuations, as well as the techniques employed to obtain them. For example, when using Pedo-Transfer functions (PTFs) to estimate soil hydraulic properties and parameterize the soil, the effect of choosing different parameterization methods on runoff components and evapotranspiration is usually disregarded. This approach may result in inadequate simulations of other hydrological components (rather than discharge) that are spatially distributed, while contradicting the notion of a behavioural model. The resulting uncertainty in the representation of the variability of the hydrological variable within a catchment then hampers the utility of the model predictions. There is thus a need to move away from the traditional calibration and evaluation framework including only aggregated observations to a more integrated framework that instead embraces spatially distributed observations, hydrological components others than discharge, and knowledge of runoff generation and soil hydraulic properties in the model evaluation process (Herman et al., 2018; Koch et al., 2017, 2016; Refsgaard, 2001; Stisen et al., 2008).

Consequently, the objective of the present PhD thesis is to address the challenges involved in assessment approaches within the context of mesoscale hydrological modeling, and to develop an evaluation framework that carefully considers information on distribution of internal process variables (also including their temporal and spatial patterns) in a hydrological boundary. The thesis aims to establish a multi-criteria evaluation approach for physically-based hydrological modeling leveraging spatially detailed information on dominant runoff generation processes, soil hydraulic properties, land cover, topography, as well as streamflow at the catchment outlet. Our approach involves utilizing the flexible framework of the WaSiM-ETH model to

create a representative mesoscale rainfall-runoff model that accurately captures the spatio-temporal dynamics of the terrestrial water cycle at an hourly resolution. In order to effectively incorporate our current knowledge of the dominant runoff generation processes, which involve the interplay between topography, physical soil properties, groundwater levels, and land cover, into a behavioural model, we will account for the spatial heterogeneity of the catchment at a resolution of 50-100 meters. In the case of a mesoscale catchment, a resolution of 50 to 100 meters is suitable for evaluating the impact of important land surface features, such as topography and soil properties. As a "behavioural" model aims to replicate not just the catchment's overall runoff but also its spatial distribution, we intend to introduce novel spatial metrics into our evaluation process to analyze the dynamic temporal and spatial patterns of both runoff generation and water balance components within the catchment. The evaluation process thus incorporates discharge data at the catchment outlet, spatial data related to the dominant runoff generation and soil hydraulic properties, and also field observations of soil water content and plant

transpiration. Through this multi-criteria evaluation approach, we will focus on addressing both global sources of uncertainty such as bias, as well as local uncertainties, such as the runoff generation processes and soil hydraulic properties. By ensuring proper evaluation, a behavioural physically-based model that is can effectively capture the impact of climate and land use variations. This, in turn, can enable us to understand how the hydrological cycle will respond to anticipated global environmental changes in the future. The PhD thesis at hand focuses on evaluating hydrological modeling with regard to different hydrological variables in three domains: (i) soil moisture content and transpiration in a plot scale in Luxembourg region; (ii) spatial distribution of soil hydraulic properties, and the spatio-temporal variation of the runoff components in a small catchment in Bavaria, Germany, and (iii) spatial patterns of dominant runoff generation processes in a mesoscale catchment in Rhineland-Palatinate, Germany. The proposed approach provides a novel tool for interpreting the model parameters with regard to their physical meaning related to the simulated hydrological processes and identifying parameter sets that simultaneously meet multiple objectives and lead to a behavioural model.

The following chapter will provide a brief background to the topic. First, we start with the section 2.1 which is devoted to a book chapter as one of the publications included in this thesis, and it provides a significant contribution to the overall body of work by offering a comprehensive overview of the topic and valuable insights into understanding the water balance and its estimation methods. Thereafter, section 2.2 explores the state of the art of modeling water fluxes

in the unsaturated zone and the interactions between soil, water, plants, and the atmosphere, followed by section 2.3 that discusses the model evaluation perspectives and their limitations. Finally, chapter 3 concludes the study by summarizing the key findings and presenting conclusive remarks. Three papers published based on the thesis outcomes can be found in the Appendix.





## **2 Scientific background**

Within this chapter, it is aimed to provide a concise background on the topic. The focal point of section 2.1 lies in a book chapter, which is among the publications encompassed in this thesis. This particular section holds immense significance within the overall body of work, as it imparts valuable insights into the overall topic, by introducing the estimation methods used to comprehend the water balance and its various components. Moving forward, section 2.2 delves into the state-of-the-art in modeling water fluxes within the unsaturated zone, exploring the intricate interactions that occur among soil, water, plants, and the atmosphere. Subsequently, section 2.3 discusses the perspectives and limitations associated with evaluating the model.

## **2.1 Understanding the water balance and its estimation methods**

## Chapter 9

# Understanding the water balance and its estimation methods

Hadis Mohajerani<sup>1</sup>, Demetrio Antonio Zema<sup>2</sup>, Manuel Esteban Lucas-Borja<sup>3</sup> and Markus Casper<sup>1</sup>

<sup>1</sup>Department of Physical Geography, Universität Trier, Trier, Germany, <sup>2</sup>Department Agraria, Mediterranean University of Reggio Calabria, Reggio Calabria, Italy, <sup>3</sup>University of Castilla-La Mancha, E.T.S.I.A.M., Albacete, Spain

### Introduction to the hydrological cycle

A system can be described as an aggregation of interrelated components subject to regular interactions. The operation of a system is to generate output from input or interrelate input and output. Therefore, a hydrologic system could be explained as a *hydrological system* (hereafter will be referred as *hydro-system*), including components of a landscape that store water in its natural state (solid, liquid, and gas) that interact regularly according to the physical laws that govern the state, movement and storage of water (Dooge, 1968).

The natural and continuous processes of water movement near or below the earth's surface form the so-called *hydrological cycle* (Fig. 9.1) where water moves either from one location to another or is being transformed from a state (i.e., liquid, solid, gas) to another. This cycle encompasses the three main terrestrial components: water bodies (including oceans), atmosphere, and land (including vegetation). The hydrological cycle starts with the evaporation from the ocean, due to the radiant (heat) energy from the sun (solar radiation). Convection lifts the water evaporated from the ocean to the atmosphere where, under suitable conditions, the vapor turns into precipitation (water, snow or ice). Precipitation can:

- First gets intercepted by the vegetation and then directly evaporates back into the atmosphere (*interception*)

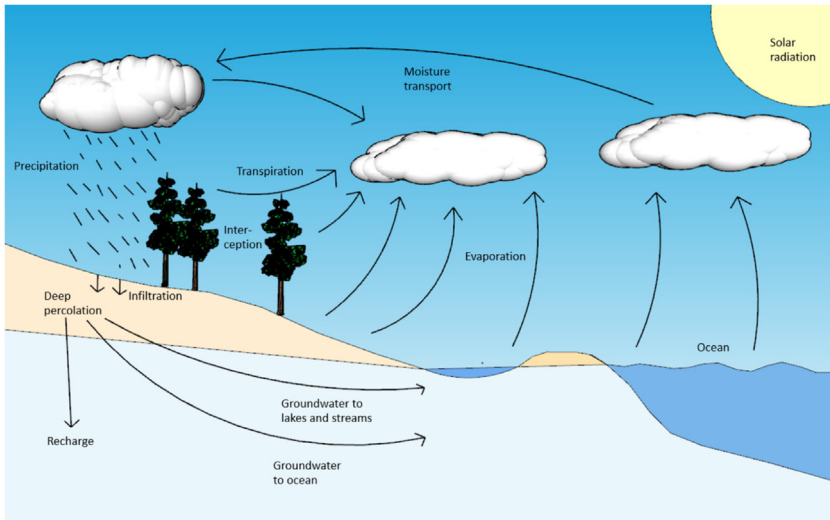


FIGURE 9.1 Different processes of the hydrological cycle.

- Infiltrates (entering the soil) and evaporates from the soil surface or transpires through vegetation (*evapotranspiration*)
- Turns into an overland water stream (*surface runoff*)
- Migrate into the deeper layers of soil (*infiltration*).

All these *hydrological processes*, which originate from the interactions among the precipitation (on its turn considered as a hydrological process) on one side and land-vegetation, water bodies and atmosphere on the other side (interception, evapotranspiration, infiltration, runoff), are components of the hydrological cycle and vary significantly in both, time, and space.

The hydrological processes generate the *water fluxes* (or *water flows*, depending on the object of focus), which are usually defined as follows:

- *Surface water flux*, which is the volumetric flow of water passing through the land surface
- *Sub-surface water flux*, which is the volumetric flow per unit of the cross-sectional area of the porous medium (soil) constituting the groundwater storage in the saturated zone
- *Atmospheric water flux*, which is either in the form of precipitation reaching the land surface from the atmosphere or returned to the atmosphere through the evapotranspiration process.

While the dimension for water flow is  $[L^3]$ , generally, the water flux is related to the surface unit of the hydro-system, and thus the dimension is  $[L]$ .

## The water balance

According to the *law of conservation of mass*, the rate of change in water storage within a hydro-system over any specific period of time must be equal to the difference between the rates of inflow and outflow of water across its boundaries (Byeon, 2014). To describe water flow into and out of a hydro-system (i.e., through the various hydrological processes) and quantify the rate of change in the water being stored in the hydro-system (i.e., in the land, atmosphere, and water bodies), a *water balance* equation is used. The spatial scale of the hydrological system for which the water balance is calculated may range from a small sample of soil (*plot scale*) to an entire catchment (*catchment scale*) or the *global/continental scale*.

To estimate the water balance, it is first necessary to define the *spatial boundaries* of the considered hydro-system (called *control volume*) and the *reference period* of time. The control volume (e.g., a catchment or a soil column) is a volume in space in which fluxes of water, energy and other mass are stored internally or transported across its boundaries. For instance, with regard to a catchment to which the water balance must be applied, the control volume is the space within (1) the ground surface; (2) the horizontal layer (roof) over the tallest vegetation; and (3) the vertical lines extruded from the perimeter of the ground/impervious surface and the roof of vegetation. The reference period is the temporal scale (event, monthly, seasonal, annual, decadal or longer) when the changes in the water storage and fluxes of the control volume are estimated. Thus, the total amount of water that is stored in a control volume is the *water storage*, with the dimension  $[L^3]$ .

A water balance accounts for the horizontal flow of water through the landscape in watercourses, for the vertical water fluxes among the atmosphere, ground surface, and groundwater and for the changes in water storage within the control volumes. In its general form, the water balance can be expressed using the following equation (Sutcliffe, 2004):

$$P + I = ET + Q + \Delta S + \Delta G + \Delta W \quad (9.1)$$

where  $P$  is precipitation,  $I$  the inflow (the water flow entering the control volume),  $ET$  the evapotranspiration,  $Q$  the outflow (the water flow leaving the control volume), and  $\Delta S$ ,  $\Delta G$  and  $\Delta W$  the changes in the water content of soil (in the unsaturated zone), groundwater storage (in the saturated zone), and water amount stored into surface water bodies, respectively. In the following, we discuss the water balance at different spatial scales.

### Plot scale

The water balance at the plot scale (Fig. 9.2) is usually applied for agricultural purposes. It considers the root zone per unit area as the control volume. The difference between the water fluxes entering and leaving the control volume must be equal to the changes in the water content, throughout the reference period. In a nutshell, the water content of the soil volume increases

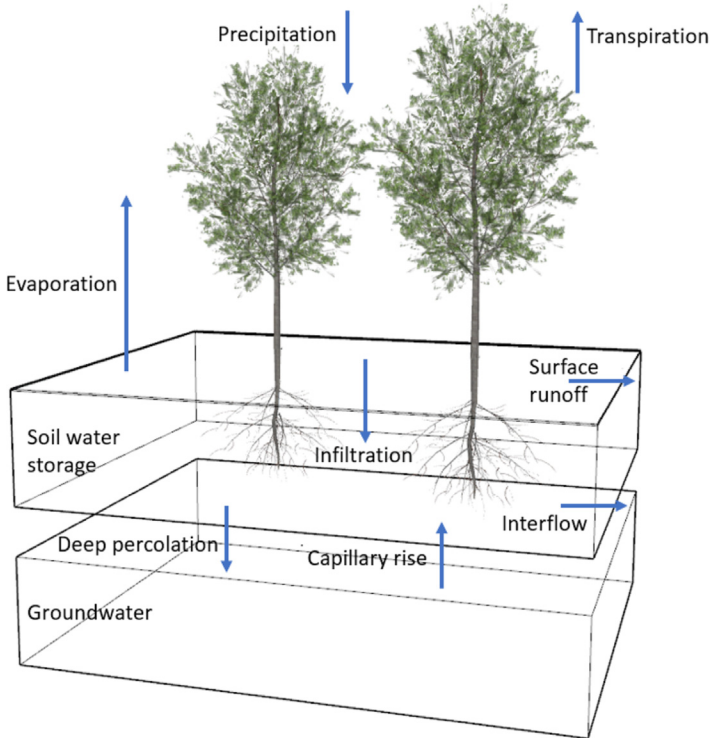


**FIGURE 9.2** Scheme of the water balance at the plot scale (root zone) (lateral flow = interflow + groundwater flow).

when water is added due to infiltration or capillary rise and decreases when water is lost by evapotranspiration or deep percolation. The water balance equation at plot scale is usually represented as follows (Zhang, Walker, & Dawes, 2002), where all the values are expressed as water fluxes or equivalent water depth throughout the reference time period:

$$\Delta S = P - I - E - T - Q - DP + CR \quad (9.2)$$

where  $\Delta S$  is the change in water content of the root zone,  $P$  is the precipitation,  $I$  is the interception,  $E$  is the direct evaporation from the soil surface,  $T$  is the transpiration through vegetation,  $Q$  is the runoff (surface runoff and interflow, see section 3.2 and 3.3),  $DP$  is the deep percolation towards the groundwater storage, and  $CR$  is the capillary rise.

### Catchment scale

A catchment, divided by watershed from the adjacent system, is the geographical unit of interest for terrestrial hydrology to apply the water balance

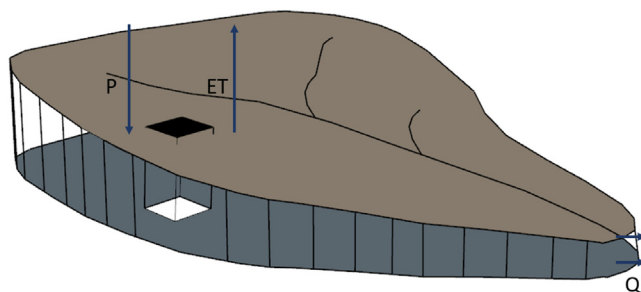


**FIGURE 9.3** Scheme of a catchment (control volume); ET = evapotranspiration; P = precipitation; Q = runoff; the brown area is the soil surface, while the gray area is the sub-soil; the vertical box is the soil column.

and part of the extensive water cycle. Precipitation is caught up by catchment, and the drainage network of the catchment collects and conveys part of this water to a common outlet. The catchment outlet can be the mouth of the main watercourse into the sea, the confluence into another stream, or the section where it flows into a lake, reservoir or wetland (Fig. 9.3). By definition, when applying the water balance at the catchment scale (i.e., when the catchment is the control volume), the streamflow at the catchment outlet represents the integrated response to all hydrological processes within the catchment (Kirchner, 2009; Singh & Woolhiser, 2002). At the catchment scale, the water balance equation can be expressed as follows (Zhang, Dawes, & Walker, 2001), where all water fluxes are estimated as the catchment-scale spatially average:

$$\Delta S + \Delta G + \Delta W = P - ET - Q \quad (9.3)$$

where  $\Delta S$ ,  $\Delta G$ , and  $\Delta W$  are the changes in water content of the soil, groundwater, and surface water bodies,  $P$  is the precipitation,  $ET$  is the evapotranspiration,  $Q$  is the runoff (streamflow).

### Global/continental scale

At global or continental scales, the water balance is generally accounted for the fundamental components, i.e., precipitation on the land surface is balanced out by streamflow, evapotranspiration, and the change in water storage. Since the water quantity of the oceans is considered to be constant for long periods of time, the streamflow (quantity of water returned from continents to the sea) and the water of oceans loss by evaporation must be equal (Marcinek, 2007). To satisfy the water balance equation at the global or continental scales, the observations of all the components of the hydrological cycle with a global perspective are required. Particularly, precipitation needs continuous monitoring, as it is the major component of the cycle.

## Water balance components/fluxes

### Atmospheric water

Atmospheric water consists of precipitation and evapotranspiration. Precipitation accounts for the major contribution to the water balance of a terrestrial control volume and consists of water that drops from the atmosphere in either liquid or solid-state. Precipitation is generated by the condensation of moisture in the atmosphere, because of the cooling of an air portion. Formation of precipitation is driven by the origin of the lifting motion that triggers it, which eventually leads to various temporal and spatial rainfall regimens, which are typical of the climatic type of an area. According to the *Köppen-Geiger Climate Classification System* (Köppen, 1936), five major climatic types are recognized based on the annual and monthly averages of temperature and precipitation:

- a. Tropical Moist Climates: all months have average temperatures above 18°C, which cause the daily intense convective precipitation
- b. Dry Climates with deficient precipitation during most of the year, which lead to convective precipitation events (while in general precipitation rate is low, but occurs in form of extreme events with high intensity)
- c. Moist Mid-latitude Climates with Mild Winters, with mid-latitude cyclones causing the winter storms
- d. Moist Mid-Latitude Climates with Cold Winters, similar to the C category, but with precipitation mostly in form of snowfall in winter
- e. Polar Climates: with extremely cold winters and summers, which cause dry conditions with a low amount of precipitation and mostly in the form of snow.

Rainfall is the liquid form of precipitation while reaching the earth. Other forms of precipitation are snowfall, which is frozen water in a crystalline state; hail that is frozen water in a massive state; sleet, which is melted snow, regarded as a mixture of snowfall and rainfall. Precipitation is characterized by high spatial and temporal variability, which can be analyzed by its main attributes:

- *Depth* (volume of precipitation accumulated on a horizontal surface area in a certain time, if precipitation can not drain, evaporate or percolate from this surface, dimensions  $[L^3/L^2]$ )
- *Duration* (the time from the start to the end of precipitation,  $[T]$ )
- *Intensity* (time rate of rainfall depth, equal to the ratio of the precipitation depth by its duration,  $[L/T]$ ).

Usually, precipitation depths and intensities of a storm are graphically reported in charts that are called *pluviographs* and *hyetographs*.

Other characteristics determining precipitation variability are:

- *Frequency* (the number of times, during a certain period, that precipitation of a specific magnitude or greater occurs)



- *Pattern* (shape of the temporal diagram of a precipitation event)
- *Areal extent*
- *Movement*
- *Location*.

Rainfall frequency provides the information on how often precipitation with a given characteristic is likely to happen, which will consequently determine the frequency of occurrence (or return period) of the resulting runoff (in particular, the frequency of the peak flow). Precipitation pattern, areal extent, and movement determine how a portion of the drainage area contributes over time to the runoff, usually caused by the type of storm (rainfall event, which is caused by the original climate conditions). For instance, precipitation associated with cold fronts (thunderstorms) tends to be more regional, faster moving, and of shorter duration, while warm fronts tend to generate slowly moving storms of broader areal extent and longer durations. Moreover, the location where a regional storm occurs in the catchment influences the temporal distribution of the runoff. To give an example, a storm falling near the catchment outlet will result in a very quick occurrence of peak flow, as well as a rapid passage of the flood. Precipitation movement affects the runoff rate, depending on the catchment shape (particularly in elongated catchments).

Duration, intensity, and frequency of precipitation are often considered in combination, to constitute the intensity-duration-frequency (IDF) curve. This is the diagram of intensity versus duration that is provided for each frequency (or return period) of precipitation. The IDF curves are specific for a given location. The storm (the so-called *critical event*) used for predicting or estimating the runoff *hydrograph* (see sub-chapter 3.5) with a specific return period (or a certain frequency) is considered as “*design storm*,” which can be derived from the IDF curves or the statistical analysis of observed rainfall. Since the amount and timing of runoff depend on the magnitude, the spatial and temporal distribution of rainfall, the hyetographs of both actual and design storms are fundamental elements for projects requiring hydrological information and for hydrological modeling (McCuen, 1982; Chow, 1964; Haan, Barfield, & Hayes, 1994).

The other component of atmospheric water is evapotranspiration (ET) that includes the processes in which water is transferred into gas flux (vapor) to the atmosphere. ET processes are generally referred to as (Labadzki, 2011):

- *Evaporation*, the water transfer from the surface of a water body or from bare soil to the atmosphere
- *Transpiration*, the water absorbed by vegetation roots from the soil and routed through the leaves (across the canopy stomata) to the atmosphere
- *Evaporation of intercepted water*, the share of precipitation which falls onto the vegetation canopy surface and is directly returned into the atmosphere.

We can distinguish potential and current ET. Potential ET can be defined as the water loss from a surface with no water limitation. It can be expressed as a function of the physical variables of the atmosphere (i.e., depends on the energy that is available to convert liquid water to vapor from climatic driving forces, like solar net radiation), where the resulting water vapor can freely move away from the surface. The water content of soil and ET are known to be highly correlated. To calculate the actual ET, potential ET is reduced based on real soil water content (Beven, 2011). Allen (1998) identified the following variables influencing ET:

- *Meteorological parameters*, such as solar radiation and air temperature, humidity, and wind speed
- *Crop parameters*, such as species, growth stage, height, ground cover, water stress, and rooting characteristics
- *Soil parameters*, such as roughness, salinity, fertility and albedo
- *Management parameters*, such as the application of fertilizers and soil cultivation practices.

The estimation of ET from vegetated areas is a basic tool to compute the water balance for estimating the water requirements of irrigated crops and for planning water management. Since direct measurements of ET are difficult, in many cases it is easier to estimate ET fluxes as a residual of the water balance equation, or by application of models using meteorological and other data as input. Generally, the difference between precipitation and ET largely controls the amount of water surplus in a hydro-system (except at the event scale). Sub-chapters 4.1.1 and 4.2 provide an overview of methods and models widely applied to measure and/or estimate ET.

## Surface water

Surface water is the hydrological response of soil to a precipitation event. During a storm, the share of atmospheric water that is not intercepted by vegetation does not infiltrate or percolate through soil (see section 1), flows by gravity over the soil along hillslopes and then in stream channels (*surface runoff*) (Fig. 9.4). Of the *total runoff*, the share directly generated by rainfall takes a rapid route to the stream channels (*direct runoff* or *quickflow*), while the other part of precipitation that infiltrates into the soil takes a much slower route (*base flow* or *delayed flow*) (Ward & Robinson, 1967). Generally, while interception, evapotranspiration and infiltration run out with precipitation, runoff may also continue in dry periods, fed by the base flow. Runoff is usually expressed as water depth per time and space units (mm, that is  $\text{m}^3$  per  $\text{m}^2$  of the area and per hour or day), which makes the comparison with precipitation (measured by the same unit) simpler.

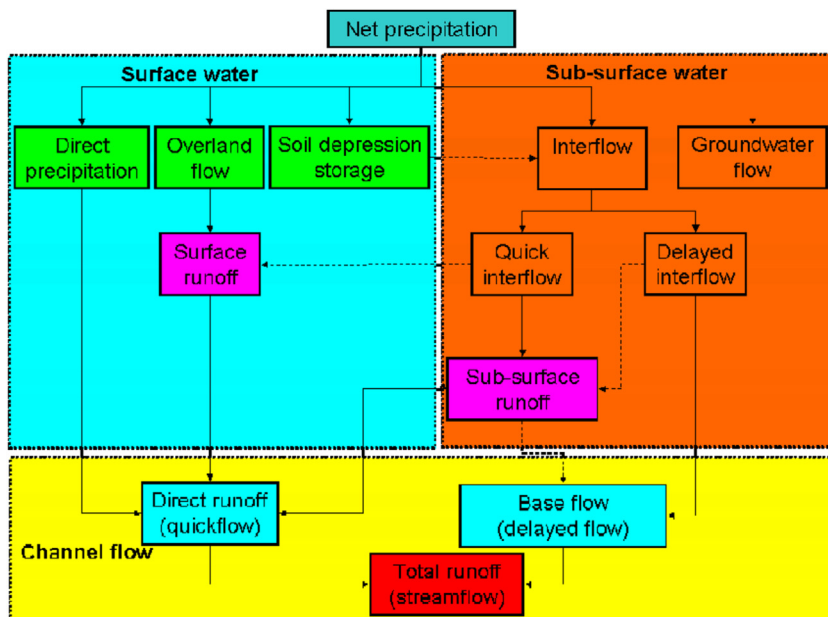


**FIGURE 9.4** Schematization of total runoff components (Ward & Robinson, 1967). Modified from R. C. Ward and M. Robinson (1967). *Principles of hydrology* (No. 551.49/W262). New York: McGraw-Hill.

The *total runoff* or *streamflow* is the result of several water flow paths (Ward & Robinson, 1967) (Fig. 9.4):

- (i) *Direct precipitation* over the water surface
- (ii) *Overland flow*
- (iii) *Interflow* (shallow sub-surface water)
- (iv) *Groundwater flow* (deep sub-surface water).

The direct precipitation is the share of the atmospheric water input that directly falls over the water surfaces (lakes, artificial reservoirs, stream channels of the hydrographic network). This share is usually limited since these surfaces cover a very small area of the catchment system.

The overland flow includes the sheet flow (the laminar water stream flowing downslope) and the concentrated flow into rills and gullies. The overland flow generates surface runoff, which is the faster component of the quick flow (Fig. 9.4).

### Sub-surface water

The interflow is the share of the water infiltrating through the soil surface that flows laterally (calculated according to Darcy's law, regulating the

filtration process into porous media) into the upper soil layer to the channel. This flow occurs in the unsaturated zone or the capillary edge over the aquifer when the horizontal hydraulic conductivity is much higher compared to the vertical conductivity into the soil profile. Moreover, the horizontal hydraulic conductivity decreases with soil layer depth (in absence of artificial disturbance, such as tillage and soil compaction), which makes the interflow of the upper soil layers much faster than the delayed interflow and groundwater flow in the deeper layers. Quick interflow and part of the delayed interflow feed the sub-surface runoff (Fig. 9.4).

The water that moves vertically is known as deep percolation, which is the water flux below the root zone. The groundwater flow is fed by the percolation of the infiltrated rainfall into the deep soil layers, reaching water tables, and runs towards the stream channel through the saturated zone. Sometimes, the infiltrated rainfall can directly generate the groundwater flow. The groundwater flow is delayed by days or even months with respect to precipitation, surface runoff or interflow, due to the very low hydraulic conductivity, but does not fluctuate rapidly (Fig. 9.5).

Groundwater flow and delayed interflow, beside a share of the sub-surface runoff, are the components of the base flow (or delayed flow) (Fig. 9.4).

The different time rates and amounts of the runoff components of the streamflow determine the nature and magnitude of the hydrological response of a territorial unit (e.g., plot, hillslope, and catchment) to precipitation.

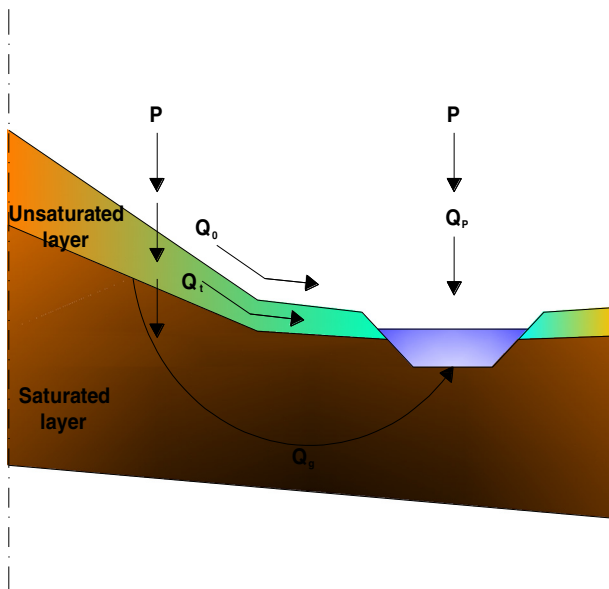


**FIGURE 9.5** The different components of runoff along a hillslope ( $P$  = precipitation;  $Q_o$  = direct precipitation over water surfaces;  $Q_o$  = overland flow;  $Q_i$  = interflow;  $Q_g$  = groundwater flow).

The current comprehension of this hydrological response can be attributed to two different runoff generation mechanisms, conceptualized by two famous hydrologists (Hewlett, 1961; Horton, 1933).

## Runoff generation mechanisms

### *Infiltration-excess (or Horton's) mechanism*

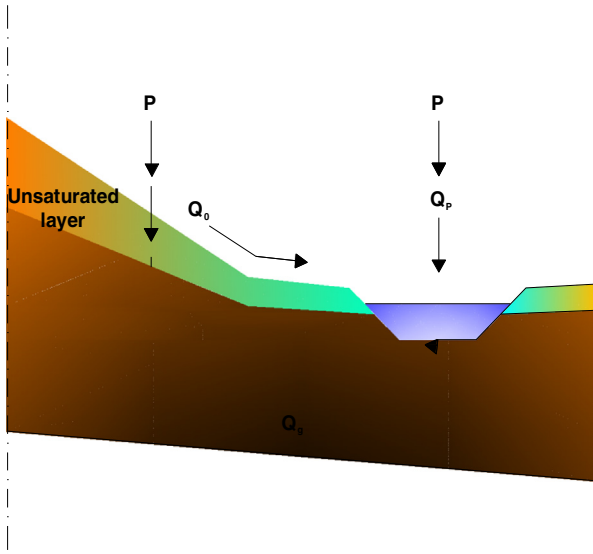
In 1933, R.E. Horton hypothesized that, at the soil surface, the shares of net precipitation infiltrating or moving over the soil as overland flow strictly depends on the *soil infiltration capacity* ( $f$ ). This is the maximum rate at which rainfall infiltrates into the soil when water is continuously and sufficiently available over its surface (Hillel, 1998). Once the storm starts,  $f$  gradually decreases with time until a steady value ( $f_c$ ), due to the progressive soil saturation during precipitation; the decrease rate of  $f$  theoretically follows an exponential law from an initial value ( $f_0$ ) until the asymptotic  $f_c$ . After the storm event, the initial  $f_0$  is recovered. If  $f$  is higher than the rainfall intensity ( $i$ ), all net precipitation infiltrates, feeding the sub-surface flows, and no runoff is observed (Fig. 9.6A). By contrast, if  $f < i$ , the excess precipitation, equal to difference  $i - f$ , is the overland flow (Fig. 9.6B), accordingly defined as *infiltration-excess (or Hortonian) overland flow*. The runoff generation mechanism conceptualized by Horton is typical of the arid or semi-arid areas, where the overland flow is produced by infrequent but heavy rainfalls and is influenced by soil surface processes, such as sealing, cracking, and freezing.

### *Saturation-excess (or Hewlett's) mechanism*

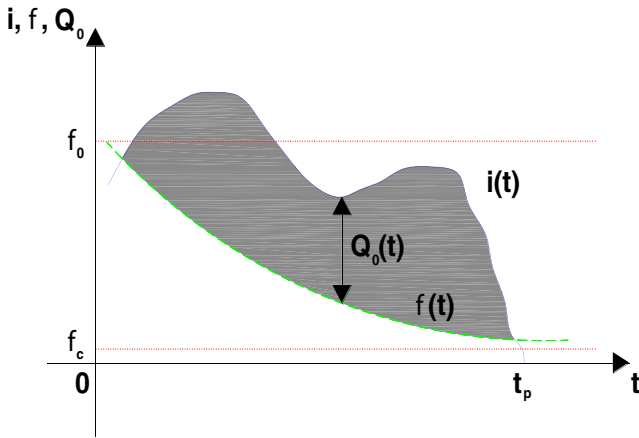
Later, in 1961, J.D. Hewlett hypothesized that, during intense and prolonged events, the precipitation infiltrating into the soil feeds the sub-surface water. Due to the progressive saturation of the soil profile, the water table rises up, primarily starting on the lower slopes of the catchment and along valley bottoms adjacent to stream channels (Fig. 9.7A). Throughout the storm, progressively larger areas, on which the soil infiltration capacity decreases to zero, saturated in the catchment, and the excess precipitation feeds the surface water, accordingly defined *saturation-excess overland flow* (Fig. 9.7B); only the saturated areas contribute to surface runoff. The runoff generation mechanism theorized by Hewlett is typical of the humid and sub-humid areas, where the morphology and other properties of soils let the water table rise easier during the precipitation events.

## Temporal evolution of surface and sub-surface water

In humid and sub-humid climates, *perennial* watercourses have permanent water flow. In arid or semi-arid areas (such as in the Mediterranean



(a)



(b)

**FIGURE 9.6** The runoff generation mechanism by infiltration excess. (A) Flow paths in the hillslope profile ( $P$  = precipitation;  $Q_p$  = direct precipitation over water surfaces;  $Q_o$  = overland flow); (B) the theoretical diagram ( $f$  = infiltration rate;  $f_c$  = steady infiltration rate;  $f_0$  = initial infiltration rate;  $t_p$  = precipitation duration;  $i$  = precipitation intensity;  $Q_o$  = overland flow).

environment), watercourses are *intermittent*. Here, the water flows in the channels for some months during the year. In *ephemeral* watercourses, the water flows only for hours or days following a storm (Wohl, 2017).

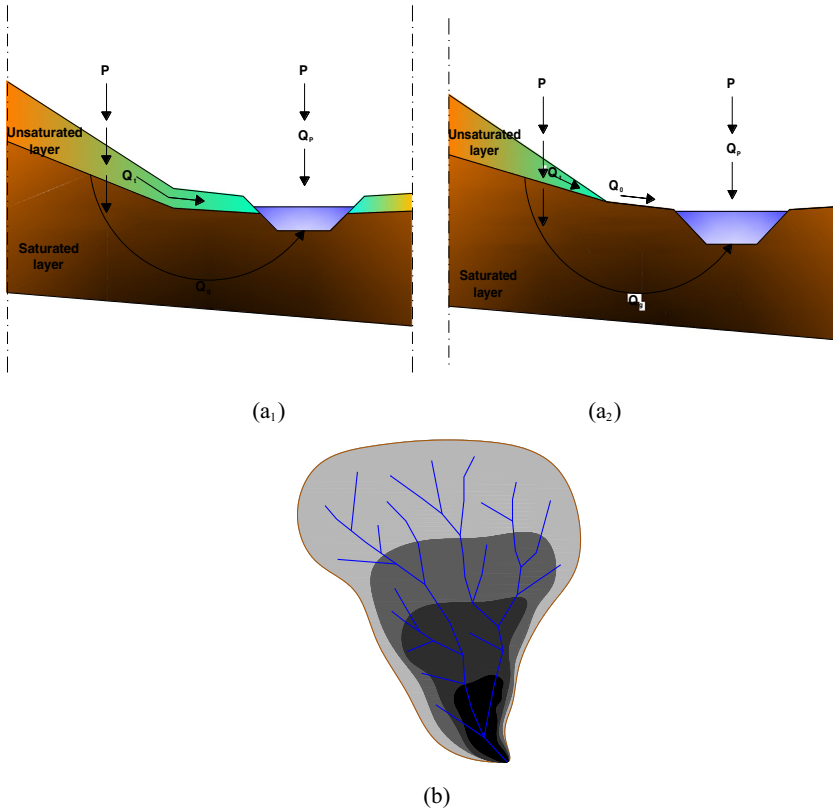


**FIGURE 9.7** The runoff generation mechanism by saturation-excess. (A) Flow paths in the hillslope profile at the start ( $a_1$ ) and during ( $a_2$ ) precipitation ( $P$  = precipitation;  $Q_p$  = direct precipitation over water surfaces;  $Q_o$  = overland flow;  $Q_t$  = interflow;  $Q_g$  = groundwater flow); (B) the progressive saturation mechanisms of the contributing areas (saturation degree increases with the gray intensity).

Usually, a diagram (hydrograph) graphically represents the time evolution of runoff, from the precipitation start until the flood depletion. The hydrograph is commonly reported together with the hyetograph (that is, the time evolution of the rainfall intensity) of the generating precipitation event. Schematically, a hydrograph consists of three components:

- A rapidly increasing curve (*concentration or rising limb*), which starts from the time when the hydrological response of the stream channel to the precipitation begins by an increase in discharge (see point  $S$  of Fig. 9.8) until to the *flood peak* (the maximum value of the surface runoff, point  $P$  of Fig. 9.8)
- The peak discharge—that is the highest point on the hydrograph, —which occurs when different parts of the catchment simultaneously contribute to the runoff at the outlet

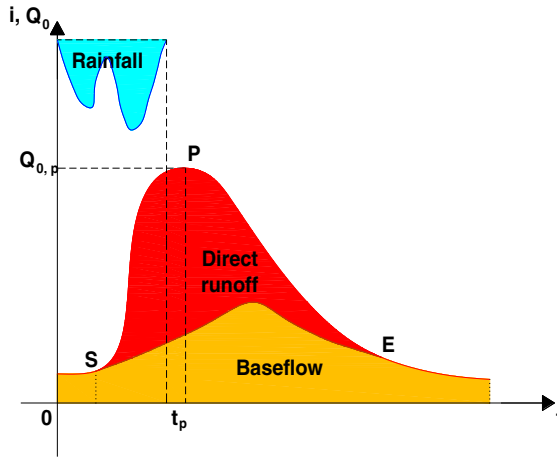


**FIGURE 9.8** Schematic flood hydrograph with a possible separation method ( $t_p$  = rainfall duration;  $Q_{0,p}$  = peak runoff;  $i$  = rainfall;  $Q_0$  = runoff;  $S$  = flood start;  $P$  = hydrograph peak;  $E$  = flood end).

- A slowly decreasing curve (*recession or falling limb*), which represents the runoff depletion after the storm until the time when the stream flow regime returns to the regular value of the dry period (baseflow).

The duration of the concentration limb is much lower compared to the recession limb. The time between the precipitation start and the flood peak is called *concentration time* (Fig. 9.8), while the time between the flood start and end is called *flood duration*.

The hydrograph shape is influenced by the amount and velocity of each runoff component. It is practically impossible to individually identify these components (except for very small catchments with a simple hydrographic network, such as the headwaters). Conversely, the separation of the *quick flow* and *delayed flow* components is generally feasible, using a set of arbitrary graphical techniques, which allows the identification of the direct runoff and the base flow hydrographs. Each separation technique requires the detection of the start and end of the flood. While the flood start is easily recognizable (it is simply the time when the hydrograph suddenly increases after the precipitation start), the identification of the flood end is much more difficult. The literature proposes hydrograph separation techniques of different complexity. The most common techniques are based on drawing a line passing across the hydrograph from the point of flood start:

- (i) A horizontal separation line
- (ii) A line of constant slope ( $0.000546 \text{ m}^3/\text{s}/\text{km}^2$ )
- (iii) A straight line to a selected point on the recession limb (point  $E$  of Fig. 9.8), which can alternatively be: (a) the point of greatest curvature close to the lower end of the recession limb; (b) the point when the



- recession limb starts to decrease according to an exponential law:
- (c) the point corresponding to a given time interval from peak flow
- (iv) the broken line consisting of (1) the line prolonged from the pre-storm hydrograph below the concentration limb until the vertical under the peak flow, and (2) the line whose extremes are the intersection of the previous line with the vertical under the peak flow and the point over the recession limb selected as above at the point (iii).

The technique (i) is simple but can lead to unrealistic results (that is, a constant hydrograph of sub-surface water, which thus does not reflect the effects of the precipitation). By contrast, the techniques (ii) to (iv), although being complex, seem to be more realistic and appropriate to reproduce the actual hydrological effects of floods.

## **Methods for components/fluxes estimation in the water balance**

### **Field measurements**

#### *Atmospheric water*

##### **Precipitation**

The amount of precipitation falling on the ground and retained over the soil without any water losses (evaporation, infiltration, depression storage) or runoff is measured (in  $\text{m}^3$  or mm) at regular time intervals (e.g., daily; hourly; every 15 min etc.) using rain gauges. These devices must be installed in the open air on a horizontal surface close to the ground (to reduce wind effects), but avoiding rain splash or submersion by floods, and far from obstacles (to prevent rainfall interception).

Rain gauges generally consist of open cylindrical vessels collecting rainfall with or without recording equipment. Some rain gauges (pluviometers) do not record the precipitation depth. A pluviometer is simply a small metal tank (diameter of about 0.10 m) placed on a horizontal plane at a height of about 0.30 m above the ground level. The tank contains an upper funnel receiving precipitation, which is collected into a lower bottle or the tank bottom; the upper net protects the pluviometer from dirt (Fig. 9.9A). Once a day, the collected rainwater is manually measured, and this record is the total rainfall of that day.

Other rain gauges (pluviographs) continuously and automatically record the precipitation depth. A writing pen activated by the surveying equipment traces the record on a graduated paper mounted on clockwork driven drum or mass memory. These records, which also report the duration of the precipitation event, allow the rainfall intensity calculation. The types of pluviographs are:

- Tipping bucket pluviograph (Fig. 9.9B), based on a pair of small buckets under the funnel, which alternatively tip, when a given rain volume falls into the buckets and actuates the writing pen

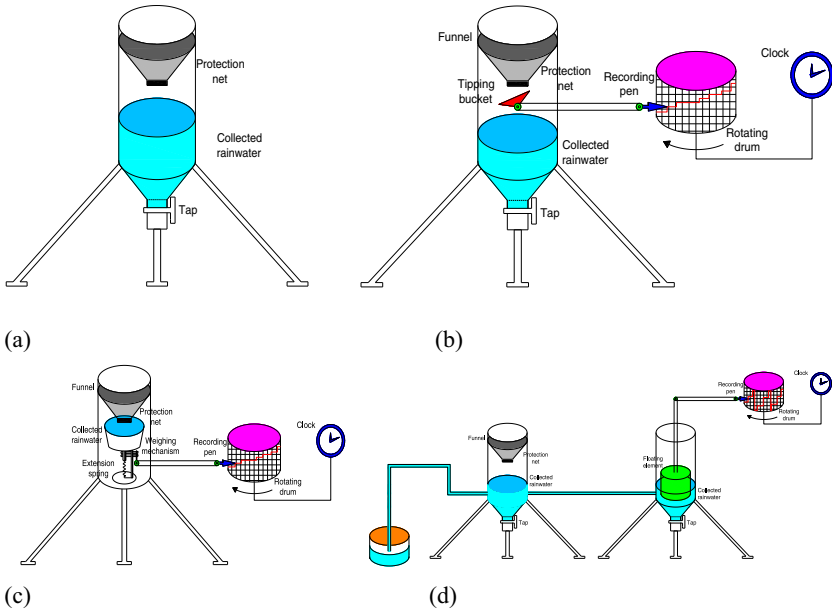


**FIGURE 9.9** Sketches of some rain gauge types (A, pluviometer; B, tipping bucket pluviograph; C, weighing pluviograph; D, natural syphon pluviograph).

- Weighing pluviograph (Fig. 9.9C), where a weighing mechanism under the tank receiving the rainwater is connected to the writing pen
- Natural syphon pluviograph (Fig. 9.9D), where the collected rainwater is poured into a float chamber, causing the float to rise and actuate the writing pen. When full, a syphon pipe automatically empties the float chamber and the writing pen is reset to zero for the next record
- Recently, the rainfall measurements of rain gauges are progressively replaced by estimations by radar. The latter devices use microwaves with a wavelength from 0.03 to 0.10 cm and operate at several hundreds of kilometers from rainstorms. Beside rainfall amounts and intensity, radar allows the simultaneous measurement of areal extent, location, and movement of the storm and even the velocity and distribution of raindrops.

**Evaporation and evapotranspiration**

Evaporation from water bodies (e.g., lakes, reservoirs, river channels) and evapotranspiration from vegetated surfaces can be directly measured or estimated using indirect methods.

Evaporation from water bodies is directly measured by evaluating the reduction of level for a sample of open water in an *evaporation pan* (with standardized size) over time; generally, the related atmospheric variables, such as the precipitation, temperature, wind speed and humidity of air are

simultaneously measured using a weather station. Daily, water evaporation from the pan (expressed in mm/day) is the difference of the water levels in two consecutive days, depurated from rainfall over the pan and other water losses, such as bird or animal consumption. The water evaporation of the specific pan must be corrected through a coefficient ( $K_p$ ), which depends on the type of pan, environment and operations.

Evapotranspiration from vegetated surfaces is directly measured using *lysimeters*. A lysimeter is a hydraulically isolated tank filled with soil cores (with or without vegetation). In this tank, evapotranspiration is evaluated weighing the lysimeter over time and simultaneously measuring the precipitation over the tank and the drainage from the sample as components of the water balance equation.

The indirect methods for estimating evaporation and evapotranspiration are:

- *Bowen ratio method*, which estimates evapotranspiration as a function of the Bowen ratio (sensible to latent heat), on its turn calculated from measures of the atmospheric temperature and humidity gradients close to vegetation
- *Eddy correlation (or covariance) method*, which estimates evapotranspiration as the temporal average from the correlation coefficient between variations in vertical wind speed and atmospheric humidity measured above the vegetation.

Recently, other methods based on remote sensing systems (such as drones and satellites) have been proposed. These systems measure atmospheric variables (such as the water vapor concentration, temperature, sensible heat, aerodynamic exchange resistance) surrounding the measurement area, and calculate the evapotranspiration fluxes from these derived measurements using mathematical algorithms and/or energy balance equations.

### Surface water

Surface runoff can be measured using methods that can be classified as follows (Dobriyal, Badola, Tuboi, & Hussain, 2017; Fig. 9.10):

- *Direct method* (it is a *volumetric method*, based on filling a tank of known volume during a given time)
- *Velocity-area methods*, based on the integration of simultaneous measures of local low velocities by cell areas of a channel cross-section, including:
  - The *float method*, where the flow velocity is the ratio between the floating distance of an object of low density and the related travel time
  - The *dilution gauging method*, which measures flow velocity as a function of the diffusion rate of a tracer, e.g., chemical or radioisotopes

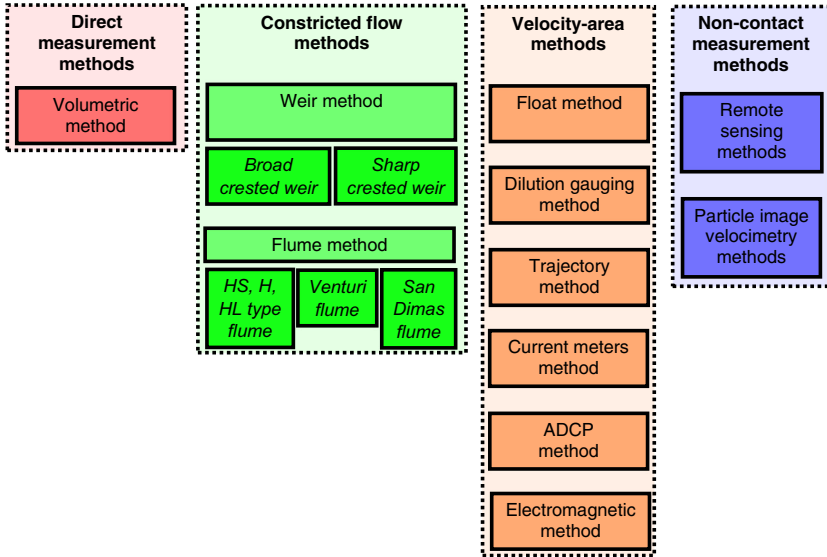


**FIGURE 9.10** Classification of methods for surface runoff measurement (Source: P. Dobriyal, R. Badola, C. Tuboi, and S.A. Hussain (2017). A review of methods for monitoring streamflow for sustainable water resource management. *Applied Water Science*, 7, 2617–2628, modified).



**FIGURE 9.11** A current meter (Valeport Inc., UK, A) and an acoustic Doppler profiler (SonTek Inc., USA, B).

- o The *trajectory method*, where the flow velocity is measured using the hydraulic equations at the outlet jet of pipeline in which all the streamflow is diverted
- o The *current meter method*, assuming that the flow velocity is proportional to the rotation speed of a mechanical rotor (Fig. 9.11A)
- o The *acoustic Doppler current profiler method*, where the flow velocity is estimated by the difference in the frequency of the sound transmitted by the device into the water and echoes received from suspended particles (Fig. 9.11B)

- The *electromagnetic method*, measuring by electromagnetic probes placed on each side of the stream the electromotive force induced in the water by a generated earth's magnetic field, which is directly proportional to the flow velocity.
- *Constricted flow methods*, based on forcing the water stream passing over a broad crested or sharp-crested weir (*weir method*, Fig. 9.12A) or an HS, H and HL type, Venturi, Parshall and San Dimas flumes (*flume method*, Fig. 9.12B) of known geometry, for which the application of the hydraulic equations to the measured water depth gives the surface runoff
- *Non-contact methods*, consisting of the *remote sensing methods* (using passive or active sensors), which provide:
  - Direct measures of water surface levels from radar altimeters/ high-resolution satellite imagery
  - Correlations of remotely-sensed water surface areas with ground measurements (water depths or discharges), and the *particle image velocimetry method* (i.e., determining the water velocity recording the laser light scattered by liquid or solid particles on a photo-camera).

Overall, the direct and constricted flow methods are quite accurate but are advised for surface runoff measures in very small channels. The other methods are more suitable for streamflow measurements in medium to large rivers. In particular, the *velocity-area methods* can be used in easily accessible watercourses for instantaneous measurements and construction of water depth-discharge equations. The non-contact methods, although being quite expensive, do not require the presence of surveyors close to the channel and are better suitable for continuous and real-time flow measurements also in the case of floods.

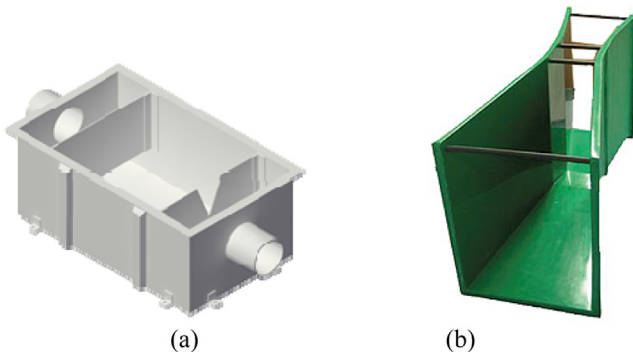


**FIGURE 9.12** A Parshall flume (Badger Meter GMBH, Germany, A) and a triangular weir (IEI Inc., USA, B).

### Sub-surface water

Measuring infiltration is of fundamental importance since the related process governs both the surface and sub-surface water. The infiltration measurements are based on field evaluation of the hydraulic conductivity, which is not constant, but varies in time (with soil saturation during a storm) and space (from point to point, depending on several soil properties, such as texture and aggregate stability). The methods for soil hydraulic conductivity measurement use *infiltrometers* or *permeameters* that can be classified as follows (Angulo-Jaramillo et al., 2000):

- *One-dimensional pressure ring-infiltrometers* (e.g., *one-ring and double-ring infiltrometers*, *mini-disk infiltrometers*, Fig. 9.13A), in which the water, supplied to the soil surface at a positive pressure head, infiltrates vertically in a ring (or two coaxial rings) pressed into the soil. This process carries on until a constant infiltration rate is observed, which is assumed to be the soil infiltration capacity;
- *Unconfined three-dimensional tension disk infiltrometers* (Fig. 9.13B), which supply the soil with water at negative pressure at its surface (to prevent wetting up of soil larger pores with possible short circuits for flow), thus allowing the evaluation of soil-water properties of the soil matrix without being dominated by flows in the larger pores (Youngs, 1991).

Infiltration can be also indirectly measured using *rainfall simulators* (Fig. 9.14). These devices generate an artificial rainfall with controlled depth, intensity and drop size; the infiltrated flow is the difference between precipitation and surface runoff, and the ratio to the infiltration time gives the hydraulic conductivity.

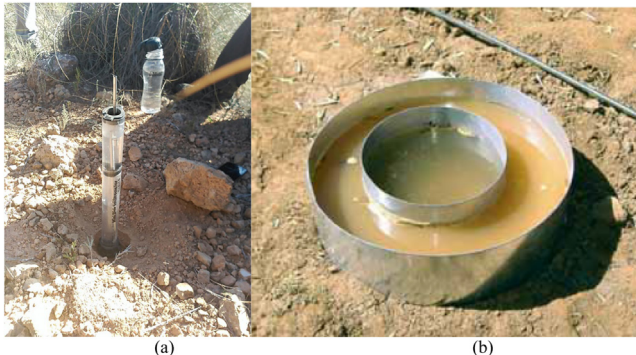


FIGURE 9.13 Minidisk infiltrometer (Decagon Inc., USA, A) and double-ring infiltrometer (B).



**FIGURE 9.14** A rainfall simulator (Eijkelkamp, Nederland).

## Modeling

Experiments about hydrology and specifically the estimation of the water balance components are usually costly and time-consuming, and sometimes not even applicable on large spatial scales and long-term periods. A possible alternative solution is the use of models in replacement of hydrological experiments and to the calculation of the water balance. In order to develop appropriate and sustainable strategies for management of water resources, the modeling approach, combined with field observations and laboratory experiments, allows a better understanding of the hydrological cycle and provides scientifically sound information about the hydrological processes and fluxes. According to the description of hydrological models provided by [Kirkby \(1996\)](#), “Models are thought experiments which help refine our understanding of the dominant processes, testing whether we have a sufficient and consistent theoretical explanation of physical processes.” Water balance models generally simulate all components of the terrestrial hydrological cycle and the interaction of surface and sub-surface processes holistically, maintaining a continuous water balance for the area of interest ([Beven, 2011](#); [Wagener, Wheater, & Gupta, 2004](#)). Some of these components are interrelated, and therefore require iterative calculations; to model some hydrological processes, the estimation of a certain number of input parameters is required. Water balance modeling is based on [Eqs. \(9.1\) to \(9.3\)](#),



depending on the control volume. In principle, modeling the water balance sounds simple; however, in practice, it is difficult to measure or estimate every single component of the hydrological cycle, particularly at larger spatial scales (i.e., from hillslope to continental scales). Such models can incorporate the spatial and temporal variability of the primary driving forces, such as precipitation and solar radiation, and land-surface heterogeneity (e.g., soil, vegetation). A mathematical description based on laws of physics (e.g., mass and momentum conservation applied to soil and water) is the first step in the formulation of a model that will produce quantitative predictions of the hydrological processes and fluxes. The general structure of all water balance models is similar. To set up a model, it is necessary to write equations that relate the rates of change in water storage in the control volume to the hydrological fluxes across its external surface throughout the reference period. To summarize, although many equations differ in their structure, complexity and input parameters, the most common equations related to the estimation of hydrological processes and/or fluxes in water balance models are the following:

- For sub-surface flow in:
  - Saturated zone: Darcy's law (1856), which assumes a linear relationship between the flow velocity and hydraulic gradient through a coefficient of proportionality (*hydraulic conductivity*)
  - Unsaturated zone: Richards' equation (1931), which is the combination of Darcy's law with the continuity or mass balance equation in a non-linear partial differential equation
- For surface flow: (1) Saint-Venant equations (1797–1886), which assume that the flow can be expressed in terms of average cross-sectional velocities and depths, and are based on the balances of both flow mass and momentum; (2) Diffusion wave and Kinematic wave equations, which are simplifications of Saint-Venant equations, where some terms are neglected (Lighthill & Whitham, 1955)
- For atmospheric water flow (evapotranspiration): (1) Penman-Monteith's equation, which is the most widely used and recommended method to directly estimate the potential ET, and indirectly actual ET by reducing the potential ET according to the actual soil water content (Monteith, Szeicz, & Waggoner, 1965); (2) Haude (1955); (3) Hamon (Federer & Lash, 1978); (iv) Hargreaves-Samani (1982); (v) Thornthwaite (1948), and other models; however, the low availability of meteorological data and field measurements may be a limiting factor in applying some of the more demanding methods/equations and particularly Penman-Monteith equation.

When it is necessary to calculate the infiltration rate at the soil surface, Horton (1933, 1940) and Green–Ampt (Green & Ampt, 1911) models can be used.



In general, the water balance models allow the estimation or prediction of surface and sub-surface flows and are commonly known as *hydrological models*. The models mostly differ in how ET and soil water content are conceptually considered and mathematically simulated. There are several classifications of hydrological models, based on structure, spatial scale, time scale, a time step of computation, interpretation of the catchment processes, etc. [Tables 9.1 and 9.2](#) illustrate two possible classifications of hydrological models. These classifications are based on *model structure* and *spatial processes*, respectively. The model structure, roughly varying from *simple model* to *complex model* based on the governing equations and number of modeled variables/input parameters, identifies how water balance components are calculated. Simple models need relatively few variables, while the most complex models (such as the physical-based models, [Fig. 9.15](#)) require a large number of interconnected variables to simulate the hydrological processes and fluxes in the water balance of the hydro-system ([Sitterson, et al., 2017](#)).

Spatial variability in geology, topography, vegetation, and soil influence the hydrological processes (and in particular the rainfall-runoff transformation) within a catchment, and, thus, should be carefully considered in modeling ([Beven, 2011](#)). According to the spatial structure classification, the hydrological models can be classified as *lumped* (average weather and geomorphological conditions are assumed for the modeled catchment), *semi-distributed* (the catchment is discretized in sub-catchments or hydrologically homogenous response units), and *fully-distributed* (a catchment is discretized in grid cells) ([Fig. 9.16 and Table 9.2](#)).

With regard to the model time scale, the water balance is generally set up for an adequately long period, such as wet/dry season, calendar or hydrological year, decade, etc. Depending on the variability of the captured hydrological flux or process of the water balance (e.g., surface water, rainfall, groundwater, or overall water availability), different temporal output data are provided, such as daily, monthly, seasonal, annual, or multi-year runoff volumes or sediment flows (averages or totals). Some hydrological models work at the event scale, that is, they estimate or predict the simulated hydrological variable as the product of a storm or a precipitation event. In addition to the time scale of models, the time step of computation (e.g., monthly, daily, hourly, etc.) is another important characteristic of the water balance models, since it influences the accuracy of the output variable and the computational time of the simulation procedure (i.e., the finer the time step, the longer the model computation).

A key issue for the practical use of the hydrological models is the reliability of their outputs for the modeler's purpose. The reliability of a model prediction or estimation is evaluated through a comparison of the modeled hydrological variable with a field measurement corresponding

**TABLE 9.1** Classification of hydrological models according to the structure (Pechlivanidis, Jackson, McIntyre, & Wheeler, 2011; Sitterson, et al., 2017).

Characteristics	Hydrological model		
	Empirical	Conceptual	Physical-based (process-based or mechanistic)
Methodological approach	Non-linear statistical relationship between inputs and outputs; observation-oriented; black-box concept	Simplified water balance equations representing hydrological components in the catchment	Physical laws formulated as partial differential hydrodynamic and porous media flow equations and resolved by numerical techniques
Advantages	Small number of input parameters; fast computational time	Simple model structure; easy to calibrate	Very accurate; the connection between model parameters and physical catchment characteristics
Limitations	Lack of physical significance between model parameters and catchment properties; input data falsification	Spatial variability within catchment not entirely addressed; lack of physical meaning in governing equations and parameters	A large number of data and parameters needed for running and calibration; catchment-specific
Most suitable applications	Ungauged catchments; runoff only desired output; rough estimation of output	Limited computational time; low detail of catchment characteristics	Availability of large and accurate input data; fine spatial and temporal scales
Examples	SCS-Curve Number; Artificial Neural Networks	TOPMODEL; HSPF; HBV; Stanford	MIKE-SHE; KINEROS; VIC; WaSiM-ETH

I. G. Pechlivanidis, B. M. Jackson, N. R. McIntyre, and H. S. Wheeler (2011). Catchment scale hydrological modelling: a review of model types, calibration approaches and uncertainty analysis methods in the context of recent developments in technology and applications. *Global NEST Journal*, 13(3), 193–214; J. Sitterson, C. Knightes, R. Parmar, K. Wolfe, M. Muehe, and B. Avant (2017). An overview of rainfall-runoff model types. United States Environmental Protection Agency, Washington, DC. EPA/600/R-17/482.

**TABLE 9.2** Classification of hydrological models according to the spatial structure (Sitterson, et al., 2017; Beven, 2011).

Characteristics	Hydrological model		
	Lumped	Semi-distributed	Distributed
Methodological approach	Spatial variability is not considered; entire catchment is modeled as one unit; calculation of one runoff value for the entire catchment at the outlet; all data are constant over space and time	Reflect some spatial variability; dividing the catchment into smaller sub-catchments (Hydrological Response Units), with different parameters for each; calculate runoff at the pour point for each sub-catchment, but do not calculate runoff at every grid cell	Accounts for detailed spatial heterogeneity in inputs and parameters by grid cells (small elements); calculates distinct hydrological response for each cell separately
Input data	All data averaged for the entire catchment	Separated within the catchment but homogenous within the sub-catchments	All specific data at grid cell: DEM; land use; precipitation; soil properties; topography; and catchment characteristics
Advantages	Fast computational time; ideal for simulating average conditions	Represents important features in the catchment; fast computational time; fewer data and parameters needed than a distributed model	Physically related to hydrological processes
Limitations	Loss of spatial variability; not representative for large areas; over- or under-parameterization	Data into sub-catchments are averaged, and manipulation of input data is possible; loss of spatial resolution	Data intense; long computational time

(Continued)

**TABLE 9.2 (Continued)**

Characteristics	Hydrological model		
	Lumped	Semi-distributed	Distributed
Most suitable applications	Regulatory purposes that look at long-term conditions	-	For management practices by providing detailed data for small elements
Examples	Empirical and conceptual models; machine learning	Conceptual and some physical models; TOPMODEL; SWAT	Physically distributed models, MIKE SHE; VELMA; WASiM-ETH

Sitterson, C. Knights, R. Parmar, K. Wolfe, M. Mucbe, and B. Avant (2017). *An overview of rainfall-runoff model types*. United States Environmental Protection Agency, Washington, DC. EPA/600/R-17/482; Beven, K.J. (2011). *Rainfall-runoff modelling: The primer*. John Wiley & Sons.

to the same meteorological input in an instrumented catchment. For example, the accuracy of a modeled peak flow for a flood after a storm is checked by its comparison with the maximum flow observed for the same storm and measured at the outlet of a catchment equipped by a flume (see sub-chapter 4.2). *Sensitivity analysis* and *calibration/validation* are useful procedures to facilitate model evaluation and application. Sensitivity analysis allows the identification of the model parameter(s) to which a model is most sensitive. Calibration adjusts one parameter or a set of parameters to make the simulated variable as close as possible to the corresponding observation. Model validation is the process to run a model by using model parameters determined during the calibration process (Moriassi, et al., 2007).

From the notion of the *global water system* and the interdependency of earth components, which needs the integration of those systems in integrated models, *Global Hydrological Models* have been developed, in which the global water flow is connected to other hydrological systems through physical relationships (Alcamo et al., 2003). They are similar to catchment models but differ in processes description, parameter estimation approaches, and the temporal and spatial resolution of input data and outputs. Global models provide useful spatial and temporal estimates of global water resources and, hence, the analysis of possible changes is attainable, particularly, under the explosion of global data availability from satellites in the last two decades (Sood & Smakhtin, 2015).

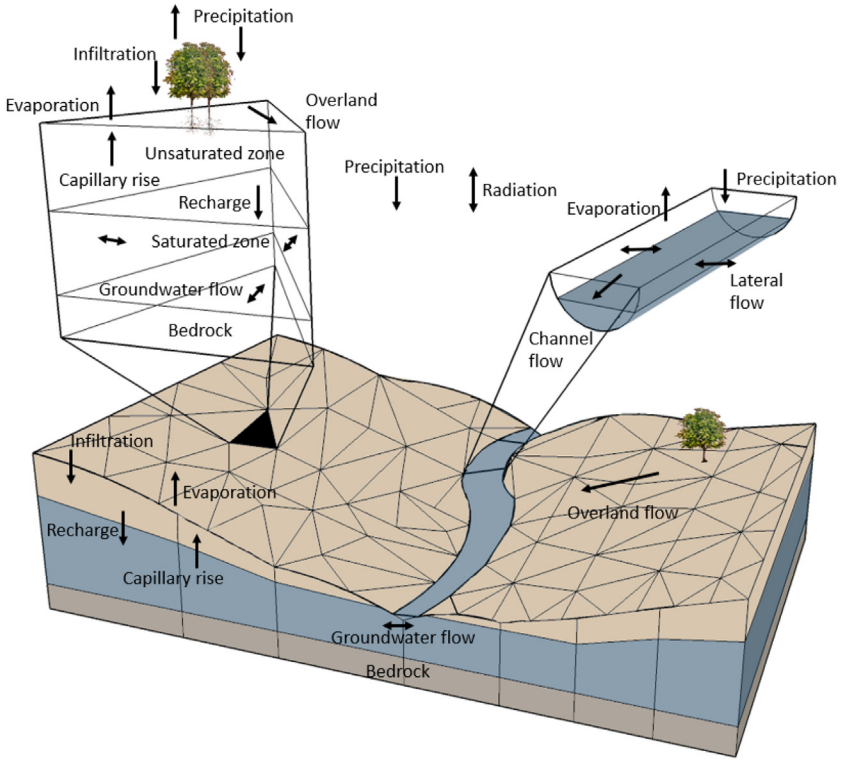


**FIGURE 9.15** Schematization of the hydrological processes and control volume (in soil layers and Triangular Irregular Network) of a physical-based model.

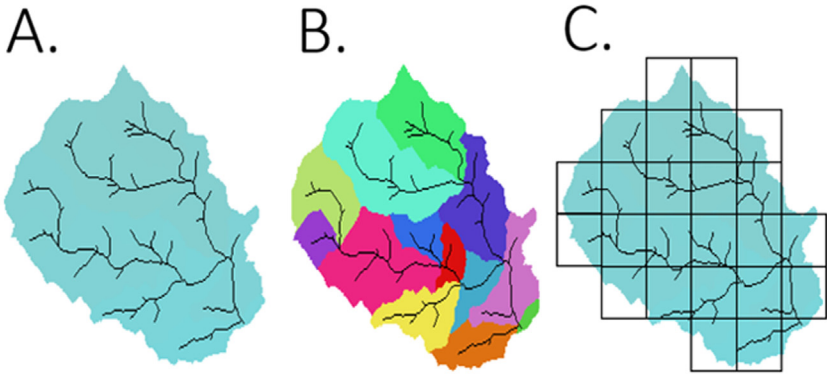


**FIGURE 9.16** Spatial structure classification of hydrological models. A: Lumped model, B: Semi-distributed model, C: Distributed model.

## References

- Alcamo, J., Döll, P., Henrichs, T., Kaspar, F., Lehner, B., Rösch, T., & Siebert, S. (2003). Development and testing of the WaterGAP 2 global model of water use and availability. *Hydrological Sciences Journal*, 48(3), 317–337.
- Allen, R. G. (1998). Crop Evapotranspiration-Guideline for computing crop water requirements. *Irrigation and Drain*, 56, 300.
- Angulo-Jaramillo, R., Vandervaere, J. P., Roulier, S., Thony, J. L., Gaudet, J. P., & Vauclin, M. (2000). Field measurement of soil surface hydraulic properties by disc and ring infiltrometers: A review and recent developments. *Soil and Tillage Research*, 55(1–2), 1–29.
- Beven, K. J. (2011). *Rainfall-runoff modelling: the primer*. John Wiley & Sons.
- Byeon, S. J. (2014). Water balance assessment for stable water management in island region. Doctoral dissertation, Université Nice Sophia Antipolis.
- Chow, V. T. (1964). *Handbook of applied hydrology*. NY, USA: McGraw-Hill.
- Darcy, H. P. G. (1856). Les Fontaines publiques de la ville de Dijon. Exposition et application des principes à suivre et des formules à employer dans les questions de distribution d'eau, etc. V. Dalamont.
- Dobriyal, P., Badola, R., Tuboi, C., & Hussain, S. A. (2017). A review of methods for monitoring streamflow for sustainable water resource management. *Applied Water Science*, 7, 2617–2628.
- Dooge, J. C. (1968). The hydrologic cycle as a closed system. *Hydrological Sciences Journal*, 13(1), 58–68.
- Federer, C. A., & Lash, D. (1978). Simulated streamflow response to possible differences in transpiration among species of hardwood trees. *Water Resources Research*, 14, 1089–1097.
- Green, W. H., & Ampt, G. A. (1911). Studies on Soil Physics. *The Journal of Agricultural Science*, 4(1), 1–24.
- Haan, C. T., Barfield, B. J., & Hayes, J. C. (1994). *Design hydrology and sedimentology for small catchments*. Elsevier.
- Hargreaves, G. H., & Samani, Z. A. (1982). Estimating potential evapotranspiration. *Journal of the Irrigation and Drainage Division*, 108(3), 225–230.
- Haude, W., 1955. *Zur Bestimmung der Verdunstung auf möglichst einfache Weise*. Dt. Wetterdienst, Bad Kissingen.
- Hewlett, J. D. (1961). Soil moisture as a source of base flow from steep mountain watersheds (p. 11). Asheville, NC, USA: Southeastern Forest Experiment Station, United States Department of Agriculture, Forest Service.
- Hillel, D. (1998). *Environmental soil physics: Fundamentals, applications, and environmental considerations*. Elsevier.
- Horton, R. E. (1933). The role of infiltration in the hydrologic cycle. *Eos, Transactions American Geophysical Union*, 14(1), 446–460.
- Horton, R. E. (1940). An approach towards the physical interpretation of infiltration-capacity (Vol. 5). Soil Science Society of America Proceedings.
- Kirchner, J. W. (2009). Catchments as simple dynamical systems: Catchment characterization, rainfall-runoff modeling, and doing hydrology backward. *Water Resources Research*, 45(2).
- Kirkby, M.J. (1996). The Scientific Nature of Geomorphology: Proceedings of the 27th Binghamton Symposium in Geomorphology. held 27-29 September. New York: Wiley.
- Koppen, W. D. (1936). Das geographische system der klimat. *Handbuch der klimatologie*, 46.
- Labeledzki, L. (Ed.). (2011). *Evapotranspiration*. BoD—Books on Demand.

- Lighthill, M. J., & Whitham, G. B. (1955). On kinematic waves I. Flood movement in long rivers. *Proceedings of the Royal Society of London. Series A. Mathematical and Physical Sciences*, 229(1178), 281–316.
- Marcinek, J. (2007). Hydrological cycle and water balance. In J. L. Lozán, et al. (Eds.), *Global change: Enough water for all* (pp. 33–37). Hamburg: Wiss. Ausw./Geo.
- McCuen, R. H. (1982). *A guide to hydrologic analysis using SCS methods*. Prentice-Hall, Inc.
- Monteith, J., Szeicz, G., & Waggoner, P. (1965). The measurement and control of stomatal resistance in the field. *Journal of Applied Ecology*, 345–355.
- Moriasi, D. N., Arnold, J. G., Van Liew, M. W., Bingner, R. L., Harmel, R. D., & Veith, T. L. (2007). Model evaluation guidelines for systematic quantification of accuracy in watershed simulations. *Transactions of the ASABE*, 50(3), 885–900.
- Pechlivanidis, I. G., Jackson, B. M., Mcintyre, N. R., & Wheatler, H. S. (2011). Catchment scale hydrological modelling: a review of model types, calibration approaches and uncertainty analysis methods in the context of recent developments in technology and applications. *Global NEST Journal*, 13(3), 193–214.
- Richards, L. A. (1931). Capillary conduction of liquids through porous mediums. *Physics*, 1(5), 318–333.
- Sitterson, J., Knightes, C., Parmar, R., Wolfe, K., Mucche, M., & Avant, B. (2017). An overview of rainfall-runoff model types. United States Environmental Protection Agency, Washington, DC. EPA/600/R-17/482.
- Singh, V. P., & Woolhiser, D. A. (2002). Mathematical modeling of watershed hydrology. *Journal of Hydrologic Engineering*, 7(4), 270–292.
- Sood, A., & Smakhtin, V. (2015). Global hydrological models: a review. *Hydrological Sciences Journal*, 60(4), 549–565.
- Sutcliffe, J. V. (2004). *Hydrology: A question of balance*. IAHS Press.
- Thornthwaite, C. W. (1948). An approach toward a rational classification of climate. *Geographical Review*, 38(1), 55–94.
- Wagener, T., Wheatler, H., & Gupta, H. V. (2004). *Rainfall-runoff modelling in gauged and ungauged catchments*. World Scientific.
- Ward, R. C., & Robinson, M. (1967). *Principles of hydrology* (No. 551.49/W262). New York: McGraw-Hill.
- Wohl, E. (2017). The significance of small streams. *Frontiers of Earth Science*, 11(3), 447–456.
- Youngs, E. G. (1991). Infiltration measurements – A review. *Hydrological Processes*, 5(3), 309–319.
- Zhang, L., Dawes, W. R., & Walker, G. R. (2001). Response of mean annual evapotranspiration to vegetation changes at catchment scale. *Water Resources Research*, 37(3), 701–708.
- Zhang, L., Walker, G. R., & Dawes, W. R. (2002). Water balance modelling: Concepts and applications. *ACIAR Monograph Series*, 84, 31–47.

## 2.2 Modeling water fluxes in the unsaturated zone

The river basin or catchment is a typical geographical scale employed in the management of water resources. Within a catchment, all precipitation within the watershed merges at a singular discharge point. At this point, water can be perceived either as a potential threat or harm in relation to flooding, or as a means to fulfill human requirements such as irrigation or potable water.

During the first century of hydrological modeling, models relied on manual calculations (such as Sherman, 1932; Mulvany, 1850, and Nash, 1959). These models were empirical and were developed through analyzing input and output data without considering hydrological processes. With the advent of computer technology, many conceptual model codes were introduced, beginning with the Stanford Watershed IV in 1966, followed by various model codes still in use today, such as NAM (Nielsen & Hansen, 1973); Sacramento (Burnash & Ferral, 1973), and HBV (Bergström & Forsman, 1973). Although these conceptual models were based on sound hydrological process knowledge, they couldn't directly exploit point-scale process equations and data, as the entire catchment served as the computational unit. The next phase towards developing model types that could encompass more hydrological field data and process knowledge was spurred by a blueprint by Freeze and Harlan (1969) and the development of the first spatially distributed process-based (physics-based) model codes such as SHE (Abbott et al., 1986a, 1986b), IHDM (Beven et al., 1987), and THALES (Grayson et al., 1992).

Computing power has undergone an exponential increase over the past 40 years, resulting in the ability to provide numerical solutions to highly non-linear equations for a wide range of initial and boundary conditions. Prior to this advancement, hydrologists were limited to analytical solutions for specific cases, such as the Burgers solution and Dirac delta solution for linearizing soil hydraulic properties to provide analytic solutions to Richards' equation (Smith et al., 2002). While these solutions continue to provide insights for verifying numerical models, numerical modeling has emerged as the preferred approach in hydrological studies. Another crucial development that has shaped the direction of hydrological modeling is the increasing



availability and resolution of digital elevation models, coinciding with the emergence of variable source area hydrology that departs from earlier Hortonian concepts of runoff dominated solely by the infiltration-excess process. The advent of geographical information systems has further accelerated the development and application of spatially distributed deterministic hydrologic models by enabling the storage, retrieval, and rapid manipulation of spatial data. Variable source area hydrology is a concept that describes how the spatial patterns of water movement and storage in a watershed can vary significantly depending on the properties of the soil, vegetation, and topography. It recognizes that in some areas, surface runoff and subsurface flow may be limited to specific locations, while in other areas, water movement may be more diffuse and widespread. In other words, variable source area hydrology emerged as an alternative to earlier concepts, such as the Hortonian overland flow model, which assumed that runoff was primarily generated by a uniform infiltration-excess mechanism over the entire watershed. This emphasizes the role of topography, soil properties, and vegetation cover in generating and storing water, and it has been widely applied in hydrological modeling studies to simulate the dynamics of water movement and storage in different types of landscapes (Litwin et al., 2023; Su et al., 2023; Guo et al., 2022; Collick et al., 2015; Pachepsky et al., 2004, and Troch et al., 2003).

Richards equation (Richards, 1931) is a mathematical model which describes the movement of water in unsaturated soils by combining the Darcy–Buckingham law with the continuity equation. This equation is widely recognized as the primary concept in soil physics and is discussed in hydrological textbooks (Ebel & Loague, 2006; Qu & Duffy, 2007; Ivanov et al., 2008). It is regarded as the fundamental principle underlying physically-based hydrological models (Mohajerani et al., 2021; Yi et al., 2023; Ebel et al., 2023). It describes how water moves through the soil matrix under the influence of gravity, capillary forces, and pressure gradients. This equation can be used to simulate soil water movement and the effects of plant and atmospheric interactions in hydrological modeling. In order to solve Richards equation, knowledge of the soil hydraulic properties is necessary. The hydraulic properties of the soil play a significant role in the primary hydrological processes that occur in catchment areas (Wösten et al., 2001; Elsenbeer, 2001; Porporato et al., 2004; Montzka et al., 2017; Vereecken et al., 2022). Hence, having information about these soil properties is essential for modeling water balance, and appropriately parameterizing soils is among the top-priority tasks in physically based catchment modeling (Arnold et al., 2000; Rieger & Disse, 2013; Novick et al., 2022). Typically, soil property parameters are assessed through point observations at a small scale. Nonetheless, when it

comes to water balance modeling in catchments, parameter values need to be determined for larger spatial scales, like grid cells or the entire catchment (Bogena et al., 2010). One can parameterize the Richards equation by utilizing either observed soil properties, which involves measured relationships between soil water content and matric potential, or constitutive equations like the Gardner-Russo model, the Brooks-Corey model (Brooks & Corey, 1966), or the Mualem-van Genuchten model (Mualem, 1976; Van Genuchten, 1980). These empirical models capture a fundamental hydro-physical characteristic of the soil, namely the relationship between soil water content and matric potential (Aubertin & Patric, 1974).

Hence, the solution for Richards equation relies on two soil water constitutive relationships that are highly nonlinear and empirical in nature. These relationships are (1) the unsaturated hydraulic conductivity function, which can be either constant or close to zero for capillary heads that are non-positive, and (2) the capillary head function, which can take on extremely small values when relative saturations are near 100%, regardless of their actual value (Farthing & Ogden, 2017). Challenges arise when solving the equation due to the extremes in the behavior of soil water, as described by the unsaturated hydraulic conductivity and the pressure head, which can cause degeneracy in the solution of Richards equation. These functions may not have smooth differentiability at these extremes, and may exhibit high slopes, hysteresis, and even discontinuity at low relative saturations. Additionally, when dry soils are infiltrated, the resulting sharp wetting fronts can produce very large spatial gradients of soil hydraulic properties (Zha et al., 2017). The presence of nonlinearities poses several challenges. For instance, in the widely used van Genuchten and Mualem constitutive relations (Van Genuchten, 1980), the pressure head function (or the suction) and specific moisture capacity (i.e., change in water content with respect to change in pressure head in a porous medium) approach zero as the moisture content nears saturation, whereas the soil-water diffusivity can increase without bound. In general, this behavior can lead to degeneracy, a condition in which the coefficients in Richards equation approach values of zero or infinity, hindering the solution. Thus, the inherent nonlinearity and degeneracy present in the behavior of soil water make it very challenging to design and analyze numerical schemes for solving Richards equation (Miller et al., 2013; Zhou et al., 2022; Maranzoni & Tomirotti, 2023; Soomere, 2023). The numerical approach developed by Celia et al. (1990) for obtaining one-dimensional solutions of Richards equation, which employs modified Picard iterations to enhance mass conservation, has become the commonly used standard method. Therefore, the method remains the basis of many production codes, including the

USDA Hydrus-1D Richards equation solver (Simunek, 2005). Infiltration is commonly considered a one-dimensional process occurring in the vertical direction (Or et al., 2015). Because of the one-dimensional vertical assumption, it is then possible for large-scale models to use multiple, separate one-dimensional computations instead of a fully coupled three-dimensional solution.

The dynamics of soil water content, simulated by Richards equation, have an impact on the availability of water to plants in hydrological modeling. Therefore, incorporating the interactions between soil, water, plants, and the atmosphere into the equation through boundary conditions is crucial. Boundary conditions that can here be taken into account are, for example, the infiltration of water into the soil, evaporation from the soil surface, and water uptake by plant roots, followed by transpiration by the crop. To include root water uptake, a boundary condition can be specified at the root surface, modeled using a sink term in the equation that represents water extraction by the roots. Likewise, evapotranspiration can be incorporated by defining a boundary condition at the soil surface that accounts for evaporation and transpiration fluxes. The root water uptake term, which is a function of depth, is determined by the potential transpiration and the root density.

Under non-stress conditions, plants can achieve their maximum potential for root water uptake. However, if the soil is either too dry or too wet, plants become stressed and their roots are unable to take up water effectively, resulting in reduced transpiration. To model the decrease in root water uptake caused by stress, a stress factor is utilized, which is dependent on soil hydraulic properties and plant characteristics (Feddes et al., 1978, Kowalik and Zaradny 1978; Pachepsky et al., 2004). In other words, the transpiration rates are influenced by soil hydraulic properties through the stress factor, and stress factor is influenced by changes in the soil's ability to conduct water. This is because the hydraulic conductivity of the soil surface decreases as water evaporates from the upper layer, which in turn affects the matric potential at the soil surface. To ensure that water can still move upwards to the drying surface, the matric potential must decrease. However, it is important to note that there is a critical threshold value below which the potential cannot drop. Once this threshold is reached, the potential at the surface remains constant, resulting in a decrease in the rate of evaporation over time. Thus, the extent to which the soil's hydraulic properties impact the evaporation rate can be predicted by using Richards' equation.

The potential evapotranspiration ( $ET_p$ ) is dependent on several factors such as the type of plant, the stage of plant-cover development, and the climatic region. It is further divided into potential evaporation from the soil surface and transpiration from the crop. The potential transpiration can then be determined by subtracting the potential evaporation from the potential evapotranspiration. To calculate the potential evapotranspiration of a cropped or bare soil surface, the reference evapotranspiration ( $ET_0$ ) is used (Doorenbos & Pruitt, 1977).  $ET_0$  represents the amount of evapotranspiration that would occur from a well-watered grass surface.  $ET_0$  is usually estimated using empirical equations that incorporate meteorological variables such as temperature, humidity, solar radiation, and wind speed. The most widely used method for calculating  $ET_0$  is the Penman-Monteith equation (Monteith, 1975; Allen et al., 1998), which is recommended by the Food and Agriculture Organization (FAO). The Penman-Monteith equation is a complex and comprehensive method that takes into account the energy balance and aerodynamic resistance of the crop, as well as the evaporative demand of the atmosphere. It requires a variety of meteorological data, including air temperature, relative humidity, wind speed, solar radiation, and atmospheric pressure. Other empirical equations that are simpler to use but less accurate than the Penman-Monteith equation are the Hargreaves equation (Hargreaves & Samani, 1985), the Priestley-Taylor equation (Priestley & Taylor, 1972), and the Blaney-Criddle equation (Blaney, 1952). These equations are widely used in situations where meteorological data are limited or not available. It is important to note that the accuracy of  $ET_0$  estimation depends on the quality and availability of meteorological data, as well as the suitability of the selected method for the specific climatic and environmental conditions.

As soils dry, the matric potential  $\Psi$  becomes more negative, resulting in a reduction of the effective radius of water-filled pores in the soil. This process shapes the water-retention curve, which is also known as the "moisture characteristic" or "water release" curve, as it illustrates the relationship between matric potential and volumetric soil moisture content  $\theta$ . It is worth noting that differences in soil physical properties can cause  $\Psi$  to vary significantly across soil types, even if  $\theta$  remains constant (Campbell, 1974; van Genuchten, 1980). In order to link water-balance equations with potential-driven flows in soil (i.e., infiltration, plant uptake, drainage, capillary rise, and evaporation), it is crucial to develop methods that establish a relationship between soil water content ( $\theta$ ) and matric potential ( $\Psi$ ) in models. Due to its widespread use and reliance on soil properties, the van Genuchten model is commonly employed by hydrological models to calculate the water retention curve when estimating this relationship (Van Looy et al.,

2017). However, in order to put this model into practice, it is crucial to obtain its unknown empirical fitting parameters through the use of known experimental data, such as a measured soil water retention curve. As the spatial scales increase, such as in catchment models, obtaining direct measurements becomes impractical due to the soil properties' heterogeneity and area coverage. Therefore, several methods have been devised to determine the van Genuchten parameters and subsequently the soil water retention curves by using easily measurable soil parameters such as texture, organic matter content, and bulk density. These functional relationships, which convert available measurable soil properties into missing soil properties such as soil hydraulic and soil chemical characteristics, are referred to as pedotransfer functions (PTFs) (Clapp & Hornberger, 1978; Bouma, 1989; Zhang & Schaap, 2017). Typically, the development of a PTF involves a two-step process. The first step involves fitting a selected water retention function, such as the van Genuchten function, to measured water retention curves. In the second step, the parameter values obtained in the fitting process are linked to the chosen soil properties (Wösten et al., 1999; Vereecken et al., 2010). Over the past three decades, soil scientists have created a vast array of PTFs that differ in terms of: (i) the techniques utilized (e.g., statistical regression methods, data exploration and mining techniques); (ii) the database of measured soil moisture retention data used to estimate the van Genuchten model; and (iii) the input parameters or predictors required (e.g., grain size distribution, bulk density, organic matter content) to develop the PTF. It has been demonstrated that the effectiveness of PTFs can be significantly influenced by several factors, such as the data utilized for calibration and assessment, the input soil properties, and the various methods employed. Notably, the databases used to generate PTFs exhibit four significant distinctions: (1) the laboratory techniques utilized to obtain a complete soil moisture retention characteristic; (2) the soil texture composition, where the extreme examples are presented in the databases of Schaap and Bouten (1996), which exclusively contain sandy materials, and Schaap and Leij (1998), which primarily feature coarse-textured soils and almost no silty soils; (3) discrepancies in the number of data points and pressure head values utilized to establish the WRC, and (4) to effectively parameterize soil hydraulic properties, it is necessary to consider hydrological processes.

The uncertainty associated with PTFs can have significant implications for water balance models (Gutmann & Small, 2005; Weihermüller et al., 2021). It is shown that van Genuchten model parameters, which are often estimated using PTFs, are the primary source of uncertainty in coupled 3D land-surface and hydrological models (Shi et al., 2014) To address this issue, it

is essential to estimate the water-retention-curve parameters locally and optimize them through data assimilation, as confirmed by observations (Shi et al., 2015). Moreover, it is crucial to select PTFs carefully when parametrizing hydrological models and only use PTFs that can result in plausible model predictions (Casper et al., 2019; Mohajerani et al., 2021; Mohajerani et al., 2023). By doing so, the uncertainty linked to PTFs can be minimized, leading to more accurate and reliable predictions in water balance models.

The WaSiM model (Version 10.06.00, 2021) utilizes Richards equation to simulate the water fluxes in unsaturated soils in a one-dimensional vertical direction. The equation is solved using a vertical finite difference (FD) scheme. The soil is represented as a series of layered columns, where each column is characterized by its distinct properties and thickness for each (Schulla & Jasper, 2012). These characteristics include the water retention curve, which is described using van Genuchten parameters, as well as the saturated hydraulic conductivity. The discharge modeled by the WaSiM-ETH is composed of three components, representing different response types: surface flow, interflow, and base flow, with varying speeds. This allows for an analysis of the runoff behavior of the catchment, with the ability to observe the effects of changes in soil hydraulic properties resulting from different soil parametrizations (utilizing various PTFs). The model incorporates the spatial variability of soil properties and land use, and as a result, it captures the spatial structure and heterogeneity of flow processes occurring at the interface between the soil and the atmosphere. In addition, the model accounts for the dynamic changes in water flow within the soil in response to the dynamic changes in boundary conditions. The infiltration is considered the upper boundary condition, which is estimated using the extended approach after Peschke (1977, 1987) following the Green and Ampt (1911) method. The lower boundary condition is the depth of the groundwater layer, which remains constant for a particular time step but varies over time due to groundwater flow, recharge, or capillary rise. The discretized Richards equation can be expressed as:

$$\frac{\Delta\theta}{\Delta q} = \frac{\Delta q}{\Delta z} = q_{in} - q_{out}$$

Where,  $Q_{in}$  is inflow into the actual soil layer [m/s], and  $Q_{out}$  is outflow from the actual soil layer (including interflow and artificial drainage) [m/s].

The model considers the hydraulic properties' dependencies on soil water content discretely. As a result, the flux  $q$  between the upper and lower layers (indexed as  $u$  and  $l$ , respectively) is expressed as:

$$q = k_{eff} \cdot \frac{h_h(\Theta_u) - h_h(\Theta_l)}{0.5 \cdot (d_u + d_l)}$$

Where,  $q$  is flux between two discrete layers [m/s],  $k_{eff}$  is effective hydraulic conductivity [m/s], and  $h_h$  is hydraulic head (dependent on the water content and given as sum of suction),  $\psi(\Theta)$  describes suction at different soil water contents,  $h_{geo}$  is geodetic altitude [m], and  $d$  is thickness of the layers under consideration [m].

### **2.3 Model evaluation and its limitation**

The purpose of hydrological models is to comprehend processes, evaluate hypotheses, and aid in decision-making. These models utilize diverse levels of complexity to solve empirical and governing equations, depending on how the governing equations are approached across various spatial configurations, such as lumped (Bergström, 1976), semi-distributed (Ajami et al., 2004), or fully distributed areas (Bitew & Gebremichael, 2011), and the degree of interrelation between variables and processes. Despite advancements in modeling to account for various complexities and processes, the modelling process still necessitates the empirical idealization and simplification of catchments. As a result, the simplified representations of real hydrological processes in catchment used in the models are subject to uncertainties in the resulting predictions. Uncertainties in hydrological models might come from parameters, model structure, observation, and input data (Jajarmizadeh et al., 2012; Pandi et al., 2021; Moges et al., 2021). Moreover, the process of simplification and separation of precipitation can introduce inaccuracies arising from insufficient understanding of the interrelationships among all the components in a catchment (Nash & Sutcliffe, 1970). In another word, every hydrological model is subject to certain limitations, leading to disparities between observed (natural system) and simulated data. Hence, the primary objective in hydrological modelling is to devise an assessment plan that yields simulations of the rainfall-runoff relationship that closely approximates reality (Krause et al., 2005).

As stated by the US EPA (2002), models must exhibit scientific soundness, robustness, and justifiability to produce satisfactory outcomes. To achieve this, the models usually need to undergo sensitivity analysis, calibration, and validation. Sensitivity analysis involves assessing the model output's responsiveness to its input and identifying the critical model parameters in the process. Calibration involves determining the identified parameters by comparing observed and predicted discharges. Finally, validation verifies that the parameters and the model, in general, yield adequately accurate predictions. The assessment of the disparities between observations and simulations serves as the foundation for evaluating the model's performance.



Mathematical criteria are frequently employed as measures of model efficiency, and they typically calculate the disparity between simulated and measured stream flow values over a specified time interval. The various efficiency measures can be broadly classified into three major types: standard regression criteria (e.g., slope and y-intercept, coefficient of determination and Pearson correlation coefficient); dimensionless criteria (e.g., Index of Agreement, Nash-Sutcliffe efficiency-NSE, NSE with logarithmic, Kling-Gupta efficiency-KGE), and error index criteria (Percent Bias-PBIAS, RMSE-observations and Standard deviation ratio) (Nash & Sutcliffe, 1970; Legates & McCabe, 1999; Krause et al., 2005; Moriasi et al., 2007; Gupta et al., 2009; Crochemore, 2011). The objective of performance criteria is not solely to measure the degree of conformity but also to utilize the insights gained to enhance the models (Krause et al., 2005). The process of evaluating a model is still quite intricate and closely tied to the specific goals of the modeling task.

The way a hydrologist views a particular hydrological system has a significant impact on the extent of conceptualization that needs to be converted into the model's structure. The significance of various system response modes that need to be simulated by the model, on the other hand, is dependent on the modeling objective. Therefore, determining the appropriate level of model complexity necessitates a thoughtful evaluation of the crucial processes integrated into the model structure and the necessary level of predictive precision (Waseem et al., 2017). Besides reducing model complexity, an alternative strategy for mitigating parameter uncertainty is to enhance the quantity of data accessible to identify the model parameters. This can be accomplished by incorporating supplementary output variables and measurements to restrict the parameter range. Nevertheless, the effectiveness of the additional data may rely on the suitability of the examined model structure. Another strategy can involve maximizing the utilization of existing information. Hence, the objective is to strike a balance between the model's performance and the ability to identify its parameters.

Advancements in data acquisition, such as earth observation techniques (e.g. McCabe et al., 2017), novel geophysical techniques (e.g. Auken et al., 2017), and citizen data collection (e.g., Le Coz et al., 2016), have ushered in a new era in hydrological modeling. These breakthroughs have made an unprecedented amount and variety of data easily accessible, coupled with the continually increasing computing power. As a result, there is an opportunity to leverage this hydrological data and process knowledge to advance hydrological modeling (e.g., Kollet et al.,

2010). It is yet to be determined how much of this potential can be fully utilized. The convergence of enhanced computer power, together with our advanced comprehension of hydrological processes, and greater accessibility to spatial data has facilitated the creation of progressively complex hydrological models with increasingly refined spatial resolutions (e.g., Liu & Gupta, 2007). However, it is crucial to acknowledge that utilizing sophisticated, high-resolution models does not necessarily ensure more precise simulations, if the internal process representation or parameterization is inadequate and if the internal processes themselves cannot be accurately represented (e.g., Refsgaard et al., 2022). For example, the availability of remotely sensed high-resolution spatial data has greatly improved in recent years. This has allowed researchers to test the ability of spatially distributed models to replicate observed spatial patterns. Nevertheless, it has been revealed through such tests that while these models may perform well in simulating observations of streamflow and groundwater heads, they often struggle to accurately simulate spatial patterns in land surface temperature and evapotranspiration (e.g., Demirel et al., 2018; Stisen et al., 2018).

Proper evaluation of hydrological models must consider uncertainties in model parameters, conceptualization, and catchment-specific information. Factors such as over-parameterization that might result in equifinality (Beven, 2006); spatial scale mismatch (Blöschl & Sivapalan, 1995; Beven, 1995); lack of high-quality data, and inadequate calibration can limit the reliability of complex models. Hence, thorough evaluation of model simulations and associated uncertainties is crucial for enhancing our understanding of hydrological processes and establishing the credibility of hydrological model simulations (Beven, 1989; Refsgaard, 1996; Jakeman et al., 2006; Refsgaard et al., 2007). However, many of hydrological process understanding has not usually been utilized in state-of-the-art catchment modelling and in evaluation strategies. When evaluating the reliability of models, it's important to consider how much catchment data and observations were used in the modeling process. This can be done by using a single objective function (usually discharge) or by performing multiple evaluations with various parameter sets and different data types. For instance, multiple parameter sets can be estimated by calibrating against both discharge and soil moisture data or by considering other water balance components such as evapotranspiration (e.g., Refsgaard et al., 2022; Acevedo et al., 2023; Mohajerani et al., 2023; Lotz et al., 2023).

Multiple studies have highlighted the constrained information provided by discharge when it comes to understanding the underlying processes and spatial variability within a catchment (e.g.,

Stisen et al., 2011; Pokhrel & Gupta, 2011). Discharge represents an aggregated measure of catchment response and has limitations in its ability to reveal detailed spatial variations within the catchment. This is due to the general lack of suitable model evaluation frameworks that are oriented towards spatial patterns. As a result, the evaluation of hydrological models is hampered by a lack of attention to spatial patterns, which can negatively impact the accuracy and reliability of spatial predictions. Furthermore, the development and application of distributed models, is based on the rationale of capturing spatial heterogeneity and variability. Therefore, it goes against this rationale to neglect the importance of spatial patterns in the evaluation of hydrological models (Freeze & Harlan, 1969; Refsgaard, 1997). For instance, in a case study conducted by Refsgaard et al. (2022), modelling was considered at two resolutions of 100 m and 500m. it was clearly observed that grids exhibiting a water level near the surface displayed cooler Land Surface Temperature (LST), while warmer grids were associated with a deeper water level. This correlation was only evident in the model with 100 m resolution, as the 500 m model failed to capture this relationship. Therefore, such local-scale differences were not captured by the objective functions used for calibration or by comparing patterns at a larger scale. It is while these local-scale differences will have significant impacts on interactions between groundwater and surface water, as well as flow paths. After a thorough evaluation using high-resolution surface wetness proxy data (LST) from Landsat, they considered the 100 m model and the resulting understanding of hydrological processes to be more reliable.

Patterns in general can arise due to the inherent properties of a system that lead to self-organization, as well as the emergence of new properties resulting from changes in scale and the presence of organizational controls within the system. These patterns can be visualized and described using a variety of tools, including (1) images and maps, (2) concepts, parameters, and statistics suitable for describing spatially distributed, temporal, and spatiotemporal data, and (3) models that can be applied to such data. When patterns are used to predict a system's behavior, it is important to quantify and characterize both the patterns themselves and the system's behavior. Identifying patterns is a crucial aspect of machine learning (Bishop, 2006). With the advent of the big data era and our ability to observe the Earth's surface and ecosystems on a larger scale, and also inexpensive in-situ measurement techniques, the importance of studying patterns has grown. The ability to generalize this data extensively is dependent on the ability to recognize patterns within it. Soil-water-vegetation-atmosphere systems display a diverse range of patterns that tend to recur and appear regularly in both space and time, and at varying scales (Vereecken

et al., 2016). These patterns present new opportunities to utilize the information they contain to enhance hydrological models and gain a deeper understanding of the intricate feedback loops between the different components of the hydrological system. The theoretical framework and terminology for the concept of spatial pattern comparisons in catchment hydrology was first established by Grayson and Blöschl (2000). Over the past decade, there has been a growing interest in emphasizing spatial patterns in hydrological modeling (Wealands et al., 2005; Grabs et al., 2009; Ryo et al., 2015; Mendiguren et al., 2017; Koch et al., 2018; Dembélé et al., 2020; Gaur et al., 2022). Therefore, comparing observed and simulated spatial patterns has become an integral component of current best practices in evaluating distributed models, while it is not an entirely new concept in the field of hydrology. This is because, instead of simply answering questions about the quantity and quality of water in a stream, it has become more crucial to determine where the water originates from and where to allocate limited financial resources for improvement. As a result, modeling spatial patterns has naturally become a more prominent focus. However, to conduct accurate evaluations of simulated spatial patterns, reliable observations are essential (Mendiguren et al., 2017).

Models that are fully-distributed have the ability to predict spatial patterns with varying levels of complexity. These patterns are influenced by the spatial variability of numerous parameters and forcing data that are used as input for the model. Essentially, any input that has a spatial dimension can potentially impact the simulated spatial patterns in the modeling outputs. Several studies, including those conducted by Chaney et al. (2015), Rosenbaum et al. (2012), Western et al. (2004), and Vereecken et al. (2007), have examined the quantification of drivers behind the spatial heterogeneity of simulated soil moisture patterns. For instance, Chaney et al. (2015) discovered a complex interplay among four drivers: soil heterogeneity, topography, land cover, and precipitation, showing distinct seasonality.

The ability to clearly differentiate between similar and dissimilar patterns is considered a crucial characteristic of a reliable performance metric, and as such, the various metrics differ in their capacity to achieve this with certainty. Over the past few years, there have been numerous studies suggesting spatial performance metrics that allow for a meaningful comparison of hydrological variables' patterns, surpassing the limitations of basic cell-to-cell comparisons (e.g., Wealands et al., 2005; Chiles & Delfiner, 2012; Renard & Allard, 2013; Wolff et al., 2014; Koch et al., 2016; Vereecken et al., 2016; Koch et al., 2018; Dembélé et al., 2020; Gaur et al., 2022). However, for instance, in a citizen science project conducted by Koch and Stisen (2017),

they utilized human perception to evaluate the similarity and dissimilarity of simulated spatial patterns in various scenarios of a hydrological catchment model. Their aim was to assess whether advanced statistical performance metrics could accurately replicate human perception in distinguishing between similarity and dissimilarity. The findings indicated that while more complex metrics did not necessarily excel in emulating human perception, they did offer additional valuable information for model diagnostics.

Overall, accurate hydrological modeling outputs rely on incorporating additional observations and reproducing spatial patterns of various hydrological variables beyond streamflow, both of which are critical components. The scientific community has, in fact, been advocating for the incorporation of spatial data in the evaluation of distributed hydrological models for a considerable period of time. For instance, remotely sensed datasets possess the capability to enhance models, either through data assimilation (Leroux et al., 2016; Tangdamrongsub et al., 2017; Tian et al., 2017) or model evaluation (Rientjes et al., 2013; Li et al., 2018; Bai et al., 2018). When utilizing remote sensing data for parameter estimation through the spatial pattern evaluation process, the current methods involve either using solely spatial patterns of remote sensed variables or a combination of remote sensing data and in-situ estimations, often streamflow data (Immerzeel & Droogers, 2008; Rajib et al., 2018; Li et al., 2018; Wambura et al., 2018). Hence, recent literatures, such as the study by Stisen et al. (2018), have increasingly explored the simultaneous assessment of hydrological models using streamflow and diverse combinations of complementary data that incorporate spatial patterns of various hydrological processes, such as dominant runoff generation, soil moisture content, and evapotranspiration. For example, Dembélé et al. (2020) propose a multivariate calibration strategy to test a hydrological model's ability to reproduce spatial patterns of evaporation, soil moisture, terrestrial water storage, and streamflow observations. The aim is to improve the model's performance by simultaneously considering multiple variables and capturing relative spatial differences within the hydrological system. In other words, the incorporation of such complementary data has the potential to significantly narrow down the range of feasible models and parameters' space, resulting in more realistic internal model dynamics and associated hydrological characteristics (Shafii & Tolson, 2015; Clark et al., 2017). Ultimately, this approach can improve the overall representation of catchment functioning. Consequently, it is essential to evaluate the model's performance in capturing different aspects of the water cycle within a catchment, particularly the dynamics of their spatial patterns. Therefore, when determining the relevant parameters in the model, it is important to

consider, for example, if we obtain realistic results with regards to spatial patterns of dominant runoff processes, soil hydraulic properties, and evapotranspiration.

### 3 Conclusion and Outlook

The quote presented below was concluded by hydrology pioneers Wagener et al. (2001), 22 years ago:

*“A framework is required that balances the level of model complexity supported by the available data with the level of performance suitable for the desired application. Tools are needed that make optimal use of the information available in the data to identify model structure and parameters, and that allow a detailed analysis of model behaviour.”*

Following that, Gupta et al. (2006) introduced a hydrological model evaluation approach with the objective of obtaining a model they referred to as a "behavioral" model, characterized by the following attributes:

*“(i) the input-state-output behavior of the model is consistent with the measurements of catchment behavior, (ii) the model predictions are accurate (i.e. they have negligible bias) and precise (i.e. the prediction uncertainty is relatively small), and (iii) the model structure and behavior are consistent with current hydrologic understanding of reality.”*

In light of the preceding insights, Wagener et al. (2010) further emphasized the necessity for a paradigm shift in hydrology, which means a fundamental change in how we approach the study of water systems. Traditionally, hydrologists have relied on observations and data from the past to make predictions about how water systems behave. However, this approach may no longer be sufficient in situations where there are significant changes in the physical characteristics of the system or when the system shows behavior that goes beyond what has been previously observed. To achieve this paradigm shift, hydrologists need to adopt two important roles: synthesists and analysts. As synthesists, they need to observe and analyze the hydrological system as a whole, considering all its interconnected components and their interactions. This holistic approach allows them to understand the system's behavior as an integrated entity, rather than focusing solely on individual elements. For example, when studying a river basin, a hydrologist might consider the rainfall patterns, the runoff processes, the water stored in soils and lakes, and the movement of groundwater. They would examine how these different components interact and influence each other, considering factors like topography, climate, land use, and

geological conditions. By analyzing the system as a whole, they gain a better understanding of its behavior and can make predictions beyond what has been previously observed. On the other hand, hydrologists also need to be analysts, meaning they should understand the functioning of individual components of the system in detail. This involves studying the properties and processes of individual elements, such as rainfall intensity, river flow dynamics, groundwater recharge rates, soil moisture distribution, dominant runoff processes, and evaporation rates. By comprehending these individual aspects, they can accurately assess how changes in specific components may impact the overall behavior of the hydrological system. For instance, an analyst might study how changes in land use, such as deforestation or urbanization, affect the rainfall patterns in a region. By understanding the relationship between land cover and rainfall, they can anticipate potential changes in the water system's behavior due to altered conditions. By combining these roles, hydrologists can effectively adapt to new challenges and uncertainties. For example, in the face of climate change, hydrologists need to predict how changes in temperature and precipitation patterns will affect water resources. By being synthesists, they can understand the broader impacts on the entire water system, including changes in river flows and groundwater levels. At the same time, by being analysts, they can study the specific mechanisms by which climate change alters evaporation rates, soil moisture, runoff generation processes, or alters the timing and intensity of storms.

The motivation behind the PhD thesis at hand is therefore encapsulated by the findings contained within the above mentioned statements. These findings emphasize the need to confront the challenges and act as a catalyst for essential enhancements in hydrological model evaluation. However, to do so, it is crucial to actively engage in a long-term initiative that adopts a model parameterization approach aligned with local topography, soil, and geology. As a result, by incorporating these site-specific characteristics into the model parameterization process and aiming to achieve a “behavioral model”, this thesis intends to contribute to improvement of hydrological modeling and provide valuable insights for robust evaluation of simulated hydrological processes.

The studies contained in this thesis question the conventional approach of model performance evaluation with respect to discharge data alone at the outlet as well as the common practice of relying on default parameterization, i.e., often using Pedo-Transfer-Functions (PTFs) without careful consideration of their suitability for the study area and their implications for the other



simulated processes. In other words, the study strikes a proper balance between the identifiability of parameters and the model's capacity to accurately depict the observed system response.

By setting up a 1-D water balance model, we tried to reproduce soil water flux dynamics and physiological control of water loss (plant transpiration) for a beech stand in Western Luxembourg. It is found that achieving consistency between model simulations and measurements of transpiration and soil moisture does not necessarily guarantee accurate estimation of runoff generation or total water balance. Therefore, to identify parameter sets that produce realistic outputs, it was necessary to set up a multi-criteria evaluation scheme that integrates various sources of information including expert knowledge of local controls and dominant hydrological processes in the region. As a result, even slight variations in parameterization, e.g., saturated water content and water retention curve, could lead to implausible model behavior (e.g., in terms of dominant runoff generation processes in the area). Consequently, in order to develop a methodology for quantifying the impact of diverse soil parameterization methods (e.g., utilizing various PTFs) on water distribution within the hydrologic system, the model was established at the catchment scale. It was discovered that the spatial variability of soil hydraulic properties, influenced by different PTFs, significantly affects the water balance and leads to a wide range of hydrological model behaviors. Surprisingly, even with variations in the runoff components generated by different PTFs, the resulting discharge hydrograph could still be adequately depicted. In order to account for the spatial variability of soil hydraulic properties and align the parameterization of soil towards capturing realistic spatial patterns of hydrological processes, supplementary information is necessary. This additional information may involve mapping dominant runoff processes or deriving patterns of soil moisture and evapotranspiration through remote sensing methods.

Taking one step further, spatial pattern information from a regional soil hydrological map was integrated into a catchment model to improve the representation of dominant runoff processes. The map contents were translated and reclassified into dominant runoff process classes consistent with the modeling approach. Various PTFs were also incorporated into the parameterization scheme to convert soil properties into model parameters. By analyzing the model's response to synthetic rainfall events and incorporating multiple PTFs, the ability of the models to reproduce the spatial patterns of dominant runoff processes was assessed. In this phase of the study, a spatial pattern-oriented evaluation of dominant runoff processes was conducted using a bias-insensitive and multicomponent metric. The identification of dominant runoff processes

was based on specific rainfall event types and location-specific soil and topographic characteristics through the use of different PTFs. As a result, distinct model reactions in reproducing the patterns of dominant runoff processes are observed, reflecting the variation in topographic relief and geomorphologic characteristics across different areas, such as uplands, hill slopes, and low-lying areas in the alluvial plain. For instance, areas with steeper slopes and fine-grained soils exhibit higher responsiveness to intense rainfall events of shorter durations, resulting in faster runoff processes (e.g., saturated over land flow). Conversely, soil water stored in steep hillslope zones play a significant role in interflow generation. Constant saturation within the riparian zone gives rise to distinct source areas marked by groundwater influences. Spatial patterns in such cases are often unaffected by climate forcing, as it is considered constant and does not leave a noticeable impact.

The integration of spatial information (e.g., from digital soil hydrological maps) provides insights into the distribution of heterogeneities that influence rapid runoff generation during wet conditions and water retention during dry conditions. Notably, in smaller catchments with complex topography, the choice of PTFs becomes critical as it has a substantial impact on hydrological fluxes within the drainage basin (e.g., Paschalis et al., 2022). This phase of the study emphasizes the improvements achieved in modeling hydrological processes by incorporating spatial patterns and addressing uncertainties related to PTFs. It showcases the progress made in accurately representing the complexities of hydrological systems.

Building upon the insights of our PhD research, our latest publication (as part of the MESOHYD project) introduces a significant enhancement through the calibration of land-use-dependent evapotranspiration parameters. This approach leverages MODIS evaporation time series data to refine the simulation of actual evapotranspiration (ET<sub>a</sub>) patterns across mesoscale catchments. By integrating land-use-specific calibration and validating against LANDSAT ET<sub>a</sub> data, we demonstrate a marked improvement in model accuracy, specifically in representing spatial ET<sub>a</sub> patterns. This publication not only complements the thesis by providing a practical example of addressing model parameterization challenges but also underscores the integration of cutting-edge remote sensing data to refine the calibration of vegetation parameters—a methodology that profoundly aligns with the thesis's broader ambition of enhancing hydrological models' fidelity through site-specific characterizations and nuanced multi-criteria evaluations (Casper et al., 2023).

The complexity of process dependency in spatial patterns extends across a broad range of spatial and temporal scales. It encompasses the intricate interactions and relationships that exist within hydrological systems at different scales. As a result, various types of patterns emerge at different scales, each associated with distinct hydrological processes. Spatial patterns in a meso-scale domain, spanning a range of 500 meters to a few kilometers, can be effectively observed using remote sensing. However, valuable insights into spatial patterns can also be derived from well-established regional digital soil hydrologic mapping or soil moisture networks in the field. The choice of modeling scale is typically constrained by the available data for informing model parameters, as well as the computational resources at hand. Nevertheless, it is expected that future advancements will allow for even finer modeling scales, thereby reshaping our understanding of the processes across different scales. Moreover, the development of the next generation of georeferenced and local-attribute-based PTFs is envisioned to be advanced, and therefore, enhance soil hydrologic process-related information by incorporating a multidimensional framework. The richness of information and advanced analytical methods will then surpass the current approach of generic-attribute-based PTFs. This provision will then foster a continuous process of improvement and enhance understanding within the field of hydrology (e.g., Arrouays et al., 2014; Vereecken et al., 2022). Furthermore, it is imperative that new evaluation approaches encompass calibration methodologies to achieve improved simulation of spatial patterns and multiple hydrological variables (e.g., Stisen et al., 2023; Refsgaard et al., 2022).

Potential future works can expand the current study by incorporating calibration strategies that utilize a spatial pattern-oriented objective function for improved estimation of evapotranspiration (ET) patterns, by integrating remotely sensed spatial patterns (e.g., Amani & Shafizadeh-Moghadam, 2023). It is particularly important at the catchment scale where land cover and soil characteristics play a significant role in driving spatial variability (e.g., Koch et al., 2022). Furthermore, the development of methods that replace fixed vegetation parameters (such as leaf area index (LAI), fractional vegetation cover (FVC), vegetation height, canopy resistance, root distribution, and phenological information) in hydrological models with remotely sensed data can enhance the estimation of ET. Integrating remotely sensed data through the parameter regionalization scheme allows for better consideration of the spatial heterogeneity of vegetation, resulting in more precise ET estimations (e.g., Soltani et al., 2021). Furthermore, it is important to evaluate the influence of soil parameterization using different

PTFs on the spatial patterns of simulated ET. Assessing the impact of different soil parameterization methods on ET estimation will provide valuable insights into the overall reliability and performance of the modeling approach. To summarize, future work can focus on implementing calibration strategies that target ET spatial patterns, incorporating remotely sensed data for vegetation parameterization and spatial pattern-oriented evaluation, and assessing the influence of different soil parameterizations on the spatial patterns of simulated ET.

## 4 References

- ABBOTT, M. B., BATHURST, J. C., CUNGE, J. A., O'CONNELL, P. E., & RASMUSSEN, J. (1986a). An introduction to the European Hydrological System—Systeme Hydrologique Euro- peen, “SHE”, 1: History and philosophy of a physically-based, distributed modelling system. *Journal of hydrology*, 87(1-2), 45-59.
- ABBOTT, M. B., BATHURST, J. C., CUNGE, J. A., O'CONNELL, P. E., & RASMUSSEN, J. (1986b). An introduction to the European Hydrological System—Systeme Hydrologique Euro- peen, “SHE”, 2: Structure of a physically-based, distributed modelling system. *Journal of hydrology*, 87(1-2), 61-77.
- ACEVEDO, S. E., MARTÍNEZ, S. I., CONTRERAS, C. P., & BONILLA, C. A. (2023). Effect of data availability and pedotransfer estimates on water flow modelling in wildfire-affected soils. *Journal of hydrology*, 617, 128919.
- AJAMI, N. K., GUPTA, H., WAGENER, T., & SOROOSHIAN, S. (2004). Calibration of a semi-distrib- uted hydrologic model for streamflow estimation along a river system. *Journal of hy- drology*, 298(1-4), 112-135.
- ALLEN, R. G., PEREIRA, L. S., RAES, D., & SMITH, M. (1998). Crop evapotranspiration. Guide- lines for computing crop water requirements. FAO Irrigation and drainage paper 56. Fao, Rome, 300(9), D05109.
- AMANI, S., & SHAFIZADEH-MOGHADAM, H. (2023). A review of machine learning models and influential factors for estimating evapotranspiration using remote sensing and ground- based data. *Agricultural Water Management*, 284, 108324.
- ARNOLD, J. G., MUTTIAH, R. S., SRINIVASAN, R., & ALLEN, P. M. (2000). Regional estimation of base flow and groundwater recharge in the Upper Mississippi river basin. *Journal of hy- drology*, 227(1-4), 21-40.
- ARROUAYS, D., GRUNDY, M. G., HARTEMINK, A. E., HEMPEL, J. W., HEUVELINK, G. B., HONG, S. Y., ... & ZHANG, G. L. (2014). GlobalSoilMap: Toward a fine-resolution global grid of soil prop- erties. *Advances in agronomy*, 125, 93-134.
- AUBERTIN, G. M., & PATRIC, J. H. (1974). *Water quality after clearcutting a small watershed in West Virginia* (Vol. 3, No. 3, pp. 243-249). American Society of Agronomy, Crop Science Society of America, and Soil Science Society of America.
- AUKEN, E., BOESEN, T., & CHRISTIANSEN, A. V. (2017). A review of airborne electromagnetic methods with focus on geotechnical and hydrological applications from 2007 to 2017. *Advances in geophysics*, 58, 47-93.

- BAI, P., LIU, X., & LIU, C. (2018). Improving hydrological simulations by incorporating GRACE data for model calibration. *Journal of hydrology*, 557, 291-304.
- BERGSTRÖM, S. (1976). *Development and application of a conceptual runoff model for Scandinavian catchments*.
- BERGSTRÖM, S., & FORSMAN, A. (1973). Development of a conceptual deterministic rainfall-runoff mode. *Nord. Hydrol*, 4, 240-253.
- BEVEN, K. (1989). Changing ideas in hydrology—the case of physically-based models. *Journal of hydrology*, 105(1-2), 157-172.
- BEVEN, K. (1995). Linking parameters across scales: subgrid parameterizations and scale dependent hydrological models. *Hydrological processes*, 9(5-6), 507-525.
- BEVEN, K. (2002). Towards an alternative blueprint for a physically based digitally simulated hydrologic response modelling system. *Hydrological processes*, 16(2), 189-206.
- BEVEN, K. (2006). A manifesto for the equifinality thesis. *Journal of hydrology*, 320(1-2), 18-36.
- BEVEN, K., CALVER, A., & MORRIS, E. M. (1987). The Institute of Hydrology distributed model.
- BISHOP, C. M. (2006). *Pattern Recognition and Machine Learning*. Springer New York, NY.
- M. M., & GEBREMICHAEL, M. (2011). Evaluation of satellite rainfall products through hydrologic simulation in a fully distributed hydrologic model. *Water Resources Research*, 47(6).
- BLANEY, H. F. (1952). Determining water requirements in irrigated areas from climatological and irrigation data.
- BLÖSCHL, G., BIERKENS, M. F., CHAMBEL, A., CUDENNEC, C., DESTOUNI, G., FIORI, A., ... & RENNER, M. (2019). Twenty-three unsolved problems in hydrology (UPH)—a community perspective. *Hydrological sciences journal*, 64(10), 1141-1158.
- BLÖSCHL, G., & SIVAPALAN, M. (1995). Scale issues in hydrological modelling: a review. *Hydrological processes*, 9(3-4), 251-290.
- BOGENA, H. R., HERBST, M., HUISMAN, J. A., ROSENBAUM, U., WEUTHEN, A., & VEREECKEN, H. (2010). Potential of wireless sensor networks for measuring soil water content variability. *Vadose Zone Journal*, 9(4), 1002-1013.
- BOUMA, J. (1989). Using soil survey data for quantitative land evaluation. *Advances in soil science*, 9(1989), 177-213.
- BROOKS, R. H., & COREY, A. T. (1966). Properties of porous media affecting fluid flow. *Journal of the irrigation and drainage division*, 92(2), 61-88.
- BURNASH, R. J., & FERRAL, R. L. (1973). *A generalized streamflow simulation system: Conceptual modeling for digital computers*. US Department of Commerce, National Weather Service, and State of California, Department of Water Resources.

- CAMPBELL, G. S. (1974). A simple method for determining unsaturated conductivity from moisture retention data. *Soil science*, 117(6), 311-314.
- CASPER, M. C., MOHAJERANI, H., HASSLER, S., HERDEL, T., & BLUME, T. (2019). Finding behavioral parameterization for a 1-D water balance model by multi-criteria evaluation. *Journal of Hydrology and Hydromechanics*, 67(3), 213-224.
- CASPER, M. C., SALM, Z., GRONZ, O., HUTENGS, C., MOHAJERANI, H., & VOHLAND, M. (2023). CALIBRATION OF LAND-USE-DEPENDENT EVAPORATION PARAMETERS IN DISTRIBUTED HYDROLOGICAL MODELS USING MODIS EVAPORATION TIME SERIES DATA. *HYDROLOGY*, 10(12), 216.
- CELIA, M.A., BOULOUTAS, E.T., & ZARBA, R.L. (1990). A general mass-conservative numerical solution for the unsaturated flow equation. *Water Resources Research* 26(7): 1483– 1496.
- CHANEY, N. W., ROUNDY, J. K., HERRERA-ESTRADA, J. E., & WOOD, E. F. (2015). High-resolution modeling of the spatial heterogeneity of soil moisture: Applications in network design. *Water resources research*, 51(1), 619-638.
- CHILES, J. P., & DELFINER, P. (2012). *Geostatistics: modeling spatial uncertainty* (Vol. 713).
- CLAPP, R. B., & HORNBERGER, G. M. (1978). Empirical equations for some soil hydraulic properties. *Water resources research*, 14(4), 601-604.
- CLARK, M. P., BIERKENS, M. F., SAMANIEGO, L., WOODS, R. A., UIJLENHOET, R., BENNETT, K. E., ... & PETERS-LIDARD, C. D. (2017). The evolution of process-based hydrologic models: historical challenges and the collective quest for physical realism. *Hydrology and Earth System Sciences*, 21(7), 3427-3440.
- COLLICK, A. S., FUKA, D. R., KLEINMAN, P. J., BUDA, A. R., WELD, J. L., WHITE, M. J., ... & EASTON, Z. M. (2015). Predicting phosphorus dynamics in complex terrains using a variable source area hydrology model. *Hydrological processes*, 29(4), 588-601.
- CROCHEMORE, L. (2011). *Evaluation of hydrological models: Expert judgement vs Numerical criteria* (Doctoral dissertation, Master II, Hydrologie, Polytech, Paris UPMC, Sciences de la Terre).
- DAVISON, J. H., HWANG, H. T., SUDICKY, E. A., & LIN, J. C. (2015). Coupled atmospheric, land surface, and subsurface modeling: Exploring water and energy feedbacks in three-dimensions. *Advances in Water Resources*, 86, 73-85.
- DEMBÉLÉ, M., HRACHOWITZ, M., SAVENIJE, H. H., MARIÉTHOZ, G., & SCHAEFLI, B. (2020). Improving the predictive skill of a distributed hydrological model by calibration on spatial patterns with multiple satellite data sets. *Water resources research*, 56(1), e2019WR026085.
- DEMIREL, M. C., MAI, J., MENDIGUREN, G., KOCH, J., SAMANIEGO, L., & STISEN, S. (2018). Combining satellite data and appropriate objective functions for improved spatial pattern performance of a distributed hydrologic model. *Hydrology and Earth System Sciences*, 22(2), 1299-1315.

- DOORENBOS, J., & PRUITT, W. O. (1977). Crop water requirements. FAO irrigation and drainage paper 24. *Land and Water Development Division, FAO, Rome, 144*(1).
- DÖLL, P., FRITSCH, M., EICKER, A., & MÜLLER SCHMIED, H. (2014). Seasonal water storage variations as impacted by water abstractions: comparing the output of a global hydrological model with GRACE and GPS observations. *Surveys in Geophysics, 35*, 1311-1331.
- EBEL, B. A., & LOAGUE, K. (2006). Physics-based hydrologic-response simulation: Seeing through the fog of equifinality. *Hydrological Processes: An International Journal, 20*(13), 2887-2900.
- EBEL, B. A., SHEPHARD, Z. M., WALVOORD, M. A., MURPHY, S. F., PARTRIDGE, T. F., & PERKINS, K. S. (2023). Modeling Post-Wildfire Hydrologic Response: Review and Future Directions for Applications of Physically Based Distributed Simulation. *Earth's Future, 11*(2), e2022EF0030368.
- EK, M. A., & HOLTSLAG, A. A. M. (2004). Influence of soil moisture on boundary layer cloud development. *Journal of hydrometeorology, 5*(1), 86-99.
- ELSENBEER, H. (2001). Hydrologic flowpaths in tropical rainforest soils— a review. *Hydrological Processes, 15*(10), 1751-1759.
- FARTHING, M. W., & OGDEN, F. L. (2017). Numerical solution of Richards' equation: A review of advances and challenges. *Soil Science Society of America Journal, 81*(6), 1257-1269.
- FEDDES, R. A., KOWALIK, P. J., & ZARADNY, H. (1978). Simulation of field water use and crop yield, Pudoc. Wageningen, Simulation Monographs.
- FREEZE, R. A., & HARLAN, R. L. (1969). Blueprint for a physically-based, digitally-simulated hydrologic response model. *Journal of hydrology, 9*(3), 237-258.
- GAUR, S., SINGH, B., BANDYOPADHYAY, A., STISEN, S., & SINGH, R. (2022). Spatial pattern-based performance evaluation and uncertainty analysis of a distributed hydrological model. *Hydrological Processes, 36*(5), e14586.
- GRABS, T., SEIBERT, J., BISHOP, K., & LAUDON, H. (2009). Modeling spatial patterns of saturated areas: A comparison of the topographic wetness index and a dynamic distributed model. *Journal of hydrology, 373*(1-2), 15-23.
- GRAYSON, R., & BLÖSCHL, G. (Eds.). (2001). Spatial patterns in catchment hydrology: observations and modelling. CUP Archive.
- GRAYSON, R. B., MOORE, I. D., & MCMAHON, T. A. (1992). Physically based hydrologic modeling: 2. Is the concept realistic?. *Water resources research, 28*(10), 2659-2666.
- GREEN, W. H., & AMPT, G. A. (1911). Studies on Soil Physics. *The Journal of Agricultural Science, 4*(1), 1-24.
- GUO, L., HUANG, K., WANG, G., & LIN, S. (2022). Development and evaluation of temperature-induced variable source area runoff generation model. *Journal of Hydrology, 610*, 127894.



- GUPTA, H. V., BEVEN, K. J., & WAGENER, T. (2006). Model calibration and uncertainty estimation. *Encyclopedia of hydrological sciences*.
- GUPTA, H. V., KLING, H., YILMAZ, K. K., & MARTINEZ, G. F. (2009). Decomposition of the mean squared error and NSE performance criteria: Implications for improving hydrological modelling. *Journal of hydrology*, 377(1-2), 80-91.
- GUTMANN, E. D., & SMALL, E. E. (2005). The effect of soil hydraulic properties vs. soil texture in land surface models. *Geophysical research letters*, 32(22).
- HARGREAVES, G. H., & SAMANI, Z. A. (1985). Reference crop evapotranspiration from temperature. *Applied engineering in agriculture*, 1(2), 96-99.
- HERMAN, M. R., NEJADHASHEMI, A. P., ABOUALI, M., HERNANDEZ-SUAREZ, J. S., DANESHVAR, F., ZHANG, Z., ... & SHARIFI, A. (2018). Evaluating the role of evapotranspiration remote sensing data in improving hydrological modeling predictability. *Journal of Hydrology*, 556, 39-49.
- HERRMANN, D. L., SCHIFMAN, L. A., & SHUSTER, W. D. (2018). Widespread loss of intermediate soil horizons in urban landscapes. *Proceedings of the National Academy of Sciences*, 115(26), 6751-6755.
- HUANG, S., KUMAR, R., FLÖRKE, M., YANG, T., HUNDECHA, Y., KRAFT, P., ... & KRYSANOVA, V. (2017). Evaluation of an ensemble of regional hydrological models in 12 large-scale river basins worldwide. *Climatic Change*, 141, 381-397.
- IMMERZEEL, W. A., & DROOGERS, P. (2008). Calibration of a distributed hydrological model based on satellite evapotranspiration. *Journal of hydrology*, 349(3-4), 411-424.
- IVANOV, V. Y., BRAS, R. L., & VIVONI, E. R. (2008). Vegetation-hydrology dynamics in complex terrain of semiarid areas: 2. Energy-water controls of vegetation spatiotemporal dynamics and topographic niches of favorability. *Water Resources Research*, 44(3).
- JAJARMIZADEH, M., HARUN, S., & SALARPOUR, M. (2012). A review on theoretical consideration and types of models in hydrology. *Journal of Environmental Science and Technology*, 5(5), 249-261.
- JAKEMAN, A. J., LETCHER, R. A., & NORTON, J. P. (2006). Ten iterative steps in development and evaluation of environmental models. *Environmental Modelling & Software*, 21(5), 602-614.
- KOCH, J., DEMIREL, M. C., & STISEN, S. (2018). The SPAtial Efficiency metric (SPAEF): Multiple-component evaluation of spatial patterns for optimization of hydrological models. *Geoscientific Model Development*, 11(5), 1873-1886.
- KOCH, J., SIEMANN, A., STISEN, S., & SHEFFIELD, J. (2016). Spatial validation of large-scale land surface models against monthly land surface temperature patterns using innovative performance metrics. *Journal of Geophysical Research: Atmospheres*, 121(10), 5430-5452.

- KOCH J., STISEN, S. (2017) Citizen science: A new perspective to advance spatial pattern evaluation in hydrology. *PLoS ONE* 12(5): e0178165. <https://doi.org/10.1371/journal.pone.0178165>
- KOCH, J., DEMIREL, M. C., & STISEN, S. (2022). Climate Normalized Spatial Patterns of Evapotranspiration Enhance the Calibration of a Hydrological Model. *Remote Sensing*, 14(2), 315.
- KOLLET, S. J., MAXWELL, R. M., WOODWARD, C. S., SMITH, S., VANDERBORGH, J., VEREECKEN, H., & SIMMER, C. (2010). Proof of concept of regional scale hydrologic simulations at hydrologic resolution utilizing massively parallel computer resources. *Water resources research*, 46(4).
- KRAUSE, P., BOYLE, D. P., & BÄSE, F. (2005). Comparison of different efficiency criteria for hydrological model assessment. *Advances in geosciences*, 5, 89-97.
- LE COZ, J., BLANQUART, B., POBANZ, K., DRAMAIS, G., PIERREFEU, G., HAUET, A., & DESPAX, A. (2016). Estimating the uncertainty of streamgauging techniques using in situ collaborative interlaboratory experiments. *Journal of Hydraulic Engineering*, 142(7), 04016011.
- LEGATES, D. R., & MCCABE JR, G. J. (1999). Evaluating the use of “goodness-of-fit” measures in hydrologic and hydroclimatic model validation. *Water resources research*, 35(1), 233-241.
- LEROUX, D. J., PELLARIN, T., VISCHÉL, T., COHARD, J. M., GASCON, T., GIBON, F., ... & SEGUIS, L. (2016). Assimilation of SMOS soil moisture into a distributed hydrological model and impacts on the water cycle variables over the Ouémé catchment in Benin. *Hydrology and Earth System Sciences*, 20(7), 2827-2840.
- LI, Y., GRIMALDI, S., PAUWELS, V. R., & WALKER, J. P. (2018). Hydrologic model calibration using remotely sensed soil moisture and discharge measurements: The impact on predictions at gauged and ungauged locations. *Journal of hydrology*, 557, 897-909.
- LITWIN, D., TUCKER, G. E., BARNHART, K. R., & HARMAN, C. J. (2023). Catchment coevolution and the geomorphic origins of variable source area hydrology.
- LIU, Y., & GUPTA, H. V. (2007). Uncertainty in hydrologic modeling: Toward an integrated data assimilation framework. *Water resources research*, 43(7).
- LOTZ, T., SUN, Z., & XUE, B. (2023). Evaluation of soil-vegetation interaction effects on water fluxes revealed by the proxy of model parameter combinations. *Environmental Monitoring and Assessment*, 195(2), 283.
- MARANZONI, A., & TOMIROTTI, M. (2023). New formulation of the two-dimensional steep-slope shallow water equations. Part II: Numerical modeling, validation, and application. *Advances in Water Resources*, 104403.
- MCCABE, M. F., RODELL, M., ALSDORF, D. E., MIRALLES, D. G., UIJLENHOET, R., WAGNER, W., ... & WOOD, E. F. (2017). The future of Earth observation in hydrology. *Hydrology and earth system sciences*, 21(7), 3879-3914.

- MENDIGUREN, G., KOCH, J., & STISEN, S. (2017). Spatial pattern evaluation of a calibrated national hydrological model—a remote-sensing-based diagnostic approach. *Hydrology and Earth System Sciences*, 21(12), 5987-6005.
- MILLER, C. T., DAWSON, C. N., FARTHING, M. W., HOU, T. Y., HUANG, J., KEES, C. E., ... & LANGTANGEN, H. P. (2013). Numerical simulation of water resources problems: Models, methods, and trends. *Advances in Water Resources*, 51, 405-437.
- MOGES, E., DEMISSIE, Y., LARSEN, L., & YASSIN, F. (2021). Sources of hydrological model uncertainties and advances in their analysis. *Water*, 13(1), 28.
- MOHAJERANI, H., JACKEL, M., SALM, Z., SCHÜTZ, T., & CASPER, M. C. (2023). Spatial Evaluation of a Hydrological Model on Dominant Runoff Generation Processes Using Soil Hydrologic Maps. *Hydrology*, 10(3), 55.
- MOHAJERANI, H., TESCHEMACHER, S., & CASPER, M. C. (2021). A comparative investigation of various pedotransfer functions and their impact on hydrological simulations. *Water*, 13(10), 1401.
- MONTEITH, J.L. (1975). *Vegetation and the atmosphere*. Academic Press, London.
- MONTZKA, C., HERBST, M., WEIHERMÜLLER, L., VERHOEF, A., & VERECKEN, H. (2017). A global data set of soil hydraulic properties and sub-grid variability of soil water retention and hydraulic conductivity curves. *Earth System Science Data*, 9(2), 529-543.
- MORIASI, D. N., ARNOLD, J. G., VAN LIEW, M. W., BINGNER, R. L., HARMEL, R. D., & VEITH, T. L. (2007). Model evaluation guidelines for systematic quantification of accuracy in watershed simulations. *Transactions of the ASABE*, 50(3), 885-900.
- MUALEM, Y. (1976). A new model for predicting the hydraulic conductivity of unsaturated porous media. *Water resources research*, 12(3), 513-522.
- MULVANY, T. J. (1850). On the use of self-registering rain and flood gauges. Making Observations of the Relations of Rain Fall and Flood Discharges in a Given Catchment. Transactions and Minutes of the Proceedings of the Institute of Civil Engineers of Ireland, Dublin, Ireland, Session, 1.
- NASH, J. E. (1959). Systematic determination of unit hydrograph parameters. *Journal of Geophysical Research*, 64(1), 111-115.
- NASH, J. E., & SUTCLIFFE, J. V. (1970). River flow forecasting through conceptual models part I—A discussion of principles. *Journal of hydrology*, 10(3), 282-290.
- NIELSEN, S. A., & HANSEN, E. (1973). Numerical simulation of the rainfall-runoff process on a daily basis. *Hydrology Research*, 4(3), 171-190.
- OR, D., LEHMANN, P., & ASSOULINE, S. (2015). Natural length scales define the range of applicability of the Richards equation for capillary flows. *Water Resources Research*, 51(9), 7130-7144.

- PACHEPSKY, Y. A., SMETTEM, K. R. J., VANDERBORGH, J., HERBST, M., VEREECKEN, H., & WÖSTEN, J. H. M. (2004). Reality and fiction of models and data in soil hydrology. *Unsaturated-Zone Modeling: Progress, Challenges and Applications*, 3-5.
- PANDI, D., KOTHANDARAMAN, S., & KUPPUSAMY, M. (2021). Hydrological models: a review. *International Journal of Hydrology Science and Technology*, 12(3), 223-242.
- PASCHALIS, A., BONETTI, S., GUO, Y., & FATICHI, S. (2022). On the uncertainty induced by pedo-transfer functions in terrestrial biosphere modeling. *Water Resources Research*, 58(9), e2021WR031871.
- PESCHKE, G., (1977): Ein zweistufiges Modell der Infiltration von Regen in geschichtete Böden, *Acta Hydrophysica XXII*, H. 1, 39-48.
- PESCHKE, G. (1987). Soil moisture and runoff components from a physically founded approach. *Acta hydrophysica (Berlin, DDR)*, 31(3/4), 191-205.
- POKHREL, P., & GUPTA, H. V. (2011). On the ability to infer spatial catchment variability using streamflow hydrographs. *Water Resources Research*, 47(8).
- PORPORATO, A., DALY, E., & RODRIGUEZ-ITURBE, I. (2004). Soil water balance and ecosystem response to climate change. *The American Naturalist*, 164(5), 625-632.
- PRIESTLEY, C. H. B., & TAYLOR, R. J. (1972). On the assessment of surface heat flux and evaporation using large-scale parameters. *Monthly weather review*, 100(2), 81-92.
- QU, Y., & DUFFY, C. J. (2007). A semidiscrete finite volume formulation for multiprocess watershed simulation. *Water Resources Research*, 43(8).
- RAJIB, A., EVENSON, G. R., GOLDEN, H. E., & LANE, C. R. (2018). Hydrologic model predictability improves with spatially explicit calibration using remotely sensed evapotranspiration and biophysical parameters. *Journal of hydrology*, 567, 668-683.
- REFSGAARD, J. C. (1997). Parameterisation, calibration and validation of distributed hydrological models. *Journal of hydrology*, 198(1-4), 69-97.
- REFSGAARD, J. C., & KNUDSEN, J. (1996). Operational validation and intercomparison of different types of hydrological models. *Water resources research*, 32(7), 2189-2202.
- REFSGAARD, J. C. (2001). Towards a formal approach to calibration and validation of models using spatial data. Spatial patterns in catchment hydrology: observations and modeling, 329-354.
- REFSGAARD, J. C., STISEN, S., & KOCH, J. (2022). Hydrological process knowledge in catchment modelling—Lessons and perspectives from 60 years development. *Hydrological Processes*, 36(1), e14463.
- REFSGAARD, J. C., VAN DER SLUIJS, J. P., HØJBERG, A. L., & VANROLLEGHEM, P. A. (2007). Uncertainty in the environmental modelling process—a framework and guidance. *Environmental modelling & software*, 22(11), 1543-1556.
- RENARD, P., & ALLARD, D. (2013). Connectivity metrics for subsurface flow and transport. *Advances in Water Resources*, 51, 168-196.

- RICHARDS, L.A. (1931). Capillary Conduction of Liquids through Porous Mediums. *Physics* 1931, 1, 318–333.
- RIEGER, W., & DISSE, M. (2013). Physically based model approach to assess the effectiveness of individual and combined decentralized flood protection measures. *hydrol. Water Conservation*, 57, 14-25.
- RIENTJES, T. H. M., MUTHUWATTA, L. P., BOS, M. G., BOOIJ, M. J., & BHATTI, H. A. (2013). Multi-variable calibration of a semi-distributed hydrological model using streamflow data and satellite-based evapotranspiration. *Journal of hydrology*, 505, 276-290.
- ROSENBAUM, U., BOGENA, H. R., HERBST, M., HUISMAN, J. A., PETERSON, T. J., WEUTHEN, A., ... & VERECKEN, H. (2012). Seasonal and event dynamics of spatial soil moisture patterns at the small catchment scale. *Water Resources Research*, 48(10).
- RYO, M., IWASAKI, Y., YOSHIMURA, C., & SAAVEDRA V, O. C. (2015). Evaluation of spatial pattern of altered flow regimes on a river network using a distributed hydrological model. *PLoS One*, 10(7), e0133833.
- SCHAAP, M. G., & LEIJ, F. J. (1998). Using neural networks to predict soil water retention and soil hydraulic conductivity. *Soil and Tillage Research*, 47(1-2), 37-42.
- SCHULLA J. JASPER K. 2012 Model Description WASIM-ETH Manual. Last updated: November 2012.
- NOVICK, K. A., FICKLIN, D. L., BALDOCCHI, D., DAVIS, K. J., GHEZZEHEI, T. A., KONINGS, A. G., ... & WOOD, J. D. (2022). Confronting the water potential information gap. *Nature geoscience*, 15(3), 158-164.
- SCHAAP, M. G., & BOUTEN, W. (1996). Modeling water retention curves of sandy soils using neural networks. *Water Resources Research*, 32(10), 3033-3040.
- SHAFII, M., & TOLSON, B. A. (2015). Optimizing hydrological consistency by incorporating hydrological signatures into model calibration objectives. *Water Resources Research*, 51(5), 3796-3814.
- SHERMAN, L. K. (1932). Stream flow from rainfall by unitgraph method. *English News Record*, 1008, 501–505.
- SHI, Y., DAVIS, K. J., ZHANG, F., & DUFFY, C. J. (2014). Evaluation of the parameter sensitivities of a coupled land surface hydrologic model at a critical zone observatory. *Journal of Hydrometeorology*, 15(1), 279-299.
- SHI, Y., DAVIS, K. J., ZHANG, F., DUFFY, C. J., & YU, X. (2015). Parameter estimation of a physically-based land surface hydrologic model using an ensemble Kalman filter: A multivariate real-data experiment. *Advances in water resources*, 83, 421-427.
- SIMUNEK, J. (2005). The HYDRUS-1D software package for simulating the movement of water, heat, and multiple solutes in variably saturated media. *HYDRUS Software Series 1*.
- SMITH, R. E., SMETTEM, K. R., & BROADBRIDGE, P. (2002). *Infiltration theory for hydrologic applications*. American Geophysical Union.

- SOLTANI, M., BJERRE, E., KOCH, J., & STISEN, S. (2021). Integrating remote sensing data in optimization of a national water resources model to improve the spatial pattern performance of evapotranspiration. *Journal of Hydrology*, 603, 127026.
- SOOMERE, T. (2023). Numerical simulations of wave climate in the Baltic Sea: a review. *Oceanologia*, 65(1), 117-140.
- STISEN, S., DEMIREL, M. C., SOLTANI, M., & KOCH, J. (2023). Spatial pattern oriented optimization of regional scale hydrological models (No. EGU23-7955). Copernicus Meetings.
- STISEN, S., JENSEN, K. H., SANDHOLT, I., & GRIMES, D. I. (2008). A remote sensing driven distributed hydrological model of the Senegal River basin. *Journal of Hydrology*, 354(1-4), 131-148.
- STISEN, S., KOCH, J., SONNENBORG, T. O., REFSGAARD, J. C., BIRCHER, S., RINGGAARD, R., & JENSEN, K. H. (2018). Moving beyond run-off calibration—Multivariable optimization of a surface–subsurface–atmosphere model. *Hydrological Processes*, 32(17), 2654-2668.
- STISEN, S., MCCABE, M. F., REFSGAARD, J. C., LERER, S., & BUTTS, M. B. (2011). Model parameter analysis using remotely sensed pattern information in a multi-constraint framework. *Journal of Hydrology*, 409(1-2), 337-349.
- SURFLEET, C. G., TULLOS, D., CHANG, H., & JUNG, I. W. (2012). Selection of hydrologic modeling approaches for climate change assessment: A comparison of model scale and structures. *Journal of Hydrology*, 464, 233-248.
- SU, T., MIAO, C., DUAN, Q., GOU, J., GUO, X., & ZHAO, X. (2023). Hydrological response to climate change and human activities in the Three-River Source Region. *Hydrology and Earth System Sciences*, 27(7), 1477-1492.
- TANGDAMRONGSUB, N., STEELE-DUNNE, S. C., GUNTER, B. C., DITMAR, P. G., SUTANUDAJA, E. H., SUN, Y., ... & WANG, Z. (2017). Improving estimates of water resources in a semi-arid region by assimilating GRACE data into the PCR-GLOBWB hydrological model. *Hydrology and Earth System Sciences*, 21(4), 2053-2074.
- TIAN, S., TREGONING, P., RENZULLO, L. J., VAN DIJK, A. I., WALKER, J. P., PAUWELS, V. R., & ALLGEYER, S. (2017). Improved water balance component estimates through joint assimilation of GRACE water storage and SMOS soil moisture retrievals. *Water Resources Research*, 53(3), 1820-1840.
- TROCH, P. A., PANICONI, C., & EMIEL VAN LOON, A. E. (2003). Hillslope-storage Boussinesq model for subsurface flow and variable source areas along complex hillslopes: 1. Formulation and characteristic response. *Water Resources Research*, 39(11).
- USEPA. (2002). Guidance for quality assurance project plans for modelling. EPA QA/G-5M.
- VAN GENUCHTEN, M. T. (1980). A closed-form equation for predicting the hydraulic conductivity of unsaturated soils. *Soil science society of America journal*, 44(5), 892-898.
- VAN LOOY, K., BOUMA, J., HERBST, M., KOESTEL, J., MINASNY, B., MISHRA, U., ... & VEREECKEN, H. (2017). Pedotransfer functions in Earth system science: Challenges and perspectives. *Reviews of Geophysics*, 55(4), 1199-1256.

- VERECKEN, H., AMELUNG, W., BAUKE, S. L., BOGENA, H., BRÜGGEMANN, N., MONTZKA, C., ... & ZHANG, Y. (2022). Soil hydrology in the Earth system. *Nature Reviews Earth & Environment*, 3(9), 573-587.
- VERECKEN, H., KAMAI, T., HARTE, T., KASTEEL, R., HOPMANS, J., & VANDERBORGHT, J. (2007). Explaining soil moisture variability as a function of mean soil moisture: A stochastic unsaturated flow perspective. *Geophysical Research Letters*, 34(22).
- VERECKEN, H., PACHEPSKY, Y., SIMMER, C., RIHANI, J., KUNOTH, A., KORRES, W., ... & SHAO, Y. (2016). On the role of patterns in understanding the functioning of soil-vegetation-atmosphere systems. *Journal of hydrology*, 542, 63-86.
- VERECKEN, H., WEYNANTS, M., JAVAUX, M., PACHEPSKY, Y., SCHAAP, M. G., & GENUCHTEN, M. T. V. (2010). Using pedotransfer functions to estimate the van Genuchten–Mualem soil hydraulic properties: A review. *Vadose Zone Journal*, 9(4), 795-820.
- WAGENER, T., BOYLE, D. P., LEES, M. J., WHEATER, H. S., GUPTA, H. V., & SOROOSHIAN, S. (2001). A framework for development and application of hydrological models. *Hydrology and Earth System Sciences*, 5(1), 13-26.
- WAGENER, T., SIVAPALAN, M., TROCH, P. A., MCGLYNN, B. L., HARMAN, C. J., GUPTA, H. V., ... & WILSON, J. S. (2010). The future of hydrology: An evolving science for a changing world. *Water Resources Research*, 46(5).
- WAMBURA, F. J., DIETRICH, O., & LISCHIED, G. (2018). Improving a distributed hydrological model using evapotranspiration-related boundary conditions as additional constraints in a data-scarce river basin. *Hydrological processes*, 32(6), 759-775.
- WASEEM, M., MANI, N., ANDIEGO, G., & USMAN, M. (2017). A review of criteria of fit for hydrological models. *International Research Journal of Engineering and Technology (IRJET)*, 4(11), 1765-1772.
- WEALANDS, S. R., GRAYSON, R. B., & WALKER, J. P. (2005). Quantitative comparison of spatial fields for hydrological model assessment—some promising approaches. *Advances in Water Resources*, 28(1), 15-32.
- WEIHERMÜLLER, L., LEHMANN, P., HERBST, M., RAHMATI, M., VERHOEF, A., OR, D., ... & VERECKEN, H. (2021). Choice of pedotransfer functions matters when simulating soil water balance fluxes. *Journal of Advances in Modeling Earth Systems*, 13(3), e2020MS002404.
- WESTERN, A. W., ZHOU, S. L., GRAYSON, R. B., MCMAHON, T. A., BLÖSCHL, G., & WILSON, D. J. (2004). Spatial correlation of soil moisture in small catchments and its relationship to dominant spatial hydrological processes. *Journal of Hydrology*, 286(1-4), 113-134.
- WOLFF, J. K., HARROLD, M., FOWLER, T., GOTWAY, J. H., NANCE, L., & BROWN, B. G. (2014). Beyond the basics: Evaluating model-based precipitation forecasts using traditional, spatial, and object-based methods. *Weather and Forecasting*, 29(6), 1451-1472.
- WOOD, E. F., ROUNDY, J. K., TROY, T. J., VAN BEEK, L. P. H., BIERKENS, M. F., BLYTH, E., ... & WHITEHEAD, P. (2011). Hyperresolution global land surface modeling: Meeting a grand challenge for monitoring Earth's terrestrial water. *Water Resources Research*, 47(5).

- WÖSTEN, J. H. M., LILLY, A., NEMES, A., & LE BAS, C. (1999). Development and use of a database of hydraulic properties of European soils. *Geoderma*, 90(3-4), 169-185.
- WÖSTEN, J. H. M., PACHEPSKY, Y. A., & RAWLS, W. J. (2001). Pedotransfer functions: bridging the gap between available basic soil data and missing soil hydraulic characteristics. *Journal of hydrology*, 251(3-4), 123-150.
- YI, B., CHEN, L., LIU, Y., GUO, H., LENG, Z., GAN, X., ... & MEI, Z. (2023). Hydrological modelling with an improved flexible hybrid runoff generation strategy. *Journal of Hydrology*, 129457.
- ZHA, Y., YANG, J., YIN, L., ZHANG, Y., ZENG, W., & SHI, L. (2017). A modified Picard iteration scheme for overcoming numerical difficulties of simulating infiltration into dry soil. *Journal of hydrology*, 551, 56-69.
- ZHANG, Y., & SCHAAP, M. G. (2017). Weighted recalibration of the Rosetta pedotransfer model with improved estimates of hydraulic parameter distributions and summary statistics (Rosetta3). *Journal of Hydrology*, 547, 39-53.
- ZHOU, P., WANG, G., MAO, H., LIAO, F., SHI, Z., & HUANG, H. (2022). Numerical modeling for the temporal variations of the water interchange between groundwater and surface water in a regional great lake (Poyang Lake, China). *Journal of Hydrology*, 610, 127827.
- ZINK, M., MAI, J., CUNTZ, M., & SAMANIEGO, L. (2018). Conditioning a hydrologic model using patterns of remotely sensed land surface temperature. *Water Resources Research*, 54(4), 2976-2998.



## 5 Appendix

## **5.1 Finding behavioral parameterization for a 1-D water balance model by multi-criteria evaluation**

# Finding behavioral parameterization for a 1-D water balance model by multi-criteria evaluation

Markus C. Casper<sup>1</sup>, Hadis Mohajerani<sup>1\*</sup>, Sibylle Hassler<sup>2,3</sup>, Tobias Herdel<sup>1</sup>, Theresa Blume<sup>2</sup>

<sup>1</sup> University of Trier, Faculty VI, Dep. of Physical Geography, Universitätsring 12, 54286 Trier, Germany.

<sup>2</sup> GFZ German Research Centre for Geosciences, Section 5.4 Hydrology, Telegrafenberg, 14473 Potsdam, Germany.

<sup>3</sup> Karlsruhe Institute of Technology (KIT), Institute for Water and River Basin Management, Chair of Hydrology, Kaiserstr. 12, 76131 Karlsruhe, Germany.

\* Corresponding author. Tel.: +49 651 2014557. FAX: +49 651 2013976. E-mail: s6hsmoha@uni-trier.de

**Abstract:** Evapotranspiration is often estimated by numerical simulation. However, to produce accurate simulations, these models usually require on-site measurements for parameterization or calibration. We have to make sure that the model realistically reproduces both, the temporal patterns of soil moisture and evapotranspiration. In this study, we combine three sources of information: (i) measurements of sap velocities; (ii) soil moisture; and (iii) expert knowledge on local runoff generation and water balance to define constraints for a “behavioral” forest stand water balance model. Aiming for a behavioral model, we adjusted soil moisture at saturation, bulk resistance parameters and the parameters of the water retention curve (WRC). We found that the shape of the WRC influences substantially the behavior of the simulation model. Here, only one model realization could be referred to as “behavioral”. All other realizations failed for a least one of our evaluation criteria: Not only transpiration and soil moisture are simulated consistently with our observations, but also total water balance and runoff generation processes. The introduction of a multi-criteria evaluation scheme for the detection of unrealistic outputs made it possible to identify a well performing parameter set. Our findings indicate that measurement of different fluxes and state variables instead of just one and expert knowledge concerning runoff generation facilitate the parameterization of a hydrological model.

**Keywords:** Forest evapotranspiration; Water balance simulation; Soil parameterization; Behavioral model.

## INTRODUCTION

Extraction of water from the soil by the root system and return of water to the atmosphere as plant transpiration are important processes in the global circulation of water (Kramer and Boyer, 1995). Quantitative means of describing transpiration are essential for an improved understanding of water and energy exchange processes between the land surface and the atmosphere. Transpiration is controlled by a combination of biotic factors (e.g. stomatal functions; leaf area; root depth and distribution, and hydraulic characteristics) and abiotic factors (e.g. soil water availability; climate, and depth to groundwater) (Durigon et al., 2016).

There is a variety of techniques to measure transpiration at different scales such as direct measurements of sap flow on individual trees (Lu et al., 2004), eddy flux gradient analyses (Saugier et al., 1997), or gauged watersheds (Wilson et al., 2001). Alternatively, simulation models are used to estimate transpiration. However, to produce accurate simulations, these usually require on-site parameterization or calibration (Durigon et al., 2016; Vose et al., 2003). Recently, a simple approach was developed by Ayyoub et al (2017) relating the normalized daily sap velocities and the daily reference evapotranspiration (ET<sub>0</sub>). This method used both, FAO-Penman-Monteith (FAO-PM) method and Hargreaves-Samani (HARG) method to estimate ET<sub>0</sub>. The FAO-PM method produced the highest correlations to daily sap velocities (Ayyoub et al., 2017).

System state (“soil moisture”) and actual evapotranspiration are known to be highly correlated. Therefore, all water balance models directly couple these two components. Wrong estimates of temporal or spatial patterns of soil moisture result in erroneous temporal or spatial patterns of transpiration (Casper and Vohland, 2008; Koch et al., 2017). Therefore, soil parameteri-

zation, and especially the representation of the Water Retention Curve - as one of the most important soil-physical characteristics - strongly influence the simulation of evapotranspiration. A similar effect can be observed when canopy resistances are wrongly estimated (Bie et al., 2015). In order to find an appropriate model parametrization, we have to verify that the model realistically reproduces both, the temporal patterns of soil moisture and evapotranspiration. This has been done in a study carried out by Holst et al. (2010) where the water balance of two beech stands in Southwest Germany was investigated using two different forest hydrological models (DNDC and BROOK90). They demonstrated that both models were able to reproduce the observed dynamics of the soil water content in the uppermost 30 cm and the transpiration estimates from sap flow measurements (Holst et al., 2010).

To analyze different assumptions on catchment behavior and hydrological processes, it is necessary to evaluate the model performance with respect to multiple indicators that evaluate the contribution of different sources of data (Gupta et al., 1998). The value of these additional data sources has been demonstrated by Fenicia et al. (2008a). They evaluated the accuracy of a hydrological simulation with respect to the observed discharge, groundwater level dynamics, and isotope signatures. If appropriate data is lacking, incorporation of expert knowledge (as an alternative source of information) into hydrological modeling and water management issues becomes more important (Bromley et al., 2005; Cash et al., 2003; Mohajerani et al., 2017). As recent studies suggest, use of expert knowledge in choosing parameter sets and introducing constraints by forcing the model to reproduce the processes observed in the real system, can also improve the model performance even without traditional calibration (Bahremand, 2016; Gharari et al., 2014; Hrachowitz et al., 2014). For instance,

having expert knowledge on local runoff generation processes, as a potential source of information in every hydrologic unit, can considerably improve hydrological simulations (Antonetti and Zappa, 2018; Casper et al., 2015; Franks et al., 1998; Seibert and McDonnell, 2002). Modelers need to consider a proper balance between parameter identifiability and the model's ability to precisely represent the observed system response. This has prompted the development of alternative approaches to hydrological modeling including the dominant process concept (Fenicia et al., 2008b; Grayson and Blöschl, 2001; Wagener et al., 2001). The concept of dominant runoff generation process (DRGP) assumes that at a particular location one particular runoff generation mechanism is dominant (Blöschl, 2001). In most of the studies, however, modelers have evaluated the model performance with respect to discharge data alone. This may cloud model realism and hamper understanding of catchment behavior. In fact, to accurately evaluate hydrological models, one has to carefully look at the hydrological responses that a model is challenged to represent rather than just being satisfied with a simple calibration. This interestingly takes us back to what Fenicia et al. (2008a) call the "Art of Modeling" and what Gupta et al. (2005) call the "Behavioral Model". The former says: "...modeling is both an Art and a Science. The science lies in the use of fundamental scientific principles and the formality of analysis; the art accounts for professional experience, insight, creativity and intuition. The latter is particularly important in developing a perceptual and conceptual model that captures the main processes at play, while maintaining minimum levels of complexity...". A "behavioral" model has the following characteristics: (i) the input-state-output behavior of the model is consistent with the measurements, (ii) the model predictions are accurate (i.e. they have negligible bias) and (iii) model structure and behavior are consistent with our hydrologic understanding of reality (Fenicia et al., 2008a; Gupta et al., 2005).

The present study combines three sources of information: measurements of sap velocities; soil moisture data; and expert knowledge of local runoff generation and water balance to define constraints for a "behavioral" forest stand water balance model. We evaluated the model by defining multi-criteria performance measures according to the constraints that data are supposed to impose on model behavior. In particular, we investigated the following research questions: (i) How can we combine different sources of information to modify the parameterization scheme in order to achieve a "behavioral model"? (ii) How does the implementation of expert knowledge of site-specific dominant runoff generation processes affect the simulation results? (iii) What are the impacts of model setup, i.e. the parameterization approach and the parameter allocation strategy on the simulated soil moisture and evapotranspiration dynamics (e.g. the effect of different parameterizations of the water retention curve of the soil)?

To address the research questions listed above, we used a one-dimensional (1-D) hydrological model (WaSiM-ETH) to simulate the soil water content as well as the actual transpiration at stand level. The basic motivation of 1-D models is often to simulate soil water content, and water balance components such as evapotranspiration, deep drainage and runoff. In the 1-D models, no groundwater flow is simulated and the upper and lower limits are soil water content at field capacity and permanent wilting point, and upper and lower loss of soil water is caused by evapotranspiration and deep percolation, respectively (Walker and Zhang, 2002). WaSiM-ETH was selected due to its highly differentiated 1-D model structure. The model represents all relevant hydrological processes at the point scale in a

physically meaningful way (Schulla, 2017). As all measured data including soil moisture and sap velocity are point measurements, setting up a "1-D model" is sufficient for our purpose. A site in the sandstone region of western Luxembourg was used as a test case. On sandstone, we expect neither stream channels nor surface runoff due to the high hydraulic conductivities of the sandy soils. The headwaters start at springs on top of the less permeable marls underlying the sandstone. While this work is not going to provide new insights of the behavior of the study catchment, it arguably is going to contribute to understanding of the value of different sources of data and information for hydrological modeling. The test case is used as a "proof-of-concept" location to investigate how different parameterization with different content of information can affect the model behavior. Our investigation is subdivided into four scenarios, i.e. different soil parameterizations. For each scenario the simulation results are evaluated by the model performance criteria defined in the section 2.4. In scenario A, the soil parameterization is taken from Tepee et al. 2003. In the two scenarios B1 and B2, we parameterize the water retention curve with three different variations of the van Genuchten parameters according to (Sauer, 2007). In a last step (scenario C), we evaluate the model performance using the soil parameter set provided by Sprenger et al. (2016). All scenarios are summarized in Table 6.

## METHODS

### Site description

The study area is the Huewelerbach, a sub-catchment (2.7 km<sup>2</sup> in area, ranging from 280 to 400 m in elevation) of the Attert River basin located in the west of Luxembourg (for detailed information see Martínez-Carreras et al. (2010)). The whole area is part of the "Catchments As Organized Systems" (CAOS) observatory investigating landscape-scale structures, patterns and interactions in hydrological processes for model development (Zehe et al., 2014). The catchment is mainly forested, but the alluvial section of the area is dominated by grassland. The mean annual precipitation of the area is approximately 850 mm (Pfister et al., 2000). In terms of lithology, the Huewelerbach catchment consists of jurassic Luxembourg sandstone which is underlain by marls (Martínez-Carreras et al., 2012, 2010). According to previous studies, the sandstone bedrock and the underlying marls produce a very stable base flow regime (Juilleret et al., 2012). Rainfall-runoff reaction is delayed on the deep sandy soils on hillslopes (deep percolation and subsurface flow). Siltation and compaction in the valley bottom may cause sporadic surface runoff (Sprenger et al., 2016). Measurements at sites Sa\_G and Sa\_K include meteorological variables such as air temperature, humidity and solar radiation and soil moisture at three depths in three different profiles. At the forested site Sa\_G there are also measurements of sap velocity at 4 trees, two of them European Beech (*Fagus sylvatica* L.) and two hornbeams (*Carpinus betulus* L.). Figure 1 shows the study area and the location of the selected sites. Dominant vegetation at site Sa\_G is a relatively young beech forest with a basal area of 16 m<sup>2</sup>/ha. Within the measurement plot we find 34 stems with a mean diameter of 19 cm (median: 14 cm).

### Hydrological model

To simulate the actual evapotranspiration (ET<sub>a</sub>), we applied a hydrological model – WaSiM-ETH (Schulla, 1997). This model is a distributed, deterministic, mainly physical and grid-based hydrological model running with variable time steps

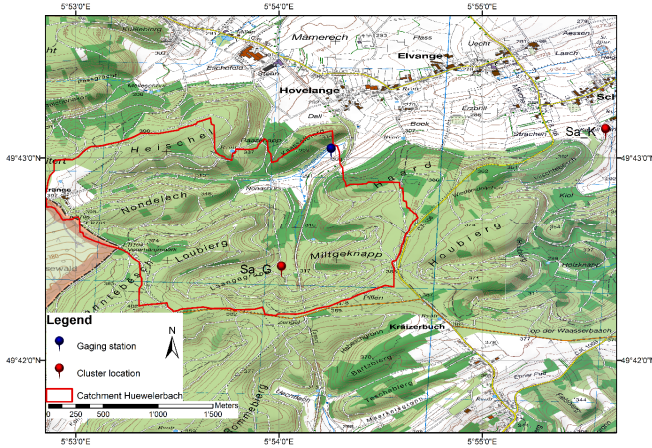


**Fig. 1.** Location of the study area Huewelerbach catchment with the test sites Sa\_G (forest) and Sa\_K (grassland).

(Schulla, 2017). The WaSiM-ETH model has performed well in sub-alpine and alpine catchments (Cullmann et al., 2006; Gurtz et al., 2003; Jasper, 2001; Jasper et al., 2002; Klok et al., 2001; Verbunt et al., 2003), also in middle-mountain (Bie et al., 2015; Grigoryan et al., 2010; Middelkoop et al., 2001), and lowland catchments (Elfert and Bormann, 2010). The model is documented in both English and German and can be used free of cost (<http://www.wasim.ch>). The model comprises different components (e.g. evapotranspiration model, soil model, snow model, glacier model, silting up, surface routing, groundwater model, discharge routing model, lake model etc.). In our case only the modules related to the soil model and evapotranspiration were used and all other components were disregarded.

#### Calculation of evapotranspiration

There are three main steps to estimate the ETa (plant transpiration as well as evaporation from the soil separately) in WaSiM-ETH. First, estimation of potential evapotranspiration (ETp) on the basis of the ground-measured meteorological data; second, simulation of soil water content in vertical direction via Richards equation (Richards, 1931). In the third step, the amount of ETa is simulated at every time step by reducing ETp according to the actual soil water content.

There are four different methods available in WaSiM-ETH model to calculate the ETp rates: Penman-Monteith approach (Monteith, 1981; Monteith et al., 1965); Wendling (Wendling, 1975); Haude (Haude, 1955) and Hamon (Federer and Lash, 1978). In this study, we choose Penman-Monteith equation (Monteith et al., 1965) (see equation 1). It is the most widely used and recommended method for ETp estimation, first developed for agricultural contexts and later also applied to other land covers such as forests (Allen et al., 1998; Droogers and Allen, 2002). This method is based on simulated potential transpiration and the available water content. In our case, actual plant transpiration is simulated in hourly time steps. However, the Penman-Monteith approach has some limitations in practical terms, as a large number of environmental variables are required to determine ETa. This is particularly challenging especially when there is a lack of appropriate atmospheric data (Allen et al., 1998).

$$\lambda E = \frac{3.6 \frac{\Delta}{\gamma_p} (Rn - G) + \frac{\rho c_p}{\gamma_p} (e_s - e) t_i}{\frac{\Delta}{\gamma_p} + 1 + \frac{r_s}{r_a}} \quad (1)$$

where  $\lambda$  is the latent vaporization heat,  $\lambda = (2500.8 - 2.372 \cdot T)$  kJ kg<sup>-1</sup>, with  $T$  is the temperature in °C;  $E$  is the latent heat flux in mm m<sup>-2</sup>  $\equiv$  kg m<sup>-2</sup>;  $\Delta$  is the tangent to the saturated vapor pressure curve in hPa K<sup>-1</sup>;  $Rn$  is the net radiation in Wh m<sup>-2</sup> and  $G = 0.1 \cdot Rn$  is the soil heat flux in Wh m<sup>-2</sup>, the factor 3.6 is used to convert both fluxes from Wh m<sup>-2</sup> to kJ m<sup>-2</sup>;  $\rho$  is the density of dry air,  $\rho = p/(RL \cdot T)$ , at 0 °C and 1013.25 hPa,  $\rho = 1.29$  kg m<sup>-3</sup>;  $c_p$  is the specific heat capacity of the dry air at constant pressure,  $c_p = 1.005$  kJ kg<sup>-1</sup> K<sup>-1</sup>;  $e_s$  is the saturation vapor pressure at temperature  $T$ , in hPa;  $e$  is the observed actual vapor pressure in hPa;  $t_i$  is the number of seconds within a time step;  $\gamma_p$  is the psychrometric constant in hPa K<sup>-1</sup>;  $r_a$  and  $r_s$  are the bulk-aerodynamic resistance and the bulk-surface resistance in s m<sup>-1</sup>, respectively.

#### Resistances for evapotranspiration

The two resistance parameters in the Penman-Monteith equation: the bulk aerodynamic resistance  $r_a$  and the bulk surface resistance  $r_s$  play an important role. However,  $r_s$  (with diurnal and seasonal variations) is more important than  $r_a$  in a forested area for ETa estimation (Beven, 1979). The bulk surface resistance  $r_s$  can be divided into two terms, the soil surface resistance  $r_{se}$  for evaporation from bare soil; and the canopy surface resistance  $r_{sc}$  describing the plant resistances in the transpiration process. There are default values of bulk surface resistance parameters in WaSiM-ETH. The maximum amount of canopy surface resistance  $r_{sc}$  is in November to February, whereas in May to September, it reduces to its annual lowest level (Bie et al., 2015; Schulla, 2017). The soil surface resistance  $r_{se}$  remains constant for the entire year. Table 1 shows the standard values applied for surface resistances parameters in the WaSiM-ETH model (Schulla, 2017).

**Table 1.** Canopy surface resistance  $r_{sc}$  (s m<sup>-1</sup>) and soil surface resistance  $r_{se}$  (s m<sup>-1</sup>).

	Jan	Feb	Mar	Apr	May	Jun	Jul	Aug	Sep	Oct	Nov	Dec
$r_{sc}$	100	100	95	75	65	65	65	65	65	85	100	100
$r_{se}$	230	230	230	230	230	230	230	230	230	230	230	230

#### Simulation of soil water content

For estimation of actual transpiration, WaSiM-ETH simulates soil moisture in the root zone. The soil module in WaSiM-ETH uses the van Genuchten method (Van Genuchten, 1980) for parameterization of the water retention curve to solve the Richard Equation. Water fluxes are simulated vertically in one dimension. Soil moisture in the root soil layer can potentially limit transpiration (Paço et al., 2014). In WaSiM-ETH, soil moisture simulation and ETa are linked, reduction of ETa would result in more water availability in the soil whereas increase of ETa will decrease the soil moisture. The Penman-Monteith equation implicitly includes the influence of soil moisture on plant transpiration through parameter  $r_{sc}$  (canopy surface resistance). Water content in soil profiles changes with time and values of the  $r_{sc}$  also show diurnal and seasonal variations. In dry periods,  $r_{sc}$  is very sensitive to soil moisture. When soil moisture content falls below a given point, the plants start decreasing transpiration to prevent internal water losses. Below that point, soil water availability becomes a key factor in obtaining ETa. ETa is gradually reduced until soil moisture reaches the wilting point at which water is no longer available for transpiration (Allen et al., 1998; Anderson et al., 2007).

### Soil parameterization

Certain predefined parameters of the WaSiM-ETH model are specific for the area where the model was developed. Thus, these parameters should be modified for each new study area. In the investigated area, the predominant soil type was described as ‘‘Podzolic Cambisol’’. The soil texture is loamy sand. It developed on a sandstone bedrock. The maximum rooting depth for the soil was observed at approx. 100 cm. The stone content is relatively low and the unaltered parent sandstone is usually not reached within the first 200 cm below soil surface (Sprenger et al., 2016). These quite sandy soils show a high permeability resulting in deep percolation as the dominant hydrological process.

In the model, the van Genuchten parameters  $\alpha$  ( $m^{-1}$ ) and  $n$  (–) are empirical constants that determine the shape of the WRC, and therefore influence substantially the behavior of the simulation model. We chose three different methods to determine the parameters of the WRC.

#### (i) Baseline parameterization after Teepe et al. 2003

We derived the corresponding van Genuchten parameters in the different soil horizons based on soil texture and bulk density classification obtained by Teepe et al. (2003). This formed our baseline parameterization of the soil in our study area (Table 2).

**Table 2.** Baseline soil parameterization of the WaSiM-ETH soil model (based on Teepe et al. (2003)).

Horizon	1	2	3	4	5	6
PMacroThresh	20					
MacroCapacity	4					
CapacityRedu	0.5					
MacroDepth	1					
Name	Ahe	Ae	Bvs	Bsv	IIBvs	IIBvs
Ksat	1.01E-4	7.95E-05	1.65E-04	1.29E-04	4.84E-05	4.84E-05
K_recession	1	1	1	1	1	1
Theta_sat	0.41	0.41	0.41	0.41	0.41	0.41
Theta_res	0.11	0.05	0.06	0.06	0.13	0.13
Alpha	0.3	0.3	0.26	0.41	0.2	0.2
Par_n	1.17	1.17	1.203	1.191	1.191	1.191
Par_tau	0.5	0.5	0.5	0.5	0.5	0.5
Thickness	0.1	0.1	0.1	0.1	0.1	1
Layers	1	1	1	3	4	7

PMacroThresh (mm/h) is given by the precipitation threshold value and if is reached or exceeded, water can infiltrate into the macropore; MacroDepth (m) is depth of the macropores; MacroCapacity (mm/h) is capacity of the macropores; CapacityRedu ( $m^{-1}$ ) defines the reduction of the macropore capacity per meter soil depth; Ksat ( $m s^{-1}$ ) is saturated hydraulic conductivity that can be given for each soil layer; K\_recession (–) is specified for each soil type describing the recession of the saturated conductivity with depth; theta\_sat ( $m^3/m^3$ ) is saturated water content; theta\_res (–) is the residual water content which cannot be extracted by transpiration;  $\alpha$  ( $m^{-1}$ ) and Par\_n (–) are empirical van-Genuchten parameters; Par\_tau is Mualem parameter; thickness (m) is the thickness of every single numerical layer in the given horizon, and layers defines the number of layers in the given horizon.

#### (ii) Parameterization after Sauer (2007)

Sauer (2007) proposes three different methods to derive the van-Genuchten parameters  $\alpha$  and  $n$ :

Variation 1: Fitting of WRC based on grain size fractions, bulk density and water content at pF 2.5 and 4.2 using the software ‘‘Rosetta Lite’’ (Schaap et al., 2001).

Variation 2: Fitting of WRC based on water content at pF 1.8, 2.5, 4.2 and Theta\_sat (= 41%) using the software ‘‘RETc’’ (Van Genuchten et al., 1991).

Variation 3: Fitting of WRC based on water content at pF 1.8, 2.5, 4.2 using the software ‘‘RETc’’ (Van Genuchten et al., 1991). See Table 3 for the three variations of parameters  $\alpha$  and  $n$ .

**Table 3.** Variations of van Genuchten parameters  $\alpha$  ( $m^{-1}$ ) and  $n$  (dimensionless) in different soil horizons as re-parameterization of the baseline (Table 2).

Horizon		Ahe	Ae	Bvs	Bsv	IIBvs	IIBvs
Variation 1	alpha	0.83	0.83	0.58	0.58	0.88	1.83
	n	1.5653	1.5653	1.6416	1.6416	1.4974	1.4553
Variation 2	alpha	2.86	2.86	3.97	3.97	4.96	1.83
	n	1.3656	1.3656	1.3965	1.3965	1.4598	1.4553
Variation 3	alpha	25.73	25.73	35.87	35.87	29.34	1.83
	n	1.2138	1.2138	1.2506	1.2506	1.3009	1.4553

#### (iii) Parameterization after Sprenger et al. (2016)

Sprenger et al. (2016) list soil parameters for the same site (Sa\_G). These parameters were obtained by fitting the simulation results to observed soil moisture and pore water stable isotope data. In this case the soil profile was divided into three different horizons (Table 4).

**Table 4.** Parameterization of WRC for the site Sa\_G (Sprenger et al., 2016).

Horizon	Ah	B	II_B
width	11 cm	110 cm	> 80 cm
theta_sat	0.546	0.319	0.470
alpha	0.033	0.005	0.005
n	1.228	1.194	1.194
k <sub>sat</sub>	6.11E-04	1.53E-04	6.16E-04

### Data description

To simulate transpiration and soil water content at the forest site Sa\_G, climate data from the grassland site Sa\_K were used as input for the model (Figure 1). These data better represent the atmospheric conditions above the trees which mainly drive the transpiration of the trees. In contrast, climate data from site Sa\_G represents the conditions inside the forest and therefore this data cannot be used in our simulation study. To run the model, climate data between 2013 and 2016 is available. All subsequent model evaluation is done for the year 2015. The years 2013 and 2014 are used as spin-up period until stabilization of the model. Climate data includes air temperature, relative humidity, wind speed, global radiation as five-minute measurements, and precipitation as hourly data. All data were checked for errors and the data gaps were filled. Soil moisture was measured in three profiles per site at 10 cm, 30 cm and 50 cm depth. For our analyses we took the average across all depths and profiles estimating the average soil moisture in the top 60 cm for each site (Hassler et al., 2018). Precipitation data (station Useldange) are available as hourly values with annual mean value of 791 mm for the year 2015 (Agrarmeteorologie Luxemburg: /http://www.agrimeteo.lu). Therefore, all other climate variables and the soil moisture measurements are averaged to hourly values.

Based on the soil moisture and grain size distribution characteristics of the study area, deep percolation is usually observed as dominant runoff generation process. Saturation excess flow or Hortonian overland flow can be excluded.

For the year 2015, transpiration of the adult beech overstory was analyzed by determining sap velocities using the heat ratio method with a central heater needle and two thermistor needles located upstream and downstream of the heater (Köstner et al., 1996). The sap velocity sensors, manufactured by East30Sensors in Washington, were installed at breast height on the north-facing side of the stem and protected with a reflective cover (Hassler et al., 2018). Sap velocities at each of those locations were calculated.

ed from the temperatures measured at the corresponding thermistor pairs according to Equation (2) (Campbell et al., 1991):

$$V_{sap} = \frac{2k}{C_w(r_u + r_d)} \ln\left(\frac{\Delta T_u}{\Delta T_d}\right) \quad (2)$$

where  $V_{sap}$  is the sap velocity ( $\text{m s}^{-1}$ ),  $k$  is the thermal conductivity of the sapwood, set to  $0.5 \text{ W m}^{-1} \text{ K}^{-1}$ ,  $C_w$  is the specific heat of water ( $\text{J m}^{-3} \text{ K}^{-1}$ ),  $r$  is the distance (m) from the heater needle to the sensor (in our case 6 mm) and  $\Delta T$  is the temperature difference (K) before heating and 60 seconds after the heat pulse. Subscripts  $u$  and  $d$  stand for location upstream and downstream of the heater.

These values were corrected to account for wounding of the xylem tissue because of the drilling according to the numerical model solutions for the heat pulse velocity method as suggested by Burgess et al. (2001):

$$V_c = bV_{sap} + cV_{sap}^2 + dV_{sap}^3 \quad (3)$$

where  $V_c$  is the corrected sap velocity ( $\text{m s}^{-1}$ ) and  $b$ ,  $c$  and  $d$  are correction coefficients; for the 2-mm-wounds we have set  $b = 1.8558$ ,  $c = -0.0018 \text{ s m}^{-1}$ ,  $d = 0.0003 \text{ s}^2 \text{ m}^{-2}$  (Burgess et al., 2001).

We selected a dataset of continuous sap velocity measurements from four trees. Daily mean values of the sap velocities were used for the photosynthetically active period from May to October 2015 in which there was a complete time series of sap flow measurements available. Simulated daily sums of actual transpiration from the model were then compared with the average sap velocity of the four trees at the site for the same period (growing season).

For better comparison sap velocities and simulated transpiration were normalized.

### Evaluation of model behavior

In our definition, a model is “behavioral”, when it is able to simulate runoff generation, water balance and the temporal pattern of soil moisture and evapotranspiration consistently with the reality. Therefore, we propose a scheme including four qualitative performance evaluation criteria to check the simulated output. This scheme allows excluding simulations that are not realistic in terms of the four sources of information mentioned above (see Table 5). Sap velocity (SV) and soil moisture (SM) criteria define the necessity of temporal consistency between observed and simulated time series of transpiration and soil water content (by comparing stand transpiration simulations with sap velocity measurements, and by comparing simulated and observed temporal pattern of soil moisture, re-

spectively). Therefore, all simulated time series that would be less consistent with the temporal variability of observations will be rejected. Since actual evapotranspiration is usually less than precipitation in the water budget (Hasenmueller and Criss, 2013), the RETa (“Realistic amount of actual evapotranspiration”) criterion eliminates simulations in which the total amount of evapotranspiration exceeds 750 mm/year. According to our knowledge of local terrain properties and field surveys, RRGP (“Realistic Runoff Generation Process”) criterion was set to deep percolation as the most plausible hydrological process at our site.

In addition to the criteria mentioned above, three widely used statistical goodness-of-fit measures complement the qualitative evaluation of model performance: Mean absolute error (MAE), correlation ( $R^2$ ) and Nash-Sutcliffe efficiency index (NSE) provide additional information on the goodness-of-fit between normalized simulated transpiration and normalized sap velocity (SV) and simulated and observed soil moisture (SM). MAE (Eq. 4) is a basic index (McKeen et al., 2005; Savage et al., 2013) derived from the mean error (difference) between simulated variable and observed variable with the same length and dimensions. This measure is recommended for model performance evaluation (Fox, 1981). It is calculated as follows:

$$MAE = N^{-1} \sum_{i=1}^N |P_i - O_i| \quad (4)$$

where  $N$  is the number of the cases,  $i = 1, 2, 3, \dots, N$ ;  $P$  is the simulation time series, and  $O$  is the observation time series.

While MAE estimates the size of difference, the correlation index  $R^2$  quantitatively estimates the agreement between observations and simulations.  $R^2$  can be expressed as the squared ratio between the covariance and the multiplied standard deviations of the predicted and observed values. Higher  $R^2$  value indicates higher correlation (Legates and McCabe, 1999; Willmott, 1982).

The Nash-Sutcliffe efficiency index (NSE), is dimensionless describing the relative error between simulations and measured data (Nash and Sutcliffe, 1970). It is calculated as:

$$NSE = 1 - \frac{\sum_{i=1}^n (O_i - P_i)^2}{\sum_{i=1}^n (O_i - \bar{O})^2} = 1 - N \frac{RMSE^2}{\sum_{i=1}^n (O_i - \bar{O})^2} \quad (5)$$

where the NSE index demonstrates the normalized ratio of residual variance (noise) to the observation variance ranging between  $-\infty$  and 1. An NSE value is considered to be acceptable when it ranges between 0 and 1. Fewer errors between simulations and observations always lead to a bigger NSE value and a better model performance. It is important to mention that a negative NSE value ( $NSE < 0$ ) indicates a bad model performance that is even worse than the mean of the observed variable.

**Table 5.** Model performance evaluation criteria.

<i>Evaluation element</i>	<i>Description</i>	<i>Evaluation criterion</i>
Sap velocity measurements (SV)	Temporal pattern of sap velocities in terms of normalized values	<b>SV criterion</b> : There should be similar variability and no high deviations between the sap velocities and simulated transpiration amounts
Soil moisture measurements (SM)	Temporal pattern of soil moisture measurements in terms of mean values (%) for uppermost 50 cm of soil layer	<b>SM criterion</b> : There should be similar variability and no high deviations between the soil moisture measurements and simulated soil moisture amounts
Realistic amount of actual evapotranspiration (RETa)	Total amount of evapotranspiration as a component of the water budget in terms of mm/year	<b>RETa criterion</b> : Total evapotranspiration simulated should be between 450 to 750 mm/year
Realistic runoff generation process (RRGP)	Derived from runoff component of the water balance	<b>RRGP criterion</b> : The simulated runoff generation process should be deep percolation <b>and</b> no direct runoff as saturation or Hortonian overland flow

Based on the four evaluation criteria from Table 5 and three performance measures, unrealistic simulations will be eliminated from consideration to attain the best parameterization which provides an overall agreement among the combined performance criteria. Therefore, only under this condition, the simulation will be categorized as “behavioral”.

Applying three groups of scenarios (Table 6), we investigated the soil parameterization that reaches to the behavioral model. The simulation results of each scenario were evaluated by the model performance criteria and statistical goodness-of-fit measures. The soil parameterization in scenario A was taken from Tepee et al. (2003). In the two scenarios B1 and B2, the water retention curve was parameterized with three different variations of the van-Genuchten parameters according to (Sauer, 2007). In scenario C, the model performance was evaluated using the soil parameter set provided by Sprenger et al. (2016).

**RESULTS**

**SCENARIO A: Model parameterization according to Tepee et al. (2003)**

Since logged air or stone fraction may reduce maximum soil moisture at saturation by up to 30% (Mualem, 1974), theta\_sat (saturated water content) is reduced in scenario A1 in three steps from 41% (baseline parameterization according to Tepee et al. (2003), see Table 2) to 35% and finally to 30%. Soil moisture simulated with the baseline parameterization of the soil Table (theta\_sat = 41%) shows much higher values than the measurements (Figure 2). As the parameter theta\_sat decreases, the simulated soil moisture values also decrease. Simulated soil water content with theta\_sat = 30% shows the highest similarity with the measurements. However, the simulated dynamics of the soil moisture simulations do not match the measured dynamics.

Sap velocity rose in the transition from spring to summer and it started to decrease again with the end of the summer (Figure 3). A rapid drop in the sap velocity was observed in June and August 2015 while there was a steep rise in July 2015 for all measuring points. The simulated transpiration with different theta\_sat values and the sap velocity measurements have a similar temporal pattern. Changing the theta\_sat value has only a negligible effect on transpiration (Figure 3).

Evaluation of the water balance (see Table A in the appendix) unveiled that total simulated evapotranspiration (775, 773 and 762 mm/year for theta\_sat = 41, 35 and 30 respectively) is too high. It is close to the annual precipitation amount (791 mm) which is not realistic. The dominant runoff

generation process was saturation excess flow or Hortonian overland flow which is not realistic according to landscape characteristics. Table 7 illustrates the model performance in scenario A1 evaluated by the three statistical efficiency measures as well as by four criteria. Meeting or not meeting a criterion is expressed in terms of “Yes” or “No” respectively. All simulations are highly correlated with the corresponding measurements ( $R^2 \geq 0.73$  for all simulations). Model performances for transpiration show the same values for all theta\_sat. While for the soil moisture, the simulation with theta\_sat = 30 Vol% shows the lowest bias (MAE = 0.02) and a positive NSE (0.55). This confirms the results obtained from visual inspection.

To investigate the effect of scaling the bulk surface resistance parameters ( $r_{sc}$  and  $r_{se}$ ), in scenario A2, the parameters  $r_{sc}$  and  $r_{se}$  are adjusted in the evapotranspiration module of the WaSiM-ETH model. The applied percentage changes were 25, 50, 75, 150, 200 and 400% according to the standard values in the model for deciduous forest (Table 1). Parameter theta\_sat was set to 30 Vol% due to the relatively satisfactory simulation results obtained from scenario A1.

Changing the bulk surface resistance parameters affects the simulated soil water content. The dynamics of the soil moisture simulations are now more consistent with measured values (Figure 2). The best fit could be obtained by decreasing the  $r_{sc}$  and  $r_{se}$  values to 75% and 50% of their standard values, respectively. By lowering the bulk surface resistance parameters, the (potential) evapotranspiration increases. This extracts more water through plant transpiration and soil evaporation. Hence, under these conditions, simulated soil moisture was reduced and became closer to the measured values. The dynamics of the simulated transpiration also corresponds well to the sap velocity measurements (Figure 3).

However, the amount of evapotranspiration losses (850 mm and 867 mm with  $r_{sc} = 75\%$  and  $r_{se} = 50\%$ , respectively) exceeded precipitation input. The simulated runoff generation process was saturation excess flow or Hortonian overland flow which was unrealistic with regard to real soil characteristics at site Sa\_G (Table A in appendix). Evaluation of the results obtained from the scenario A2 is shown in Table 8. Here, all measures indicate an almost perfect fit after scaling the bulk surface resistance (NSE = 0.74 for transpiration, and NSE = 0.85 or 0.91 for soil moisture). This confirms a substantial improvement of simulation accuracy. Nevertheless, runoff generation process and water balance are not correctly reproduced.

**Table 6.** Overview of different scenario combinations.

SCENARIO A (using soil parameterization after Tepee et al. (2003))	A1 (Scaling theta_sat)	-41% -35% -30%	
	A2 Scaling bulk surface resistances theta_sat = 30%	A2-1 (Scaling soil surface resistance $r_{se}$ )	25%-50%-75%-100%- 150%-200%-400%
		A2-2 (Scaling canopy surface resistance $r_{sc}$ )	25%-50%-75%-100%- 150%-200%-400%
	SCENARIO B (using soil parameterization after Sauer (2007))	B1 Re-parameterization of Water Retention Curve with theta_sat = 30%	-Variation 1 -Variation 2 -Variation 3
B2 Re-parameterization of Water Retention Curve with theta_sat = 41%		-Variation 1 -Variation 2 -Variation 3	
SCENARIO C		Soil parameterization after Sprenger et al. (2016)	Comparison to best performing parameter set (theta_sat = 41%, Var1)



**Table 7.** Criteria evaluation and efficiency measures in scenario A1.

Scenario A1: scaling theta_sat						
Criterion	30 Vol%		35 Vol%		41 Vol%	
SV	Yes		Yes		Yes	
SM	No		No		No	
RETA	No		No		No	
RRGP	No		No		No	
Efficiency measure	Transpiration	Soil moisture	Transpiration	Soil moisture	Transpiration	Soil moisture
	R <sup>2</sup>	0.73	<b>0.95</b>	0.73	0.95	0.73
MAE	0.42	<b>0.02</b>	0.42	0.08	0.42	0.13
NSE	0.71	<b>0.55</b>	0.71	-2.66	0.71	-8.92

**Table 8.** Criteria evaluation and efficiency measures in scenario A2.

Criterion	30 Vol% (baseline)		A2-1 (r <sub>sc</sub> = 50%)		A2-2 (r <sub>sc</sub> = 75%)	
SV	Yes		Yes		Yes	
SM	No		Yes		Yes	
RETA	No		No		No	
RRGP	No		No		No	
Efficiency measure	Transpiration	Soil moisture	Transpiration	Soil moisture	Transpiration	Soil moisture
	R <sup>2</sup>	0.73	0.95	0.73	<b>0.94</b>	0.76
MAE	0.42	0.02	0.39	<b>0.01</b>	0.39	<b>0.01</b>
NSE	0.71	0.55	0.74	<b>0.91</b>	0.74	<b>0.85</b>

**Table 9.** Criteria evaluation and efficiency measures for model performances in scenarios B1 and B2.

Criterion	Re-parameterization of the water retention curve – scenario B															
	scenario B1 (theta_sat = 30 %)								scenario B2 (theta_sat = 41%)							
	Baseline		Var1		Var2		Var3		Baseline		Var1		Var2		Var3	
SV	Yes	No	No	No	No	No	No	No	Yes	Yes	No	No	No	No	No	No
SM	No	No	No	No	No	No	No	No	No	Yes	No	No	No	No	No	No
RETA	No	Yes	Yes	Yes	Yes	Yes	Yes	Yes	No	Yes	Yes	Yes	Yes	Yes	Yes	Yes
RRGP	No	Yes	Yes	Yes	Yes	Yes	Yes	Yes	No	Yes	Yes	Yes	Yes	Yes	Yes	Yes
Efficiency measure	SM	Tr	SM	Tr	SM	Tr	SM	Tr	SM	Tr	SM	Tr	SM	Tr	SM	Tr
	R <sup>2</sup>	0.95	0.73	0.75	0.64	0.60	0.37	0.62	0.11	0.93	0.61	<b>0.74</b>	<b>0.73</b>	0.67	0.5	0.62
MAE	0.02	0.42	0.05	0.53	0.07	0.75	0.06	0.97	0.13	0.42	<b>0.02</b>	<b>0.43</b>	0.04	0.66	0.06	0.97
NSE	0.55	0.71	-0.44	0.6	-1.98	0.21	-1.64	-0.34	-8.92	0.71	<b>0.65</b>	<b>0.71</b>	-0.01	0.41	-1.64	-0.34

**SCENARIO B: Re-parameterization of Water Retention Curve**

In scenario B1, van Genuchten parameters of the baseline parametrization of the soil were re-parameterized according to Sauer (2007), where three variations of the parameters “alpha” and “n” were proposed for the same soil type “loamy sand”. Figure 2 depicts soil moisture of the three variations of van Genuchten parameters for a soil with theta\_sat = 30%. All variants underestimate the measured values. Variation of van Genuchten parameters also affects simulated actual transpiration rates: In Figure 3, we clearly see that simulated transpiration does not match the temporal pattern of sap velocity measurements.

In all three variations, the soil was significantly dryer than the measured value. In variation 2 and 3 the soil water content came close to the residual water content. For the simulated transpiration, its temporal consistency with sap velocity decreased from variation 1 to 3. As all three variations performed worse than the best A1 scenario all three variants are rejected.

In scenario B2 we changed theta\_sat from 30 to 41 Vol% and then repeated the three variations of alpha and n after Sauer (2007) and then checked both soil moisture (Figure 2) and

transpiration dynamics (Figure 3). Simulation results with theta\_sat = 41% for the transpiration dynamics are relatively consistent with the observed sap velocities over the entire vegetation period for variation 1. In scenario B2, variation 1 provided sufficient soil water during the vegetation period for plant transpiration. This corresponds well to temporal patterns of sap velocities. Nevertheless, in variation 2 and 3, simulated transpiration did not reproduce the temporal patterns of the sap velocity data. There is a strong deviation in July and August 2015 and at some points the simulated transpiration drops to zero. This is the result of the low soil water content in summer (close to residual water content) for these two variations.

Table 9 provides all evaluation results related to the scenario B. Runoff generation process for all three variations with theta\_sat = 30% and 41% is now deep percolation (Table A in appendix). Furthermore, the total amount of evapotranspiration was less than 750 mm for all variations. Variation 1 with theta\_sat = 41% fulfills all four evaluation criteria. This is confirmed by the three statistical efficiency measures. Here, variation 1 with theta\_sat = 41% clearly performs the best. In accordance with our definition we can label this model parameterization as “behavioral”.

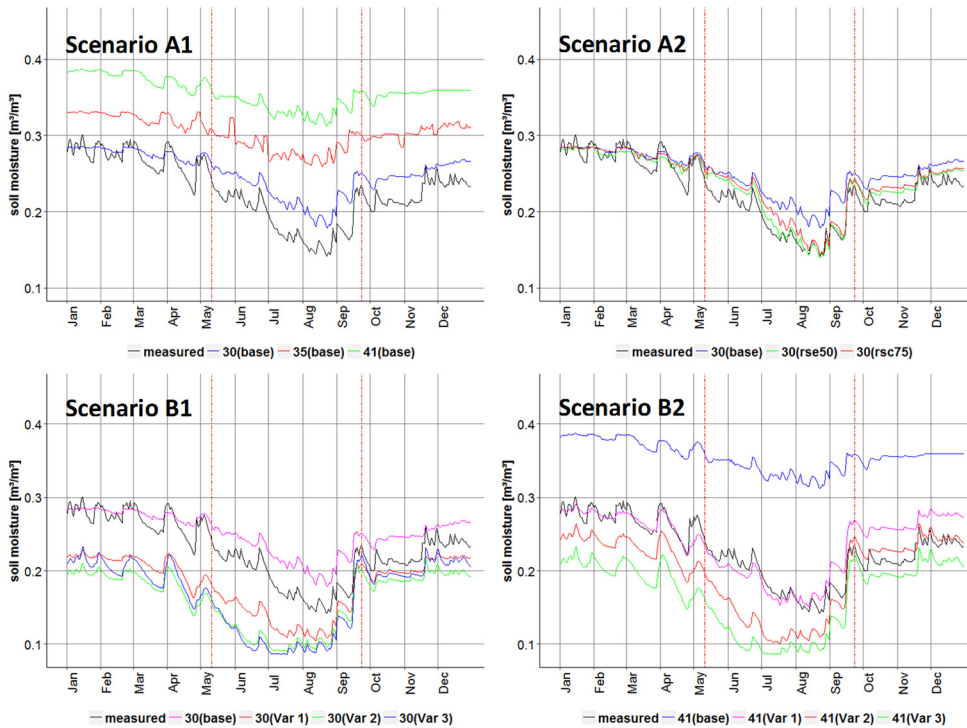


Fig. 2. Simulated and measured soil moisture in the root zone (Vol%) in 2015 for Scenarios A1, A2, B1 and B2. Red vertical lines indicate the growing season.

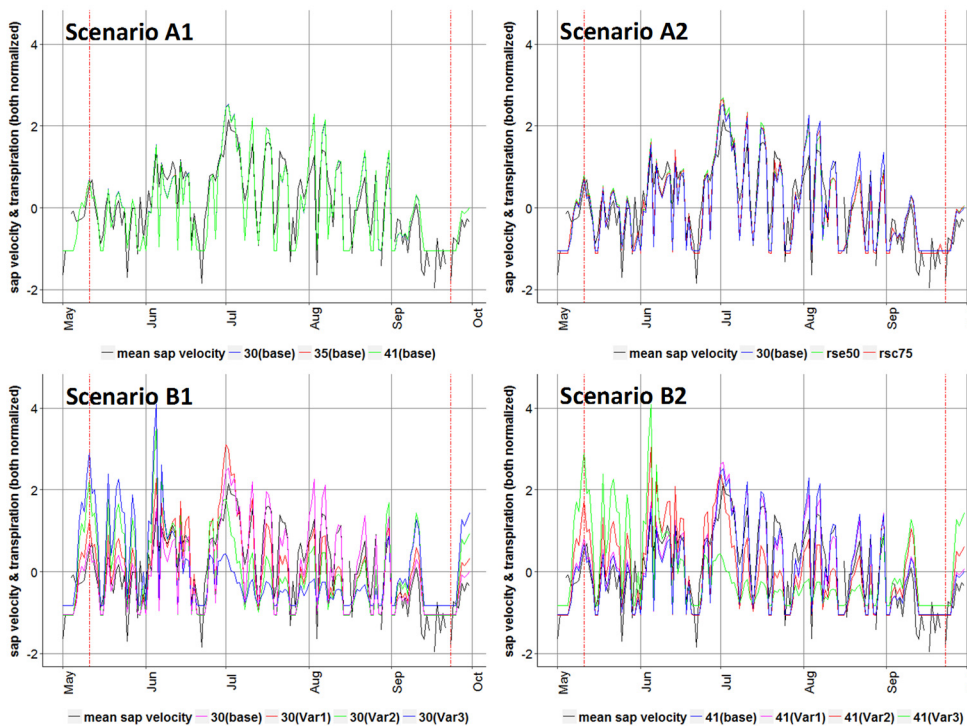


Fig. 3. Simulated transpiration (normalized) and normalized mean values of sap velocity (measured) for growing season 2015 (Scenarios A1, A2, B1, B2). In Scenario A1 all simulations show the same transpiration (identical lines).

**SCENARIO C: Soil parameterization after Sprenger et al. (2016)**

Sprenger et al. (2016) provided a soil parameter set for the Site Sa\_G. In the scenario C, this parameter set was determined by automatic fitting to soil moisture measurements and stable isotope data. We compared this parameterization with our best performing model from the previous section (variation 1 from scenario B2 with  $\theta_{sat} = 41\%$ ).

The simulated runoff generation process was deep percolation which is plausible (Table A in appendix). Total

evapotranspiration (602 mm) was estimated to be lower than precipitation (791 mm) which is also correct. But it can be seen in Figure 4 that soil moisture simulation does not show the correct dynamics compared to the measured time series. Here again, the parameterization of WRC is the reason that the soil is drying out in summer. This causes a significant reduction in transpiration during August which does not correspond to our sap velocity measurements. Additionally, the statistical efficiency measures (Table 10) reveal that the model performs very weak in simulating soil moisture (negative value for NSE). Simulated transpiration is therefore not consistent with the

corresponding sap velocity time series (Figure 5). It shows an overestimation in spring and a slight underestimation in summer, which is also indicated by lower model performance measures compared to the simulation with the optimal parameter set (B2, variation 1 with  $\theta_{\text{sat}} = 41\%$ ) from the previous section.

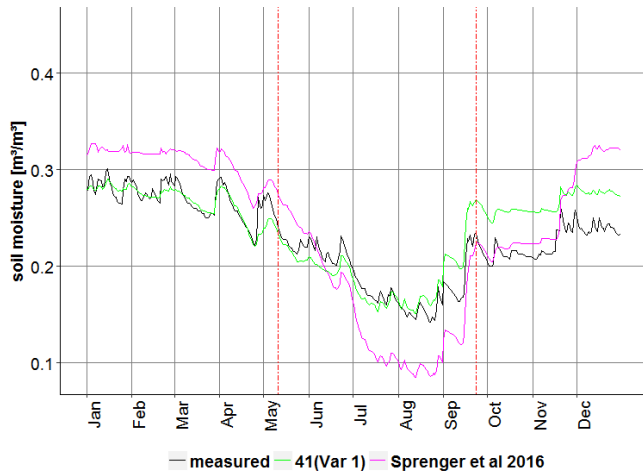


**Fig. 4.** Simulated soil water content for soil parameters according to Sprenger et al. 2016 compared to corresponding measured values and simulated soil moisture from variation 1 ( $\theta_{\text{sat}} = 41\%$ ) in 2015. Red vertical lines indicate the growing season.

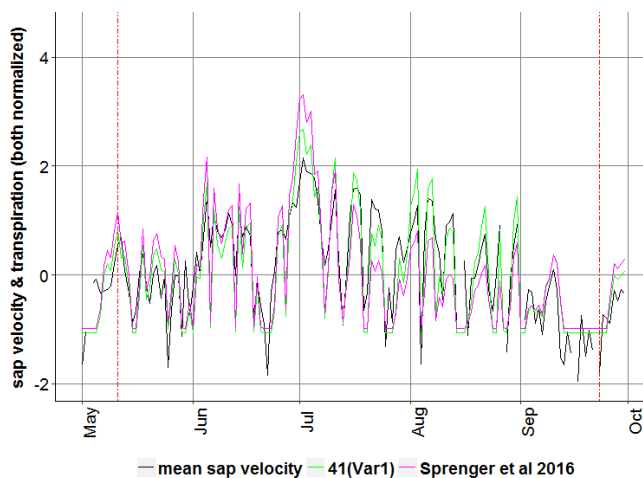


**Fig. 5.** Normalized simulated transpiration for soil parameters according to Sprenger et al. 2016 compared to normalized mean sap velocity (measured) and normalized simulated transpiration for variation 1 ( $\theta_{\text{sat}} = 41\%$ ) in growing season 2015.

**Table 10.** Criteria evaluation and efficiency measures for soil parameterization according to Sprenger et al. (2016).

Criterion	Optimal parameter set ( $\theta_{\text{sat}} = 41\%$ , Variation 1)		Sprenger et al. 2016	
	Transpiration	Soil moisture	Transpiration	Soil moisture
SV	Yes		No	
SM	Yes		No	
REtr	Yes		Yes	
RRGP	Yes		Yes	
Efficiency measure				
	R <sup>2</sup>	0.73	0.74	0.61
	MAE	0.43	0.02	0.55
	NSE	0.71	0.65	0.57
				0.89
				0.04
				-0.11

## DISCUSSION

The main objective of this study was to build up a behavioral forest stand water balance model to characterize the temporal changes in hydrological components of water balance by making use of both observed soil moisture and sap velocities as well as expert knowledge of local runoff generation processes. A behavioral model was defined as a model in which simulation results have to be consistent with measurements of soil moisture and sap velocity and with our hydrologic understanding of runoff generation processes in the area of investigation. To accomplish the objectives, a multi-criteria evaluation scheme was developed. While 24 model realizations were tested, only one model realization could be categorized as “behavioral”.

Results of this study demonstrated that without the use of additional information (e.g. using sap velocity measurements for transpiration dynamics; different soil parameterizations, and expert knowledge), it is not possible to identify a model which captures these processes and dynamics adequately. This sheds light on the value of the contribution of different forms of data in representing the catchment behavior. In a case study in a Swiss Pre-Alpine catchment, it was also found that the application of expert knowledge and the concept of dominant processes can increase the realism of the hydrological models (Antonetti and Zappa, 2018). Taking into consideration that model evaluation would always be partly subjective, we looked at the model behavior from different perspectives through application of multi criteria evaluation that integrated this additional information. Therefore, we were able to select a behavioral parameter set from a number of equally likely soil parameterizations. The development of a multi-criteria approach for model evaluation is based on the consideration that a single measure of performance does not properly extract the information contained in the data (Gupta et al., 1998). This approach includes multiple performance measures and allows to evaluate if the hydrological model is able to represent the behavior of internal catchment processes (Fenicia et al., 2008b). Moreover, our results are also in line with Livneh (2012). He improved model performance significantly by the application of a multi-criteria scheme to evaluate multiple model outputs and by adding supplementary information in the parameterization process (Livneh, 2012). Another study showed that the introduction of constraints was efficient in reducing simulation uncertainty, in conditioning parameters, and in identifying critical parameters (Senapati et al., 2016).

All functions describing soil water retention imply a specific soil hydraulic behavior. Soil parameterization schemes according to Teepe et al. (2003) and Sauer (2007) use different amounts of soil information to derive pedo-transfer functions to translate soil information into van Genuchten parameters. Our results revealed that different parameterizations of the corresponding soil led to diverse simulation results. This issue is of great significance in all models applying the Richard’s equation (e.g. WaSiM-ETH). Therefore, finding a behavioral model for evapotranspiration is highly dependent on the identification of an appropriate WRC. This is consistent with the results of Garrigues et al. (2018). They compared the performance of two water transfer models in simulating evapotranspiration using different soil parameterizations. They found an unexpectedly high model sensitivity to soil moisture at field capacity, root extinction coefficient, and the proportion of homogeneous root distribution (Garrigues et al., 2018). In our proof-of-concept study based on a 1-D model, we took the measurements of sapflow and soil moisture as representative for the “sandstone area” where the dominant hydrologic process is deep percola-

tion. This made it possible to identify a behavioral model. It is known that models might work for the wrong reasons (i.e. reproducing discharge with incorrect process representations) (Beven, 2006; Walker and Zhang, 2002). This makes it advisable to implement expert knowledge to develop a proper parameterization to reflect our perceptions of the processes observed.

## CONCLUSION

A considerable amount of effort is still being devoted to the development of hydrological models, and there is a continuing need to advance the techniques for their parameter estimation. It is also important to develop a good working knowledge of their sensitivity, and strengths and weaknesses.

This study underlines the importance of correctly setting up the 1-D water balance simulation model WaSiM-ETH in order to reproduce the dynamics of soil water fluxes and the physiological control of water loss through transpiration at a specific site (beech forest in Western Luxembourg). Adjustment of the parametrization of the WRC showed a high impact on simulation results. Our main finding was that: even though all parameter sets refer to the same soil ("loamy sand"), a slightly different parameterization of soil moisture at saturation ( $\theta_{sat}$ ), bulk surface resistance parameters and WRC may result in implausible model behavior. Even if transpiration and soil moisture are simulated consistently with our observations, runoff generation or total water balance may be wrongly estimated. Therefore, only the introduction of a multi-criteria evaluation scheme for exclusion of unrealistic outputs allowed finding a well performing parameter set for our test site. These findings suggest that using different sources of information such as expert knowledge on the dominant hydrological processes and the understanding of local controls facilitate parameterization and evaluation of a hydrological model. We should question the generally accepted procedure to parametrize soils using "default" parameter sets based on soil texture description or similar. Only if porosity and WRC for all soil horizons are correctly adjusted, a "physically based" model may simulate runoff processes and transpiration consistently with observations. Only in this case, we may refer to a model as "behavioral" (Gupta et al., 2005). We recommend finding "prototype soils" which are in accordance with soil description (e.g. texture) and expert knowledge on runoff processes in the area under investigation. This in turn implies that model parameterization, evaluation or calibration has to incorporate this "soft" knowledge.

Setups identified as optimal for 1-D simulations will go a long way of improving the application of WaSiM-ETH water balance model on catchment scale to answer questions about watershed characteristics and water resources management. Since point measurements are not valid on catchment scale, we may try to address the spatiotemporal distribution of evapotranspiration, soil moisture and runoff generation processes at catchment scale as well as the estimation of overall water balance at the corresponding gaging station(s) (Koch et al., 2016, 2015). The current study showed that soil parameterization affects not only the temporal distribution of soil moisture and transpiration, but also the runoff generation process. This also highlights the need to consider the incorporation of several data products to increase knowledge about the hydrological processes on catchment scale (Casper et al., 2015). Remotely sensed data will open up the possibility to analyze spatial patterns of actual evapotranspiration (ETa) or soil moisture (Koch et al., 2017). Together with additional knowledge of the spatial distribution of dominant runoff processes on catchment scale this

will facilitate the parameterization of the hydrological model WaSiM-ETH and its subsequent optimization by extending the traditional model evaluation procedure at gaging stations with the search for a best fit of spatial patterns of ETa and runoff processes on catchment scale. A number of automatic mapping approaches for delineation of dominant runoff process exist, which can be used to constrain the uncertainty of hydrological simulations (Antonetti et al., 2016; Behrens et al., 2010). The model RoGeR (Runoff Generation Research) demonstrated its ability to quantify runoff process in high spatial and temporal resolution without the need of parameter calibration (Steinbrich et al., 2016). This approach combines knowledge of runoff process gained through long term research with spatially distributed data sets and can thus be used to extend the here presented approach to the catchment scale.

*Acknowledgements.* The data was collected within the DFG Research Unit FOR 1598 "Catchments As Organized Systems (CAOS)" in a project led by Markus Weiler and Theresa Blume. All datasets can be obtained from Theresa Blume (blume@gfz-potsdam.de) upon request. We thank the technicians Britta Kattenstroth and Tobias Vetter for the maintenance of the sensor network.

## REFERENCES

- Allen, R.G., Pereira, L.S., Raes, D., Smith, M., others, 1998. Crop evapotranspiration-guidelines for computing crop water requirements. FAO Irrigation and Drainage Paper 56. FAO Rome 300, D05109.
- Anderson, M.C., Norman, J.M., Mecikalski, J.R., Otkin, J.A., Kustas, W.P., 2007. A climatological study of evapotranspiration and moisture stress across the continental United States based on thermal remote sensing: 1. Model formulation. *J. Geophys. Res.-Atmospheres*, 112, Article Number: D10117.
- Antonetti, M., Buss, R., Scherrer, S., Margreth, M., Zappa, M., 2016. Mapping dominant runoff processes: an evaluation of different approaches using similarity measures and synthetic runoff simulations. *Hydrol. Earth Syst. Sci.*, 20, 2929–2945. <https://doi.org/10.5194/hess-20-2929-2016>
- Antonetti, M., Zappa, M., 2018. How can expert knowledge increase the realism of conceptual hydrological models? A case study based on the concept of dominant runoff process in the Swiss Pre-Alps. *Hydrol. Earth Syst. Sci.*, 22, 4425–4447.
- Ayyoub, A., Er-Raki, S., Khabba, S., Merlin, O., Ezzahar, J., Rodriguez, J., Bahlaoui, A., Chehbouni, A., 2017. A simple and alternative approach based on reference evapotranspiration and leaf area index for estimating tree transpiration in semi-arid regions. *Agric. Water Manag.*, 188, 61–68.
- Bahreman, A., 2016. HESS Opinions: Advocating process modeling and de-emphasizing parameter estimation. *Hydrol. Earth Syst. Sci.*, 20, 1433–1445.
- Behrens, T., Zhu, A.-X., Schmidt, K., Scholten, T., 2010. Multi-scale digital terrain analysis and feature selection for digital soil mapping. *Geoderma*, 155, 175–185. <http://dx.doi.org/10.1016/j.geoderma.2009.07.010>
- Beven, K., 2006. A manifesto for the equifinality thesis. *J. Hydrol.*, 320, 18–36.
- Beven, K., 1979. A sensitivity analysis of the Penman-Monteith actual evapotranspiration estimates. *J. Hydrol.*, 44, 169–190.
- Bie, W., Casper, M.C., Reiter, P., Vohland, M., 2015. Surface resistance calibration for a hydrological model using evapotranspiration retrieved from remote sensing data in Nahe catchment forest area. *Proc. Int. Assoc. Hydrol. Sci.*, 368, 81–86. <https://doi.org/10.5194/piahs-368-81-2015>
- Blöschl, G., 2001. Scaling in hydrology. *Hydrol. Process.*, 15, 709–711.
- Bromley, J., Jackson, N.A., Clymer, O., Giacomello, A.M., Jensen, F.V., 2005. The use of Hugin® to develop Bayesian networks as an aid to integrated water resource planning. *Environ. Model. Softw.*, 20, 231–242.

- Burgess, S.S., Adams, M.A., Turner, N.C., Beverly, C.R., Ong, C.K., Khan, A.A., Bleby, T.M., 2001. An improved heat pulse method to measure low and reverse rates of sap flow in woody plants. *Tree Physiol.*, 21, 589–598.
- Campbell, G., Calissendorff, C., Williams, J., 1991. Probe for measuring soil specific heat using a heat-pulse method. *Soil Sci. Soc. Am. J.*, 55, 291–293.
- Cash, D.W., Clark, W.C., Alcock, F., Dickson, N.M., Eckley, N., Guston, D.H., Jäger, J., Mitchell, R.B., 2003. Knowledge systems for sustainable development. *Proc. Natl. Acad. Sci.*, 100, 8086–8091.
- Casper, M.C., Gronz, O., Gemmar, P., 2015. Process-oriented parameterisation and calibration of a water balance model. *Hydrol. Wasserbewirtsch.*, 59, 136–144.
- Casper, M.C., Vohland, M., 2008. Validation of a large scale hydrological model with data fields retrieved from reflective and thermal optical remote sensing data – A case study for the Upper Rhine Valley. *Phys. Chem. Earth Parts ABC*, 33, 1061–1067. <http://dx.doi.org/10.1016/j.pce.2008.06.001>
- Cullmann, J., Mishra, V., Peters, R., 2006. Flow analysis with WaSiM-ETH? model parameter sensitivity at different scales. *Adv. Geosci.*, 9, 73–77.
- Droogers, P., Allen, R.G., 2002. Estimating reference evapotranspiration under inaccurate data conditions. *Irrig. Drain. Syst.*, 16, 33–45.
- Durigon, A., Van Lier, Q.D.J., Metselaar, K., 2016. Forcing variables in simulation of transpiration of water stressed plants determined by principal component analysis. *Int. Agrophysics*, 30, 431–445.
- Elfert, S., Bormann, H., 2010. Simulated impact of past and possible future land use changes on the hydrological response of the Northern German lowland ‘Hunte’ catchment. *J. Hydrol.*, 383, 245–255.
- Federer, C.A., Lash, D., 1978. Simulated streamflow response to possible differences in transpiration among species of hardwood trees. *Water Resour. Res.*, 14, 1089–1097.
- Fenicia, F., McDonnell, J.J., Savenije, H.H., 2008a. Learning from model improvement: On the contribution of complementary data to process understanding. *Water Resour. Res.*, 44, 6, Article Number: W06419.
- Fenicia, F., Savenije, H.H., Matgen, P., Pfister, L., 2008b. Understanding catchment behavior through stepwise model concept improvement. *Water Resour. Res.*, 44, 1, Article Number: W01402.
- Fox, D.G., 1981. Judging air quality model performance. *Bull. Am. Meteorol. Soc.*, 62, 599–609.
- Franks, S.W., Gineste, P., Beven, K.J., Merot, P., 1998. On constraining the predictions of a distributed model: the incorporation of fuzzy estimates of saturated areas into the calibration process. *Water Resour. Res.*, 34, 787–797.
- Garrigues, S., Boone, A., Decharme, B., Olioso, A., Albergel, C., Calvet, J.-C., Moulin, S., Buis, S., Martin, E., 2018. Impacts of the soil water transfer parameterization on the simulation of evapotranspiration over a 14-year Mediterranean crop succession. *J. Hydrometeorol.*, 19, 3–25.
- Gharari, S., Hrachowitz, M., Fenicia, F., Gao, H., Savenije, H., 2014. Using expert knowledge to increase realism in environmental system models can dramatically reduce the need for calibration. *Hydrol. Earth Syst. Sci.*, 18, 4839.
- Grayson, R., Blöschl, G., 2001. Summary of pattern comparison and concluding remarks. In: Grayson, R., Blöschl, G. (Eds): *Spatial Patterns in Catchment Hydrology – Observations and Modelling*. Cambridge University Press, Cambridge, UK, pp. 355–367.
- Grigoryan, G.V., Casper, M.C., Gauer, J., Vasconcelos, A.C., Reiter, P.P., 2010. Impact of climate change on water balance of forest sites in Rhineland-Palatinate, Germany. *Adv. Geosci.*, 27, 37–43. <https://doi.org/10.5194/adgeo-27-37-2010>
- Gupta, H.V., Beven, K.J., Wagener, T., 2005. Model calibration and uncertainty estimation. In: Anderson, M. (Ed.): *Encyclopedia of Hydrological Sciences*, Vol. 3, Chapter 131, pp. 2015–2032.
- Gupta, H.V., Sorooshian, S., Yapo, P.O., 1998. Toward improved calibration of hydrologic models: Multiple and noncommensurable measures of information. *Water Resour. Res.*, 34, 751–763.
- Gurtz, J., Zappa, M., Jasper, K., Lang, H., Verbunt, M., Badoux, A., Vitvar, T., 2003. A comparative study in modelling runoff and its components in two mountainous catchments. *Hydrol. Process.*, 17, 297–311.
- Hasenmueller, E.A., Criss, R.E., 2013. Water balance estimates of evapotranspiration rates in areas with varying land use. In: Alexandris, S. (Ed.): *Evapotranspiration-An Overview*. IntechOpen, DOI: 10.5772/52811.
- Hassler, S.K., Weiler, M., Blume, T., 2018. Tree-, stand- and site-specific controls on landscape-scale patterns of transpiration. *Hydrol. Earth Syst. Sci.*, 22, 13–30.
- Haude, W., 1955. Zur Bestimmung der Verdunstung auf möglichst einfache Weise. *Dt. Wetterdienst*, Bad Kissingen.
- Holst, J., Grote, R., Offermann, C., Ferrio, J.P., Gessler, A., Mayer, H., Rennenberg, H., 2010. Water fluxes within beech stands in complex terrain. *Int. J. Biometeorol.*, 54, 23–36.
- Hrachowitz, M., Fovet, O., Ruiz, L., Euser, T., Gharari, S., Nijzink, R., Freer, J., Savenije, H., Gascuel-Oudou, C., 2014. Process consistency in models: The importance of system signatures, expert knowledge, and process complexity. *Water Resour. Res.*, 50, 7445–7469.
- Jasper, K., 2001. Hydrological modelling of Alpine river catchments using output variables from atmospheric models (PhD Thesis). ETH Zurich.
- Jasper, K., Gurtz, J., Lang, H., 2002. Advanced flood forecasting in Alpine watersheds by coupling meteorological observations and forecasts with a distributed hydrological model. *J. Hydrol.*, 267, 40–52.
- Juilleret, J., Iffly, J.-F., Hoffmann, L., Hissler, C., 2012. The potential of soil survey as a tool for surface geological mapping: a case study in a hydrological experimental catchment (Huewelerbach, Grand-Duchy of Luxembourg). *Geologica Belgica*, 15, 1–2, 36–41.
- Klok, E., Jasper, K., Roelofsma, K., Gurtz, J., Badoux, A., 2001. Distributed hydrological modelling of a heavily glaciated Alpine river basin. *Hydrol. Sci. J.*, 46, 553–570.
- Koch, J., Jensen, K.H., Stisen, S., 2015. Toward a true spatial model evaluation in distributed hydrological modeling: Kappa statistics, Fuzzy theory, and EOF-analysis benchmarked by the human perception and evaluated against a modeling case study. *Water Resour. Res.*, 51, 1225–1246. <https://doi.org/10.1002/2014WR016607>
- Koch, J., Mendiguren, G., Mariethoz, G., Stisen, S., 2017. Spatial sensitivity analysis of simulated land surface patterns in a catchment model using a set of innovative spatial performance metrics. *J. Hydrometeorol.*, 18, 1121–1142. <https://doi.org/10.1175/JHM-D-16-0148.1>
- Koch, J., Siemann, A., Stisen, S., Sheffield, J., 2016. Spatial validation of large-scale land surface models against monthly land surface temperature patterns using innovative performance metrics. *J. Geophys. Res. Atmospheres*, 121, 5430–5452.
- Köstner, B., Biron, P., Siegwolf, R., Granier, A., 1996. Estimates of water vapor flux and canopy conductance of Scots pine at the tree level utilizing different xylem sap flow methods. *Theor. Appl. Climatol.*, 53, 105–113.
- Kramer, P.J., Boyer, J.S., 1995. *Water Relations of Plants and Soils*. Academic Press.
- Legates, D.R., McCabe, G.J., 1999. Evaluating the use of “goodness-of-fit” measures in hydrologic and hydroclimatic model validation. *Water Resour. Res.*, 35, 233–241.
- Livneh, B., 2012. Development of a unified land model with multi-criteria observational data for the simulation of regional hydrology and land-atmosphere interaction. PhD Thesis. University of Washington, Seattle, USA.
- Lu, P., Urban, L., Zhao, P., 2004. Granier’s thermal dissipation probe (TDP) method for measuring sap flow in trees: theory and practice. *ACTA Bot. Sin. (Engl. Ed.)*, 46, 631–646.
- Martínez-Carreras, N., Krein, A., Gallart, F., Iffly, J.-F., Hissler, C., Pfister, L., Hoffmann, L., Owens, P.N., 2012. The influence of sediment sources and hydrologic events on the nutrient and metal content of fine-grained sediments (Attert River basin, Luxembourg). *Water. Air. Soil Pollut.*, 223, 5685–5705.
- Martínez-Carreras, N., Udelhoven, T., Krein, A., Gallart, F., Iffly, J.F., Ziebel, J., Hoffmann, L., Pfister, L., Walling, D.E., 2010. The use of sediment colour measured by diffuse reflectance spectrometry to determine sediment sources: application to the Attert River catchment (Luxembourg). *J. Hydrol.*, 382, 49–63.
- McKeen, S., Wilczak, J., Grell, G., Djalalova, I., Peckham, S., Hsie, E.-Y., Gong, W., Bouchet, V., Menard, S., Moffet, R., others, 2005. Assessment of an ensemble of seven real-time ozone forecasts over eastern North America during the summer of 2004. *J. Geophys. Res.-Atmospheres*, 110, Article Number: D21307.
- Middelkoop, H., Daamen, K., Gellens, D., Grabs, W., Kwadijk, J.C.,



Lang, H., Parmet, B.W.A.H., Schädler, B., Schulla, J., Wilke, K., 2001. Impact of climate change on hydrological regimes and water resources management in the Rhine basin. *Clim. Change*, 49, 105–128.

Mohajerani, H., Kholghi, M., Mosaedi, A., Farmani, R., Sadoddin, A., Casper, M., 2017. Application of Bayesian decision networks for groundwater resources management under the conditions of high uncertainty and data scarcity. *Water Resour. Manag.*, 31, 1859–1879.

Monteith, J., 1981. Evaporation and surface temperature. *Q. J. R. Meteorol. Soc.*, 107, 1–27.

Monteith, J., Szeicz, G., Waggoner, P., 1965. The measurement and control of stomatal resistance in the field. *J. Appl. Ecol.*, 345–355.

Mualem, Y., 1974. A conceptual model of hysteresis. *Water Resources Research*, 10, 514–520.

Nash, J.E., Sutcliffe, J.V., 1970. River flow forecasting through conceptual models part I—A discussion of principles. *J. Hydrol.*, 10, 282–290.

Paço, T.A., Pôças, I., Cunha, M., Silvestre, J.C., Santos, F.L., Paredes, P., Pereira, L.S., 2014. Evapotranspiration and crop coefficients for a super intensive olive orchard. An application of SIMDualKc and METRIC models using ground and satellite observations. *J. Hydrol.*, 519, 2067–2080.

Pfister, L., Humbert, J., Hoffmann, L., 2000. Recent trends in rainfall-runoff characteristics in the Alzette river basin, Luxembourg. *Clim. Change*, 45, 323–337.

Richards, L.A., 1931. Capillary conduction of liquids through porous mediums. *Physics*, 1, 318–333.

Sauer, T., 2007. Modellierung von Bodenwasserhaushalt und Abflussprozessen auf der Plotskale in Abhängigkeit von Substrat und Landnutzung (Dissertation). University of Trier, Trier, Germany.

Saugier, B., Granier, A., Pontailler, J., Dufrene, E., Baldocchi, D., 1997. Transpiration of a boreal pine forest measured by branch bag, sap flow and micrometeorological methods. *Tree Physiol.*, 17, 511–519.

Savage, N., Agnew, P., Davis, L., Ordóñez, C., Thorpe, R., Johnson, C., O'Connor, F., Dalvi, M., 2013. Air quality modelling using the Met Office Unified Model (AQUAM OS24-26): model description and initial evaluation. *Geosci. Model Dev.*, 6, 353.

Schaap, M.G., Leij, F.J., Van Genuchten, M.T., 2001. Rosetta: A computer program for estimating soil hydraulic parameters with hierarchical pedotransfer functions. *J. Hydrol.*, 251, 163–176.

Schulla, J., 2017. Model Description WaSiM (Water balance Simulation Model), completely revised version 2017. Zür. Switz. Hydrol. Softw. Consult., 347.

Schulla, J., 1997. Hydrologische Modellierung von Flussgebieten zur Abschätzung der Folgen von Klimaänderungen. PhD Thesis. ETH Zurich.

Seibert, J., McDonnell, J.J., 2002. On the dialog between experimentalist and modeler in catchment hydrology: Use of soft data for multicriteria model calibration. *Water Resour. Res.*, 38, 11, Article Number: 1241.

Senapati, N., Jansson, P.-E., Smith, P., Chabbi, A., 2016. Modelling heat, water and carbon fluxes in mown grassland under multi-objective and multi-criteria constraints. *Environ. Model. Softw.*, 80, 201–224.

Sprenger, M., Seeger, S., Blume, T., Weiler, M., 2016. Travel times in the vadose zone: Variability in space and time. *Water Resour. Res.*, 52, 5727–5754.

Steinbrich, A., Leister, H., Weiler, M., 2016. Model-based quantification of runoff generation processes at high spatial and temporal resolution. *Environ. Earth Sci.*, 75, 1423.

Teepe, R., Dilling, H., Beese, F., 2003. Estimating water retention curves of forest soils from soil texture and bulk density. *J. Plant Nutr. Soil Sci.*, 166, 111–119.

Van Genuchten, M.T., 1980. A closed-form equation for predicting the hydraulic conductivity of unsaturated soils 1. *Soil Sci. Soc. Am. J.*, 44, 892–898.

Van Genuchten, M.T., Leij, F.J., Yates, S.R., Williams, J.R., 1991. The RETC code for quantifying the hydraulic functions of unsaturated soils. U.S. Salinity Laboratory, USDA, Riverside, California.

Verbunt, M., Gurtz, J., Jasper, K., Lang, H., Warmerdam, P., Zappa, M., 2003. The hydrological role of snow and glaciers in alpine river basins and their distributed modeling. *J. Hydrol.*, 282, 36–55.

Vose, J.M., Harvey, G.J., Elliott, K.J., Clinton, B.D., 2003. Measuring and modeling tree and stand level transpiration. In: Lehr, J.H., Keeley, J. (Eds.): *Water Encyclopedia*, Volume 3, Surface and Agricultural Water. Wiley, pp. 732–740.

Wagner, T., Boyle, D.P., Lees, M.J., Wheeler, H.S., Gupta, H.V., Sorooshian, S., 2001. A framework for development and application of hydrological models. *Hydrol. Earth Syst. Sci.*, 5, 13–26.

Walker, G.R., Zhang, L., 2002. Plot Scale Models and their Application to Recharge Studies. Part 10 of Basics of Recharge and Discharge Series. CSIRO Publishing.

Wendling, U., 1975. Zur Messung und Schätzung der potentiellen Verdunstung. *Z. Für Meteorol.*, 25, 103–111.

Willmott, C.J., 1982. Some comments on the evaluation of model performance. *Bull. Am. Meteorol. Soc.*, 63, 1309–1313.

Wilson, K.B., Hanson, P.J., Mulholland, P.J., Baldocchi, D.D., Wullschleger, S.D., 2001. A comparison of methods for determining forest evapotranspiration and its components: sap-flow, soil water budget, eddy covariance and catchment water balance. *Agric. For. Meteorol.*, 106, 153–168.

Zehe, E., Ehret, U., Pfister, L., Blume, T., Schröder, B., Westhoff, M., Jackisch, C., Schymanski, S. J., Weiler, M., Schulz, K., Allroggen, N., Tronicke, J., van Schaik, L., Dietrich, P., Scherer, U., Eccard, J., Wulfmeyer, V., Kleidon, A., 2014. HESS Opinions: From response units to functional units: a thermodynamic reinterpretation of the HRU concept to link spatial organization and functioning of intermediate scale catchments. *Hydrol. Earth Syst. Sci.*, 18, 4635–4655.

Received 30 April 2018  
Accepted 14 November 2018

APPENDIX

Table A. Water balance for all simulation runs, DP = Deep Percolation, SOF = Saturation Overland Flow, HOF = Hortonian Overland Flow.

Scenario	A1			A2		B1:			B2			C
	base-line 41	baseline 35%	baseline 30%	r <sub>sc</sub> 75%	r <sub>se</sub> 50%	Var. 1 30%	Var. 2 30%	Var. 3 30%	Var. 1 41%	Var. 2 41%	Var. 3 41%	
Pot. Evaporation	270	270	270	281	471	270	270	270	270	270	270	270
Real Evaporation	261	259	250	254	372	174	167	179	183	168	179	160
Interception Evaporation	146	146	146	157	146	146	146	146	146	146	146	146
ETp	851	851	851	978	1051	851	851	851	851	851	851	851
ETr	776	774	762	850	867	613	536	497	676	569	497	602
ETr_Layer1 = Transpiration	368	368	365	438	348	293	222	172	347	255	172	296
Baseflow	145	166	107	117	73	212	278	316	251	267	316	196
Direct Runoff	161	11	82	63	73	0	0	0	0	0	0	0
Interflow	0	0	0	0	0	0	0	0	0	0	0	0
Total Runoff	306	177	190	180	146	212	278	316	251	267	316	196
GW recharge	68	114	94	103	64	190	268	307	130	248	307	156
Delta Storage	-290	-160	-161	-239	-222	-33	-22	-22	-136	-45	-22	-7
Precipitation	791	791	791	791	791	791	791	791	791	791	791	791
Total Balance Error	0	0	0	0	0	0	0	0	0	0	0	0
Runoff Process	SOF/H OF	SOF/HOF/DP	SOF/HOF	SOF/HOF	SOF/HOF	DP	DP	DP	DP	DP	DP	DP

## **5.2 A Comparative Investigation of Various Pedotransfer Functions and Their Impact on Hydrological Simulations**

## Article

# A Comparative Investigation of Various Pedotransfer Functions and Their Impact on Hydrological Simulations

Hadis Mohajerani <sup>1,\*</sup>, Sonja Teschemacher <sup>1,2</sup>  and Markus C. Casper <sup>1</sup> 

<sup>1</sup> Department of Physical Geography, Faculty VI, University of Trier, Universitätsring 12, 54296 Trier, Germany; sonja.teschemacher@tum.de (S.T.); casper@uni-trier.de (M.C.C.)

<sup>2</sup> TUM Department of Civil, Geo and Environmental Engineering, Technical University of Munich (TUM), Arcisstrasse 21, 80333 München, Germany

\* Correspondence: mohajerani@uni-trier.de; Tel.: +49-651-2014557; Fax: +49-651-2013976

**Abstract:** Soil hydraulic properties, which are basically saturated and unsaturated hydraulic conductivity and water retention characteristics, remarkably control the main hydrological processes in catchments. Thus, adequate parameterization of soils is one of the most important tasks in physically based catchment modeling. To estimate these properties, the choice of the PTFs in a hydrological model is often made without taking the runoff characteristics of the catchment into consideration. Therefore, this study introduces a methodology to analyze the sensitivity of a catchment water balance model to the choice of the PTF. To do so, we define 11 scenarios including different combinations of PTFs to estimate the van Genuchten parameters and saturated hydraulic conductivity. We use a calibrated/validated hydrological model (WaSiM-ETH) as a baseline scenario. By altering the underlying PTFs, the effects on the hydraulic properties are quantified. Moreover, we analyze the resulting changes in the spatial/temporal variation of the total runoff and in particular, the runoff components at the catchment outlet. Results reveal that the water distribution in the hydrologic system varies considerably amongst different PTFs, and the water balance components are highly sensitive to the spatial structure of soil hydraulic properties. It is recommended that models be tested by careful consideration of PTFs and orienting the soil parameterization more towards representing a plausible hydrological behavior rather than focusing on matching the calibration data.

**Keywords:** pedotransfer functions; soil hydraulic parameterization; catchment water balance; runoff components; hydrologic modeling; spatial pattern comparison; water retention curve



**Citation:** Mohajerani, H.; Teschemacher, S.; Casper, M.C. A Comparative Investigation of Various Pedotransfer Functions and Their Impact on Hydrological Simulations. *Water* **2021**, *13*, 1401. <https://doi.org/10.3390/w13101401>

Academic Editor: Jan Wesseling

Received: 22 April 2021

Accepted: 14 May 2021

Published: 17 May 2021

**Publisher's Note:** MDPI stays neutral with regard to jurisdictional claims in published maps and institutional affiliations.



**Copyright:** © 2021 by the authors. Licensee MDPI, Basel, Switzerland. This article is an open access article distributed under the terms and conditions of the Creative Commons Attribution (CC BY) license (<https://creativecommons.org/licenses/by/4.0/>).

## 1. Introduction

The projected future changes in the land-use, climate, and water cycle lead to an increasing demand for modeling approaches and frameworks for the simulation of hydrological processes at local and regional scale of water resource management. Therefore, a well parameterized and calibrated physically based hydrological model, which is capable of realistically reproducing the behavior of the hydrologic system, is considered particularly important in order to provide decision makers in water resources management with reliable predictions [1]. Soil hydraulic properties have a major impact on the main hydrological processes in catchment areas [2,3]. Therefore, information on these soil properties plays a key role in water balance modeling, and an adequate parameterization of soils is one of the most important tasks in physically based catchment modeling [4,5]. Richard's equation [6], which describes the water flow in unsaturated soil by combining the Darcy–Buckingham law with the continuity equation, is the dominant concept of soil physics in hydrological textbooks [7–9]. It can be considered as the fundamental concept underlying “physically-based” hydrological models [10]. To solve this equation, information on soil hydraulic properties is required [11].

Parameters of soil properties are usually measured as point observations at small scales. However, water balance modeling in catchments requires parameter values at larger



spatial scales such as grid cells or the entire catchment [12]. The Richard's equation is parameterized by either observed soil properties (i.e., measured relations of soil water content and matric potential) or constitutive equations such as the Gardner–Russo model [13], the Brooks-Corey model [13], or the Mualem–van Genuchten model [14,15]. These empirical models represent a basic hydro-physical characteristic of the soil: the relation between soil water content and matric potential [16].

Among the empirical models developed to parameterize the water flow in unsaturated soils, the traditional van Genuchten parameterization [15] has evolved to a de facto standard and is widely used because of its higher degree of fit to observed soil water retention data [17]. Nevertheless, to practically apply this model, obtaining its unknown empirical fitting parameters based on known experimental data (namely, a measured soil water retention curve) is essential. Moreover, at larger spatial scales, such as those of catchment models, direct measurements are not feasible due to the area coverage and the heterogeneity of the soil properties. Therefore, various methods have been developed to determine the van Genuchten parameters, and subsequently, the soil water retention curves using soil parameters that are easier to measure, such as texture, organic matter content, and bulk density. The term pedotransfer function (PTF) has been introduced to define these functional relationships that transfer available measurable soil properties into missing soil properties (e.g., soil hydraulic and soil chemical characteristics) [18]. The derivation of a PTF is usually based on a two-step process. First, the selected water retention function (e.g., van Genuchten) is fitted to measured water retention curves. In the second step, the parameter values determined in this process are related to the selected soil properties [17,19]. During the last three decades, soil scientists have developed a broad set of PTFs that differ with respect to:

1. Applied methods (e.g., statistical regression techniques, data mining and exploration techniques);
2. The underlying database of measured soil moisture retention data used to fit van Genuchten model estimates; and
3. Required input parameters or predictors (e.g., grain size distribution, bulk density, organic matter content) to derive PTF.

Extensive reviews on this content were given by Pachepsky and Rawls (2004) [20]; Wösten et al. (2001) [11]; Vereecken et al. (2010) [17]; and Patil and Singh (2016) [21]. Accuracy and uncertainty of PTFs were evaluated by Schaap and Leij (1998) [22]. They showed that the performance of PTFs may depend strongly on: the data employed for calibration and evaluation, input soil properties, and different applied methods. The databases that have been used to derive PTFs show four remarkable differences:

1. The measurement methods and techniques used to obtain the complete soil moisture retention characteristic in the laboratory;
2. The sample size used at different pressure heads is not the same;
3. The soil textural composition, here the extreme examples are the databases of Schaap and Bouten (1996) [23] which contain only sandy materials, and of Schaap and Leij, (1998) [22] which includes a large number of coarse textured soils and practically no silty soils;
4. Variations in the number of data points, as well as the values of pressure heads used to determine the WRC [17].

Parameterization of soil hydraulic properties should be done in such a way that the hydrological processes simulated using a water balance model match the locally observed processes [24,25]. From a modeler's perspective, the inconsistencies in the data bases used for deriving the different PTFs complicate the evaluation of their reliability in a specific case. For instance, Vereecken et al. (1992) [26] showed that 90% of the variation in predicted moisture supply was attributed to estimation errors in hydraulic properties when using the PTFs developed by Vereecken et al. (1989, 1990) [27,28]. In another study, Chirico et al. (2010) [29] analyzed the effect of PTF prediction uncertainty on soil water

balance components at the hillslope scale. They found that simulated evaporation is more affected by the PTF model error than by errors due to uncertainties in model input data. This sensitivity can result in a compensation of structural model errors by soil parameters, if no careful evaluation of the parameterization of soil hydraulic properties or the simulation of depth-dependent soil moisture content is made [30]. As a result, investigating the model behavior in response to change in the method used to estimate soil hydraulic properties, such as using different types of PTFs, is of major relevance to modelers. However, selection of PTF is usually not guided by its effect on the runoff behavior of the catchment model.

Therefore, the aim of this paper is to evaluate the impact of PTF selection on subsequent changes in the hydrological model behavior. We hypothesize that the PTF-specific soil water retention and hydraulic conductivity curves distinctly affect the water balance and runoff characteristics of the hydrological model, and the resulting differences may be related to the respective soil hydraulic properties of the study area as well as to the methodology to derive the PTF. To test the hypothesis (i) we adapted the soil parameterization in a calibrated and validated hydrological model by varying the underlying PTFs and determined the effects on the soil hydraulic properties of the catchment; and (ii) we analyzed the resulting changes in the model behavior with respect to the catchment outlet, as well as the spatial and temporal variation of the total flow and the flow components.

## 2. Materials and Methods

### 2.1. Study Area

The Glonn catchment area is located in the Tertiary Molasse Hills in Bavaria, Germany. The region is characterized by a low to moderate river density and a runoff coefficient of about 35% [31]. The Molasse basin consists of deposits from the Alps, so the study area comprises a wide range of different grain size compositions. The investigated area of the Glonn catchment has a size of 104 km<sup>2</sup> and an elevation difference of 95 m (Figure 1a), resulting in an average terrain gradient of 4.7%. The soil types were derived from the Übersichtsbodenkarte Bayern (ÜBK25) and consist mainly of Cambisol (65%) and Gley (19%), which is located near the watercourse. These grain size compositions of the soil types are displayed in Figure 1b and cover 71% of the KA5-texture classes [32] and 85% of the FAO texture classes.

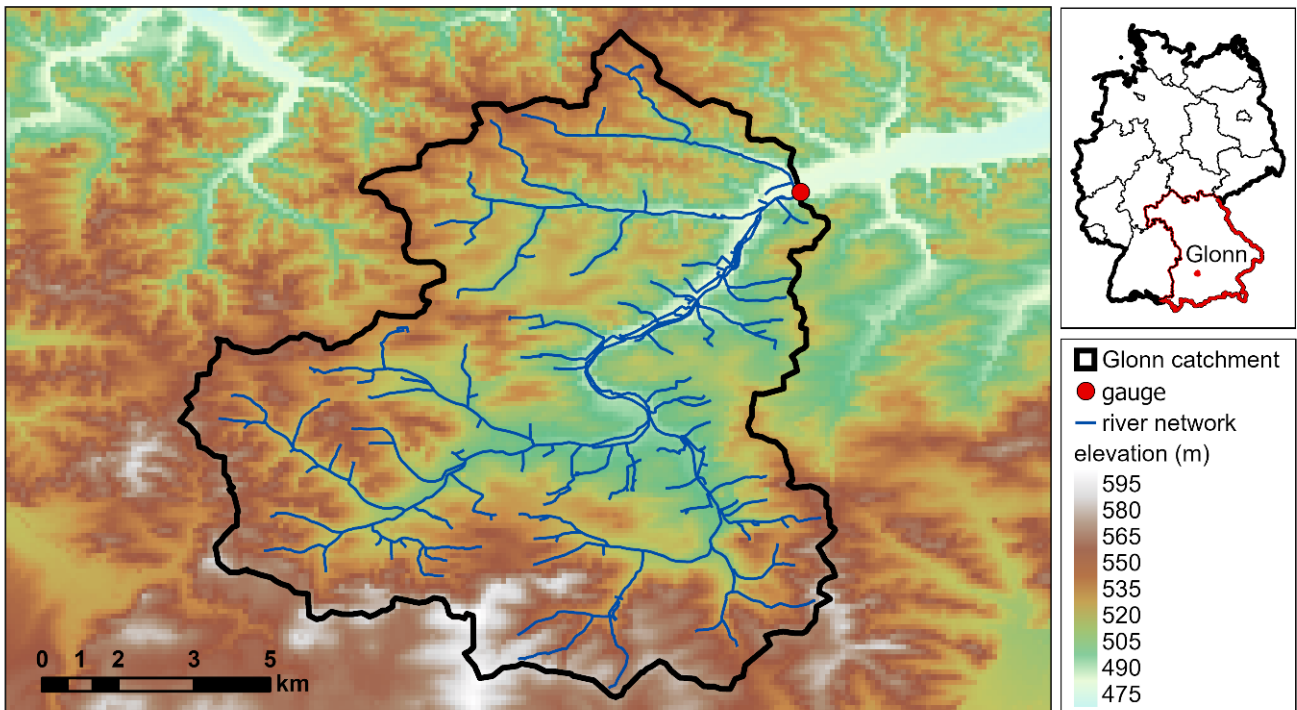
The analysis of the land use distribution is based on a combination of the ATKIS dataset and the INVEKOS data and reveals an extensive agricultural use of the catchment area (Figure 1c). Cropland is the largest land use in the area with 56%, followed by forest (23%) and grassland (12%). Sealed areas (9%) are dominant at the outlet of the catchment area but are more or less evenly distributed over the entire catchment area.

Since the Glonn catchment embraces a high variety of soil and land use types, we consider this catchment to be well suited to study the general effects of different PTFs on the distribution of water in the system and on runoff generation processes.

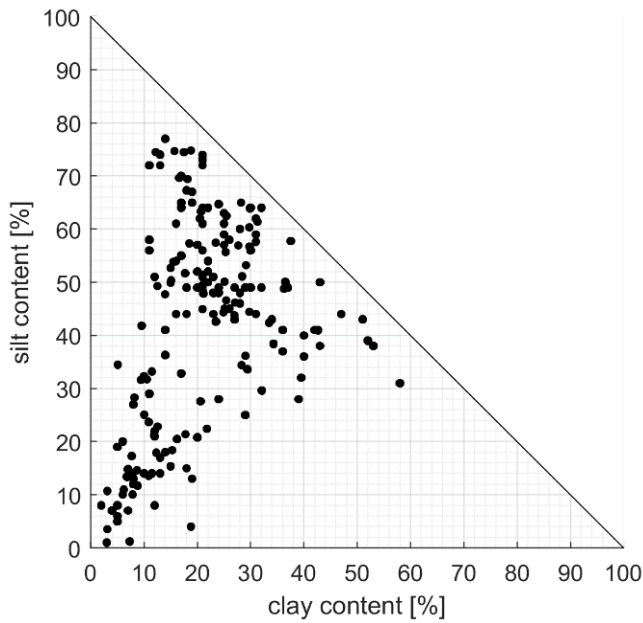
### 2.2. Model Setup and Calibration

The water balance in the catchment area was investigated by applying the hydrological model WaSiM (<http://www.wasim.ch>, accessed on 14 May 2021). WaSiM is a distributed and deterministic model, which includes mostly physical descriptions of the hydrological processes involved. WaSiM is considered illustrative for distributed hydrological models that apply the Richard equation and PTFs to parameterize the soil hydraulic properties. The Richards approach simulates the unsaturated water flow in the soil [6]. In WaSiM, the soil is represented as layered soil columns, in which the thickness as well as the soil characteristics can be defined individually for every horizon. The description of the soil horizons comprises the water retention curve, which are described using van Genuchten parameters [15] and the saturated hydraulic conductivity (Table 1). The modeled discharge has three components (surface flow, interflow, base flow), which represent different response types (fast, intermediate, slow). The model thus allows analyzing the effects of

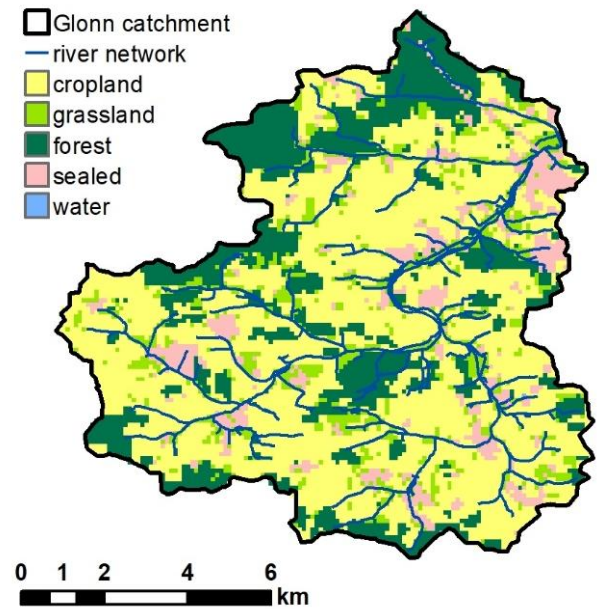
change in soil hydraulic properties caused by multiple soil parametrizations (with different PTFs) on the runoff behavior of the catchment.



(a) Digital elevation model, location, and river network



(b) Distribution of grain size compositions



(c) Land use distribution

Figure 1. Topography (a), soil characteristics (b), and land use (c) of the Glonn catchment.

**Table 1.** Mandatory parameters to describe a soil horizon in the WaSiM control file.

Parameter	Description
Horizon	ID for each soil horizon; one value per horizon.
Layer	Number of numerical layers for each horizon.
Thickness	Thickness of each single numerical layer in this horizon in m; one value per horizon.
$K_{\text{sat}}$	Saturated hydraulic conductivity in m/s; one value per soil horizon.
$\Theta_{\text{sat}}$	Saturated water content (fillable porosity in 1/1); one value per soil horizon.
$\Theta_{\text{res}}$	Residual water content (in 1/1, water content which cannot be extracted by transpiration, only by evaporation); one value per soil horizon.
$\alpha$	van Genuchten Parameter $\alpha$ ; one value per soil horizon.
$n$	van Genuchten Parameter $n$ ; one value per soil horizon.
$K_{\text{recession}}$	$K_{\text{sat}}$ recession with depth: factor of recession per meter (only applied for the uppermost 2 m of the soil); one value per horizon.

We set up the model on a spatial scale of 100 m and a temporal scale of 1 h. The required topographic spatial data (e.g., slope, flow accumulation, sub-catchment structure) were derived from TANALYS (i.e., a pre-processing tool of WaSim-ETH) [33] by performing a complex analysis of the DEM. The land use map is equivalent to the above-mentioned combination of ATKIS and INVEKOS data (Figure 1c). The soil map is derived and parameterized based on the Übersichtsbodenkarte Bayern (ÜBK25). The depth profiles of the bulk density and organic matter content of the soil types were adapted according to the overlying main land use type. For the calibration of the baseline scenario, we choose: (1) the PTF of [19] to derive the van Genuchten parameters, and (2) the KA5 [32] which contains a table for the derivation of saturated hydraulic conductivities from texture classes. The considered input time series contain precipitation, temperature, relative humidity, global radiation, and wind speed interpolated from station data.

We calibrated the model manually based on stream flow data at the gaging station of Odelzhausen near the catchment outlet. The evaluation of the model runs was based on a visual analysis, obtaining a plausible water balance, and statistical indices. These indices are the NSE (Nash–Sutcliffe Efficiency), NSE log (NSE with logarithmic values), and PBIAS (percent bias) [34]. The evaluation results show a good representation of the runoff characteristics of the catchment, while underestimating the runoff volume during the calibration period and slightly overestimating it during the validation period (Table 2). The volume shares of the water balance components are in a plausible range with a runoff coefficient of about 32% to 33%, which is close to the literature value of the region [31]. The calibrated model is regarded as a benchmark model (“baseline scenario”, see Table 3). Therefore, the effect of PTF selection will be investigated through multiple scenarios (Table 3) without the interference of a recalibration. This means, the exact representation of the reality is of minor importance.

**Table 2.** Goodness of fit criteria and shares of water balance components for the calibration and validation period.

Parameter	Calibration	Validation
Time period	1 November 1995–31 October 2004	1 November 2004–31 October 2013
NSE	0.74	0.65
NSE <sub>log</sub>	0.61	0.67
PBIAS	13.2	−1.9
<b>Volume share of</b>		
Baseflow	0.16	0.14
Interflow	0.14	0.14
Surface runoff	0.04	0.05
Evapotranspiration	0.68	0.67

**Table 3.** Scenario definition: combinations of PTFs to determine the van Genuchten parameters ( $\theta_{\text{sat}}$ ,  $\theta_{\text{res}}$ ,  $\alpha$ ,  $n$ ) and the saturated hydraulic conductivity ( $K_{\text{sat}}$ ).

Scenario	Van Genuchten Parameter	Saturated Hydraulic Conductivity
Baseline	Wösten et al. (1999) [19]	Ad-Hoc AG Boden (2006) [32]
1	Renger et al. (2009) [35]	Ad-Hoc AG Boden (2006) [32]
2	Weynants et al. (2009) [36]	Ad-Hoc AG Boden (2006) [32]
3	Zacharias & Wessolek (2007) [37]	Ad-Hoc AG Boden (2006) [32]
4	Teepe et al. (2003) [38]	Ad-Hoc AG Boden (2006) [32]
5	Zhang & Schaap (2017): Rosetta H2w [39]	Ad-Hoc AG Boden (2006) [32]
6	Zhang & Schaap (2017): Rosetta H3w [39]	Ad-Hoc AG Boden (2006) [32]
7	Wösten et al. (1999) [19]	Wösten et al. (1999) [19]
8	Renger et al. (2009) [35]	Renger et al. (2009) [35]
9	Zhang & Schaap (2017): Rosetta H2w [39]	Zhang & Schaap (2017): Rosetta H2w [39]
10	Zhang & Schaap (2017): Rosetta H3w [39]	Zhang & Schaap (2017): Rosetta H3w [39]

### 2.3. Scenario Definition

The influence of the PTF selection on the catchment runoff behavior was investigated through different simulation runs. These include 11 scenarios in which the PTFs used to determine the van Genuchten parameters and saturated hydraulic conductivity were altered. The respective combinations are summarized in Table 3. The so-called “baseline scenario” is the model run for which the calibration and validation was performed (Section 2.2). It serves as the benchmark for the other scenarios and thus as the basis for the scenario comparison. The soil profiles that were modified because of the PTF selection were limited to areas with cropland, grassland, and forest land use. The parameterization of sealed surfaces and water surfaces were identical in all scenarios. The definition of the saturated hydraulic conductivities by using the table of Ad-Hoc AG Boden (2006) [32] (Scenarios 1 to 6) or the corresponding equations of selected PTFs (Scenarios 7 to 10) allows a separate consideration of their respective influence on the runoff behavior.

The seven PTFs adopted for scenario development (Table 3), are described in Table 4. The selection was based on the wide distribution and extensive application of the PTFs in European studies [38,40–43]. Their potential applicability to the study area and the respective performance were not considered in order to obtain a wider range of possible results. The van Genuchten parameters  $\theta_{\text{sat}}$ ,  $\theta_{\text{res}}$ ,  $\alpha$ ,  $n$ , which are required for the soil description in WaSiM, are specified by all selected PTFs. The PTFs of Wösten et al. (1999) [19],



Renger et al. (2009) [35] and Zhang & Schaap (2017) [39] additionally contain a definition of the parameter  $K_{\text{sat}}$  (saturated hydraulic conductivity). The key differences among the PTFs, apart from the underlying databases, are the number of considered soil samples and the selected predictors. While soil texture is included in all PTFs as a predictor, in some other PTFs, bulk density (BD), and organic matter content (OM) are not always taken into account.

**Table 4.** Overview of the selected PTFs including their main characteristics.

PTF	Method	Database	Sample Size	Predictors
Wösten et al. (1999) [19]	Regression analysis	HYPRES [19]	5521	Clay, Silt, OM, BD, topsoil/subsoil
Renger et al. (2009) [35]	Regression analysis	various sources	unknown	Sand, Silt, Clay
Weynants et al. (2009) [36]	Regression analysis	Vereecken et al., 1989 [27]	166	Sand, Silt, Clay, BD, OM
Zacharias and Wessolek (2007) [37]	Regression analysis	IGBP-DIS soil data (Tempel et al., 1996) [44]; UNSODA (Nemes et al., 2001) [43]	676	Sand, Silt, Clay, BD
Teepe et al. (2003) [38]	Regression analysis	Teepe et al. (2003) [38]	1850	Lookup table: Sand, Silt, Clay, BD
Zhang & Schaap (2017), Rosetta H2w [39]	Single Artificial Neural Network	Schaap et al. (2001) [45]	2134 for WRC, 1306 for $K_{\text{sat}}$	Sand, Silt, Clay
Zhang & Schaap (2017), Rosetta H3w [39]	Single Artificial Neural Network	Schaap et al. (2001) [45]	2134 for WRC, 1306 for $K_{\text{sat}}$	Sand, Silt, Clay, BD

Clay: percentage of clay, Silt: percentage of silt, OM: percentage of organic matter, BD: bulk density.

## 2.4. Evaluation Strategies

The differences among the modeling scenarios are caused by the respective soil hydraulic properties, which are dependent on the underlying PTFs. Therefore, the basis for the scenario evaluation was to identify features or patterns in the input and output data, and to determine the causal relationships of these patterns. This process involves various model parameters used to examine the influence of PTFs on the runoff behavior of the catchment quantitatively and qualitatively. The evaluation strategy is to analyze the changes in: (1) soil hydraulic properties; (2) runoff response at the catchment outlet; (3) the partitioning of the water balance components in time and space, and (4) the resulting dominant runoff processes. Through this, each scenario evaluation was carried out in relation to the calibrated baseline scenario.

### 2.4.1. Soil Hydraulic Properties

The van Genuchten parameters, which are determined using the different PTFs, define the shape of the water retention curve, i.e., the relationship between soil moisture and suction. This relationship specifies the pore volume that is available for water retention at a given matric potential. Accordingly, it has a distinct effect on the runoff characteristics of a catchment. In combination with the saturated hydraulic conductivity, the water retention curve also has an influence on the relationship between soil moisture and unsaturated hydraulic conductivity. This dependency influences the vertical water movement in the soil and thus the infiltration characteristics.

In order to quantitatively evaluate and compare the characteristics of the water retention curves and hydraulic conductivities of the different PTFs, we considered the variables of plant-available water capacity (AWC), field capacity (FC), and saturated hydraulic conductivity ( $K_{\text{sat}}$ ). The FC corresponds to the pore volume which is filled with water at a matric potential of  $pF = 1.8$ . The AWC is the respective pore volume between  $pF = 1.8$  and  $pF = 4.2$ . Values of FC and AWC were determined for each grid cell for the uppermost

meter of the soil profile, and  $K_{\text{sat}}$  was analyzed for individual soil horizons. The distribution of these values were statistically examined using box plots analysis, considering only cropland, grassland, and forest areas. In addition, demonstration of the spatial distribution of these three variables (AWC, FC,  $K_{\text{sat}}$ ) can be used to establish qualitative relationships between soil hydraulic properties and land use distribution or topography.

#### 2.4.2. Runoff Response

The total runoff at the catchment outlet or a gauging station is the most common model parameter used for the calibration or evaluation of a hydrological model. Since the model calibration was only performed for the baseline scenario, a comparison of the other scenarios with the measured hydrographs is not meaningful. Therefore, the scenario hydrographs were solely compared to the respective hydrograph simulated by the baseline scenario. The evaluation includes both a visual inspection of the event characteristics and a quantitative analysis of the differences between baseline and scenarios using signature indices.

The calculation of the signature indices is based on the flow duration curve (FDC). FDC is equivalent to the flow exceedance probability curve and is commonly used to represent and classify the catchment functioning. Accordingly, the FDC indicates the ability of the catchment to produce runoff values of different magnitudes and is therefore dependent on the vertical redistribution of the soil water content [46,47]. This vertical redistribution results in 'fast', 'intermediate', and 'slow' runoff components within the discharge hydrograph associated with surface runoff, interflow, and baseflow [48]. A set of signature indices is considered to be a characteristic fingerprint of the respective hydrological response of the catchment in terms of producing different runoff components. Thus, signature indices can be used to evaluate runoff components and parameters that control the runoff processes as well as the overall water balance. In this study, we derive the following signature indices:

1. %BiasRR: The percent bias in overall runoff ratio is a diagnostic signature index of the total water balance. It is expected to show primary sensitivity to model parameters that control evapotranspiration.
2. %BiasMidslope: The percent bias of the mid-segment slope of the FDC (between 20% and 70% exceeding probability) indicates the reactivity of the catchment to the rainfall events and quantifies the rainfall-runoff response rate.
3. %BiasFHV: The percent bias in high-segment volumes of the FDC (<2% exceeding probability) is related to the surface runoff and compares the peak discharges for heavy rainfall events.
4. %BiasFLV: The percent bias in low-segment volumes of the FDC (>70% exceeding probability), that reflects the minimum discharge values and is related to the base flow.

A detailed description of the general procedure and the relevant equations is presented in Casper et al. (2012) [49].

#### 2.4.3. Water Balance Components

We provide a deeper insight into the catchment behavior by a quantification of the differences amongst scenario simulations corresponding to runoff and water balance components, which are caused by the choice of the PTF. The components were considered and compared at different spatial and temporal resolutions or clusters.

A detailed analysis of the water balance components was performed for the outlet gage of the catchment using annual sums. It includes runoff components (surface runoff, interflow, and baseflow), evaporation components (evaporation, transpiration, interception evaporation, and snow evaporation) and storage components (soil storage, interception storage, and snow storage). In addition, we considered the amount and distribution of infiltration components to explain the changes in the water balance and link them to the soil hydraulic properties obtained from the different PTFs. The investigation of the temporal and spatial differences resulting from the PTF selection was limited to the runoff

components of surface runoff, interflow, and baseflow. We considered the frequency of certain shares of the flow components on the total runoff.

#### 2.4.4. Spatial Pattern Analysis

To compare spatial pattern of water balance components simulated in different scenarios, we use two different metrics: (i) the Pearson correlation coefficient  $\alpha$  between the spatial water balance components of the baseline model (A) and PTF scenarios (B); and (ii) the percentage of histogram intersection  $\gamma$  [50].  $\gamma$  reveals only the agreement on the distribution of the variable in space [51]. The term  $\gamma$  is calculated for a given histogram K of the baseline maps (A) and the histogram L of the PTF scenario maps, each comprising 'n' bins, here we use 100 bins.

$$\alpha = \rho(A, B) \quad (1)$$

$$\gamma = \frac{\sum_{j=1}^n \min(K_j, L_j)}{\sum_{j=1}^n K_j} \quad (2)$$

### 3. Results

#### 3.1. Soil Hydraulic Properties

The distribution of the selected soil hydraulic properties in the Glonn catchment is displayed in Figure 2. The data contains all cells with cropland, grassland and forest land use, whereas sealed areas and water bodies are not included. AWC and FC were summarized for the uppermost meter of the soil profile. In contrast, the  $K_{\text{sat}}$  is presented for the top layer (horizon 1) and for the soil horizon 3, which accounts for a depth of about 75 cm. The thickness of the horizons, and consequently the depths of them, vary among the soil types. For AWC and FC, we included all PTFs, which have their own specific equation to estimate  $K_{\text{sat}}$ , and those that consider the parametrization of Ad-hoc-AG Boden [32] for  $K_{\text{sat}}$ .

The median values of the soil hydraulic properties as well as the size of the interquartile ranges show a clear dependency on the respective PTF. The range of the median values is larger for AWC than for FC, whereas the size of the interquartile ranges or the total variability is larger for FC. Accordingly, for each PTF, AWC is relatively similar within one PTF for all soil types within the catchment, most notably in the PTFs of Wösten et al. (1999) [19], Renger et al. (2009) [35], and Weynants et al. (2009) [36]. The values of AWC for the PTF of Wösten et al. (1999) [19], which is considered in the baseline scenario, range within the values of the other PTFs. The lowest AWC values were determined using the PTF of Zacharias & Wessolek (2007) [37]. The PTF with the most frequent large AWC values is the one of Zhang & Schaap (2017) [39] that does not consider bulk density as input (Rosetta H2w). The distinction in the ranges of AWC values amongst the PTFs are pronounced differently from those of FC. This indicates the variability of the available soil water storage volumes depending on the preconditions.

The range of simulated  $K_{\text{sat}}$  by the baseline scenario (defined according to Ad-Hoc AG Boden, 2006) [32] is within the values of the other PTFs for the considered horizons. The largest median of  $K_{\text{sat}}$  was defined via Renger et al. (2009) [35]. This PTF is also the only one for which the median increases from horizon 1 to horizon 3. The distinctly smaller variability of  $K_{\text{sat}}$  in Rosetta H2w compared to Rosetta H3w is due to the lack of consideration of the bulk density in Rosetta H2w.

The largest spatial variation of the AWC differences ( $\Delta\text{AWC}$ ) was found for Teepe et al. (2003) [38]. Here, the soil water storage capacities of flat areas with forest or grassland cover are increased (compared to baseline scenario), while decreased for other land uses. This observation is in accordance with the distribution displayed in Figure 2, which shows a similar median as the baseline scenario, but a distinctly larger variability. The PTF of Zacharias & Wessolek (2007) [37] results in an overall lower soil water storage with lower values in valleys and thus a contrasting behavior compared to Teepe et al. (2003) [38]. Weynants et al. (2009) [36] and both versions of Zhang & Schaap (2017) [39] show a



predominantly higher soil water storage with some exceptions next to the rivers. In most cases, the areas of lower AWC in Weynants et al. (2009) [36] are not equal to those of Zhang & Schaap (2017) [39].

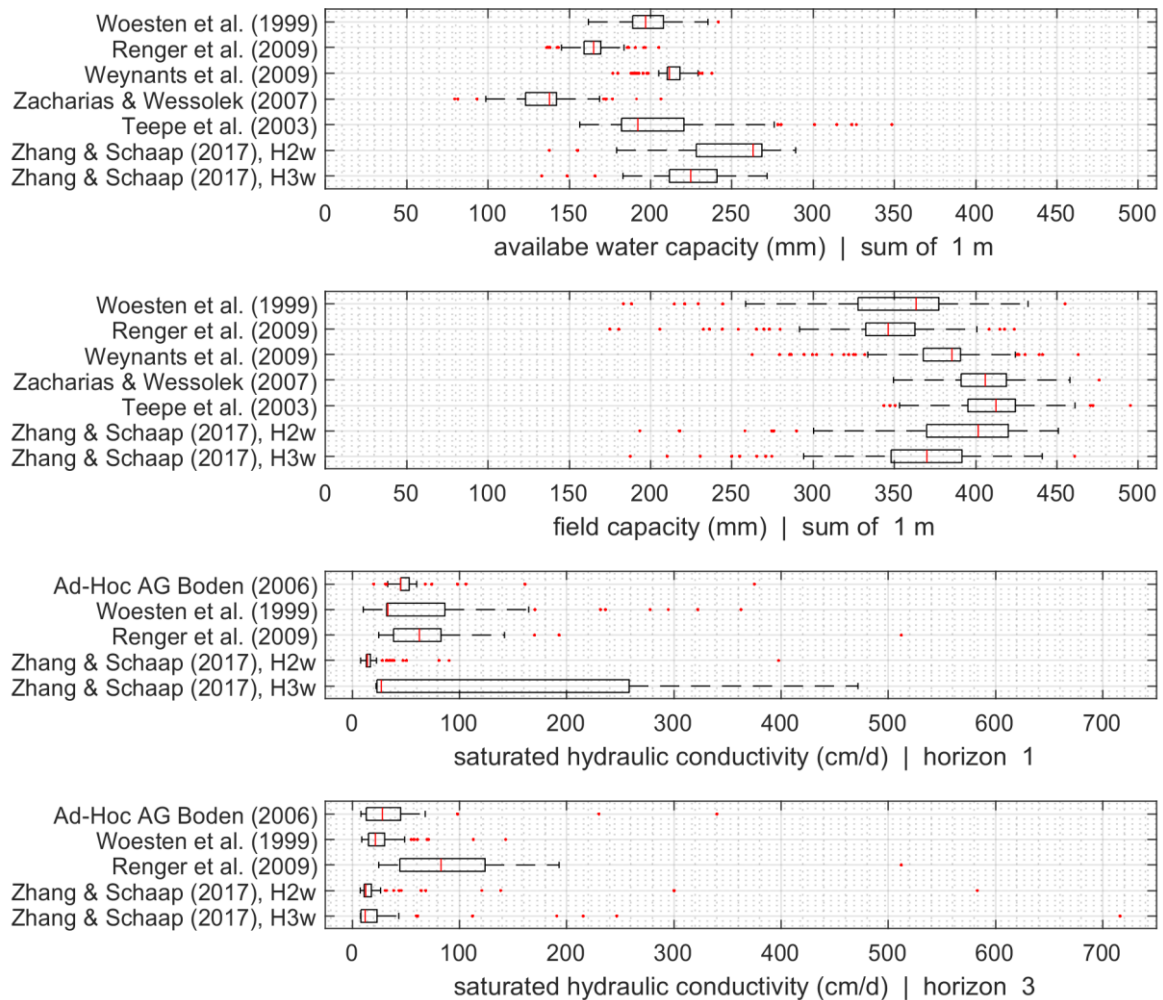
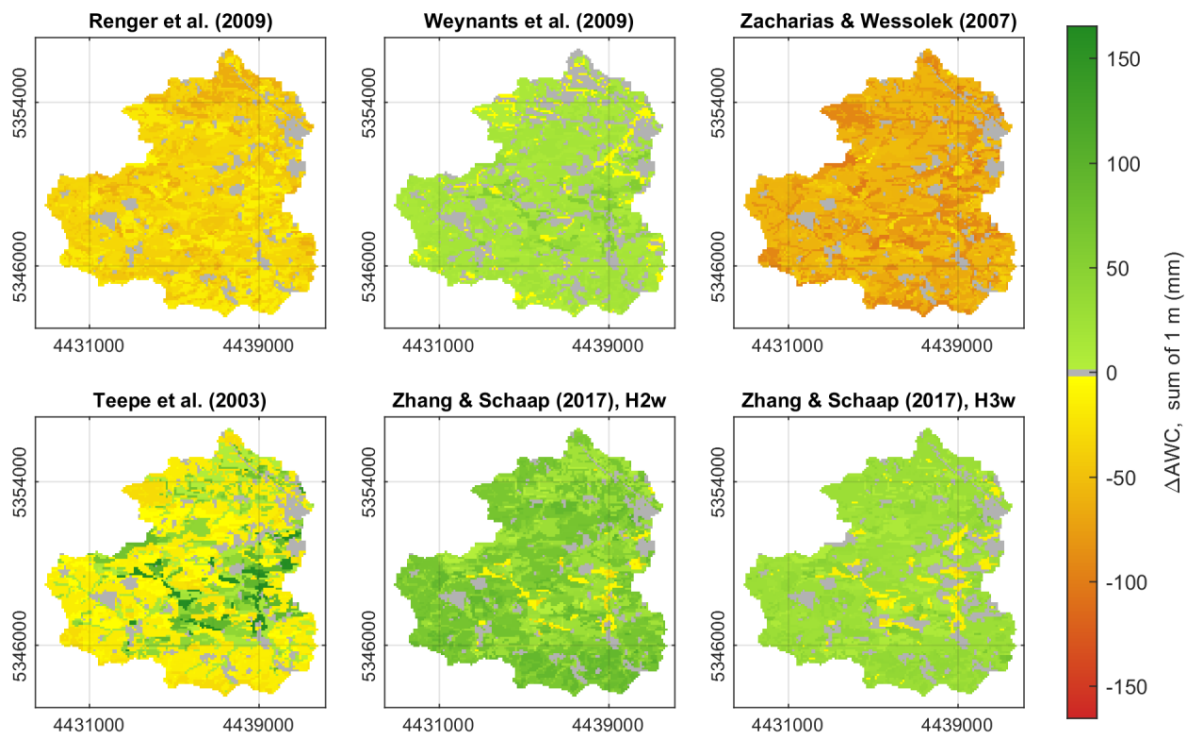


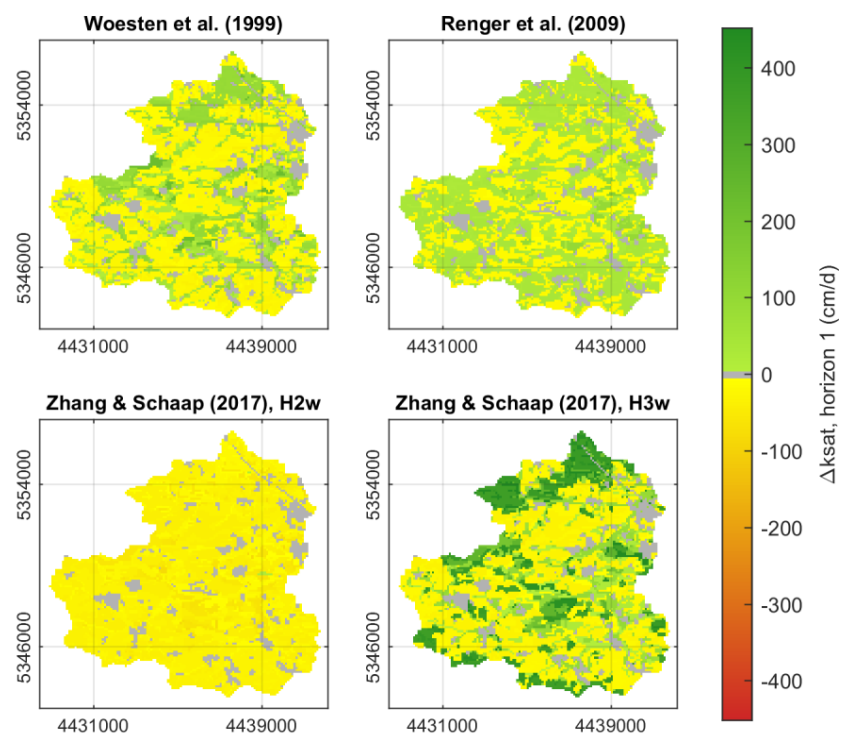
**Figure 2.** Distribution of the soil hydraulic properties AWC, FC, and  $K_{sat}$  for the land use types cropland, grassland and Forest in the Glonn catchment.

The shapes of the water retention curves are influenced by the input parameters of the PTFs as well as the databases used for their development (Table 4). Accordingly, the dependency of the soil water storage capacity can be related to the land use types, which affect the bulk density and organic matter content of the respective soil type. Furthermore, the variation of the soil texture class can have different effects on soil water holding capacities depending on the PTF that results in the observed non-linear shift of the soil hydraulic properties between the scenarios and the baseline scenario.

The saturated hydraulic conductivities in the topmost soil horizon of Renger et al. (2009) [35] are mostly larger than those of Ad-Hoc AG Boden (2006) [32], whereas those of Zhang & Schaap (2017), H2w [39] are lower (Figure 3b). The largest differences compared to the baseline scenario ( $\Delta K_{sat}$ ) were observed in Zhang and Schaap (2017), H3w [39]. Forest sites result in much higher values of  $K_{sat}$ , while the increase is less distinct on grassland sites. On cropland, the  $K_{sat}$  values of Zhang & Schaap (2017) [39], H3w are mostly lower than those of Ad-Hoc AG Boden (2006) [32]. The differences in Wösten et al. (1999) [19] are also attributed to the land use type but less distinguished. The dependency of  $K_{sat}$  on the land use type is driven by the inclusion of bulk density and/or organic matter content in the PTFs.



(a) available water capacity AWC (baseline: Wösten et al. (1999) [19])



(b) saturated hydraulic conductivity  $K_{sat}$  (baseline: Ad-Hoc AG Boden (2006) [32])

**Figure 3.** Spatial distribution of differences in soil hydraulic properties ( $\Delta AWC$ ,  $\Delta K_{sat}$ ). AWC is calculated for the first meter of the soil profile and the  $K_{sat}$  at the uppermost horizon of the soil profiles.

### 3.2. Runoff Response

The different soil hydraulic properties of the PTFs result in a change in runoff behavior that is evident in both the total volume and the event characteristics. Figure 4 shows the hydrographs of the different scenarios (model runs) for two exemplary flood events. The quantitative evaluation of the peak and volume changes are summarized in Table 5. The double-peaked event in June 2013 was analyzed separately for the first and second wave. The range of runoff peaks of the different scenarios compared to the baseline scenario is between +43% and −65% (Table 5).

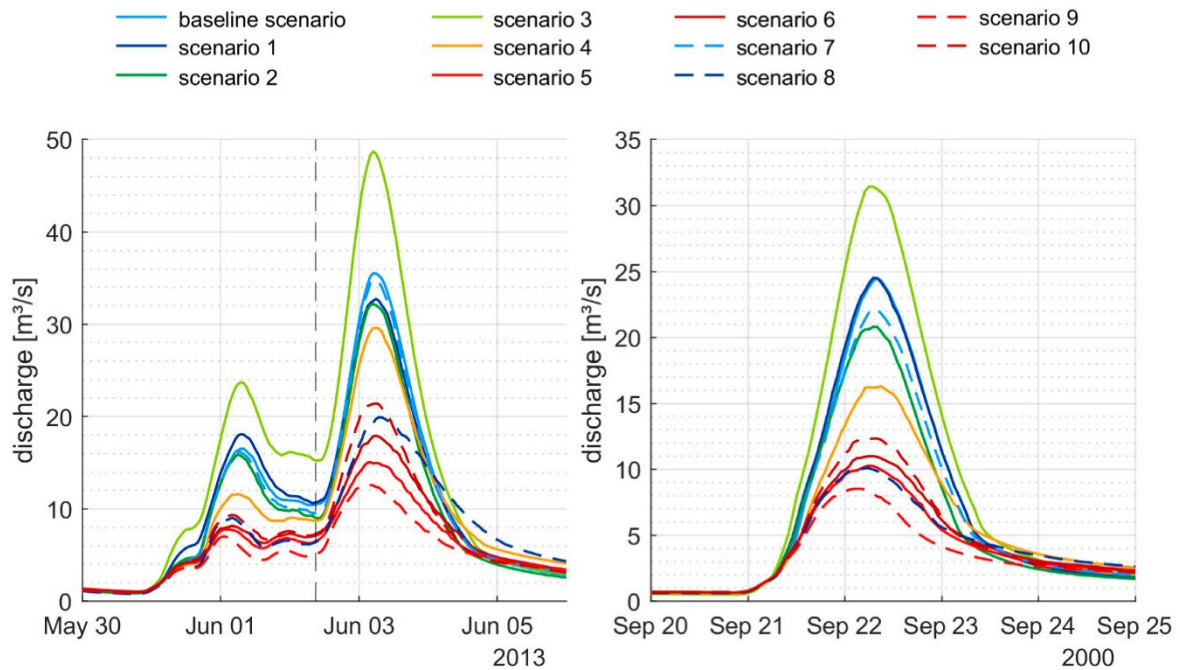


**Figure 4.** Hydrographs of the baseline scenario and the 10 scenario runs for two exemplary events (scenario description: Table 3).

**Table 5.** Peak changes (%) and volume changes (%) of the selected events in Figure 4 and the calibration and validation periods the event in June 2013 is evaluated separately for both peaks.

Scenario	Peak Change (%)			Volume Change (%)				
	06/2013 (1)	06/2013 (2)	09/2000	06/2013 (1)	06/2013 (2)	09/2000	calib.	valid.
1	9.4	−7.9	0.0	10.0	−4.6	1.0	−4.7	−0.5
2	−3.8	−9.4	−15.1	−5.4	−11.1	−13.0	−5.2	−4.5
3	43.4	37.0	28.3	44.1	29.2	26.8	−6.7	−4.7
4	−29.8	−16.7	−33.6	−20.7	−8.0	−18.9	−5.7	−4.6
5	−52.9	−57.6	−58.0	−39.9	−42.6	−41.1	−0.6	−0.7
6	−50.5	−49.5	−55.1	−36.2	−34.6	−36.9	−0.9	−0.6
7	−2.2	−1.9	−9.5	−3.6	−2.7	−6.6	0.0	0.4
8	−45.3	−43.9	−58.8	−39.5	−21.7	−39.3	−2.4	0.3
9	−57.4	−64.6	−65.2	−49.8	−50.1	−50.4	−0.6	−0.8
10	−43.3	−39.7	−49.6	−32.3	−30.4	−34.3	−1.9	−1.6

The largest runoff response occurred in scenario 3, which is based on the PTF of Zacharias & Wessolek (2007) [37], which resulted in the lowest AWC values, in comparison

to other PTFs (Figure 2). The lowest runoff peaks and volumes occur in Scenarios 5 and 9, which are based on Rosetta (H2w). This PTF resulted in the largest AWC values compared to the different PTFs (Figure 2). The distinctly larger antecedent soil moisture conditions during the second peak of the flood event in June 2013 results in a different change in runoff behavior depending on the PTF. It can lead to a decrease in the percent peak change (Scenario 4), an increase in the percent peak change (Scenario 2), or even in a reversal in the direction of the peak change (Scenario 1) compared to the baseline scenario (Figure 2, Table 5). The volume changes of the calibration and validation period are small compared to those of the events. The variations indicate a different behavior in distinct discharge ranges, whose separate analysis is therefore of special interest.

For a quantitative analysis of the change in modeled runoff behavior caused by the choice of PTFs as well as the change in distinct discharge ranges, the flow duration curves at the basin outlet were compared, and four signature indices were calculated (Table 6).

**Table 6.** Signature indices of the 10 scenarios compared to the baseline scenario; evaluation period: 1 November 1995–31 October 2013.

Scenario	%BiasRR	%BiasMidslope	%BiasFHV	%BiasFLV
1	−2.6	7.5	10.1	−16.8
2	−4.8	1.0	−3.9	−11.2
3	−5.7	87.5	43.5	−47.2
4	−5.1	43.3	−11.8	−25.4
5	−0.6	20.2	−24.6	−11.1
6	−0.7	38.1	−20.8	−25.7
7	0.2	1.0	−2.5	−0.3
8	−1.0	−0.1	−23.5	6.1
9	−0.7	−3.6	−34.7	14.1
10	−1.7	27.1	−18.0	−21.3

As expected, Scenario 7 shows only minor deviations in catchment behavior. However, there are obvious deviations in estimating the water balance by different scenarios (%Bias<sub>RR</sub>; e.g., underestimated up to −5.7% for scenario 4), revealing that the choice of PTF has a considerable impact on the estimated evapotranspiration. Regarding the reactivity (%Bias<sub>Midslope</sub>), the tendency of scenarios 3, 4, and 6 is similar: showing markedly increased values (highly overestimated compared to the baseline scenario), that indicates a fast reaction of catchment to rainfall events and its direct transformation into runoff. In contrast, most scenarios exhibit an underestimation of the discharge peaks, only the scenarios 1 and 3 overestimate the peaks (positive value of %Bias<sub>FHV</sub>). Concerning the low flows (related to base flow components), we can see a contrasting model behavior for the scenarios: While the hydrological model tends to underestimate low flows for most of the scenarios (distinctly pronounced in case 3, 4, and 6), a severe underestimation of low flows results from scenario 3 (−47.2%).

### 3.3. Water Balance Components and Spatial Pattern Analysis

The differences in the runoff behavior amongst the scenarios can be addressed by analyzing the respective water balance and infiltration components. As displayed in Table 7, there are noticeable changes occurring in the runoff components as well as in the components influenced by the soil hydraulic properties, i.e., evaporation from the soil and change in soil water storage. The soil hydraulic properties also control the amount of matrix infiltration, which affects the infiltration excess and consequently the surface runoff.

**Table 7.** Mean annual amount of the water balance and infiltration components for the baseline scenario and the 10 scenarios.

	Water Balance Components (mm/a)								Infiltration Components (mm/a)						
	Surface Runoff	Interflow	Base Flow	Transpiration	Evaporation	Snow Evaporation	Interception Evaporation	Change in Soil Storage	Change in Snow Storage	Infiltration Excess	Macropore infiltration	Matrix Infiltration	Interception Evaporation	Snow Evaporation	
<b>Baseline</b>	39	117	121	99	302	14	163	4	0	39	19	625	163	14	
<b>Scenario</b>	<b>1</b>	42	121	108	98	303	14	163	10	0	42	19	622	163	14
	<b>2</b>	41	113	110	99	316	14	163	4	0	41	19	624	163	14
	<b>3</b>	50	117	95	99	323	14	163	0	0	50	18	615	163	14
	<b>4</b>	37	89	136	99	322	14	163	0	0	37	19	627	163	14
	<b>5</b>	34	120	122	97	310	14	163	0	0	34	19	630	163	14
	<b>6</b>	34	135	106	97	310	14	163	0	0	34	19	630	163	14
	<b>7</b>	39	121	119	99	302	14	163	4	0	39	19	625	163	14
	<b>8</b>	36	123	117	99	299	14	163	10	0	36	19	628	163	14
	<b>9</b>	35	107	133	97	309	14	163	1	0	35	19	629	163	14
	<b>10</b>	35	133	108	97	311	14	163	0	0	35	19	629	163	14

The large runoff reactivity of scenario 3 (Figure 3) can be attributed to an increased amount of surface runoff (Table 7) which is caused by a reduction in matrix infiltration and a resulting decrease in baseflow. Compared to the baseline scenario, scenario 4 shows a slightly increased matrix infiltration and correspondingly a reduced surface runoff volume. Larger differences occur in the slower runoff components, with a significant reduction in the interflow volume and an increase in the magnitude of the baseflow. Although there is only little increase in total infiltration compared to the baseline scenario, the change in soil hydraulic properties results in a more efficient transport of water to deeper soil layers. The evaporation volumes of the scenarios 3 and 4 are the largest in comparison to other scenarios, and are about 7% higher than the baseline scenario.

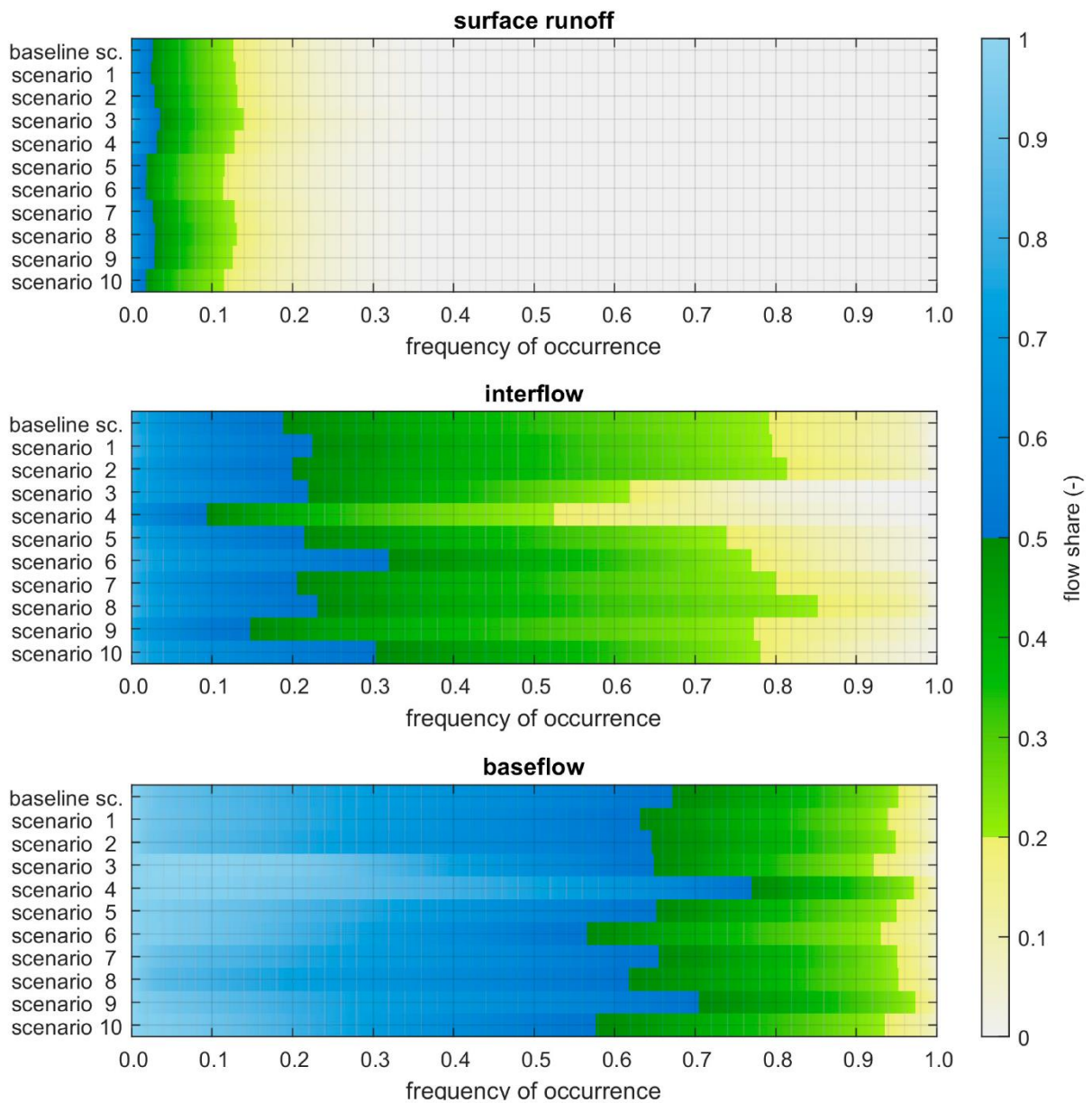
The lowest runoff response of the all scenarios occurs for the scenarios 5, 6, 9, and 10. In these scenarios, surface runoff volumes are reduced in a uniform manner by about 10–13% compared to the baseline scenario. The changes in interflow and baseflow are more diverse. While the volumes are only slightly changed in scenario 5, a significant increase in interflow with a simultaneous large reduction in baseflow could be observed in scenarios 6 and 10. In contrast, in scenario 9, the interflow is reduced and the baseflow is increased, resulting in an enhanced proportion of surface runoff during the events and leading to the earlier and lower peak discharge as observed in Figure 3 compared to scenario 5. We can conclude that in both cases the use of  $K_{sat}$  estimated by the respective PTFs leads to a reduction in interflow and an increase in baseflow (scenarios 5 and 6 compared to 9 and 10). This behavior is more pronounced between scenarios 5 and 9 (Rosetta, H2w) than between scenarios 6 and 10 (Rosetta, H3w).

Figure 5 shows the frequency of occurrence of different flow shares for all runoff components. Blue colors indicate the dominance of the respective component (probability > 50%), green colors indicate a flow share of 20–50%, whereas yellow to grey colors indicate a probability below 20% for the respective runoff component. Scenarios 5, 6, and 10 show the shortest time periods dominated by surface runoff. While Scenario 5 shows dominance of baseflow in relatively longer time periods, Scenarios 6 and 10 remarkably indicate longer periods with interflow as dominant runoff generation process. Scenarios 4 and 9 have the shortest periods with dominant interflow but the longest with baseflow as the dominant runoff generation process.

In order to compare the spatial patterns of the evapotranspiration and runoff components simulated by 10 scenarios to the baseline scenario, we analyzed the Pearson correlation coefficient  $\alpha$  and percentage of histogram overlap  $\gamma$ , considering the spatial mean of direct runoff, interflow, baseflow, and actual evapotranspiration (ETa) (Table 8).

For direct runoff, the spatial correlation of occurrence is very high but the absolute amount is different, which is indicated by a low histogram overlap. For interflow, some scenarios show both low spatial correlation and low histogram overlap, indicating that the PTF has a high impact on this runoff generation process in the model. In contrast, the baseflow pattern is similar in all scenarios. Interestingly, in all scenarios, the ETa pattern show a high correlation, however, the absolute values seem to differ considerably (relatively low values for histogram overlap).





**Figure 5.** Frequency of occurrence of flow shares for all runoff components (scenario description: Table 3).

**Table 8.** Spatial correlation (correl) and histogram overlap (histo) of the 10 scenarios compared to the baseline scenario, for spatial mean of direct runoff, Interflow, baseflow, and ETa.

Scenario	Correl	Histo	Correl	Histo	Correl	Histo	Correl	Histo
	Direct Runoff		Interflow		Baseflow		ETa	
1	0.997	0.804	0.942	0.893	0.996	0.985	0.997	0.819
2	0.999	<b>0.697</b>	0.975	0.892	0.998	0.976	0.998	0.727
3	0.992	<b>0.423</b>	<b>0.782</b>	<b>0.769</b>	0.978	0.970	0.988	<b>0.349</b>
4	0.997	0.786	<b>0.500</b>	<b>0.381</b>	0.976	0.987	0.997	0.744
5	0.997	0.653	0.835	0.829	0.990	0.966	0.996	<b>0.652</b>
6	0.995	<b>0.473</b>	0.916	0.874	0.995	0.965	0.998	<b>0.653</b>
7	0.999	0.683	0.962	0.898	0.999	0.994	1.000	0.827
8	0.997	0.758	0.913	0.910	0.997	0.988	0.997	0.846
9	0.997	0.712	<b>0.795</b>	<b>0.746</b>	0.990	0.975	0.995	<b>0.626</b>
10	0.996	0.782	0.900	0.909	0.994	0.965	0.997	<b>0.618</b>

#### 4. Discussion

The selection of the PTF to estimate the soil hydraulic properties which are included in a hydrological model is often done without taking the runoff characteristics of the catchment into consideration. Therefore, it is of particular interest to the modeling community to have a quantitative description of the change in model behavior caused by the choice of PTF, in order to make decisions that are more informed. We hypothesized that the water balance and runoff behavior of a catchment are distinctly affected by the characteristics of the PTFs that primarily represent the water retention and hydraulic conductivity curves. Thus, we considered the soil parameterization of different PTFs in a hydrological catchment model to quantify the changes in soil hydraulic properties of the Glonn catchment as well as to analyze the resulting shifts in its water balance components and runoff characteristics.

As shown in Figure 1b, the Glonn catchment covers a wide range of different soil texture classes. It is therefore well suited for studying the influence of PTFs on soil hydraulic properties as well as the resulting runoff behavior. This high diversity allowed holding a more profound analysis of the spatial and temporal variability of different runoff characteristics depending on the choice of the respective PTF. The good representation of the runoff behavior by WaSiM-ETH suggests the general suitability of this hydrological model for the intended investigation. Moreover, the implementation of a layered soil structure made it possible to consider the underlying soil properties in detail.

The baseline scenario and the 10 other scenarios (Table 3) were chosen in such a way that the influence of modified van-Genuchten parameters or saturated hydraulic conductivities could be separately explored. Since the calibration was only performed for the baseline scenario, the differences in the runoff behavior amongst scenarios can be directly attributed to the modified soil parameters. Nevertheless, this approach cannot provide a definitive assessment of the suitability of the PTFs to represent the runoff behavior in the catchment. This evaluation would require the calibration of all scenarios using the same calibration strategy. However, due to the resulting over-imposition of the runoff behavior by the calibration parameters, the direct analysis of the particular influence of the changed soil properties would no longer be possible. Therefore, the calibration of the scenarios was not performed. Nevertheless, the parameters of the calibrated baseline scenario are within the parameter space of the other scenarios, and thus their hydrographs scatter around the measured runoff.

The considered PTFs resulted in a wide range of different shapes for the water retention and saturated hydraulic conductivity curves. The shape of the water retention curve is mainly associated with the parameters  $n$  and  $\alpha$  which are included in the soil parameterization in WaSiM-ETH (Table 1). The parameters are related to the process of



saturation and desaturation of the soil [52]. The hydraulic parameters AWC, FC, and  $K_{\text{sat}}$  determined for a quantitative comparison of the curves showed significant differences in their spatial distribution (Figure 2). These differences become particularly evident when comparing the individual scenarios with the baseline scenario. This issue is important because spatial variability of soil hydraulic properties is regarded as a significant factor to water distribution in the catchment [53].

The quality and quantity of the changes in the soil hydraulic properties induced by different PTFs are remarkably affected by their underlying databases, predictors, and methods used to develop the predictive equations. For example, apart from the soil texture classes, there is a significant effect on estimates of soil hydraulic properties, when both OM and BD variables and when only one of them are inputs to the equations (PTFs) [54]. Consequently, the impact of land use and geographic attributes on soil BD and OM [55] leads to a different description of the same soil in the PTFs (i.e., different input values into the equation) and this may account for the observed variation in soil hydraulic properties [11,43]. As a result, the spatial distribution of the differences that we observed between AWC and  $K_{\text{sat}}$  simulated by the scenarios and those of the baseline scenario could be attributed to the land use distribution as well as the proximity to watercourses (Figures 1 and 3). AWC depends to a large extent on the bulk density and the silt content. Hence, PTFs that do not include BD typically result in lower AWC values in soils with lower bulk densities, such as those found in the upper soil horizons of forest soils in a study by [56,57]. They also identified the BD and soil texture as major factors explaining spatial variance in AWC for a study area in China.

The qualitative and quantitative analysis of the discharge hydrographs (Figure 4 and Table 5) as well as the respective signature indices analysis (Table 6) showed distinct differences in the runoff behavior of the catchment through investigated PTFs. The variation of the peak discharge differences between the scenarios and the baseline scenario is caused by the respective pre-event conditions, including the initial soil moisture, and consequently the available soil water storage volume, as well as infiltration capacity.

The differences in model behavior due to soil parameterizations through different PTFs were already analyzed in a study by [58] using a 1D hydrological model. They showed that even when the very same soil was considered in the entire parameterization scheme, and simulated transpiration and soil moisture were consistent with observations, yet the runoff processes or total water balance could be estimated incorrectly. Based on a multi-criteria evaluation, they found that only one of 24 investigated parameterizations resulted in a realistic behavioral model. The complexity of this evaluation is increased by focusing on a closed hydrological catchment, as it was considered in this study. Here, in comparison to above-mentioned 1D model (i.e., only one cell), adjusting the soil hydraulic properties in our catchment model by various PTFs affects the neighboring cells in the spatial domain as well.

In addition, the runoff behavior in the model is influenced by the choice of the calibration parameters. As a result, an insufficient parameterization of the soil can be at least partially compensated by an appropriate adjustment of the model calibration. However, even after calibration, a model may still represent an unrealistic water distribution across the landscape [59]. Therefore, in addition to get the right answer, for example by comparing runoff hydrographs at the catchment outlet, it is also required to analyze whether we are getting the “right answers for the right reasons” [60].

Ultimately, depending on the soil and topographic characteristics, we tracked the spatial distributions of the changes in the main hydrological processes (Tables 7 and 8, Figure 5).

Our results led to a similar conclusion where remarkable differences amongst water balance components of the individual scenarios against the calibrated case were obtained. Furthermore, analysis of frequency of occurrence of runoff components (Figure 5) displayed a pronounced contrast amongst scenarios. This indicates that the dominance of surface runoff, interflow, and baseflow within the catchment and during time periods can be

shifted depending on how the soil hydraulic properties are parameterized. In addition to temporal patterns of runoff components, we examined the spatial patterns of runoff and evapotranspiration in the catchment (Table 8). The outcome was relevant to the previous mentioned argument, where spatial patterns were also quite distinguishable amongst different scenarios. The quantified influence of various PTFs on temporal and spatial patterns of water budget components provided the same evidence to the fact that spatial variability in soil hydraulic characteristics and model errors initiated from application of different PTF cases, may introduce their own uncertainty to model simulation. This is consistent with what has been found by [61]. They compared the performance of two different soil hydraulic parameterization techniques in terms of outputs of catchment water balance simulated by the model HydroGeoSphere, and underlined the potential flaws of choosing different parameterizations in spatially distributed modeling.

Finally, it may be concluded that the information contained in streamflow data is not sufficient to derive physically reasonable soil parameter values only via calibration. This indicates that the resulted uncertainty most likely comes from different descriptions of soil water characteristics (i.e., PTF cases). On this account, deriving the “spatial distribution of variability” from different scenarios, our methodology revealed that choosing a specific PTF may significantly influence the spatial distribution of soil hydraulic properties (e.g.,  $K_{sat}$  and AWC) and also the way water is being distributed across the landscape prior to the catchment outlet. As a result, owing to the fact that the spatial variability of  $K_{sat}$  and AWC affects the temporal response of the catchment to precipitation and runoff concentration, one can consider that selection of a particular PTF makes evident changes in the distribution among groundwater infiltration, runoff and evapotranspiration in the catchment [53,62].

It is important to highlight the fact that most of the PTFs yet show limitations considering the effects of soil inhomogeneity due to structure or macropores, and widely available soil datasets (e.g., FAO Harmonized World Soil Database) may fail to reflect actual field conditions. This warrants further evaluation of PTFs using extensive observed data and particular inclusion the effects of soil structure and macropores [39,63]. Moreover, since soil hydrological parameters vary significantly even within a small area, most of the PTFs are usually applicable with acceptable accuracy only in the regions where those functions were developed [64]. This study showed that the uncertainly forced by selection of PTFs are mainly represented in the spatial distribution of runoff components which are not distinctly addressed by hydrological model calibration against observed discharge time series at the catchment outlet. This recommends that emphasis should be made to soil parameterization oriented towards a “plausible hydrological behavior in terms of spatial patterns of runoff components” during catchment modeling.

According to our knowledge, no comprehensive work was dedicated to carefully analyze the impact of different PTF selection on spatial distribution of internal hydrological processes in the catchment, which underlines the novelty of this research. Indeed, at this stage of understanding, the question of “which PTFs are performing the best?” still remains to be addressed. Since answering this question is beyond the topic of this paper, we therefore believe that future research is clearly required to quantify and qualify the spatial difference in distribution of internal hydrological processes introduced by various PTFs. In other words, application of PTFs in hydrological models without evaluating the spatial patterns of soil moisture, evapotranspiration, and runoff processes produced by different PTFs may ultimately lead to implausible results and possibly to incorrect decisions in water management. This entails investigation of additional information, which usually has to be elaborately collected, for instance, by mapping the dominant runoff generation processes in the area, or retrieving the spatial patterns of evapotranspiration and soil moisture using remote sensing methods, and evaluation at a scale commensurate with hydrological model [51,65].

## 5. Conclusions

The knowledge of soil hydraulic properties and land use effects on these properties are important for efficient soil and water management. Hence, the motivation for this study was to examine a methodology to quantify the effect of modeler's choice of PTF on van Genuchten parameters, and accordingly, analyze the sensitivity of simulated hydrological processes to the spatial variability in soil hydraulic characteristics associated with different PTFs. Our results cast a new light on the way that PTFs are routinely being opted for parameterization of hydrologic modeling (i.e., parameters of van Genuchten). It was revealed that elements of the water balance are highly sensitive to the spatial structure of soil hydraulic properties, and a wide range of different hydrological model behavior can be created just by the option of PTFs. Despite the different proportions of various runoff components produced by a variety of PTFs, this might still result in an acceptable representation of the discharge hydrograph. As a result, model calibration exclusively at catchment outlet may lead to implausible results and possibly to incorrect decisions. Since the distribution of water in the hydrologic system differs greatly amongst PTF cases, we recommend aligning the soil parameterization more towards mapping a plausible hydrological behavior. Nevertheless, to this end, additional information is required, which usually has to be intricately clustered together, for example, by mapping the dominant runoff processes in the hydrologic system; or deriving the soil moisture and evapotranspiration patterns by remote sensing methods.

**Author Contributions:** Conceptualization, H.M. and M.C.C.; Methodology, S.T., H.M. and M.C.C.; Software, S.T. and M.C.C.; Validation, H.M., S.T. and M.C.C.; Resources, M.C.C.; Data curation, S.T. and M.C.C.; Writing—original draft preparation, H.M.; Writing—review and editing, H.M., S.T. and M.C.C.; Visualization, S.T.; Supervision, M.C.C.; Project administration, M.C.C.; Funding acquisition, M.C.C. All authors have read and agreed to the published version of the manuscript.

**Funding:** This work has been funded by the Deutsche Forschungsgemeinschaft (DFG, German Research Foundation)—426111700.

**Institutional Review Board Statement:** Not applicable.

**Informed Consent Statement:** Not applicable.

**Data Availability Statement:** The data presented in this study are available on request from the corresponding author.

**Conflicts of Interest:** The authors declare no conflict of interest.

## References

- Gupta, H.V.; Beven, K.J.; Wagener, T. Model Calibration and Uncertainty Estimation. In *Encyclopedia of Hydrological Sciences*; John Wiley & Sons, Ltd.: Hoboken, NJ, USA, 2006. [\[CrossRef\]](#)
- Elsenbeer, H. Hydrologic Flowpaths in Tropical Rainforest Soilscapes—A Review. *Hydrol. Process.* **2001**, *15*, 1751–1759. [\[CrossRef\]](#)
- Montzka, C.; Herbst, M.; Weihermüller, L.; Verhoef, A.; Vereecken, H. A Global Data Set of Soil Hydraulic Properties and Sub-Grid Variability of Soil Water Retention and Hydraulic Conductivity Curves. *Earth Syst. Sci. Data* **2017**, *9*, 529–543. [\[CrossRef\]](#)
- Arnold, J.G.; Muttiah, R.S.; Srinivasan, R.; Allen, P.M. Regional Estimation of Base Flow and Groundwater Recharge in the Upper Mississippi River Basin. *J. Hydrol.* **2000**, *227*, 21–40. [\[CrossRef\]](#)
- Rieger, W.; Disse, M. Physikalisch Basierter Modellansatz Zur Beurteilung Der Wirksamkeit Einzelner Und Kombinerter Dezentraler Hochwasserschutzmaßnahmen. *Hydrol. Wasserbewirtsch.* **2013**, *57*, 14–25. [\[CrossRef\]](#)
- Richards, L.A. Capillary Conduction of Liquids through Porous Mediums. *Physics* **1931**, *1*, 318–333. [\[CrossRef\]](#)
- Ebel, B.A.; Loague, K. Physics-Based Hydrologic-Response Simulation: Seeing through the Fog of Equifinality. *Hydrol. Process. Int. J.* **2006**, *20*, 2887–2900. [\[CrossRef\]](#)
- Qu, Y.; Duffy, C.J. A Semidiscrete Finite Volume Formulation for Multiprocess Watershed Simulation. *Water Resour. Res.* **2007**, *43*, W08419. [\[CrossRef\]](#)
- Ivanov, V.Y.; Bras, R.L.; Vivoni, E.R. Vegetation-Hydrology Dynamics in Complex Terrain of Semiarid Areas: 1. A Mechanistic Approach to Modeling Dynamic Feedbacks. *Water Resour. Res.* **2008**, *44*, W03429. [\[CrossRef\]](#)
- Te Chow, V. *Applied Hydrology*; Tata McGraw-Hill Education: Pennsylvania Plaza, NY, USA, 2010.
- Wösten, J.; Pachepsky, Y.A.; Rawls, W. Pedotransfer Functions: Bridging the Gap between Available Basic Soil Data and Missing Soil Hydraulic Characteristics. *J. Hydrol.* **2001**, *251*, 123–150. [\[CrossRef\]](#)

12. Bogaen, H.; Herbst, M.; Huisman, J.; Rosenbaum, U.; Weuthen, A.; Vereecken, H. Potential of Wireless Sensor Networks for Measuring Soil Water Content Variability. *Vadose Zone J.* **2010**, *9*, 1002–1013. [[CrossRef](#)]
13. Brooks, R.H.; Corey, A.T. Properties of Porous Media Affecting Fluid Flow. *J. Irrig. Drain. Div.* **1966**, *92*, 61–88. [[CrossRef](#)]
14. Mualem, Y. A New Model for Predicting the Hydraulic Conductivity of Unsaturated Porous Media. *Water Resour. Res.* **1976**, *12*, 513–522. [[CrossRef](#)]
15. Van Genuchten, M.T. A Closed-Form Equation for Predicting the Hydraulic Conductivity of Unsaturated Soils 1. *Soil Sci. Soc. Am. J.* **1980**, *44*, 892–898. [[CrossRef](#)]
16. Aubertin, G.M.; Patric, J.H. Water Quality after Clearcutting a Small Watershed in West Virginia. *J. Environ. Qual.* **1974**, *3*, 243–249. [[CrossRef](#)]
17. Vereecken, H.; Weynants, M.; Javaux, M.; Pachepsky, Y.; Schaap, M.; Van Genuchten, M.T. Using Pedotransfer Functions to Estimate the van Genuchten–Mualem Soil Hydraulic Properties: A Review. *Vadose Zone J.* **2010**, *9*, 795–820. [[CrossRef](#)]
18. Bouma, J. Using Soil Survey Data for Quantitative Land Evaluation. In *Advances in Soil Science*; Springer: Berlin/Heidelberg, Germany, 1989; pp. 177–213.
19. Wösten, J.; Lilly, A.; Nemes, A.; Le Bas, C. Development and Use of a Database of Hydraulic Properties of European Soils. *Geoderma* **1999**, *90*, 169–185. [[CrossRef](#)]
20. Pachepsky, Y.; Rawls, W.J. *Development of Pedotransfer Functions in Soil Hydrology*; Elsevier: Amsterdam, The Netherlands, 2004; Volume 30, ISBN 978-0-444-51705-0.
21. Patil, N.G.; Singh, S.K. Pedotransfer Functions for Estimating Soil Hydraulic Properties: A Review. *Pedosphere* **2016**, *26*, 417–430. [[CrossRef](#)]
22. Schaap, M.G.; Leij, F.J. Using Neural Networks to Predict Soil Water Retention and Soil Hydraulic Conductivity. *Soil Tillage Res.* **1998**, *47*, 37–42. [[CrossRef](#)]
23. Schaap, M.G.; Bouten, W. Modeling Water Retention Curves of Sandy Soils Using Neural Networks. *Water Resour. Res.* **1996**, *32*, 3033–3040. [[CrossRef](#)]
24. Grayson, R.B.; Blöschl, G.; Western, A.W.; McMahon, T.A. Advances in the Use of Observed Spatial Patterns of Catchment Hydrological Response. *Adv. Water Res.* **2002**, *25*, 1313–1334. [[CrossRef](#)]
25. Beven, K. Towards an Alternative Blueprint for a Physically Based Digitally Simulated Hydrologic Response Modelling System. *Hydrol. Process.* **2002**, *16*, 189–206. [[CrossRef](#)]
26. Vereecken, H.; Diels, J.; Van Orshoven, J.; Feyen, J.; Bouma, J. Functional Evaluation of Pedotransfer Functions for the Estimation of Soil Hydraulic Properties. *Soil Sci. Soc. Am. J.* **1992**, *56*, 1371–1378. [[CrossRef](#)]
27. Vereecken, H.; Maes, J.; Feyen, J.; Darius, P. Estimating the Soil Moisture Retention Characteristic from Texture, Bulk Density, and Carbon Content. *Soil Sci.* **1989**, *148*, 389–403. [[CrossRef](#)]
28. Vereecken, H.; Maes, J.; Feyen, J. Estimating Unsaturated Hydraulic Conductivity from Easily Measured Soil Properties. *Soil Sci.* **1990**, *149*, 1–12. [[CrossRef](#)]
29. Chirico, G.; Medina, H.; Romano, N. Functional Evaluation of PTF Prediction Uncertainty: An Application at Hillslope Scale. *Geoderma* **2010**, *155*, 193–202. [[CrossRef](#)]
30. Seibert, J. Regionalisation of Parameters for a Conceptual Rainfall-Runoff Model. *Agric. For. Meteorol.* **1999**, *98*, 279–293. [[CrossRef](#)]
31. Eckelmann, W.; Sponagel, H.; Grottenthaler, W.; Hartmann, K.-J.; Hartwich, R.; Janetzko, P.; Joisten, H.; Kühn, D.; Sabel, K.-J.; Traidl, R. *Bayrisches Landesamt für Wasserwirtschaft: Fließgewässerlandschaften in Bayern*; BAYERN | DIREKT: München, Germany, 2002.
32. *Ad-hoc-AG Boden Bodenkundliche Kartieranleitung*, 5th ed.; Schweizerbart Science Publishers: Stuttgart, Germany, 2006; ISBN 978-3-510-95920-4.
33. Schulla, J. *Model Description WaSiM (Water Balance Simulation Model)*; Hydrology Software Consulting: Zürich, Switzerland, 2019; p. 379.
34. Moriasi, D.N.; Arnold, J.G.; Van Liew, M.W.; Bingner, R.L.; Harmel, R.D.; Veith, T.L. Model Evaluation Guidelines for Systematic Quantification of Accuracy in Watershed Simulations. *Trans. ASABE* **2007**, *50*, 885–900. [[CrossRef](#)]
35. Renger, M.; Bohne, K.; Facklam, M.; Harrach, T.; Riek, W.; Schäfer, W.; Wessolek, G.; Zacharias, S. Ergebnisse Und Vorschläge Der DBG-Arbeitsgruppe “Kennwerte Des Bodengefüges” Zur Schätzung Bodenphysikalischer Kennwerte. *Acad. Accel. World’s Res.* **2008**, *40*, 4–51.
36. Weynants, M.; Vereecken, H.; Javaux, M. Revisiting Vereecken Pedotransfer Functions: Introducing a Closed-Form Hydraulic Model. *Vadose Zone J.* **2009**, *8*, 86–95. [[CrossRef](#)]
37. Zacharias, S.; Wessolek, G. Excluding Organic Matter Content from Pedotransfer Predictors of Soil Water Retention. *Soil Sci. Soc. Am. J.* **2007**, *71*, 43–50. [[CrossRef](#)]
38. Teepe, R.; Dilling, H.; Beese, F. Estimating Water Retention Curves of Forest Soils from Soil Texture and Bulk Density. *J. Plant Nutr. Soil Sci.* **2003**, *166*, 111–119. [[CrossRef](#)]
39. Zhang, Y.; Schaap, M.G. Weighted Recalibration of the Rosetta Pedotransfer Model with Improved Estimates of Hydraulic Parameter Distributions and Summary Statistics (Rosetta3). *J. Hydrol.* **2017**, *547*, 39–53. [[CrossRef](#)]
40. Tóth, B.; Weynants, M.; Pásztor, L.; Hengl, T. 3D Soil Hydraulic Database of Europe at 250 m Resolution. *Hydrol. Process.* **2017**, *31*, 2662–2666. [[CrossRef](#)]



41. Rajkai, K.; Kabos, S.; Van Genuchten, M.T. Estimating the Water Retention Curve from Soil Properties: Comparison of Linear, Nonlinear and Concomitant Variable Methods. *Soil Tillage Res.* **2004**, *79*, 145–152. [[CrossRef](#)]
42. Wessolek, G.; Duijnsveld, W.; Trinks, S. Hydro-Pedotransfer Functions (HPTFs) for Predicting Annual Percolation Rate on a Regional Scale. *J. Hydrol.* **2008**, *356*, 17–27. [[CrossRef](#)]
43. Nemes, A.; Schaap, M.; Leij, F.; Wösten, J. Description of the Unsaturated Soil Hydraulic Database UNSODA Version 2.0. *J. Hydrol.* **2001**, *251*, 151–162. [[CrossRef](#)]
44. Tempel, P.; Batjes, N.; Van Engelen, V. IGBP-DIS Soil Data Set for Pedotransfer Function Development. *ISRIC* **1996**, 447365.
45. Schaap, M.G.; Leij, F.J.; Van Genuchten, M.T. Rosetta: A Computer Program for Estimating Soil Hydraulic Parameters with Hierarchical Pedotransfer Functions. *J. Hydrol.* **2001**, *251*, 163–176. [[CrossRef](#)]
46. Vogel, R.M.; Fennessey, N.M. Flow-Duration Curves. I: New Interpretation and Confidence Intervals. *J. Water Res. Plan. Manag.* **1994**, *120*, 485–504. [[CrossRef](#)]
47. Smakhtin, V.U. Low Flow Hydrology: A Review. *J. Hydrol.* **2001**, *240*, 147–186. [[CrossRef](#)]
48. Yilmaz, K.K.; Gupta, H.V.; Wagener, T. A Process-Based Diagnostic Approach to Model Evaluation: Application to the NWS Distributed Hydrologic Model. *Water Resour. Res.* **2008**, *44*, W09417. [[CrossRef](#)]
49. Casper, M.C.; Grigoryan, G.; Gronz, O.; Gutjahr, O.; Heinemann, G.; Ley, R.; Rock, A. Analysis of Projected Hydrological Behavior of Catchments Based on Signature Indices. *Hydrol. Earth Syst. Sci.* **2012**, *16*, 409–421. [[CrossRef](#)]
50. Swain, M.J.; Ballard, D.H. Color Indexing. *Int. J. Comput. Vis.* **1991**, *7*, 11–32. [[CrossRef](#)]
51. Demirel, M.C.; Mai, J.; Mendiguren, G.; Koch, J.; Samaniego, L.; Stisen, S. Combining Satellite Data and Appropriate Objective Functions for Improved Spatial Pattern Performance of a Distributed Hydrologic Model. *Hydrol. Earth Syst. Sci.* **2018**, *22*, 1299–1315. [[CrossRef](#)]
52. Wang, J.-P.; Hu, N.; François, B.; Lambert, P. Estimating Water Retention Curves and Strength Properties of Unsaturated Sandy Soils from Basic Soil Gradation Parameters. *Water Resour. Res.* **2017**, *53*, 6069–6088. [[CrossRef](#)]
53. Zheng, J.; Shao, M.; Zhang, X. Spatial Variation of Surface Soil's Bulk Density and Saturated Hydraulic Conductivity on Slope in Loess Region. *J. Soil Water Conserv.* **2004**, *18*, 53–56. [[CrossRef](#)]
54. Nemes, A.; Rawls, W.J.; Pachepsky, Y.A. Influence of Organic Matter on the Estimation of Saturated Hydraulic Conductivity. *Soil Sci. Soc. Am. J.* **2005**, *69*, 1330–1337. [[CrossRef](#)]
55. Azuka, C.; Igué, A. Surface Runoff as Influenced by Slope Position and Land Use in the Koupendri Catchment of Northwest Benin: Field Observation and Model Validation. *Hydrol. Sci. J.* **2020**, *65*, 995–1004. [[CrossRef](#)]
56. Dobarco, M.R.; Bourennane, H.; Arrouays, D.; Saby, N.P.; Cousin, I.; Martin, M.P. Uncertainty Assessment of GlobalSoilMap Soil Available Water Capacity Products: A French Case Study. *Geoderma* **2019**, *344*, 14–30. [[CrossRef](#)]
57. Li, X.; Shao, M.; Zhao, C.; Jia, X. Spatial Variability of Soil Water Content and Related Factors across the Hexi Corridor of China. *J. Arid Land* **2019**, *11*, 123–134. [[CrossRef](#)]
58. Casper, M.C.; Mohajerani, H.; Hassler, S.K.; Herdel, T.; Blume, T. Finding Behavioral Parameterization for a 1-D Water Balance Model by Multi-Criteria Evaluation. *J. Hydrol. Hydromech.* **2019**, *67*, 213–224. [[CrossRef](#)]
59. Rajib, A.; Evenson, G.R.; Golden, H.E.; Lane, C.R. Hydrologic Model Predictability Improves with Spatially Explicit Calibration Using Remotely Sensed Evapotranspiration and Biophysical Parameters. *J. Hydrol.* **2018**, *567*, 668–683. [[CrossRef](#)] [[PubMed](#)]
60. Kirchner, J.W. Getting the Right Answers for the Right Reasons: Linking Measurements, Analyses, and Models to Advance the Science of Hydrology. *Water Resour. Res.* **2006**, *42*. [[CrossRef](#)]
61. Nasta, P.; Boaga, J.; Deiana, R.; Cassiani, G.; Romano, N. Comparing ERT-and Scaling-Based Approaches to Parameterize Soil Hydraulic Properties for Spatially Distributed Model Applications. *Adv. Water Res.* **2019**, *126*, 155–167. [[CrossRef](#)]
62. Herbst, M.; Diekkrüger, B. The Influence of the Spatial Structure of Soil Properties on Water Balance Modeling in a Microscale Catchment. *Phys. Chem. Earth Parts A/B/C* **2002**, *27*, 701–710. [[CrossRef](#)]
63. Bayabil, H.K.; Dile, Y.T.; Tebebu, T.Y.; Engda, T.A.; Steenhuis, T.S. Evaluating Infiltration Models and Pedotransfer Functions: Implications for Hydrologic Modeling. *Geoderma* **2019**, *338*, 159–169. [[CrossRef](#)]
64. Li, Y.; Chen, D.; White, R.E.; Zhu, A.; Zhang, J. Estimating Soil Hydraulic Properties of Fengqiu County Soils in the North China Plain Using Pedo-Transfer Functions. *Geoderma* **2007**, *138*, 261–271. [[CrossRef](#)]
65. Casper, M.C.; Vohland, M. Validation of a Large Scale Hydrological Model with Data Fields Retrieved from Reflective and Thermal Optical Remote Sensing Data—A Case Study for the Upper Rhine Valley. *Phys. Chem. Earth Parts A/B/C* **2008**, *33*, 1061–1067. [[CrossRef](#)]

### **5.3 Spatial Evaluation of a Hydrological Model on Dominant Runoff Generation Processes Using Soil Hydrologic Maps**

## Article

# Spatial Evaluation of a Hydrological Model on Dominant Runoff Generation Processes Using Soil Hydrologic Maps

Hadis Mohajerani <sup>1,\*</sup>, Mathias Jackel <sup>1,2</sup>, Zoé Salm <sup>1</sup>, Tobias Schütz <sup>2</sup> and Markus C. Casper <sup>1</sup><sup>1</sup> Department of Physical Geography, University of Trier, 54286 Trier, Germany<sup>2</sup> Hydrology Department, University of Trier, 54286 Trier, Germany

\* Correspondence: mohajerani@uni-trier.de

**Abstract:** The aim of this study was to simulate dominant runoff generation processes (DRPs) in a mesoscale catchment in southwestern Germany with the physically-based distributed hydrological model WaSiM-ETH and to compare the resulting DRP patterns with a data-mining-based digital soil map. The model was parameterized by using 11 Pedo-transfer functions (PTFs) and driven by multiple synthetic rainfall events. For the pattern comparison, a multiple-component spatial performance metric (SPAEF) was applied. The simulated DRPs showed a large variability in terms of land use, applied rainfall rates, and the different PTFs, which highly influence the rapid runoff generation under wet conditions.

**Keywords:** data-mining-based digital soil mapping; spatial pattern comparison; water balance modeling; spatial efficiency metric

## 1. Introduction

Distributed physically-based hydrological models have been the mainstream in the community of hydrological modelers, providing significant insights into understanding and predicting hydrological fluxes and states [1,2]. Based on the rainfall–runoff response, these models account for the spatio-temporal dynamics of hydrological processes at various scales [3–6]. Modeling the interplay of hydrological processes in a spatially distinct manner provides the required tool to tackle the issues at hand driven by global climate change and land use intensification. The capability of a model to predict the spatial variabilities of hydrological processes, however, poses evident challenges to its modeling structure. Thereby, considering the complex feedbacks between the hydrological processes that drive spatial variability, distributed hydrological model applications are a challenge for spatial pattern-oriented evaluations [7–9]. The spatial predictability of distributed model output can only be thoroughly verified when evaluating the outputs against spatial observations [9,10], whereas, in particular, discharge data at the catchment outlet does not provide sound information about the spatial distribution of runoff processes within the catchment [11].

Changes in the underlying land surface conditions caused by land use, soil types, geological, and topographical factors may alter the spatial patterns of runoff generation processes in a catchment area, which might then cause extreme flood or drought events. Such events may further influence the subsequent processes that govern the runoff response of a region, particularly in smaller catchments. For example, for water resource management and early flood warning, it is important to conduct quantitative measurements of the effects of urbanization on surface runoff. A recent study approached runoff fluctuations in an urban region using GIS and remote sensing technologies as well as the SCS-CN model [12]. It was found that within the period of 15 years, the region experienced a significant growth of urban impervious areas and a notable decline in vegetated land cover, being the predominant drivers of surface runoff change. The rise in surface runoff was found to be positively correlated to the growth in urbanization and negatively correlated



**Citation:** Mohajerani, H.; Jackel, M.; Salm, Z.; Schütz, T.; Casper, M.C. Spatial Evaluation of a Hydrological Model on Dominant Runoff Generation Processes Using Soil Hydrologic Maps. *Hydrology* **2023**, *10*, 55. <https://doi.org/10.3390/hydrology10030055>

Academic Editor: Giorgio Baiamonte

Received: 6 January 2023

Revised: 11 February 2023

Accepted: 17 February 2023

Published: 22 February 2023



**Copyright:** © 2023 by the authors. Licensee MDPI, Basel, Switzerland. This article is an open access article distributed under the terms and conditions of the Creative Commons Attribution (CC BY) license (<https://creativecommons.org/licenses/by/4.0/>).

to the decreased vegetation cover. Another study analyzed the effects of land use change on runoff production by using the SCS-CN approach, remote sensing data, and GIS tools, where runoff was predicted from precipitation, land use, and hydrological soil groups using the SCS-CN model [13]. According to another study, the influence of different land use covers on the soil hydraulic properties was investigated, and consequently, different soil hydrological behaviors to heavy storms were found, and therefore, different runoff productions were observed [14].

A well-performing hydrological model of a given catchment is in essence a virtual reflection of how the runoff generation processes vary spatially and temporally and switch between major flow mechanisms (i.e., surface runoff, subsurface flow, or base flow) [15]. While various runoff processes may occur on a site, only the dominant processes most likely contribute to the total runoff of the catchment and are significantly dependent on the site characteristics and the nature of the precipitation event [16,17]. For instance, relatively flat areas adjacent to the flow channel are disposed to faster saturation (i.e., even during slight precipitation events) and can quickly transfer water to the river network, which generally results in a fast runoff response (e.g., saturation overland flow). In contrast, runoff responses from hillslope zones are relatively slower, even during higher intensity rainfall events, and may largely contribute to processes such as interflow. Therefore, models that correctly discern the spatial variability of dominant runoff processes (DRPs) and identify flow pathways consistent with spatial observations can serve as tools to make predictions and test the hypotheses of the controls on hydrological responses [18–22]. The spatial information of DRPs in a catchment allow for a thorough evaluation of how a model represents the spatial distribution of runoff generation and the contributing areas under different rainfall characteristics and initial catchment conditions. The various mapping approaches for DRPs differ regarding the time and data required for mapping, and accordingly, the defined DRP classes might then be different [16,23,24].

While better process representations are required, it has always been quite a challenge to acquire good quality observed datasets with minimal uncertainty for hydrological model testing. Such datasets should then ideally transfer information about the changes in storage and variations in travel time distributions as a catchment wets and dries out, so that models can confidently be evaluated against the spatial distribution of runoff generation processes and the internal moisture state in catchments with different properties [25–27]. This highlights the principle that the model evaluation should thus make use of all sources of data available in a catchment area [25,28]. Antonetti et al. (2019) applied multiple DRP maps to incorporate the knowledge on DRPs into hydrological modeling. They presented divergent catchment reactions in terms of DRPs to precipitation events for flash flood predictions. They implemented synthetic runoff simulations to assess the sensitivity of the hydrograph to the mapping approach and found that simulations following the simplified procedures resulted in the strongest deviations from the reference map. Furthermore, in the Nahe catchment in Rhineland-Pfalz, Haag et al. (2016) [29] also integrated spatially distributed information on DRPs based on the classification of Scherrer and Naef (2003) [30] into LARSIM (large area runoff simulation model) for operational flood forecast [31] and applied different soil parameterizations corresponding to DRPs in the catchment area.

Thereupon, in the present study, we attempted to utilize an available soil hydrological map for the state of Rhineland-Palatinate (western Germany) from which the DRPs in a landscape unit are identified [32]. This map reflects different flow processes, which are plausible based on the site's characteristics. In this paper, we intend to integrate this process information into rainfall–runoff model evaluation. Therefore, a methodology was developed that translates the map content into runoff classes that are consistent with the model structure in use. This would then enable spatial pattern-oriented evaluation on DRPs, for which we adopted a multiple-component spatial performance metric (SPAEF) [33]. We then defined a series of synthetic rainfall events with different intensities on a system moisture state around field capacity to assess how different rainfall intensities affect the spatial patterns of DRPs in the catchment. Furthermore, we applied 11 different Pedo-transfer



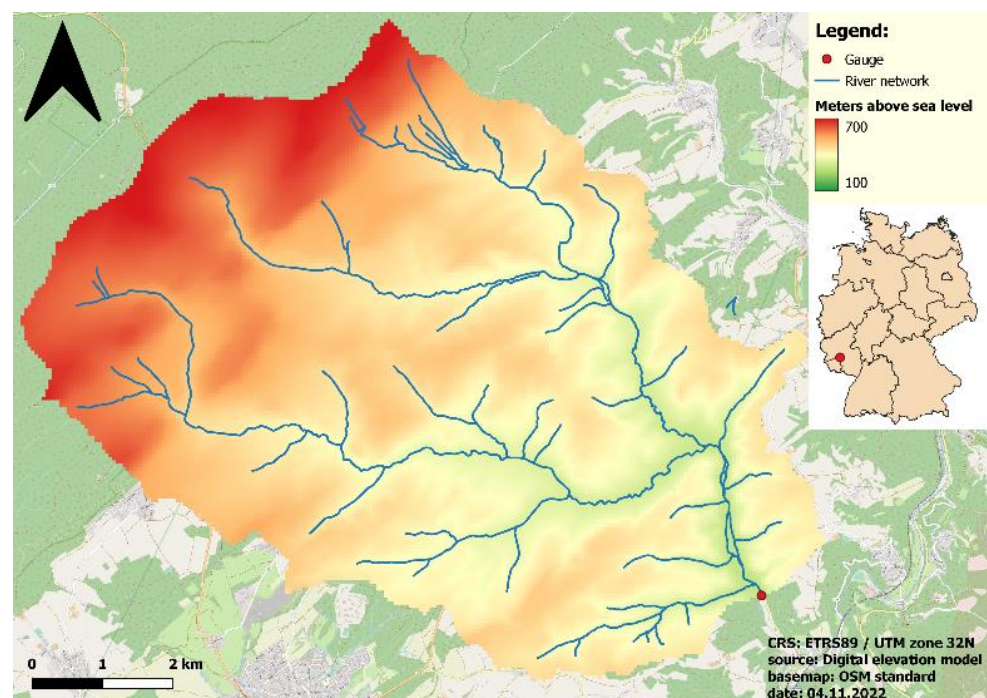
functions (PTFs) to translate the information on soil properties into model parameters, since the choice of PTFs has a distinctive effect on the water balance and runoff generation [7]. Overall, this study aimed to provide a basis to understand and evaluate the observed differences in the spatial patterns of DRPs at the catchment scale and to use this information as a significant constraint in the evaluation process of a hydrological model. This would allow for the selection of behavioral model parameterizations (rather than compensating through calibration).

## 2. Materials and Methods

### 2.1. Study Area

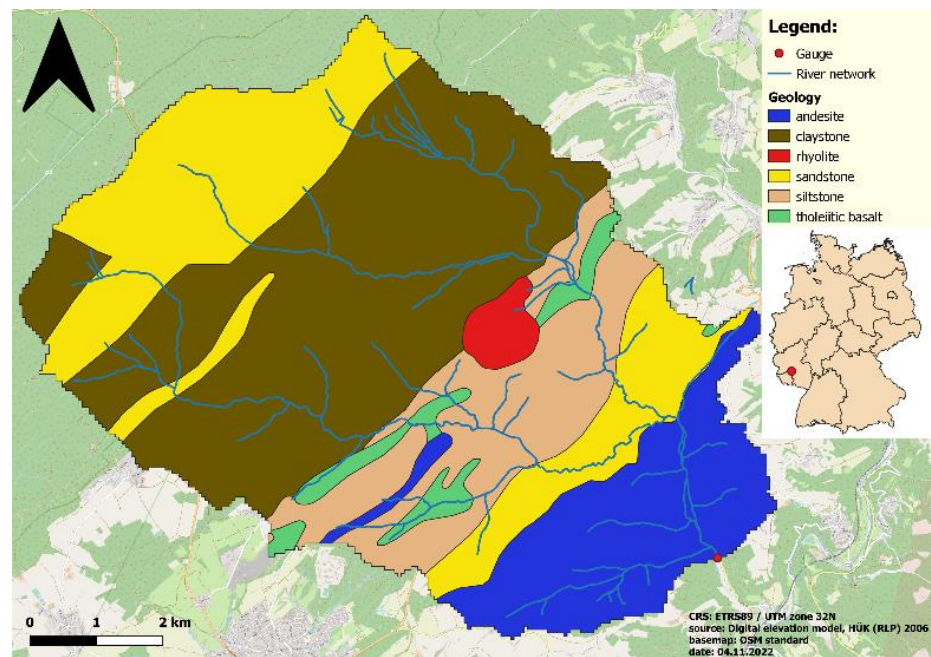
The Kronweiler catchment in the Nahe Valley is located in the state of Rhineland-Palatinate in the southwest of Germany. The catchment, with an area of 64 km<sup>2</sup>, has a distinct river network, and the elevation ranges from 298 m a.s.l. (in the southeast) to above 720 m a.s.l. (in the north and northwest), resulting in a mean slope gradient of 8.6 and a notable altitude difference (see Figure 1a; [34]). Soil and geological information (Figure 1b) were derived from the “Hydrologische Übersichtskarte Rheinland-Pfalz” (2006). Sandstone mainly occurs in the northern parts, and siltstone underlies the southwest parts of the region. Dominant soil types are Gleyic and Humic Podzols and Cambisols.

Land use information (Figure 1c) was taken from the Corine land cover dataset (CLC, 2006), which represents forested areas as the largest land use (66%) followed by grassland (29%), cropland (3.9%), urban (0.9%), and wasteland (0.2%). While forests are patchily scattered throughout the catchment, they large cover the northern areas and the areas around the river network in the south. There are also grasslands distributed evenly over the entire area, except for the highlands in the north.

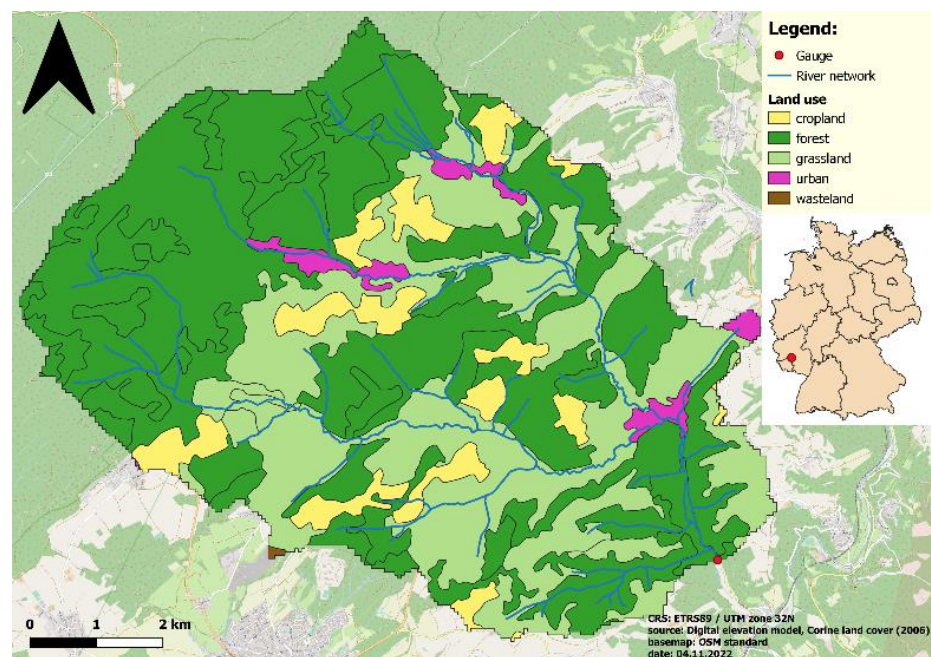


(a)

Figure 1. Cont.



(b)



(c)

**Figure 1.** Topography (a), geology (b), and land use (c) of the Kronweiler catchment.

## 2.2. Model Setup and Parameterization

The hydrological model WaSiM (<http://www.wasim.ch>, accessed on 17 February 2023) was applied to analyze the water balance and runoff generation processes in the catchment. As a distributed and deterministic model, WaSiM provides physical descriptions of the involved hydrological processes. It applies Richard's equation [35] to simulate unsaturated water fluxes in the soil and uses van Genuchten parameters [36] for the parameterization of the soil hydraulic properties. WaSiM represents the soil as a layered column. This means, for each soil horizon, that the layer thickness and water retention curve are separately defined. Every

horizon within a soil profile is characterized with a specific permeability. To describe the water retention curve, estimations of the van Genuchten parameters as well as the saturated hydraulic conductivities are required (i.e., by using PTFs). The model indicates different runoff response types (fast, intermediate, slow) by simulating the three runoff components surface runoff, interflow, and base flow. A detailed description of the procedure by which the model determines the DRPs in the catchment is presented in the Section 2.4.2).

The model was set up with a spatial resolution of 50 m and a temporal resolution of 1 h. The required input time series of precipitation, temperature, relative humidity, global radiation, and wind speed were taken from the meteorological station of Dienstweiler (<https://www.wetter.rlp.de/agrarmeteorologie>, accessed on 17 February 2023). The pre-processing tool of WaSim-ETH TANALYS was applied to derive the necessary spatial data (e.g., slope, flow accumulation, sub-catchment structure, and stream network). The depth of the bulk density and organic matter content for each soil type and horizon were adapted considering the main land use types. The input time series of 6 years (2009–2014) was used for the model stabilization. Then, the system moisture state on 31 December 2014 represents the catchment moisture condition around field capacity.

Overall, without the interference of model calibration, the model allows for the analysis of the effects of changes in the soil hydraulic properties and rainfall event characteristics on the dominant runoff behavior of the catchment and its spatial patterns. In other words, for the purpose of this study, the exact description of the reality was of minor importance.

A combination of 11 PTFs were applied through different simulation runs to consider the effect of the different soil parameterizations by PTFs on the spatial patterns of runoff processes in the catchment. Defined PTF combinations (Table 1) determined the van Genuchten parameters (i.e.,  $\theta_{sat}$ ,  $\theta_{res}$ ,  $n$ ) and saturated hydraulic conductivity  $K_{sat}$ . Determination of the  $K_{sat}$  for the combinations of 1 to 7 was carried out according to the table of the Ad-hoc-AG Boden (2005) [37], while for the combinations of 8 to 10, the corresponding equations of selected PTFs were applied. The main differences among the PTFs were the underlying databases, number of considered soil samples, and the selected input predictors to the equations (i.e., soil texture is included in all PTFs as an input, but bulk density and organic matter content are not always considered in some of the PTFs). For detailed information on the following PTF combinations, see [7].

**Table 1.** PTF combinations to estimate the parameters of van Genuchten ( $\theta_{sat}$ ,  $\theta_{res}$ ,  $n$ ) and saturated hydraulic conductivity  $K_{sat}$ .

PTF Combination	Van Genuchten Parameters	Soil Hydraulic Conductivity $K_{sat}$
1	Wösten et al. (1999) [38]	Ad-hoc-AG Boden (2005) KA5 [37]
2	Renger et al. (2009) [39]	Ad-hoc-AG Boden (2005) KA5 [37]
3	Weynants et al. (2009) [40]	Ad-hoc-AG Boden (2005) KA5 [37]
4	Zacharias and Wessolek (2007) [41]	Ad-hoc-AG Boden (2005) KA5 [37]
5	Teepe et al. (2003) [42]	Ad-hoc-AG Boden (2005) KA5 [37]
6	Zhang and Schaap (2017): Rosetta H2w [43]	Ad-hoc-AG Boden (2005) KA5 [37]
7	Zhang and Schaap (2017): Rosetta H3w [43]	Ad-hoc-AG Boden (2005) KA5 [37]
8	Wösten et al. (1999) [38]	Wösten et al. (1999) [38]
9	Renger et al. (2009) [39]	Renger et al. (2009) [39]
10	Zhang and Schaap (2017): Rosetta H2w [43]	Zhang and Schaap (2017): Rosetta H2w [43]
11	Zhang and Schaap (2017): Rosetta H3w [43]	Zhang and Schaap (2017): Rosetta H3w [43]



### 2.3. Synthetic Rainfall Events

We defined a series of synthetic rainfall events with different intensities but fixed volume to analyze their impact on the spatial patterns of DRPs in the catchment. Instead of focusing on how well the model reproduces a measured discharge, the word “synthetic” implies that the focus of this study was exclusively on the differences between the simulated patterns and patterns derived from a digital soil map. The synthetic rainfall event series had a consistent total rainfall amount of 100 mm of precipitation and accordingly, ascending rainfall durations resulted in descending intensities (Table 2). According to the available rainfall data on large precipitation events in the area, the amount of 100 mm rainfall in 3 to 10 h is realistic. In addition, this amount is high enough to force the model to reach the maximum infiltration rates and eventually produce overland flow. In other words, during the 3 up to 10 h of synthetic rainfall, the changes in the spatial distribution of surface runoff, interflow, and deep percolation were analyzed.

**Table 2.** Overview of the rainfall characteristics of the synthetic rainfall events. Total rainfall amounts up to 100 mm of precipitation for all events.

Rainfall Duration (Hours)	Rainfall Intensity (mm/h)
3	33.33
4	25
5	20
6	16.66
7	14.29
8	12.5
9	11.11
10	10

The simulation period was set to 7 days to consider the contribution of delayed flow processes. To ensure that no process other than the main runoff processes (i.e., overland flow, interflow, and deep percolation) was triggered within the catchment, the air humidity was set to a constant value of 100%, which prevents evaporation processes. Air temperatures above 0 °C prevent any snow contribution. This ensures that the defined precipitation amount predominantly transforms into runoff production.

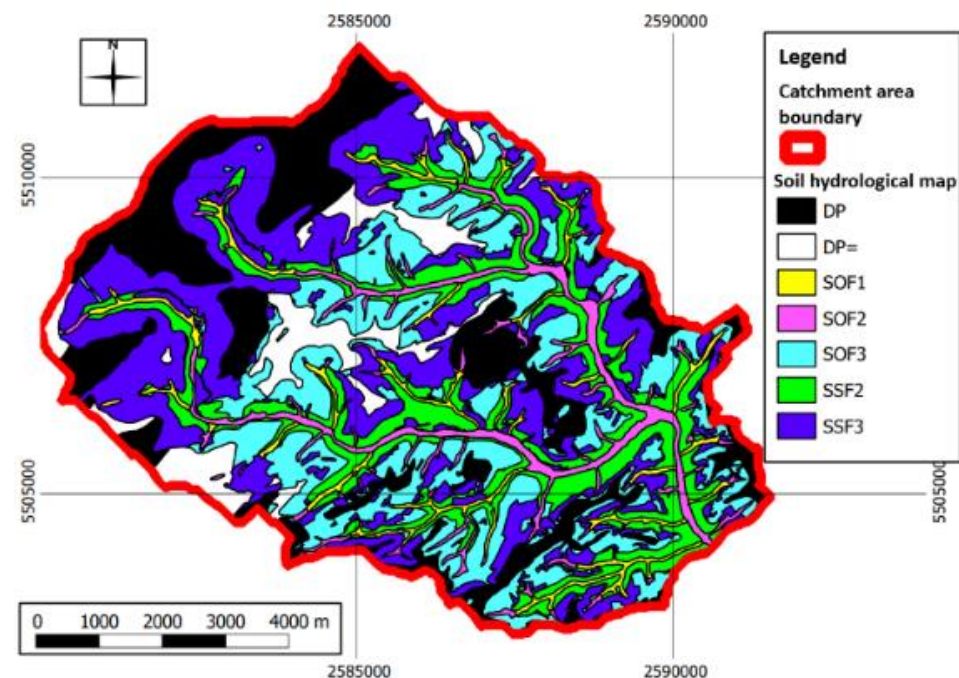
### 2.4. Determination of Dominant Runoff Generation Process (DRP)

#### 2.4.1. DRP by Reference Soil Hydrological Map

Information on the spatial distribution of runoff processes in a catchment can be visualized in maps discerning different types of runoff [24]. There are different mapping techniques for DRPs regarding the required time and data for mapping, and therefore, the DRP classes might be differently defined [16,23,24,30]. For the Nahe River Basin located in the state of Rhineland-Palatinate in southwest Germany, a runoff generation (reference) map is available, which also encompasses the study area Kronweiler [32]. To create this reference map, in a first step, four reference areas were mapped by experts using the mapping scheme of Scherrer (2006) [44]. In a second step, a data-driven artificial intelligence method used (i) these maps, (ii) the output from digital terrain analysis (e.g., slope, distance to stream) [45], and (iii) spatial information about geology, soil, and land use to generate the final product, a map of the dominant runoff generation processes, and the reaction time (Table 3) [46,47]. The resulting spatial structure of DRPs is plausible, for instance, if a location is close to the stream channels or on steep slopes, runoff generation is faster and overland flow or interflow, respectively, are more likely (Figure 2). If a location is dominated by permeable soils or permeable geology, deep percolation or (on slopes) interflow are more likely as dominant DRPs [32].

**Table 3.** List of the DRP classes defined in the reference soil hydrological map [32,44].

DRP Class	Description
SOF 1	Saturated overland flow Level 1
SOF 2	Saturated overland flow Level 2
SOF 3	Saturated overland flow Level 3
SSF 1	Subsurface flow Level 1
SSF 2	Subsurface flow Level 2
SSF 3	Subsurface flow Level 3
DP	Deep percolation

**Figure 2.** Reference soil hydrological map—spatial distribution of DRPs in the catchment area Kronweiler [48].

In Table 3:

- (1) Saturated overland flow (SOF) describes the surface runoff, occurring when the storage capacity is exceeded due to saturation of the soil profile. The levels (or subclasses) describe the pace of the flow process from very fast (1) to delayed (2) and strongly delayed (3). Subclass SOF1 arises when the soil is saturated very fast. The subclasses SOF2 and SOF3 show an increasing saturation deficit, where saturation happens with a delay.
- (2) Subsurface flow (SSF) describes the flow processes within the soil profile, where precipitation water infiltrates through the soil surface. There, it can either be stored or continues to percolate until reaching the groundwater table. When a well-permeable soil horizon lies above a less permeable horizon, lateral subsurface runoff can also occur.
- (3) Deep percolation (DP) describes the percolation of water to deeper soil horizons.

#### 2.4.2. Determining DRPs Using a Hydrological Model

The rainfall–runoff transformations simulated with WaSiM are represented by three runoff components. Surface runoff and interflow simulations are directly produced by the model runs, and by subtracting these runoff components from the total runoff, deep percolation can be estimated. As a result, each grid cell of the catchment area individually

represents a runoff process. Here, the evaporation or other intermediate storage is not triggered. A runoff component comprising 75% of the precipitation is considered dominant. Therefore, the DRPs can be initially defined into three classes:

- 1 = Deep percolation is dominant;
- 2 = Interflow is dominant;
- 3 = Surface runoff is dominant.

This classification holds true if the respective runoff process is triggered from at least 75% of the total precipitation. However, when there is no runoff process with a 75% contribution rate and the runoff shares are very close to each other, two further classes can be defined considering the second largest runoff shares. Accordingly, the grid cells are assigned to the corresponding DRP classes (Table 4).

**Table 4.** Dominant runoff classification in WaSiM.

DRP Class	Description
1	DP > 75, and/or DP > SR and DP > IF
1.5	IF > 50 and DP > 25 DP > 50 and IF > 25 DP > 50 and SR > 25
2	IF > 75 IF > 50 and IF > DP IF > SR and IF > DP
2.5	SR > 50 and DP > 25 IF > 50 and SR > 25
3	SR > 75 SR > 50 and IF > 25 SR > IF and SR > DP

For instance, class 1.5 is assigned whenever one or more of the following conditions apply:

- (1) When interflow (IF) is greater than 50% and DP is greater than 25% at the same time, or
- (2) If DP is greater than 50% and at the same time IF is greater than 25%, or
- (3) When DP is greater than 50% and at the same time the surface runoff (SR) is greater than 25%.

#### 2.4.3. Reclassification of the Reference Map for DRPs

A common classification must be set because the classes used for the determination of DRPs for the model simulations and those of the reference map do not match. For this purpose, the classes of the reference map were adapted to those of the simulation model. Table 5 shows the reclassification. To give an example, since class DP and DP = in the map and class 1 in the model both represent deep percolation as DRP, DP and DP = classes of the reference map were assigned to class 1.

**Table 5.** Reclassification of the soil hydrologic map corresponding to the hydrological model DRP classes.

DRP Classes in Reference Hydrological Map	Corresponding DRP Classes in WaSiM Model
DP	1
SSF 3	1.5
SSF 1 and SSF 2	2
SOF 3	2.5
SOF 1 and SOF 2	3

### 2.5. Quantitative Evaluation of Spatial Patterns of DRPs

The accordance of the spatial patterns between the model and reference map was evaluated by using a spatial efficiency metric (SPAEF, see Equation (1)) developed by Demirel et al. (2018) [33]. The SPAEF is a multi-component statistical metric inspired by the Kling–Gupta efficiency [49] that quantifies the spatial similarity between the simulation patterns and spatial observation. The three components of the SPAEF are (i) the Pearson correlation coefficient ( $\alpha$ ); (ii) the coefficient of variation ( $\beta$ ); and (iii) percentage of histogram intersection ( $\gamma$ ), as follows:

**Equation (1).** SPAEF spatial efficiency metric formula.

$$\text{SPAEF} = 1 - \sqrt{(\alpha - 1)^2 + (\beta - 1)^2 + (\gamma - 1)^2} \quad (1)$$

where

$$\alpha = \rho(A, B); \beta = \left(\frac{\sigma_A}{\mu_A}\right) / \left(\frac{\sigma_B}{\mu_B}\right); \gamma = \frac{\sum_{j=1}^n \min(K_j, L_j)}{\sum_{j=1}^n K_j}$$

where  $\alpha$  is the Pearson correlation coefficient between  $A$  (spatial observation by the reference map) and  $B$  (simulated patterns).  $\beta$  is the fraction of the coefficient of variation representing spatial variability.  $\gamma$  is the histogram overlap for the given histograms  $K$  of the patterns of  $A$  and  $L$  of the patterns of  $B$ , each containing  $n$  bins. The spatial efficiency scale value ranges from  $-\infty$  to 1. If the value is above 0, a pattern match can be seen. The better the similarity between the patterns, the closer the efficiency metric value approaches unity.

### 3. Effects of Rainfall Intensities on Spatial Patterns of Simulated Runoff Processes

Different rainfall intensities together with different soil hydraulic properties (i.e., derived from various PTF combinations) can be applied to simulate the runoff processes (i.e., surface runoff, interflow, and deep percolation) occurring in the catchment, and accordingly, the changes in the spatial patterns are illustrated (Figures 3–5). The moisture pre-condition for the catchment system is considered as the moisture content at the root zone after an extended rainfall period, which amounts to soil water content near field capacity. Here, we present only PTF combination 5 [37,42] because it showed the highest similarity to the reference map.

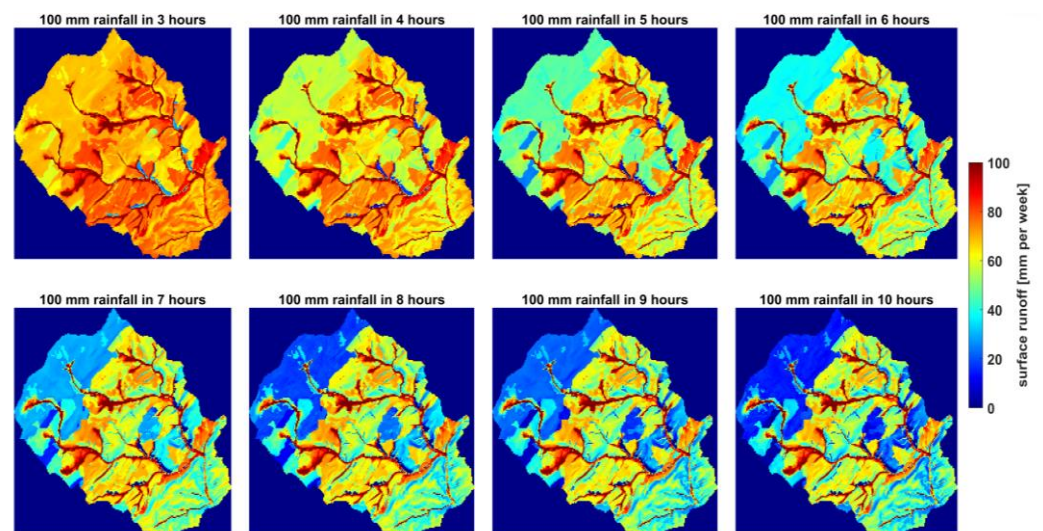


**Figure 3.** Variability in the spatial patterns of the simulated surface runoff within the catchment under different synthetic rainfall intensities (PTF combination 5 in Table 1).



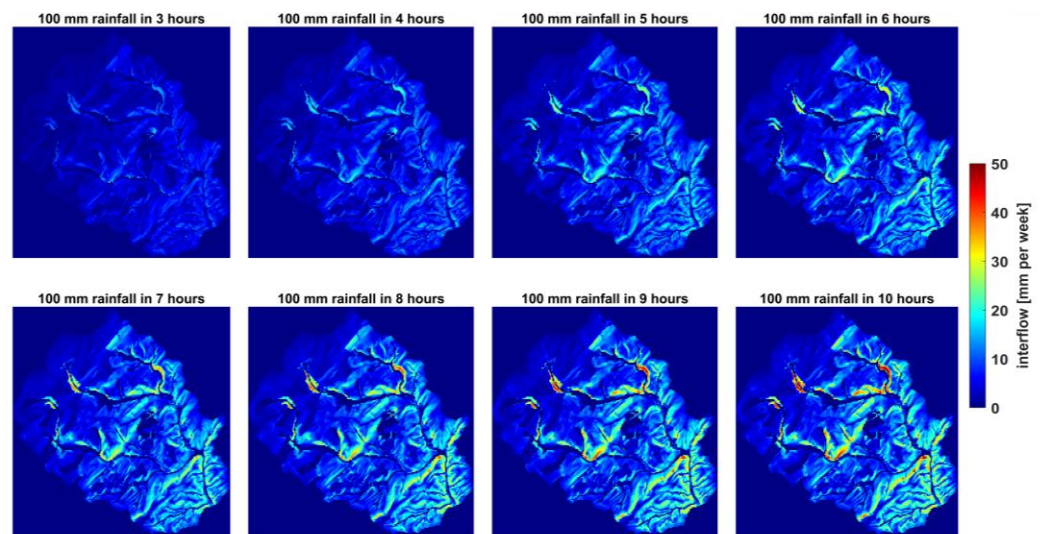


**Figure 4.** Variability in the spatial patterns of simulated interflow within the catchment, under different synthetic rainfall intensities (PTF combination 5 from Table 1).

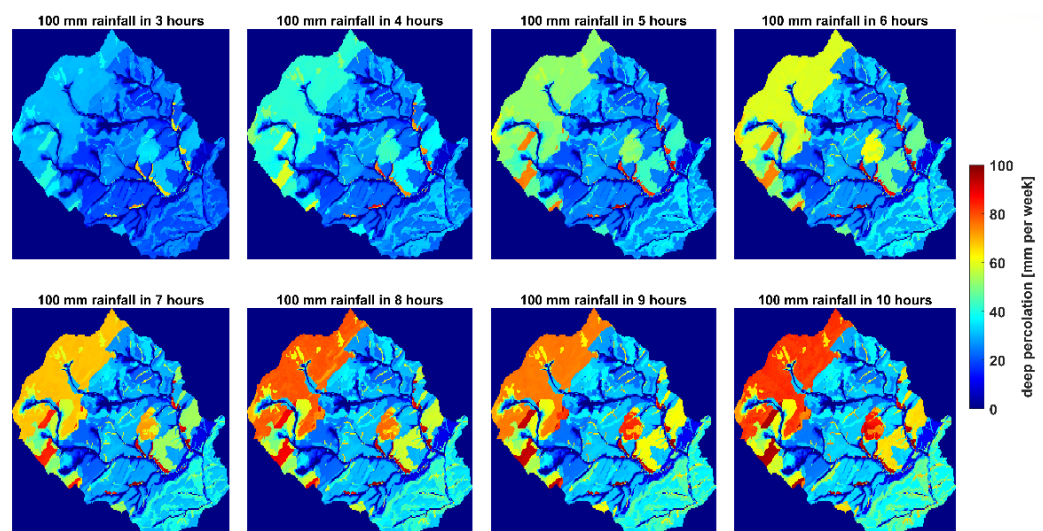


**Figure 5.** Variability in the spatial patterns of simulated deep percolation within the catchment under different synthetic rainfall intensities (PTF combination 5 from Table 1).

A clear variability could be seen in the spatial patterns (Figure 3). For all rainfall intensities, the patterns of surface runoff with the highest values (about 80 to 100 mm) were observed in the stream channels or in the adjacent areas, except for some spots close to the channels (in blue colors), which resulted lower amounts of surface runoff. These exceptions showed a remarkable decreased runoff value of about 35 mm for the rainfall intensity of 100 mm/3 h (displayed in light blue) and continued to show lower runoff values with increasing precipitation duration until it no longer generated surface runoff for a 6 h precipitation duration and longer (displayed in darker blue colors). In general, with an increase in the precipitation duration (i.e., decreasing rainfall intensity), spatial patterns showed a significant decline in the amount of surface runoff, distinctly in the distant locations from the river courses. These patterns were particularly recognizable in the high elevations of the catchment in the north and northwest as well as in the low elevations in the south and southeast, and a sub-area in the center of the catchment.

Obviously, with an increasing rainfall duration, and therefore a decreasing rainfall intensity, the interflow amount rose (Figure 4). It can be stated that the interflow largely developed near the river courses (i.e., not in them). It is also remarkable that the interflow



patterns in the catchment did not change from a precipitation duration of 6 h up to 10 h. If the total catchment is considered, the interflow usually amounted to 15–20 mm. However, interflow occasionally reached 35–50 mm in simulations with higher rainfall intensities (e.g., 100 mm in 3 and 4 h) and only in a small area close to the channels.

Total deep percolation increased mostly within the catchment, as the rainfall duration became longer (Figure 5). This overall change was markedly pronounced up to the rainfall event of 100 mm/7 h, while a further reduction in rainfall intensity did not show a clear increase in deep percolation. Under the highest rainfall intensity (i.e., 100 mm/3 h), the simulations still showed development of the spatial patterns of deep percolation in the catchment. These patterns reached amounts between 30 mm and 45 mm in deep percolation over large areas in the north, northwest, and central areas between the river courses and eastern parts of the catchment. For the lowest precipitation intensity of 100 mm/10 h, the upland areas with higher permeability transformed almost all the precipitation water into deep percolation and produced patterns with amounts of 65–90 mm. Overall, the areas developing the highest deep percolation shares corresponded to forest land use.

#### 4. Spatial Evaluation of Simulated DRP Patterns

Simulated spatial patterns of DRPs by applying synthetic rainfall events and 11 PTF combinations were evaluated using a regional reference runoff process map as the perceived reality. Here, we only present the pattern of simulated DRPs for the rainfall event of 100 mm/7 h due to its pronounced visual similarity to the reference map (Figure 6).

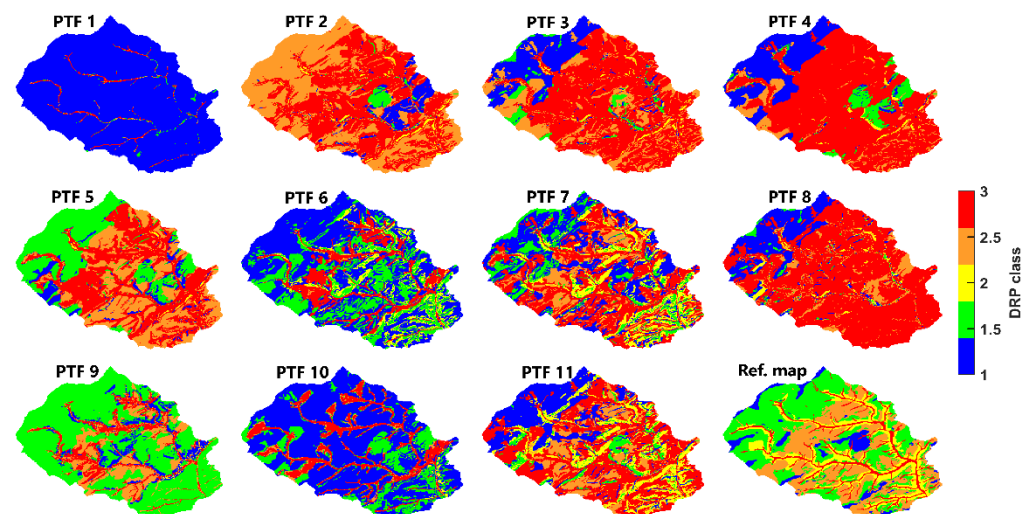


**Figure 6.** Spatial patterns of the simulated DRP classes for 11 PTFs and synthetic rainfall event of 100 mm/7 h, and the corresponding reclassified reference map.

Looking at the DRPs all over the reference map, distinct spatial patterns were visible (Figure 6, bottom right corner). DRP-class 3, which stands for fast surface runoff processes, was distributed exclusively in the stream channels and riverbanks. Spatial patterns of DRP-class 2.5, representing a combination of surface and fast sub-surface runoff, covered a larger area and were mostly located on the steep slopes near the streamflow, forming a broad strip from the west to the northeast of the catchment. This class was discerned only occasionally and on a very small scale in the high altitudes of the north and northwest. Patterns of DRP-class 2 indicating interflow formed a fringe alongside the river courses. Class 1.5, which represents a shared dominance of rapid and delayed sub-surface runoff, covered larger parts of the catchment, particularly, in the high elevations in the north and northwest of the catchment. Patterns of DRP class 1 referring to delayed sub-surface runoff (deep percolation) were sporadically distributed within the area such as small spots in the north and northwest boundaries of the catchment, and a more extensive pattern was distinct in the central part.

By performing visual inspection, it was observed that PTF combination 5 (Table 1) showed noticeable spatial similarities with the reference map while also encompassing differences (Figure 7). These similarities were evident between the simulated and observed spatial patterns of DRP class 1.5 derived from the digital soil reference map (i.e., delayed subsurface runoff processes with dominance of deep percolation), in terms of spatial distribution and area shares, particularly in the north, northwest, and some spots in the east and mid-catchment area. Moreover, the spatial distribution as well as the area share of the simulated DRP class 2.5 (i.e., which is more for faster runoff processes such as fast interflow and surface runoff) clearly corresponded to the reference map (i.e., 28% area share for simulations and 28.35% in reference map). Patterns of DRP class 1 (i.e., dominance of deep percolation processes) in the simulations and reference map were evidently consistent in terms of area share (i.e., 6.45% in the simulations and 7% in the reference map), although the spatial distributions indicated only slight commonality. The area share of simulated DRP class 3 (i.e., showing the dominance of fast runoff reactions such as saturated overland flows) was clearly overestimated, while the spatial distribution of this class was consistent with the reference map. Nevertheless, simulations with PTF combination 5 represented only negligible amounts of interflow as the dominant runoff process (class 2) in the entire catchment, which did not correspond to the reference map.

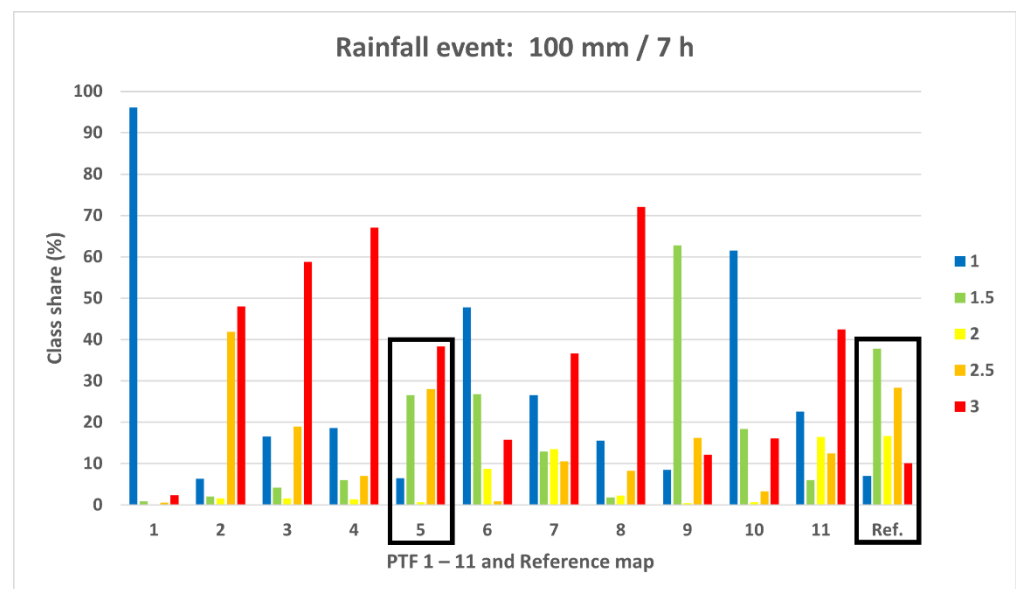


**Figure 7.** Percentage share of DRP classes for the entire catchment in the reclassified reference map and corresponding simulations for all PTFs and a precipitation intensity of 100 mm/7 h.

In addition to the visual inspection, the spatial patterns of simulated DRPs were evaluated using the spatial efficiency metric (SPAEF), and the spatial similarities were quantified. Table 6 accordingly reports the results of the spatial evaluation after applying all PTF combinations and rainfall events, while the green fields indicate positive SPAEF values.

There was an evident variation in the measure of spatial similarity amongst the simulated DRP patterns. By using different PTFs, the SPAEF values clearly changed. The highest SPAEF values were found for PTF combination 5, while it increased from 0.06 for 100 mm/5 h rainfall intensity to 0.32 for 7 h and dropped again to 0.17 until 10 h rainfall. It is also remarkable that in the case of PTF combination 9 and 100 mm/7 h rainfall intensity, SPAEF reached a maximum value of 0.20, and decreased again for the lower rainfall intensities to the value of 0.02.

**Table 6.** Spatial similarities (SPAEF values) between the simulated patterns of DPR (i.e., for all PTF combinations and synthetic rainfall intensities) and the reclassified reference runoff process map. Positive values are in green.

PTFs Rainfall Intensity	1	2	3	4	5	6	7	8	9	10	11
100 mm/3 h	−0.36	−0.64	−0.60	0.05	−0.34	−0.35	−0.39	−0.66	−0.62	−0.10	−0.49
100 mm/4 h	−1.13	−0.52	−0.37	−0.01	−0.28	−0.02	−0.23	−0.36	−0.49	0.00	−0.37
100 mm/5 h	−5.01	−0.19	−0.34	0.11	0.06	−0.04	0.17	−0.35	−0.48	−0.41	−0.39
100 mm/6 h	−6.19	−0.36	−0.33	0.11	0.15	−0.36	−0.01	−0.43	−0.18	−0.89	−0.22
100 mm/7 h	−7.22	−0.07	0.15	0.12	0.32	−0.49	−0.05	0.00	0.20	−0.98	0.02
100 mm/8 h	−7.26	−0.21	0.20	0.07	0.27	−0.69	−0.04	−0.03	−0.12	−1.07	0.01
100 mm/9 h	−7.38	0.15	0.22	0.07	0.23	−0.81	−0.25	0.06	−0.03	−1.18	0.02
100 mm/10 h	−7.44	0.13	0.09	0.13	0.17	−0.90	−0.30	0.01	−0.18	−1.28	0.08

Furthermore, PTFs 1, 6, and 10 did not produce positive values. PTF 3 showed comparatively high values from a duration of 7 h, which increased up to 9 h (0.15 to 0.20 to 0.22), and in turn decreased significantly at 10 h to 0.09. PTF 4 showed consistently positive values (except for the 4 h duration), even if these only reached a maximum SPAEF of 0.13. PTFs 2, 7, 8, and 11 only showed negligible positive values.

## 5. Discussion

A spatial pattern-oriented evaluation on dominant runoff processes was performed by integrating the process information of the reference soil hydrological map of the region. The map contents were translated and reclassified into the DRP classes that were consistent with the corresponding modeling approach. Model reactions to the precipitation intensities in terms of producing spatial patterns of DRPs were analyzed regarding the spatial structure of the catchment. To translate the information on soil properties into the model parameters, 11 PTF combinations were incorporated into the model parameterization scheme as the test cases exploring how the hydrological system functions. As a result, information on soil water retention and hydraulic conductivity, together with the given precipitation data, were considered to determine the runoff processes across the catchment.

The results described here reveal the wide range of model reactions to precipitation events. Runoff patterns varying from tiny percentages to more than 90% of the applied rainfall rates were observed within the catchment area. Moreover, different PTF combinations also caused a large variability in the spatial distribution and magnitude of the simulated DRPs. PTFs impact the soil water capacity and hydraulic conductivity. This may then control the types of catchment reaction to the rainfall event (i.e., fast, or slow) in terms of percolation or water redistribution, leading to different runoff generation processes in hillslopes and alluvial plain [50].

The above results show that simulations of surface runoff, interflow, and deep percolation (Figures 3–5) exhibited discernable variations in developing the spatial patterns within the catchment under different rainfall events. In general, this can be mainly explained by the spatial structure of the catchment under study, and thus attributed to the drivers such as precipitation intensity and duration, varying physiographic features of the catchment (i.e., the soils, topography, land slope and aspect, and local climate), infiltration capacity, and antecedent conditions [15]. Areas with steeper slopes and fine-grained soils (e.g., in the mid-catchment, east and western parts) were more responsive to rainfalls with higher intensity and shorter duration in promoting the generation of faster runoff processes. Highest surface runoff patterns were largely found in the river courses and riparian zones in the alluvial plain. Moreover, in the model, there was continuous connectivity between the groundwater module and the stream network, where interactions of shallow groundwater and surface water system further increased the soil moisture in the unsaturated zone due

to capillary rise. In fact, in alluvial plains, a shallow groundwater table plays a key role in controlling the hydrological processes within the soil [51–53]. As a result, we saw the remarkable development of surface runoff patterns in the valley floor and in a strip bordering the stream network with a constant and gentle slope gradient. This is also consistent with the results of Wang et al. (2022) [54] and Nanda and Sen (2021) [55], showing that nearly all precipitation contributed to surface runoff as the soil reached a saturated moisture content. Detty and McGuire (2010) [56] suggested that in such runoff production processes, when the groundwater level rises to a near-surface soil, surface runoff is generated because of the increased effective saturated hydraulic conductivity, which involves the transmission feedback mechanism. In contrast, soil water stored in steep hillslope zones (i.e., particularly in the parts between the north and northwest and the alluvial plain, and those on the south and southwest) contributed largely to interflow generation, while it might only be released and produce surface runoff only during higher intensity rainfall events [15]. This might be due to the difference in the topographic relief and geomorphologic characteristics between the uplands and the low-lying areas in the alluvial plain. The direction of the slope is from the northwest to the southeast, and evidently, the patterns of interflow occurred greatly on the steep slopes, and they continued developing until the longest rainfall event. The far stream uplands of the north and northwest with very gentle slopes is where the geology contributes to the development of sandy soils, and thereupon, lower surface runoff and higher deep percolation (and maybe partly interflow) have occurred. Sandy soils are characterized by intense macropores and a good matrix permeability. Therefore, geological substratum and terrain slope trigger larger interflow and deep percolation processes, particularly during longer and less intense rainfall events [57]. This may also be attributed to greater depths to the saturated zone in the upland areas of the north and northwest, which equals more available storage in the unsaturated zone and a longer percolation path [50,58]. In addition, extending the rainfall duration leads to greater infiltration of precipitation water into the deeper soils, and therefore, while surface runoff generation tends to lessen in longer rainfall events, the interflow and deep percolation processes showed growing patterns. As a result, an overall tendency of the runoff generation patterns simulated by the model could be discerned, which was the increase in surface runoff generation while deep percolation and interflow declined.

To reflect the antecedent soil moisture, we considered the condition after a persistent period of rainfall through December 2014 that corresponded to some moisture storage availability for the event water (i.e., soil water deficit), allowing for the infiltration of the rainfall into soil [50]. For example, even for the highest rainfall intensities, there may still be about 30–35% of deep percolation generated in areas on the alluvial plains in the vicinity of the river network, which still showed a slight infiltration capacity, and even 60% of deep percolation generated in some parts of the uplands during intensive rainfalls. Production of these patterns may be due to the high permeability of the soil, which still exists in these spots of the catchment.

By reclassifying the regionalized data-mining-based digital DRP map (reference map), the corresponding DRPs could be translated into numerical classes that were commensurate to the model's definition of DRPs. This allowed for a spatial comparison of the simulated DRPs and the reference map (i.e., as a benchmark for our perceived reality) for which a measure of spatial similarity was applied. The spatial efficiency metric (SPAEF) quantified the overall similarities (i.e., that encompasses both the amount and distribution of the processes in the spatial domain) between the simulated patterns and discerned the DRP patterns by the reference map. Regarding a defined system moisture precondition, a runoff process was identified to be dominant for a given rainfall event type and specific soil and topographic characteristics at a certain location, and subsequently by using different PTFs into modeling. Accordingly, the results showed that only the simulations for the rainfall event of 100 mm/7 h embraced the most pronounced visual similarity to the reference map. In contrast, shorter rainfall events with higher intensities (e.g., 3 and 4 h rainfall events) produced the lowest spatial contrast and the smallest similarities to the reference

map. Surface runoff was the dominant runoff process in the catchment. The application of synthetic precipitation events to modeling makes the spatial evaluation of the DRPs more feasible as it excludes certain influencing factors such as evapotranspiration.

Using this methodology, we could, in general, examine the effects of different PTFs showing a decisive role on dominant runoff production on a specific location and under the given rainfall characteristics. Paschalis et al. (2022) explained that the complex topography (e.g., in small catchments) particularly amplifies the importance of PTF uncertainties, where the choice of PTF indicates a significant effect on the hydrological fluxes within the drainage basin [59]. Furthermore, through a sensitivity analysis, Weihermüller et al. (2021) [60] also emphasized that choosing different PTFs in hydrological models causes a substantial variability in the simulated fluxes and soil water capacity distribution across the land. In our results, as far as the overall similarity is concerned, PTF combination 5 (Table 1) most closely corresponded to the pattern of DRPs in the existing reference map (i.e., in terms of producing the reasonable patterns for all three processes of surface runoff, interflow as well as deep percolation across the catchment area). However, when looking at individual DRPs separately, we could see, for instance, no similarity between PTF combination 5 and the reference map regarding the patterns of interflow whereas PTFs of 10 and 11 could represent the spatial patterns of interflow with higher similarities to the reference map. A possible explanation for why PTF combination 5 showed the greatest overall similarity might be that the soil database used to develop the PTF was extracted from the forest and agricultural soil in Germany [42]. This is perhaps one of the reasons why the soil samples used in Teepe et al. (2003) [42] corresponded more closely to the soil types in our study area, with 66% forests and about 33% agricultural land, whereas the rest of the PTFs used soil samples from around the world, and not just from Germany.

This study demonstrates that a local reference map of DRPs provides a useful tool for model evaluation. The availability of good quality datasets would ultimately allow for the examination of fitness-for-purpose models across a wide range of conditions [25,61–63]. For example, performing the spatial pattern-oriented evaluation, Gaur et al. (2022) [10] estimated the uncertainty associated with the spatial pattern-based evaluation of the MIKE SHE model for the Subarnarekha Basin. In another study, Dembélé et al. (2020) introduced a new bias-insensitive metric based on pixel-by-pixel locational matching that could be used to improve the calibration of a hydrological model on the spatial patterns of hydrological processes derived from a data-mining-based digital soil map [64]. While our study was in essence a sensitivity analysis, it did not include model verification using measured fluxes and it only employed one model.

## 6. Conclusions

The overall goal of the current work was to focus on improving the spatial representation of dominant runoff processes in a hydrological model using spatial pattern information from a regional soil hydrological map. Evaluating the plausibility of reproduced dynamics of the hydrological system, a bias-insensitive and multicomponent metric was applied for spatial pattern matching. Dealing with the issues of inadequate spatial observations for rigorous spatial model evaluation, we made use of a reference soil hydrologic map available for the study area to discern the expected dominant runoff processes across a wide range of hydrological conditions. Considering the spatial structure of the catchment, we analyzed the model's reaction to various synthetic rainfall events in terms of reproducing the spatial patterns of DRPs. Moreover, multiple PTFs were incorporated in the model parameterization scheme as the test cases translating the information on soil properties into model parameters. In general, the information on the soil hydraulic properties, together with the given rainfall data, were considered to determine the runoff process dynamics. As a result, the different models' reactions to reproduce the patterns of DRPs could be distinguished. This spatial information would ultimately reflect the distribution of heterogeneities that are important in rapid runoff generation under wet conditions or retention under dry conditions. Such improvements will be an asset for spatial hydrology and large-



domain water management applications (e.g., flood forecast, drought monitoring, and water accounting). This, in fact, will contribute to solving some of the issues (e.g., spatial variability and modeling methods) identified as the 23 unsolved problems in hydrology in the 21st century [65]. However, to the best of our knowledge, only a few studies have applied the spatial observation of DRP by regional soil maps into the spatial evaluation of models. The present study, nevertheless, will progress toward a comprehensive model calibration procedure considering multiple data sources simultaneously, with the specificity of incorporating the spatial patterns of satellite remote sensing data as well as reference DRP maps in the parameter estimation method to reproduce the plausible dynamics of the various hydrological processes (e.g., evapotranspiration, soil water storage, and runoff).

**Author Contributions:** Conceptualization, M.C.C., M.J. and H.M.; methodology, M.C.C. and M.J.; software, M.J.; validation, M.J., M.C.C. and H.M.; formal analysis, M.J. and M.C.C.; investigation, M.J.; resources, M.C.C. and T.S.; data curation, M.J.; writing—original draft preparation, H.M., M.J., Z.S. and M.C.C.; writing—review and editing, H.M., Z.S., M.C.C. and T.S.; visualization, M.J.; supervision, M.C.C.; project administration, M.C.C.; funding acquisition, M.C.C. All authors have read and agreed to the published version of the manuscript.

**Funding:** Funded by the Deutsche Forschungsgemeinschaft (DFG, German Research Foundation)—Projektnummer 426111700.

**Data Availability Statement:** The data presented in this study are available on request from the corresponding authors.

**Conflicts of Interest:** The authors declare no conflict of interest.

## References

1. Horton, P.; Schaefer, B.; Kauzlaric, M. Why Do We Have so Many Different Hydrological Models? A Review Based on the Case of Switzerland. *WIREs Water* **2022**, *9*, e1574. [[CrossRef](#)]
2. Sitterson, J.; Knightes, C.; Parmar, R.; Wolfe, K.; Avant, B.; Muche, M. An Overview of Rainfall-Runoff Model Types. In Proceedings of the International Congress on Environmental Modelling and Software, Fort Collins, CO, USA, June 2018; Volume 41.
3. Yang, Y.; Anderson, M.C.; Gao, F.; Hain, C.R.; Semmens, K.A.; Kustas, W.P.; Noormets, A.; Wynne, R.H.; Thomas, V.A.; Sun, G. Daily Landsat-Scale Evapotranspiration Estimation over a Forested Landscape in North Carolina, USA, Using Multi-Satellite Data Fusion. *Hydrol. Earth Syst. Sci.* **2017**, *21*, 1017. [[CrossRef](#)]
4. Baroni, G.; Schalge, B.; Rakovec, O.; Kumar, R.; Schüler, L.; Samaniego, L.; Simmer, C.; Attinger, S. A Comprehensive Distributed Hydrological Modeling Intercomparison to Support Process Representation and Data Collection Strategies. *Water Resour. Res.* **2019**, *55*, 990–1010. [[CrossRef](#)]
5. Krogh, S.A.; Pomeroy, J.W.; Marsh, P. Diagnosis of the Hydrology of a Small Arctic Basin at the Tundra-Taiga Transition Using a Physically Based Hydrological Model. *J. Hydrol.* **2017**, *550*, 685–703. [[CrossRef](#)]
6. Mohajerani, H.; Zema, D.A.; Lucas-Borja, M.E.; Casper, M. Chapter 9—Understanding the Water Balance and Its Estimation Methods. In *Precipitation*; Rodrigo-Comino, J., Ed.; Elsevier: Amsterdam, The Netherlands, 2021; pp. 193–221. ISBN 978-0-12-822699-5.
7. Mohajerani, H.; Teschemacher, S.; Casper, M.C. A Comparative Investigation of Various Pedotransfer Functions and Their Impact on Hydrological Simulations. *Water* **2021**, *13*, 1401. [[CrossRef](#)]
8. Koch, J.; Demirel, M.C.; Stisen, S. Climate Normalized Spatial Patterns of Evapotranspiration Enhance the Calibration of a Hydrological Model. *Remote Sens.* **2022**, *14*, 315. [[CrossRef](#)]
9. Koch, J.; Siemann, A.; Stisen, S.; Sheffield, J. Spatial Validation of Large-Scale Land Surface Models against Monthly Land Surface Temperature Patterns Using Innovative Performance Metrics. *J. Geophys. Res. Atmos.* **2016**, *121*, 5430–5452. [[CrossRef](#)]
10. Gaur, S.; Singh, B.; Bandyopadhyay, A.; Stisen, S.; Singh, R. Spatial Pattern-Based Performance Evaluation and Uncertainty Analysis of a Distributed Hydrological Model. *Hydrol. Process.* **2022**, *36*, e14586. [[CrossRef](#)]
11. Fekete, B.M.; Vörösmarty, C.J.; Grabs, W. High-Resolution Fields of Global Runoff Combining Observed River Discharge and Simulated Water Balances. *Glob. Biogeochem. Cycles* **2002**, *16*, 15-1–15-10. [[CrossRef](#)]
12. Das, P.C.; Esraz-Ul-Zannat, M.D. Assessing the Impacts of Land Use–Land Cover Changes on Direct Surface Runoff: A Remote Sensing Approach in Khulna City. *Water Sci. Technol.* **2022**, *85*, 3122–3144. [[CrossRef](#)]
13. Ahmadi-Sani, N.; Razaghnia, L.; Pukkala, T. Effect of Land-Use Change on Runoff in Hyrcania. *Land* **2022**, *11*, 220. [[CrossRef](#)]
14. Lucas-Borja, M.E.; Zema, D.A.; Plaza-Álvarez, P.A.; Zupanc, V.; Baartman, J.; Sagra, J.; González-Romero, J.; Moya, D.; de las Heras, J. Effects of Different Land Uses (Abandoned Farmland, Intensive Agriculture and Forest) on Soil Hydrological Properties in Southern Spain. *Water* **2019**, *11*, 503. [[CrossRef](#)]
15. Sinha, S.; Rode, M.; Borchardt, D. Examining Runoff Generation Processes in the Selke Catchment in Central Germany: Insights from Data and Semi-Distributed Numerical Model. *J. Hydrol. Reg. Stud.* **2016**, *7*, 38–54. [[CrossRef](#)]

16. Müller, C.; Hellebrand, H.; Seeger, M.; Schobel, S. Identification and Regionalization of Dominant Runoff Processes—A GIS-Based and a Statistical Approach. *Hydrol. Earth Syst. Sci.* **2009**, *13*, 779–792. [[CrossRef](#)]
17. Scherrer, S.; Naef, F.; Faeh, A.O.; Cordery, I. Formation of Runoff at the Hillslope Scale during Intense Precipitation. *Hydrol. Earth Syst. Sci.* **2007**, *11*, 907–922. [[CrossRef](#)]
18. Casper, M.C.; Mohajerani, H.; Hassler, S.K.; Herdel, T.; Blume, T. Finding Behavioral Parameterization for a 1-D Water Balance Model by Multi-Criteria Evaluation. *J. Hydrol. Hydromech.* **2019**, *67*, 213–224. [[CrossRef](#)]
19. Farsi, N.; Mahjouri, N. Evaluating the Contribution of the Climate Change and Human Activities to Runoff Change under Uncertainty. *J. Hydrol.* **2019**, *574*, 872–891. [[CrossRef](#)]
20. Liu, J.; Luo, M.; Liu, T.; Bao, A.; De Maeyer, P.; Feng, X.; Chen, X. Local Climate Change and the Impacts on Hydrological Processes in an Arid Alpine Catchment in Karakoram. *Water* **2017**, *9*, 344. [[CrossRef](#)]
21. Yin, J.; He, F.; Xiong, Y.J.; Qiu, G.Y. Effects of Land Use/Land Cover and Climate Changes on Surface Runoff in a Semi-Humid and Semi-Arid Transition Zone in Northwest China. *Hydrol. Earth Syst. Sci.* **2017**, *21*, 183–196. [[CrossRef](#)]
22. Jiang, T.; Fischer, T.; Lu, X. Larger Asian Rivers: Climate Change, River Flow, and Watershed Management. *Quat. Int.* **2010**, *226*, 1–3. [[CrossRef](#)]
23. Antonetti, M.; Buss, R.; Scherrer, S.; Margreth, M.; Zappa, M. Mapping Dominant Runoff Processes: An Evaluation of Different Approaches Using Similarity Measures and Synthetic Runoff Simulations. *Hydrol. Earth Syst. Sci.* **2016**, *20*, 2929–2945. [[CrossRef](#)]
24. Schmockler-Fackel, P.; Naef, F.; Scherrer, S. Identifying Runoff Processes on the Plot and Catchment Scale. *Hydrol. Earth Syst. Sci. Discuss.* **2006**, *3*, 2063–2100. [[CrossRef](#)]
25. Semanova, O.; Beven, K. Barriers to Progress in Distributed Hydrological Modelling. *Hydrol. Process.* **2015**, *29*, 2074–2078. [[CrossRef](#)]
26. Tetzlaff, D.; Buttle, J.; Carey, S.K.; McGuire, K.; Laudon, H.; Soulsby, C. Tracer-Based Assessment of Flow Paths, Storage and Runoff Generation in Northern Catchments: A Review. *Hydrol. Process.* **2015**, *29*, 3475–3490. [[CrossRef](#)]
27. Kuczera, G.; Renard, B.; Thyer, M.; Kavetski, D. There Are No Hydrological Monsters, Just Models and Observations with Large Uncertainties! *Hydrol. Sci. J.* **2010**, *55*, 980–991. [[CrossRef](#)]
28. Beven, K. A Manifesto for the Equifinality Thesis. *J. Hydrol.* **2006**, *320*, 18–36. [[CrossRef](#)]
29. Haag, I.; Luce, A.; Henn, N.; Demuth, N. Consideration of spatially differentiated runoff process maps in the water balance model LARSIM. *Forum Hydrol. Wasserbewirtschaft.* **2016**, *36*, 51–62.
30. Scherrer, S.; Naef, F. A Decision Scheme to Indicate Dominant Hydrological Flow Processes on Temperate Grassland. *Hydrol. Process.* **2003**, *17*, 391–401. [[CrossRef](#)]
31. Bremicker, M. *Das Wasserhaushaltsmodell LARSIM: Modellgrundlagen Und Anwendungsbeispiele*; Institution für Hydrologie der University Freiburg: Freiburg, Germany, 2000.
32. Steinrücken, U.; Behrens, T. *Bodenhydrologische Karte—Nahe-Rheinland-Pfalz Südwest: Stand 04/2010*; LUWG-Bericht; LUWG: Mainz, Germany, 2010.
33. Demirel, M.C.; Mai, J.; Mendiguren, G.; Koch, J.; Samaniego, L.; Stisen, S. Combining Satellite Data and Appropriate Objective Functions for Improved Spatial Pattern Performance of a Distributed Hydrologic Model. *Hydrol. Earth Syst. Sci.* **2018**, *22*, 1299. [[CrossRef](#)]
34. Casper, M.C.; Grigoryan, G.; Gronz, O.; Gutjahr, O.; Heinemann, G.; Ley, R.; Rock, A. Analysis of Projected Hydrological Behavior of Catchments Based on Signature Indices. *Hydrol. Earth Syst. Sci.* **2012**, *16*, 409–421. [[CrossRef](#)]
35. Richards, L.A. Capillary Conduction of Liquids through Porous Mediums. *Physics* **1931**, *1*, 318–333. [[CrossRef](#)]
36. Van Genuchten, M.T. A Closed-Form Equation for Predicting the Hydraulic Conductivity of Unsaturated Soils 1. *Soil Sci. Soc. Am. J.* **1980**, *44*, 892–898. [[CrossRef](#)]
37. Boden, A.-h.-A.G. *Bodenkundliche Kartieranleitung. KA5*; Schweizerbart Science Publishers: Stuttgart, Germany, 2005; ISBN 978-3-510-95920-4.
38. Wösten, J.; Lilly, A.; Nemes, A.; Le Bas, C. Development and Use of a Database of Hydraulic Properties of European Soils. *Geoderma* **1999**, *90*, 169–185. [[CrossRef](#)]
39. Renger, M.; Bohne, K.; Facklam, M.; Harrach, T.; Riek, W.; Schäfer, W.; Wessolek, G.; Zacharias, S. Ergebnisse Und Vorschläge Der DBG-Arbeitsgruppe Kennwerte Des Bodengefüges. *Zur Schätzung Bodenphysikalischer Kennwerte* **2009**, *40*, 4–51.
40. Weynants, M.; Vereecken, H.; Javaux, M. Revisiting Vereecken Pedotransfer Functions: Introducing a Closed-Form Hydraulic Model. *Vadose Zone J.* **2009**, *8*, 86–95. [[CrossRef](#)]
41. Zacharias, S.; Wessolek, G. Excluding Organic Matter Content from Pedotransfer Predictors of Soil Water Retention. *Soil Sci. Soc. Am. J.* **2007**, *71*, 43–50. [[CrossRef](#)]
42. Teepe, R.; Dilling, H.; Beese, F. Estimating Water Retention Curves of Forest Soils from Soil Texture and Bulk Density. *J. Plant Nutr. Soil Sci.* **2003**, *166*, 111–119. [[CrossRef](#)]
43. Zhang, Y.; Schaap, M.G. Weighted Recalibration of the Rosetta Pedotransfer Model with Improved Estimates of Hydraulic Parameter Distributions and Summary Statistics (Rosetta3). *J. Hydrol.* **2017**, *547*, 39–53. [[CrossRef](#)]
44. Scherrer, S. *Bestimmungsschlüssel zur Identifikation von Hochwasserrelevanten Flächen: Landesamt für Umwelt*; Wasserwirtschaft; Landesamtes für Umwelt, Wasserwirtschaft und Gewerbeaufsicht: Mainz, Germany, 2006; p. 126.
45. Behrens, T.; Zhu, A.-X.; Schmidt, K.; Scholten, T. Multi-Scale Digital Terrain Analysis and Feature Selection for Digital Soil Mapping. *Geoderma* **2010**, *155*, 175–185. [[CrossRef](#)]

46. Behrens, T.; Förster, H.; Scholten, T.; Steinrücken, U.; Spies, E.-D.; Goldschmitt, M. Digital Soil Mapping Using Artificial Neural Networks. *J. Plant Nutr. Soil Sci.* **2005**, *168*, 21–33. [[CrossRef](#)]
47. Behrens, T.; Scholten, T. Digital Soil Mapping in Germany—A Review. *J. Plant Nutr. Soil Sci.* **2006**, *169*, 434–443. [[CrossRef](#)]
48. Gronz, O. *Nutzung von Abflussprozessinformation in LARSIM*; Universität Trier: Trier, Germany, 2013.
49. Gupta, H.V.; Kling, H.; Yilmaz, K.K.; Martinez, G.F. Decomposition of the Mean Squared Error and NSE Performance Criteria: Implications for Improving Hydrological Modelling. *J. Hydrol.* **2009**, *377*, 80–91. [[CrossRef](#)]
50. Pavlin, L.; Széles, B.; Strauss, P.; Blaschke, A.P.; Blöschl, G. Event and Seasonal Hydrologic Connectivity Patterns in an Agricultural Headwater Catchment. *Hydrol. Earth Syst. Sci.* **2021**, *25*, 2327–2352. [[CrossRef](#)]
51. Pirastru, M.; Niedda, M. Evaluation of the Soil Water Balance in an Alluvial Flood Plain with a Shallow Groundwater Table. *Hydrol. Sci. J.* **2013**, *58*, 898–911. [[CrossRef](#)]
52. Krause, S.; Bronstert, A. The Impact of Groundwater–Surface Water Interactions on the Water Balance of a Mesoscale Lowland River Catchment in Northeastern Germany. *Hydrol. Process.* **2007**, *21*, 169–184. [[CrossRef](#)]
53. Jung, M.; Burt, T.P.; Bates, P.D. Toward a Conceptual Model of Floodplain Water Table Response. *Water Resour. Res.* **2004**, *40*, W12409. [[CrossRef](#)]
54. Wang, S.; Peng, H.; Hu, Q.; Jiang, M. Analysis of Runoff Generation Driving Factors Based on Hydrological Model and Interpretable Machine Learning Method. *J. Hydrol. Reg. Stud.* **2022**, *42*, 101139. [[CrossRef](#)]
55. Nanda, A.; Sen, S. A Complex Network Theory Based Approach to Better Understand the Infiltration-Excess Runoff Generation Thresholds. *J. Hydrol.* **2021**, *603*, 127038. [[CrossRef](#)]
56. Detty, J.M.; McGuire, K.J. Topographic Controls on Shallow Groundwater Dynamics: Implications of Hydrologic Connectivity between Hillslopes and Riparian Zones in a till Mantled Catchment. *Hydrol. Process.* **2010**, *24*, 2222–2236. [[CrossRef](#)]
57. Ran, G.; Jian, S.; Wu, Q.; Zhang, L.; Hu, C. Exploring the Dominant Runoff Processes in Two Typical Basins of the Yellow River, China. *Water* **2020**, *12*, 3055. [[CrossRef](#)]
58. Klaus, J.; Jackson, C.R. Interflow Is Not Binary: A Continuous Shallow Perched Layer Does Not Imply Continuous Connectivity. *Water Resour. Res.* **2018**, *54*, 5921–5932. [[CrossRef](#)]
59. Paschalis, A.; Bonetti, S.; Guo, Y.; Fatichi, S. On the Uncertainty Induced by Pedotransfer Functions in Terrestrial Biosphere Modeling. *Water Resour. Res.* **2022**, *58*, e2021WR031871. [[CrossRef](#)]
60. Weihermüller, L.; Lehmann, P.; Herbst, M.; Rahmati, M.; Verhoef, A.; Or, D.; Jacques, D.; Vereecken, H. Choice of Pedotransfer Functions Matters When Simulating Soil Water Balance Fluxes. *J. Adv. Model. Earth Syst.* **2021**, *13*, e2020MS002404. [[CrossRef](#)]
61. Beven, K.; Smith, P. Concepts of Information Content and Likelihood in Parameter Calibration for Hydrological Simulation Models. *J. Hydrol. Eng.* **2015**, *20*, A4014010. [[CrossRef](#)]
62. Hrachowitz, M.; Savenije, H.; Blöschl, G.; McDonnell, J.; Sivapalan, M.; Pomeroy, J.; Arheimer, B.; Blume, T.; Clark, M.; Ehret, U.; et al. A Decade of Predictions in Ungauged Basins (PUB)—A Review. *Hydrol. Sci. J.* **2013**, *58*, 1198–1255. [[CrossRef](#)]
63. Beven, K.J. Preferential Flows and Travel Time Distributions: Defining Adequate Hypothesis Tests for Hydrological Process Models. *Hydrol. Process.* **2010**, *24*, 1537–1547. [[CrossRef](#)]
64. Dembélé, M.; Hrachowitz, M.; Savenije, H.H.G.; Mariéthoz, G.; Schaeffli, B. Improving the Predictive Skill of a Distributed Hydrological Model by Calibration on Spatial Patterns with Multiple Satellite Data Sets. *Water Resour. Res.* **2020**, *56*, e2019WR026085. [[CrossRef](#)]
65. Blöschl, G.; Bierkens, M.F.; Chambel, A.; Cudennec, C.; Destouni, G.; Fiori, A.; Kirchner, J.W.; McDonnell, J.J.; Savenije, H.H.; Sivapalan, M.; et al. Twenty-Three Unsolved Problems in Hydrology (UPH)—A Community Perspective. *Hydrol. Sci. J.* **2019**, *64*, 1141–1158. [[CrossRef](#)]

**Disclaimer/Publisher’s Note:** The statements, opinions and data contained in all publications are solely those of the individual author(s) and contributor(s) and not of MDPI and/or the editor(s). MDPI and/or the editor(s) disclaim responsibility for any injury to people or property resulting from any ideas, methods, instructions or products referred to in the content.



## Curriculum Vitae

---

Name Hadis  
Surname Mohajerani  
Contact info [mohajerani@uni-trier.de](mailto:mohajerani@uni-trier.de);  
[hadisa.mohajerani@gmail.com](mailto:hadisa.mohajerani@gmail.com)



## Professional Experience

---

- 01/2018 - Present    **Scientific Employee**  
**Trier University, Department of Physical Geography, Trier, Germany:**
- Developed preliminary work for DFG grant application by publishing in peer-reviewed journals and presenting in scientific conferences/meetings.
  - Collaborated with Leipzig University (Prof. Michael Volland) to prepare the original grant proposal, organized team meetings, and contributed to a successful research proposal submission to DFG.
- DFG Project: "Improving the spatio-temporal accuracy of mesoscale hydrological modeling using remote sensing products" (07/2019 - Present)**
- Focused on Catchment Hydrological processes/Water Balance Simulation
  - Conducted project groups, organized meetings, and prepared project reports.
  - Planned and operated hydrological simulation work and interpreted water balance modeling outputs.
  - Designed and authored project outcomes for peer-reviewed journals.
  - Organized and moderated international meetings and workshops.
  - Provided guidance to the students.
- 03/2017-03/2018    **Academic Assistant**  
**Trier University, Department of Physical Geography, Trier, Germany**  
Worked on grant proposal ideas and materials for fundraising applications in water balance and catchment hydrology modeling.
- 10/2012-10/2014    **Academic Assistant**  
**Department of Water Engineering, University of Gorgan, Gorgan, Iran**  
Provided guidance to undergraduate students on Groundwater Management and Bayesian Network studies for their theses and scientific papers.

## Academic Formation

---

- 01/2016 – 22/11/2023    **PhD**
- Department of Physical Geography, Trier University, Germany
  - PhD research: "Towards Behavioral Model Parameterization: Integrated Evaluation of Hydrological Modeling and Parameterization Schemes,

Considering Pedo-transfer Functions and Spatial Patterns of Runoff Generation Processes" under the supervision of Prof. Markus Casper.

- 10/2008 - 10/ 2011      **Master of Science (M.Sc)**
- Water Resources Engineering, Gorgan University of Agricultural Sciences and Natural Resources, Iran
  - Research: "Groundwater Management Using Bayesian Decision Network."
- 10/2003 - 10/ 2007      **Bachelor Degree (B.Sc)**
- Agricultural Engineering -Irrigation, Mazandaran University, Iran
- 10/1998 - 10/ 2001      **Diploma (High school)**
- Mathematics and Physics, Tehran, Iran
  - Background of studying at NODET high schools (National Organization for Development of Exceptional Talents).

### ***Awards***

---

- 01/11/2023 – 31/01/2024      DAAD Iran Bridge Scholarship  
Aimed to support doctoral/postdoctoral researchers from Iran to continue their research project in German higher education institutes

### ***Selected Professional Development Activities***

---

- 2023
- Organized, coordinated, and moderated panel discussion series with the IAHR on "Capacity of the youth and international organizations towards partnership, cooperation, and environmental protection to accelerate SDGs" (05.06.2023):  
<https://www.youtube.com/watch?v=XiTT1p9kT6Q&pp=ygUWSUFIUiBjYXBhY2l0eSBvZiB5b3V0aA%3D%3D>  
& <https://www.iahr.org/index/detail/1031>
  - Organized and coordinated the joint international workshop (by Hadis Mohajerani) on "Water balance, Planetary boundaries, and Sustainable development goals" in Nong Lam University, Ho Chi Minh City, Vietnam (09.03.2023).
  - \* Coordinated a seminar for graduate students at the University of Economy (UEH), Ho Chi Minh City, Vietnam on "Sustainability, planetary boundaries, and economic growth" (05.03.2023).
  - \* Talk at 9th International Conference on Environment and Renewable Energy (ICERE 2023). 24-26.02.2023, Hanoi, Vietnam. Mohajerani, H., Jackel, M., & Casper, M. "Spatial Evaluation of a Hydrological Model on Dominant Runoff Generation Processes Using Soil Hydrologic Maps."
  - \* Attended the Workshop on "Organizing an Academic Conference" Graduiertenzentrum Universität Trier (GUT), April 2023
  - \* Attended the Presentation Masterclass by Sam Horn -virtual training to master presentation and public speaking skills, 18-20 April 2023
- 2022
- Talk at the 39th IAHR World Congress "From Snow to Sea" in Granada, Spain (19-24 June 2022). Mohajerani, H., Casper, M., Hutengs, C., Jackel, M., Rodrigo-Comino, J. & Voland, M. "Combining satellite data on Evapotranspiration for improved spatial pattern of hydrological model: Impact on appropriate Pedo-Transfer Function selection."

- EGU General Assembly 2022 (23-27.03.2022), Vienna, Austria . Jackel, M., Mohajerani, H., & Casper, M. “The effect of different pedotransferfunctions on the spatial distribution and intensity of runoff processes using the hydrological model WaSiM-ETH.”
- \* Attended the Workshop „Chancengleichheit in Forschungsverbänden“  
Referat für Gleichstellung der Universität Trier. 2022. Mentoring als Gleichstellungsmaßnahme. Abgerufen am 13.05.2022
- 2021 \* Participated in the Research Management Training Workshop (ReMaT) by Tutech Innovation, Hamburg (21 & 22 October 2021).
- \* Attended the Workshop on „How to Write a Competitive Proposal for Horizon Europe“  
Dr. Seán McCarthy & Sylvia McCarthy - Hyperion Ltd. (Training Courses for European Researchers) - 11.2021
- \* Participated in the Mentoring-Program (Karriereplanung für Wissenschaftlerinnen der Universität Trier)  
Universität Trier, Referat für Gleichstellung, from 01.06.2019 to 30.06.2021
- 2020 • Tag Der Hydrology, 03.2020, Potsdam, Germany Poster (German), Casper, M., Teschemacher, S., Mohajerani, H., & Gronz, O: “Der Zusammenhang zwischen Pedotransferfunktion und Modellverhalten”
- \* Attended the workshop „Drittmitteleinwerbung und Karriereförderung  
Förderprogramme der DFG“ by Dr. Gisela Minn, Forschungsreferat, Universität Trier – 09.2020
- \* Attended the Workshop „Souverän handeln im beruflichen Kontext“  
Trier University, 30.09. und 01.10.2020
- 2019 • Organization & moderation of session at 5th Biohydrology meeting, 20-27.07.2019, Valencia, Spain, Session title: “Learning from Biohydrological Journey of Evapotranspiration: Departing from soil reservoir, transferring to the plant roots and leaf stomata and arriving at the atmosphere”.
- \* Attended the workshop on “Good Scientific Practice”, by Graduiertenzentrum der Universität Trier (GUT), Dr. Michael Gommel, 10.2019
- 2017 \* Presented at EGU. Mohajerani, H., Casper, M., Kholghi, M., Mosaedi, A., Farmani, R., Saadoddin, A., & Meftah Halaghi, M. (2017, April). Application of Bayesian Decision Networks for sustainable groundwater resources management in semi-arid regions. In EGU General Assembly Conference Abstracts (p. 2297).
- \* Attended The 2nd IAHS Panta Rhei International Conference on Water System Knowledge Innovation and its Practices in Developing Countries, Gorgan, Iran (20-22.11.2017).

### ***Scientific Publications***

---

- 2024 Heuer, M., Casper, M., & Mohajerani, H. 2024. Multi-criteria runoff process-related evaluation of a behavioral hydrological model. Hydrological Science Journal (under-review).
- 2023 Casper, M. C., Salm, Z., Gronz, O., Hutengs, C., Mohajerani, H., & Vohland, M. (2023). Calibration of Land-Use-Dependent Evaporation Parameters in Distributed Hydrological Models Using MODIS Evaporation Time Series Data. Hydrology, 10(12), 216.
- 2023 Mohajerani, H., Jackel, M., Salm, Z., Schütz, T., & Casper, M. C. (2023). Spatial Evaluation of a Hydrological Model on Dominant Runoff Generation Processes Using Soil Hydrologic Maps. Hydrology, 10(3), 55.

- 2021 Mohajerani, H.; Teschemacher, S.; Casper, M.C. A Comparative Investigation of Various Pedotransfer Functions and Their Impact on Hydrological Simulations. *Water* 2021, 13.
- 2021 Mohajerani, H., Zema, D. A., Lucas-Borja, M. E., & Casper, M. (2021). Understanding the water balance and its estimation methods. In *Precipitation* (pp. 193-221). Elsevier.
- 2019 Casper, M. C., Mohajerani, H., Hassler, S., Herdel, T., & Blume, T. (2019). Finding behavioral parameterization for a 1-D water balance model by multi-criteria evaluation. *Journal of Hydrology and Hydromechanics*, 67(3), 213-224.
- 2017 Mohajerani, H., Kholghi, M., Mosaedi, A., Farmani, R., Sadoddin, A., & Casper, M. (2017). Application of Bayesian Decision Networks for Groundwater Resources Management Under the Conditions of High Uncertainty and Data Scarcity. *Water Resources Management*, 31(6), 1859-1879.
- 2017 Comino, J. R., Bogunovic, I., Mohajerani, H., Pereira, P., Cerdà, A., Ruiz Sinoga, J. D., & Ries, J. B. (2017). The impact of vineyard abandonment on soil properties and hydrological processes. *Vadose Zone Journal*, 16(12), 1-7.

---

***Reviewer in Scientific journals***

---

- **Journal of Water Resources Management WARM:**  
<https://www.springer.com/earth+sciences+and+geography/hydrogeology/journal/11269>
- **Air, Soil and Water Research Journal :** <https://us.sagepub.com/en-us/nam/air-soil-and-water-research/journal202616>
- **Hydrological Sciences Journal :** <https://www.tandfonline.com/loi/thsj20>